

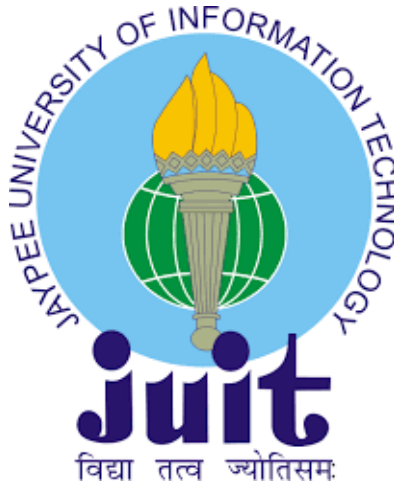
# **DESIGN AND DEVELOPMENT OF COMPACT MIMO/DIVERSITY BAND NOTCHED UWB ANTENNAS**

*Thesis submitted in fulfillment of the requirements for the Degree of*

**Doctor of Philosophy**

**By**

**EKTA THAKUR**



Department of Electronics and Communication Engineering  
JAYPEE UNIVERSITY OF INFORMATION TECHNOLOGY  
WAKNAGHAT, SOLAN, H.P., INDIA  
AUGUST, 2020

@ Copyright JAYPEE UNIVERSITY OF INFORMATION TECHNOLOGY,  
WAKNAGHAT,  
December, 2020  
ALL RIGHT RESERVED

# TABLE OF CONTENT

<b>CONTENTS</b>	<b>PAGE NO.</b>
<b>DECLARATION BY THE SCHOLAR .....</b>	<b>i</b>
<b>SUPERVISOR’S CERTIFICATE.....</b>	<b>ii</b>
<b>ACKNOWLEDGEMENT .....</b>	<b>iii</b>
<b>LIST OF SYMBOLS.....</b>	<b>iv</b>
<b>LIST OF ABBREVIATIONS AND ACRONYMS .....</b>	<b>vi</b>
<b>LIST OF FIGURES .....</b>	<b>ix</b>
<b>LIST OF TABLE .....</b>	<b>xiv</b>
<b>ABSTRACT.....</b>	<b>xv</b>
<b>CHAPTER 1 .....</b>	<b>2</b>
<b>Introduction .....</b>	<b>2</b>
1.1 Introduction .....	2
1.2 UWB Technology.....	2
1.3 Monopole Antenna .....	4
1.4 Multiple Antennas.....	6
1.5 Motivation for the Present Research.....	7
1.6 Challenges in antenna design .....	8
1.7 Research Problem Statement.....	8
1.8 Objectives.....	9
1.9 Thesis organization .....	10
1.10 Summary .....	11
<b>CHAPTER 2 .....</b>	<b>13</b>
<b>Literature Review .....</b>	<b>13</b>
2.1 UWB Background.....	13
2.2 Monopole Antennas .....	15

2.2.1 Feeding Techniques .....	16
2.2.2 Analytical Modelling of PMAs: Related Issues .....	19
2.3 UWB Antennas.....	21
2.3.1 Advantages .....	21
2.4 Multiple-Input-Multiple-Output Communication systems .....	22
2.4.1 MIMO system.....	22
2.5. UWB MIMO Antenna characteristics .....	27
2.5.1 Challenges in designing UWB MIMO systems.....	28
2.6 Polarization.....	28
2.6.1 Axial ratio and Polarization ellipse .....	29
2.6.2 Antenna polarization loss factor (PLF) .....	30
2.6.3 Advantages of circular polarization .....	31
2.7 Application of UWB MIMO antenna system.....	32
2.7.1 RFID Radio Frequency Identification (RFID) .....	32
2.7.2 Precision asset location (PAL) system .....	33
2.7.3 Communication.....	34
2.7.4 Medicine .....	34
2.7.5 Commercial UWB systems .....	35
2.8 Metamaterial.....	35
2.8.1 Electromagnetic Band Gap (EBG) Structures .....	36
2.8.2 EBG Structure and characterization.....	36
2.8.4 EBG Structure Miniaturization .....	38
2.9 Band notch operation in patch antenna using EBG Structures .....	40
2.10 Designing of different feeding methods in Microstrip Antenna .....	43
2.10.1 Antenna Design and discussion .....	43
2.11 Summery .....	50
<b>CHAPTER 3.....</b>	<b>53</b>
<b>Compact Band notched UWB MIMO Antenna using Quarter wavelength slots.....</b>	<b>53</b>
3.1 Introduction .....	53
3.2 Proposed UWB MIMO Antenna with triple notches.....	54

3.2.1 Antenna Design and Analysis.....	54
3.3 Parametric study .....	55
3.3.1 Variation of Slot length .....	55
3.3.2 Effect of Variation of Ground Plane .....	57
3.3.3 Current Distribution Analysis .....	59
3.4 Fabrication and Experimental demonstration.....	60
3.4.1. Measured Scattering Parameters and radiation pattern .....	60
3.4.2 MIMO performances:.....	62
3.5 Summery .....	71
<b>CHAPTER 4 .....</b>	<b>73</b>
<b>Band rejected UWB MIMO/DIVERSITY antenna with TVC EBG Structure .....</b>	<b>73</b>
4.1 Introduction .....	73
4.2 Suggested TVC- EBG unit cell .....	74
4.2.1. TVC- EBG Structure Design .....	74
4.3. Suggested UWB MIMO/DIVERSITY antenna with TVC-EBG unit cell.....	77
4.4 Experimental results and Discussion .....	77
4.4.1 Measured scattering parameters.....	77
4.4.2 Radiation patterns characteristics .....	78
4.4.3 MIMO Characteristics.....	78
4.4.3 Comparison of the proposed antenna with published work .....	83
4.5 Four elements band-notched UWB MIMO antenna.....	85
4.5.1Antenna Design.....	85
4.5.2Equivalent circuit Model .....	86
4.6.1 Numerical Results and discussion .....	93
4.6.2 Radiation pattern plots and gain .....	93
4.6.3 MIMO characteristics.....	95
4.7 Summery .....	100

<b>CHAPTER 5 .....</b>	<b>103</b>
<b>Circularly Polarized Ultra-Wideband MIMO/Diversity antenna .....</b>	<b>103</b>
5.1 Introduction .....	103
5. 2 Circular Polarized UWB Antenna .....	104
5. 2.1 Design and Analysis .....	104
5. 3 Results and Parametric analysis .....	105
5 3.1 Variations in the ring slot ( $G_P$ ) .....	105
5.3.2 Variations in the ground slot ( $S_1$ ).....	106
5.3.3 Variation of the slot length ( $S_3$ ) .....	106
5.3.4 Variations in the ground slot ( $S_4$ ).....	107
5.4 Circular Polarized band-notched UWB MIMO Antenna.....	113
5.4.1 Band notched CP UWB MIMO antenna.....	116
5.4.2 Circular polarization phenomenon.....	116
5.5 Experimental results and validation.....	120
5.6 Comparison of different CP UWB MIMO Antenna.....	123
5.7 Summery .....	124
<b>CHAPTER 6 .....</b>	<b>128</b>
<b>Compact UWB MIMO Antenna with Enhanced Bandwidth .....</b>	<b>128</b>
6.1 Introduction .....	128
6.2 UWB MIMO Antenna with Enhanced Bandwidth.....	128
6. 2.1. Antenna Design and Analysis .....	128
6.2.2 Deviations in the ground plane of presented antenna: .....	129
6.2.3 Surface Current circulation of the Ultra-Wide MIMO antenna.....	129
6.3. Experimental results and discussion .....	133
6.4 Summery .....	140
<b>CHAPTER 7 .....</b>	<b>144</b>
<b>Conclusion and Future scope .....</b>	<b>144</b>
7.1 Overview of research .....	144
7.2 Conclusions .....	147

7.3 Future work ..... 148  
PUBLICATIONS ..... 150  
REFERENCES ..... 152  
APPENDIX..... 182

## **DECLARATION BY THE SCHOLAR**

I hereby declare that the work which is being presented in this thesis entitled “**Design and Development of compact MIMO/diversity band-notched UWB antennas**” in fulfilment of the required for the degree of Doctor of Philosophy in electronics and communication engineering in the department of electronics and communication engineering of the Jaypee University of Information Technology, Waknaghat, Solan, Himachal Pradesh, India is an authentic record of my work carried out under the supervision of **Dr. Naveen Jaglan and Prof. Samir Dev Gupta**. I have not submitted this work elsewhere for any other degree or any other Institute/University.

**Ekta Thakur**

Enrolment No. 176001

Department of Electronics and Communication Engineering,

Jaypee University of Information Technology, Solan, India

Date: 26-08-2020



## JAYPEE UNIVERSITY OF INFORMATION TECHNOLOGY

(Established by H.P. State Legislative vide Act No. 14 of 2002)

P.O. Wagnaghat, Teh. Kandaghat, Distt. Solan - 173234 (H.P.) INDIA

Website: [www.juit.ac.in](http://www.juit.ac.in) Phone No. (91)01792-257999

Fax: +91-01792-245362

### SUPERVISOR'S CERTIFICATE

This is to certify that the work reported in the Ph.D. thesis entitled “**Design and Development of Compact MIMO/Diversity Band Notched UWB Antennas**”, submitted by **Ekta Thakur** in fulfillment of the requirement for the award of the degree of Doctor of Philosophy in Electronics and Communication Engineering and submitted in the Department of Electronics and Communication Engineering of **Jaypee University of Information Technology, HP, India**, is a bonafide record of her original work carried out under my supervision.

This work presented in this thesis has not been submitted elsewhere for any other degree or diploma.

**Dr. Naveen Jaglan**

**Assistant Professor**

Department of Electronics &

Communication Engineering

Jaypee University of Information

Technology,

Wagnaghat, H.P., India

**Prof. Samir Dev Gupta**

**Dean of Academics**

Department of Electronics &

Communication Engineering

Jaypee University of Information

Technology,

Wagnaghat, H.P., India

## ACKNOWLEDGEMENT

*“There is nothing noble in being superior to your fellow man; true nobility is being superior to your former self”*

*First of all, I express my sincere gratitude to my supervisors, **Prof. Samir Dev Gupta**, and **Dr. Naveen Jaglan**, Jaypee University of Information Technology (JUIT), Wahnaghat, Solan, for their guidance and encouragement. Their vast experience and deep understanding of the subject proved to be an immense help to me. My sincere thanks to Vice-Chancellor, and Head of Electronics and Communication Engineering (ECE) Department, JUIT, Solan for providing me all the needed support to complete the research work. I am sincerely thankful to my committee members, **Prof. Sunil Kumar Khah**, **Dr. Vikas Bhagal**, and **Dr. Nafis Khan** for their constructive feedback and comments that have helped me in improving my thesis. I also sincerely thank every member of the ECE Department and Administration of the JUIT, Solan, for their kind support. My special thanks to **Prof. B.K. Kanaujia**, JNU, Delhi, for providing encouragement and measurement facilities in his lab.*

*I give my greatest gratitude to my parents, who have been offering all-around support during the period of my studies and research. It is the tremendous blessings and endless sacrifice of my parents. They have shown immense patience and supported me in every possible way. I also thank my friends and lab-mates including **Dr. Ashutosh Sharma**, **Dr. Jyotsna Dogra**, **Dr. Prabhat Thakur**, **Dr. Amit Sharma**, **Charu Bhardwaj**, **Dr. Urvashi Shrama**, **Mahima Poonia** and **Kirti** for their encouragement and maintaining a stress-free environment. I would like to thank all those people from the core of my heart who made this thesis possible.*

*Thanks to all of you!*

*Ekta Thakur*

## LIST OF SYMBOLS

$\lambda_g$	Guided Wavelength inside substrate (mm)
$\Gamma$	Reflection coefficient
$\sigma$	Conductivity (S/m)
$\eta_{rad}$	Radiation efficiency
$\beta$	Bloch propagation constant
$c$	Speed of light in free space = $2.99792458 \times 10^8$ (m/s)
$C$	Capacitance(F)
$dB$	Decibel
$\epsilon_r$	Dielectric constant (Dimensionless)
$\epsilon_{eff}$	Effective dielectric constant (Dimensionless)
$\epsilon_0$	Permittivity of free space = $8.854 \times 10^{-12}$ (F/m)
$E$	Electric Field Strength (V/m)
$D$	Electric Flux density (C/m <sup>2</sup> )
$D$	Directivity
$f_r$	Resonance frequency (Hz)
$f$	Operating frequency (Hz)
$f_c$	Cut off frequency (Hz)
$G$	Gain
$GHz$	Gigahertz, (KHz)
$h$	Thickness of the substrate (mm)
$H$	Magnetic Field Strength (A/m)
$k$	Wave vector
$KHz$	Kilohertz, $10^3$ hertz
$N_r$	Number of receiving antennas
$N_t$	Number of transmitting antennas
$MHz$	Megahertz, $10^6$ hertz
$Q$	Quality factor
$R$	Resistance( $\Omega$ )

$S_{ij}$	Scattering matrix elements
$L$	Inductance (H)
$P_c$	Complex cross-correlation coefficient
$\rho_e$	Envelope correlation coefficient
$Tan(\delta)$	Dielectric loss tangent
$\mu$	Absolute permeability = $\mu_0 \cdot \mu_r$ (H/m)
$\mu_0$	Permeability of free space = $4\pi \times 10^{-7}$ (H/m)
$\omega_0$	Angular frequency = $2\pi f$ (rad/sec)
$Z_c$	Characteristic impedance ( $\Omega$ )
$Z_{in}$	Input Impedance ( $\Omega$ )
$G_t$	Gain of the transmitting antenna
$G_r$	Gain of the receiving antenna
$P_t$	Transmitted power
$P_r$	Received power
$\gamma$	Propagation Constant
$\alpha$	Attenuation Constant
$\beta$	Phase Constant
$\lambda_g$	Guided Waveguide
$\Gamma$	Reflection coefficient
$\sigma$	Conductivity

## LIST OF ABBREVIATIONS AND ACRONYMS

1-D	One Dimensional
2-D	Two Dimensional
3-D	Three Dimensional
3G	Third Generation
4G	Fourth Generation
5G	Five Generation
AMC	Artificial Magnetic Conductor
ARBW	Axial Ratio bandwidth
BW	Bandwidth
CPW	Co-Planar Waveguide
CRLH	Combined Right/Left Handed
CP	Circularly Polarized
CLL	Channel Capacity loss
CMT	Conventional Mushroom Shaped
DGS	Defected Ground Structure
DNG	Double Negative
DPS	Double Positive
DG	Diversity Gain
EBG	Electromagnetic Band Gap
ECC	Envelope Correlation Coefficient
EDG	Effective Diversity Gain
EIRP	Effective isotropic radiated power
ELV	Edge Located Via
EM	Electromagnetic

ENG	Epsilon Negative
EP	Ever Precision
IB	Impedance Bandwidth
ISM	Industrial, Scientific and Medical
IEEE	Institute of Electrical and Electronics Engineer
FBW	Fractional Bandwidth
FCC	Federal Communication Commission
FDTD	Finite Difference Time Domain
FEM	Finite Element Method
FR	Flame Retardant,
FSS	Frequency Selective Surface
GPS	Global Positioning System
GSM	Global System for Mobile Communications
HIS	High Impedance Surface
HFSS	High Frequency Structure Simulator
LHCP	Left Hand Circularly Polarized
LTE	Long Term Evolution
MIMO	Multiple Input Multiple Output
MISO	Single Input Single Output
MMIC	Monolithic Microwave Integrated Circuits
MNG	Mu Negative
MoM	Method of Moment
MPA	Microstrip Patch Antenna
MEG	Mean Effective Gain
MPA	Microstrip Patch Antenna
MSS	Mushroom Shaped Structure

PBC	Perfect Boundary Condition
PBG	Photonic Band Gap
PEC	Perfect Electric Conductor
PMC	Perfect Magnetic Conductors
PML	Perfect Matched Layer
RE	Radiation Efficiency
RF	Radio Frequency
RFID	Radio Frequency Identification Device
RHCP	Right Hand Circularly Polarized
RL	Return loss
SISO	Single Input Single Output
SIMO	Single Input Multiple Output
SM	Spatial multiplexing
SNG	Single Negative
SMA	Sub Miniature version A
SRR	Split Ring Resonator
TEM	Transverse Electromagnetic
TVC-EBG	Two Via Compact Electromagnetic Band Gap
TARC	Total Active Reflection Coefficient
UMTS	Universal Mobile Telecommunications System
UWB	Ultra-Wide Band
VSWR	Voltage Standing Wave Ratio
WiMAX	World Wide Interoperability for Microwave Access
WLAN	Wireless Local Area Network
XPR	Cross-Polarization Power Ratio

## LIST OF FIGURES

<b>Figure 1.1:</b> UWB system overlap with the narrowband system	3
<b>Figure 1.2:</b> Monopole Antenna	4
<b>Figure 1.3:</b> Various Planar configuration [9]	5
<b>Figure 1.4:</b> MIMO Antennas Configuration [15]	7
<b>Figure 2.1:</b> Monopole antenna [33]	16
<b>Figure 2.2:</b> Microstrip patch antenna with different feeds by (a) Microstrip feedline, (b) Proximity coupling, (c) aperture coupling [52]	18
<b>Figure 2.3:</b> MIMO Channel Model.	24
<b>Figure 2.4:</b> Different type of polarization [105]	29
<b>Figure 2.5:</b> Faraday rotation effect [110]	32
<b>Figure 2.6:</b> Various EBG unit cell geometries	37
<b>Figure 2.7 :</b> Different Analysis Methods for EBGs [165]	39
<b>Figure 2.8:</b> a) Band-notched UWB MIMO Antenna (b) VSWR Plot [179]	41
<b>Figure 2.9:</b> (a) Monopole UWB Antenna with triple band-notched (b) VSWR plot [180]	41
<b>Figure 2.10:</b> (a) Triple band-notched UWB MIMO Antenna (b) VSWR plot[183].	42
<b>Figure 2.11 :</b> ( a) Band-notched UWB Antenna (b) VSWR of triple band-notched UWB MIMO antenna [183]	42
<b>Figure 2.12:</b> (a) Pentagonal UWB monopole antenna (b) VSWR Plot [184].	43
<b>Figure 2.13:</b> layout MPA with Coaxial probe feed	46
<b>Figure 2.14:</b> Return loss of inset feed	46
<b>Figure 2.15:</b> Layout of MPA with inset feed	47
<b>Figure 2.16:</b> Return loss of MPA	48
<b>Figure 2.17:</b> Radiation curves of coaxial feed MPA	48
<b>Figure 2.18:</b> Radiation curves of inset feed MPA	49
<b>Figure 2.19</b> Return loss	49
<b>Figure 2.20:</b> MPA with Quarter wavelength feed	49
<b>Figure 2.21:</b> Radiation curve	50
<b>Figure 3.1:</b> Design of Ultra wideband antenna with three quarter wavelength slots	55
<b>Figure 3.2:</b> Stepwise expansion	56
<b>Figure 3.3:</b> Variation of different antenna structure	57

<b>Figure 3.4:</b> Variation of WiMAX Length	57
<b>Figure 3.5:</b> Variation of WLAN Length	58
<b>Figure 3.6 :</b> Variation of X Band Length	58
<b>Figure 3.7:</b> Extension of the metallic ground surface	59
<b>Figure 3.8:</b> Variation of mutual coupling in the different ground plane	59
<b>Figure 3.9:</b> Current distribution of the suggested antenna at notched frequencies	61
<b>Figure 3.10</b> a) Upper sight b) Foot sight of fabricated Suggested antenna	61
<b>Figure 3.11:</b> Photograph of the VSWR of the proposed antennas measured using a networ	62
<b>Figure 3.12:</b> Photograph of the mutual coupling of the proposed antennas measured using a network	63
<b>Figure 3.13</b> Measures and simulated VSWR	63
<b>Figure 3.14 :</b> Measures and simulated isolation	64
<b>Figure 3.15:</b> Photograph of the measurement of radiation pattern and gain in the anechoic chamber	65
<b>Figure 3.16:</b> Radiation plot of the suggested antenna (a) 3GHz (b) 5GHz and (c) 9.5GHz	66
<b>Figure 3.17:</b> Difference between measured and simulated of ECC and DG	66
<b>Figure 3.18 :</b> TARC variation with frequency	67
<b>Figure 3.19:</b> Radiation Efficiency plot of Suggested Antenna	68
<b>Figure 3.20:</b> MEGs of two Antenna elements	70
<b>Figure 3.21:</b> Deviation of Gain with frequency	70
<b>Figure 4.1 :</b> (a) Geometry of the TVC-EBG unit cell (b) Circuit model (c) of TVC-EBG unit cell	75
<b>Figure 4.2:</b> Extension of the TVC-EBG unit cell	76
<b>Figure 4.3 :</b> UWB MIMO structure with TVC-EBG cell	77
<b>Figure 4.4 :</b> VSWR of the presented structure	79
<b>Figure 4.5:</b> a) Upper sight b) Foot sight	80
<b>Figure 4.6 :</b> Measurement set up for proposed dual notch fabricated prototype antenna in anechoic chamber	81
<b>Figure 4.7 :</b> VSWR of the fabricated prototype	81
<b>Figure 4.8:</b> Mutual couplings of the presented structure	82
<b>Figure 4.9:</b> Radiation plots of the presented structure (a) 3 GHz (b) 5 GHz and (c) 10 GHz	83
<b>Figure 4.10 :</b> ECC and DG with frequency	84

<b>Figure 4.11:</b> Variation of TARC with frequency	84
<b>Figure 4.12 :</b> Deviation of gain and radiation efficiency	85
<b>Figure 4.13 :</b> Layout of 4 element suggested antenna	89
<b>Figure 4.14 :</b> Transmission line over modified EBG structure	89
<b>Figure 4.15:</b> Transmission coefficient for modified EBG structure	90
<b>Figure 4.16 :</b> Equivalent circuit Model	91
<b>Figure 4.17 :</b> Prototype of proposed four element UWB MIMO antenna	92
<b>Figure 4.18:</b> Deviation of VSWR with frequency	92
<b>Figure 4.19:</b> Variation of VSWR with the frequency of different port	93
<b>Figure 4.20 :</b> Variation of Measured VSWR	93
<b>Figure 4.21 :</b> Deviation of mutual coupling with frequency	94
<b>Figure 4.22 :</b> Variation of mutual coupling with frequency	95
<b>Figure 4.23 :</b> Normalized radiation plot at (a) 4 GHz (b) 6.3 GHz and (c) 7.6 GHz	97
<b>Figure 4.24 :</b> Deviation of gain with frequency	98
<b>Figure 4.25 :</b> Deviation of ECC and DG with frequency	100
<b>Figure 4.26 :</b> Deviation of TARC	100
<b>Figure 4.27 :</b> Deviation of MEG	101
<b>Figure 5.1:</b> Suggested UWB antenna with enhanced bandwidth	105
<b>Figure 5.2:</b> (a) Uppermost view, (b) foot view	106
<b>Figure 5.3:</b> Tested and simulated VSWR	107
<b>Figure 5.4:</b> Tested and simulated axial ratio.	107
<b>Figure 5.5:</b> Variation of VSWR for different ring slot width	109
<b>Figure 5.6:</b> Deviation of Axial ratio for different ring slot width.	109
<b>Figure 5.7:</b> Deviation of VSWR for dissimilar ground slot length ( $S_1$ )	110
<b>Figure 5.8:</b> Deviation of Axial ratio for dissimilar ground slot length ( $S_1$ ).	110
<b>Figure 5.9:</b> Deviation of VSWR for dissimilar the length of the slot ( $S_3$ )	110
<b>Figure 5.10:</b> Deviation of Axial Ratio for dissimilar the length of the slot ( $S_3$ )	111
<b>Figure 5.11.:</b> Deviation of VSWR for dissimilar ground slot length ( $S_4$ )	111
<b>Figure 5.12 :</b> Deviation of Axial ratio for dissimilar ground slot length ( $S_4$ )	112
<b>Figure 5.13:</b> Current density at 6 GHz with the dissimilar phase of $0^\circ$ , $90^\circ$ , $180^\circ$ , and $270^\circ$ .	112

<b>Figure 5.14:</b> Radiation plot (a) E -plane and (b) H-plane at 5 GHz c) E-plane and (d) H-plane at 7 GHz	113
<b>Figure 5.15:</b> The plot of radiation efficiency	113
<b>Figure 5.16:</b> The plot of radiation efficiency and Gain	114
<b>Figure 5.17:</b> Layout of the triple band-notched CP UWB antenna	115
<b>Figure 5.18:</b> Stepwise expansion of the presented antenna.	117
<b>Figure 5.19:</b> Axial ratio of different stages of the presented antenna.	117
<b>Figure 5.20:</b> VSWR of different stages of triple band-notched CP UWB antenna.	118
<b>Figure 5.21:</b> Geometric layout of the presented structure	118
<b>Figure 5.22:</b> Prototype of the made-up structure	120
<b>Figure 5.23:</b> Simulated surface currents with when port 1 is excited	121
<b>Figure 5.24:</b> Simulated surface currents with when port 2 is excited	122
<b>Figure 5.25:</b> VSWR of the presented structure.	
<b>Figure 5.26:</b> A R of the presented structure	123
<b>Figure 5.27:</b> Measured and simulated Mutual coupling of the band notched CP UWB MIMO antenna	124
<b>Figure 5.28:</b> Tested and Simulated radiation plot with port 1 excitation (a) E-plane plot at 5 GHz (b) H-plane plot at 5 GHz c) E-plane plot at 7 GHz (d) H-plane plot at 7 GHz	125
<b>Figure 5.29:</b> Measured and simulated ECC and DG	125
<b>Figure 6.1:</b> Layout of the presented antenna	130
<b>Figure 6.2.</b> Extension of the presented antenna	130
<b>Figure 6.3:</b> Deviation of the ground plane	131
<b>Figure 6.4:</b> Circulation of the surface current on the presented structure	132
<b>Figure 6.5:</b> (a) Topmost vision, (b) foot vision of the made-up presented structure.	132
<b>Figure 6.6:</b> Measures and simulated VSWR	133
<b>Figure 6.7:</b> Measures and simulated Mutual coupling	133
<b>Figure 6.8:</b> Measurement set up for proposed dual notch fabricated prototype antenna in the anechoic chamber	134
<b>Figure 6.9.:</b> Difference between the measured and simulated radiation plot at for dissimilar frequencies	136
<b>Figure 6.10:</b> Measured and simulated deviation of ECC and DG	137
<b>Figure 6.11:</b> Deviation of TARC vs frequency	138

<b>Figure 6.12:</b> MEGs of the presented system.	138
<b>Figure 6.13:</b> Deviation of CCL vs frequency	139
<b>Figure 6.14:</b> Graph of radiation efficiency and Gain	139

## LIST OF TABLE

<b>Table 2.1:</b> Parameters of inset feed MPA Design	44
<b>Table 2.2:</b> Parameters of Coaxial feed MPA Design	45
<b>Table 2.3:</b> Parameters of Quarter wavelength feed MPA Design	47
<b>Table 2.4:</b> Comparison of numerous feeding methods	50
<b>Table 3.1:</b> Augmented dimensions of the Ultra-Wideband antenna	54
<b>Table 3.2 :</b> Evaluation of designed Antenna with existing antenna design	69
<b>Table 4.1 :</b> Augmented dimensions of the presented antenna	78
<b>Table 4.2 :</b> Assessment of suggested EBG unit cell Designs	86
<b>Table 4.3 :</b> Evaluation of Proposed structure with different antenna	87
<b>Table 4.4 :</b> Parameters of four element UWB MIMO Antenna	90
<b>Table 4.5 :</b> Evaluation of proposed antenna with the existing structure	99
<b>Table 5.1.:</b> Dimensions of Suggested Antenna	108
<b>Table 5.2:</b> Performance comparison of the suggested antenna	114
<b>Table 5.3.:</b> Optimized dimension of the proposed antenna	116
<b>Table 5.4 :</b> Circularly Polarized UWB MIMO Antenna Dimension	119
<b>Table 5.5:</b> Evaluation of presented antenna with dissimilar antenna	126
<b>Table 6.1:</b> Optimized size of the Ultra-Wide MIMO antenna with enhanced bandwidth	129
<b>Table 6.2:</b> Evaluation of the presented structure with present work	141

## ABSTRACT

The allocation of 7.5 GHz of bandwidth by the Federal Communication Commission (FCC) for Ultra-Wideband (UWB) applications has provided an exciting and challenging opportunity to design short-range wireless communication. To fully realize the potential of the UWB system, wireless communication systems are required to operate on the entire UWB frequency band. The combination of the wide bandwidth requirement and the target application of the UWB systems have led to a surge of interest in designing of novel integrated circuits and antennas for the UWB applications. In any communication system like Radio Frequency Identification system, the antenna has a fundamental influence on the system enactment, and as a result, it has attracted considerable research interest. Significant analysis has been prepared in the usage of UWB schemes from the time when the FCC unconstrained the BW 3.1-10.6 GHz. Many narrowband applications also function in this range of 3.1-10.6 GHz. To avoid possible interventions with these narrowband systems it is desired to propose a UWB system with band rejection features. Another biggest challenge for wireless communication systems is the polarization mismatch loss amid the transmitting and receiving antenna. To overcome the polarization mismatch loss and multiple path interference it is essential to propose an antenna with Circular Polarization (CP) features. In conventional narrow-band communications, MIMO techniques compromise attractive features in the communication system. These MIMO techniques help in achieving great channel capacity using spatial multiplexing or provide a rise of link toughness. Mutual Coupling (MC) is the major concern in MIMO antenna when located on the identical PCB, Isolation is one of the significant factors to contemplate while simulating MIMO antennas. Mutual coupling among the antenna elements affecting the MIMO performance, in terms of radiation plots, the return loss, and -10dB bandwidth. Furthermore; it reduces the antenna efficiency and directivity. This thesis emphasizes the UWB MIMO antennas that are suitable for various wireless communication systems. Different planar antennas are fed with Microstrip feed line are presented in this work. Firstly, twisted quarter wavelength slots are used to achieve band rejection features with a reduction in antenna dimensions. The designed band-notched UWB MIMO antenna can be used in medical imaging etc. Measurement and simulation results indicate that antenna achieves input impedance matching in a bandwidth of more

than 7.5 GHz with band notch characteristics. Secondly, the two MIMO antennas are designed to work for Radio identification system applications. TVC EBG Structure is used to avoid intrusion due to narrowband communication systems. Thirdly, two circularly polarized UWB antennas are designed. To avoid interference band notch characteristics are achieved using TVC EBG Structure. Finally, the enhanced bandwidth UWB MIMO antenna is designed to operate for various applications. The details of the system used are: **Intel(R) Core(TM) i-5 2450M CPU @ 2.50GHz, 4 GB RAM.** Simulations are performed using **Ansoft HFSS v.14**, and **Matlab R 2013**. The fabrication machine is prepared through the **EP 2006 PCB Prototype machine**. The S Parameters of fabricated antennas are tested using **Rohde and Schwarz ZVL Vector Network Analyzer**. The layout used in antenna fabrication is prepared using **AutoCAD 2013**. Microwave shielded **Anechoic chamber** is used for far-field measurements.

# **CHAPTER 1**

## **INTRODUCTION**

# CHAPTER 1

## Introduction

### 1.1 Introduction

In wireless communication technology, tremendous growth has been seen in the past two decades. In reality, the growth in the wireless system provided new applications to consumers and become a part of our everyday life. In wireless communication devices ‘antennas’ are the spine with which the technology reached this point. As per IEEE Standard, antennas can be well-defined as “a means for radiating and receiving electromagnetic waves” [1]. So, the growing propensity of wireless devices considerably demands compact size, cost-effective, and low profile without compromising its performance [2].

Firstly, this chapter deliberates the UWB technology, followed by the vital of planar monopole antenna and multiple input multi-output antennas. In this chapter, the description of the encouragement behind the research work is also presented.

### 1.2 UWB Technology

In April 2002, the FCC allocated the unrestricted 3.1-10.6 GHz band for commercialized use. Ultra-wideband technology earlier known as ‘impulse radio’ that can revolutionize the prevalent communication systems. UWB technology transmits data over a wide range of frequencies using -41.3dBm/MHz power density and very short duration pulses. Since this technology offers a very high-speed therefore it is another to an existing wireless system for example WLAN, Hiper LAN. Therefore, the UWB system has fascinated the abundant attention of the researcher and has turn out to be the main center of research in industrial and academic. The channel capacity or the maximum achievable data rate can be related to the bandwidth and the SNR ratio by using the Shannon-Nyquist criterion [3]. Therefore, channel capacity is defined as the sum of information transmitted bits per second over a transmission channel and expressed as [4]:

$$C = B \log_2 (1 + SNR), \quad (1.1)$$

Where  $C$  is the transmission data rate,  $B$  is bandwidth and  $SNR$  is referred to as signal to noise ratio. The equation illustrates that the transmission data rate is linearly proportional to bandwidth. This equation suggests that capacity can be increase quickly by varying the BW than  $SNR$ . Another important term for the UWB transmitter is and it is well-defined as the multiplications of its gain and power. According to the FCC regulations EIRP emission level is set to  $-41.3\text{dBm/MHz}$  all over the entire UWB band. For legal operation, UWB systems must work within the specified spectral mask to fulfill FCC standards and regulations [5].

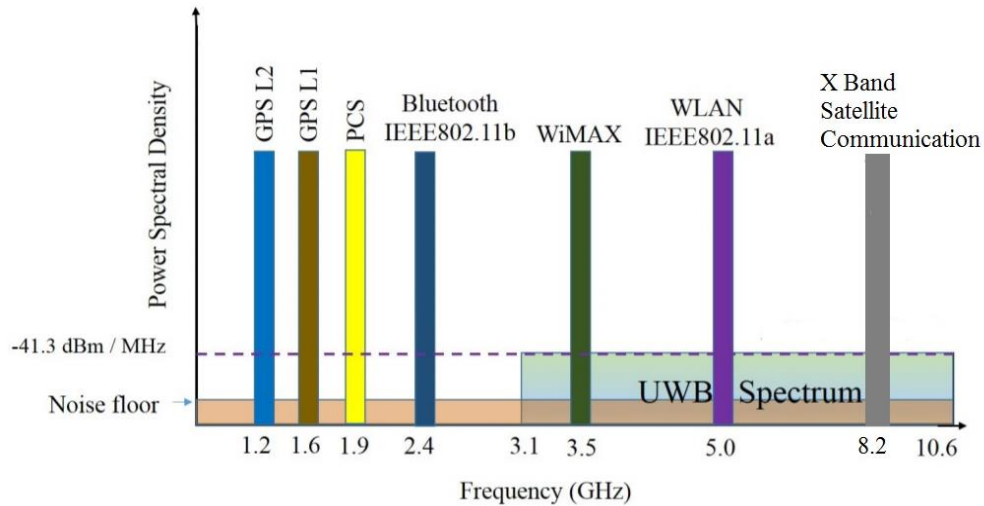


**Figure 1.1:** UWB system overlap with the narrowband system

In comparison to narrowband systems, the spectrum of the UWB system is larger in terms of bandwidth and emitted power. The band assigned by FCC constitutes a bandwidth of 7.5 GHz which is 110% fractional bandwidth. The UWB signals occupy larger bandwidth where the energy of radio frequency spreads over the entire band. The maximum power available to the antenna will be 0.556 mW when the overall band allocated by FCC is fully employed. In contrast to other radio communication systems, the UWB transmission has very low power and high sensitivity. Thus, the UWB system has great data rates for short-range communications systems and fewer data rates for mid-range communications. Ultra-wideband system has many assistances such as high data rate, less power intake, cheap, immunity to multipath intrusion. UWB signal offers a carrier-free transmission because it uses whole frequency as carrier frequency, this suppers the requirement of extra RF mixers.

Therefore, the entire UWB system can be incorporated with a single CMOS which consequently results in low cost, low complexity, low power, and small size. In multi-path surroundings, the transmitted signal arrives at the receiver via different paths and the signal gets distorted. UWB uses short-duration pulses for transmission that provides a resolution to distorted pulses at the receiver. Therefore, UWB communications can resolve numerous paths and provides multipath diversity. Because of the aforesaid advantages, UWB technology has enormous indoor applications transmitting at Mbps to several Gbps within a space of 20 meters as WPANs and USB connectivity another major application is Wireless Sensor Network (WSN) useful in medical and tracking applications [6].

### 1.3 Monopole Antenna

In UWB communication technology, one of the major problems is the design of a compact, modest, and multifunctional antenna. In this segment, the basics of the monopole antenna that can be used for UWB applications will be explained. When half i.e one arm of the dipole is substituted by an infinite ground plane monopole antenna came into the picture as shown in Figure 1.2. It is defined as a thin wire of length  $L$  mounted above the infinite ground plane. When the antenna is positioned beyond a metallic ground surface it acts as a dipole due to reflections, meanwhile, the ground surface behaves like an electric mirror. The fields of the antenna and dipole antenna above the ground plane will be similar. The monopole antenna has zero radiation below the ground plane. The monopole antennas are suitable to match 50 ohms and are unbalanced [7]. Hence, it is convenient to be connected to feed at one side and grounded to the outer shield.

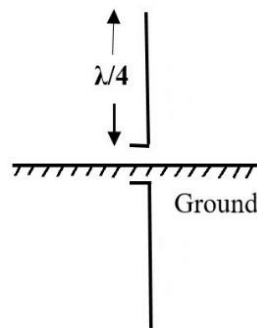


**Figure 1.2:** Monopole Antenna

Modern and future communication system demands antenna for multiband and broadband operations with low cost and desired performance. The antennas were formed by substituting the wire elements of the traditional antenna with the planar element. They have enormous advantages, for instance, planar structure, low fabrication cost, small volume, low profile, and easy integration due to which they are significantly suitable for various wireless applications. A different planar configuration such as circular, elliptical, rectangular, and triangular [8] as shown in Figure1.3 have been studied, this configuration in comparison to conventional monopole increases the surface area which in turn has a direct impact on bandwidth.

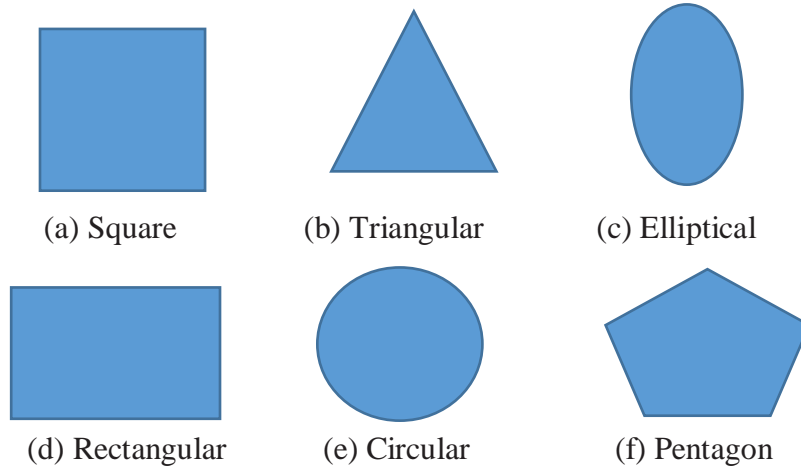


**Figure1.3:** Various Planar configuration [9]

Planar monopole antennas are modified form of microstrip antenna but conventional Microstrip antenna has narrow bandwidth due to its resonant nature while planar monopoles have broad bandwidth. But, by modifying the antenna structure two or more resonant overlaps broadband bandwidth performance [10]. Thus, the microstrip antenna is required to be modified to support the multi-resonance. However, the BW of the antenna can also be better by using a thicker substrate but this approach is limited. Moreover, many other techniques, for example, the use of an asymmetrical feeding, slanting plate, a double feeding arrangement, or by amending the gapping among the radiator and ground surface are also available in the literature to enhance the performance of Microstrip planar antenna in terms of operating

frequency, BW and radiation pattern[11]. The planar monopoles have enormous advantages, such as easy integration into planar circuits and low manufacturing cost. Therefore, planar monopole antennas have been extensively employed in the wireless communication system

## **1.4 Multiple Antennas**

The new generation of wireless communication systems requires high-speed data rates with a low error rate and increase channel capacity and conventional wireless systems are unable to meet this requirement due to multipath fading and co-channel interference [12]. When the signal at the receiver is received via multiple paths then the signal gets faded which is known as multipath fading. Another term is co-channel interference and it is defined as the intrusion produced by dissimilar signals consuming identical frequency. Later, to improve quality and channel capacity multiple antennas have to be employed. The basic concept to increase channel capacity is to equip multiple antennas either in the transmitter/receiver or both of them [13]. Therefore, there was an emergent interest in the development of codes and techniques for multiple antennas. In 1987, a diversity antenna technique for radio communication in which he used  $M$  number of transmitting receiving antennas to study the fundamental limits on the data rate of multiple antenna systems in a Rayleigh fading environment. The main focus was to employ an equal number of antenna array elements at both sides to improve the channel capacity. MIMO is a smart antenna technology for the current wireless communication system [14]. It has been evidenced to be one of the finest methods for the enhancement in channel capacity without the requirement of additional bandwidth and power. The employment of multiple antennas on both the transmitter and receiver leads to MIMO systems. They can be characterized by various:

MIMO is the arrangement of several antenna systems for example SISO, SIMO, and MISO.

SISO is a conformist system where the transmitter and receiver have one element.

SIMO this formation has only transmitter elements and multiple receiver elements.

MISO has many transmitter elements and only the receiver element.

MIMO has many transmitter elements and receiver elements.

## 1.5 Motivation for the Present Research

Over the past few years, the advancements in UWB technology have greatly improved the interest in the UWB antenna due to miniaturization with a high frequency of operation. Therefore, there is a huge demand for devices having a compact structure and low cost. This has induced the need for small size antennas that has to be well-matched with various wireless devices. The diversity techniques are employed to cater to the growing demand for wireless communication systems with an increased data rate. Diversity systems spread an identical amount of power using different antennas at either side of the system thus increases the capacity without the requirement of extra power. Dimensions of the antenna element are significant concerns in the design of diversity antenna as the space for antenna integration is limited in portable devices such as PCs and mobile devices. For an efficient diversity antenna system isolation among the antennas element that is located close to each other should be as low as possible throughout the entire operating band. These design issues and required features for achieving miniaturization with enhanced bandwidth serves as motivation to the authors. This thesis work encourages the design of UWB antennas to meet some of these challenging demands. Therefore, this thesis aims to investigate the UWB technology with monopole antenna and MIMO antennas in detail.

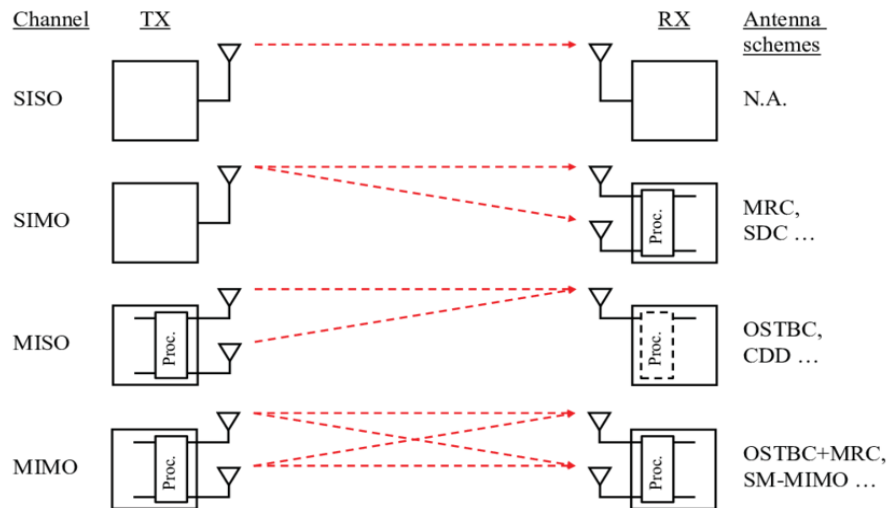


**Figure 1.4:** MIMO Antennas Configuration [15]

## **1.6 Challenges in antenna design**

The modern wireless system has met numerous important expansions in current years. Though, several challenges in creating this system to its complete potential out of which antennas design are the major challenge. In antenna design, the major challenge is to design an antenna that covers the whole band approved by FCC. A recent trend in wireless technology demands a miniaturized UWB MIMO antenna to be companionable with wireless devices. As devices shortly are going to be more compact and the space for antenna integration is also reducing, the antennas must be placed more closely in limited space. But the reduction in the size of the antenna will affect its radiation characteristics. Another challenge in the UWB antenna design is electromagnetic interference due to the coexistence of narrowband systems such as WIMAX/C-band with the center frequency at 3.5GHz, WLAN the center frequency at 5.5GHz, and X Band Satellite communication system the center frequency at 8.6 GHz that lies within UWB range. The narrowband antennas are highly efficient as they are used for long-range applications whereas the UWB antennas are not that efficient since they are used for short-range applications. Therefore, the impact of interference of the UWB spectrum with that narrowband is an important issue and has to be eliminated. Further, the expansion of UWB-MIMO antenna systems adds extra difficulty in antenna design. The designs of the MIMO antenna system are provoked with similar design constraints as that of a single antenna with additional challenges of isolation, the correlation between radiation patterns, and diversity gain. Mutual coupling between antennas in a space-limited device is of major concern where antennas are located nearby. As it not only disturbs the antenna performance but also impacts the envelop correlation. Another difficult task that occurs during the designing of a MIMO antenna is the concurrent enhancement of isolation and impedance bandwidth.

## **1.7 Research Problem Statement**

With the advent and escalating growth of ultra-wideband systems, wideband antennas find increasing applications in short-range communication. The compact size and interference from existing narrowband communication systems are major challenges to the UWB antenna design.

1. Overlapping of the UWB spectrum with the wireless narrowband communication system. To avoid the interference between the Ultra-wideband (3.1 -10.6 GHz) with a narrow-band application, for example, WiMAX, WLAN, and X band satellite communication band which cause. As a result, the UWB antenna with a band-rejection feature is mandatory.
  2. To reduce radiation losses due to perturbation on the patch to attain the band notch features. To resolve this problem, the EBG structure is used by placing near the feed line of the proposed antenna structure.
  3. Another major challenge for wireless communication systems is the polarization mismatch loss between the transmitter and the receiver. Therefore, a circularly polarized Ultra Wide Band MIMO antenna with frequencies-rejection features is required to eliminate the necessity to align the orientation of the receiver and transmitter.
  4. To operate various applications such as GPS, GSM, ISM, and Bluetooth using a single UWB antenna, Therefore, an improved bandwidth UWB MIMO antenna is necessary.
- This thesis aims to contribute towards the research of UWB MIMO antenna structure combined with EBG structures.

## **1.8 Objectives**

To fulfill the requirement of UWB wireless gadgets, the antenna design must be compact with multi-operational characteristics. This research has identified the following objectives for the study and development of band rejected UWB MIMO antennas;

### **Objective I.**

*To design a miniaturized notched UWB MIMO Antenna using] quarter wavelength slots*

### **Objectives II.**

*To design a compact band-rejected UWB MIMO antenna with TVC-EBG structure*

### **Objectives III.**

*To design, a miniaturized band rejected Circularly Polarized Ultra Wide Band MIMO Antenna.*

### **Objectives IV.**

*To design a miniaturized UWB MIMO antenna with Enhanced Bandwidth.*

## **1.9 Thesis organization**

The research accomplished in this work is organized in the following seven chapters:

Chapter 1: This chapter delivers the introduction of the thesis. In this, a brief description of UWB technology, the stimulus behind the research work, and thesis arrangement are presented.

Chapter 2: This chapter discusses the state-of-art of the present work. In this, a literature review on UWB technology, planar monopole antennas, and band rejected UWB antennas for wideband applications are presented and summarized.

Chapter 3: Band rejected UWB MIMO antenna is introduced in this chapter. The presented antenna rejects the WiMAX/C Band, WLAN, and X Band system. The parameters analysis and MIMO performance parameters were comprehensively studied. The ultra-wideband characteristic of the suggested antenna is evaluated in terms of VSWR, gain, and radiation efficiency, and radiation patterns; validated by both simulations and measurements. The designed antenna has a compact size and simple structure as compared to the previously reported antennas.

Chapter 4: A diminished band rejected UWB MIMO antenna using a Two via compact (TVC-EBG) structure is investigated In this chapter. The TVC EBG structure is designed and studied based on obtained band rejection in the UWB MIMO antenna. The working mechanism of mushroom type EBG structure is described by LC Model and transmission method. This chapter introduces the design of triple band-notched UWB MIMO for Radio Frequency Identification systems, radio altimeters, and radar applications.

Chapter 5: In this chapter, the miniaturized circularly polarized UWB MIMO antenna is presented. The suggested antenna utilizes a TVC-EBG structure to attain band-notched characteristics with wide axial ratio bandwidth. The proposed antenna rejects a narrowband system that intrusion in the UWB range.

Chapter 6: In this chapter, the enhanced bandwidth UWB MIMO antenna is introduced. The MIMO antenna has a small dimension and provides good impedance bandwidth of 1-30 GHz. This antenna is designed to access various applications like GSM/UMTS, GPS, ISM WLAN/Wi-Fi, radio applications, UWB communication, radio astronomy, and 5G.

Chapter 7: In this chapter, the overall work supported out in this thesis is summarized and the scope for future research is also suggested and sketched. The outcome of the present research work (i.e. published papers) embodied in this thesis is also listed.

## **1.10 Summary**

A brief overview was presented on the UWB system followed by a planar monopole antenna and MIMO antennas in this chapter. This chapter also summarizes the motivation and the challenges behind the present research. This chapter delivers a comprehensive sketch of the thesis in an inclusive style. After acquainted with the fundamentals of UWB monopole antennas and multiple antennas, a brief historical review will be carried out in the next chapter.

**CHAPTER 2**  
**LITERATURE**  
**REVIEW**

## **CHAPTER 2**

### **Literature Review**

#### **2.1 UWB Background**

UWB technologies are different from all different communication strategies as it works very narrow radio frequency impulse to speak among transmitters and receivers. Employing short-duration impulse as the structure blocks for communications without delay produces a very extensive bandwidth and deals with numerous advantages, for example, great throughput, concealment, toughness to congestion, and existence with contemporary radio offerings. UWB technology is no longer a novel tool; actually, it used to be first worked by Marconi in 1901 to send Morse code series means of the spark-gap radio device. Though, the advantage of a wide BW and the functionality of performing multiple-user schemes delivered by EM pulses were in no way regarded at that point. Around some years afterward, Marconi worked on the modern-day pulse-based transmission that comes into existence in the form of impulse radars. The current expansion in micro handling and quick substituting in semiconductor science has made UWB prepared for industrial applications. So, it is extra suitable for a long-existing communication system. As concern in the commercial of UWB has improved above the previous several years, builders of UWB structures started out forcing the FCC to accept UWB for profitable use. In April 2002, the FCC authorized for industrial use of UWB science below strict strength emission limits for several devices.

The concept of electromagnetic wave radiation in space was proved by the experimentation led by Heinrich Rudolf Hertz in the year 1888 [16]. Jagdish Chandra Bose an Indian Physicist in 1897 confirmed a whole transmitter and receiver systems communicating in the millimeter-wave spectrum at around 60 GHz [17]. He has used cylindrical horn antennas to achieve wireless connectivity. The concept of monopole antenna was brought up by Sir Oliver Lodge in the year 1889 [18]. He has invented the bow tie and bi-conical antenna. Thereafter with the practical realization of the radio system by Marconi using the fan and conical monopole antennas with enhanced radiation power to achieve long-range communication [19], the use of the UWB antenna system has slowly moved towards narrowband systems [20]. After 1933

when Edwin Armstrong invented the wideband frequency modulation system and the Television was invented, the old narrowband amplitude modulation systems are slowly replaced by the wideband system. Thereafter the wideband technology has drawn much attention in the mind of researchers. The first tapered feed mechanism connected to a bi-conical antenna was used by carter in the year 1939 [21]. He was the first person to incorporate a broadband transition between a feed line and the radiating element. This lead to a revolution in antenna technology in designing bulky three-dimensional structures like horn antennas, log-periodic antennas, spiral antennas, etc. [22]. These broadband antennas were prone to dispersion and not suitable for UWB applications [23]. Although the footprints of the planar antennas were seen in the 1950s the appreciable growth in the microstrip based planar antenna designs were observed after the FCC declassified the UWB spectrum for commercial applications in 2002.

The FCC releases 7.5 GHz bandwidth for ultra-wideband communication systems. Development in UWB technology is enhanced due to the FCC's definition of a spectral mask, to allow operation of UWB radios at the noise floor across a wide spectrum. UWB is adopted for short-range communication with EIRP less than -41.3 dBm/MHz [24]. This allocation has stimulated antenna designers to look for challenging designs for low-cost UWB antennas. The UWB systems attractive because of benefits for example large channel capacity, low power consumption, the capability to operate with low SNR ratio, jamming, and low cost. The main factor that discriminates the UWB antennas from the other antennas is its impedance bandwidth. Therefore, the absolute bandwidth of the UWB antennas should be larger than 500 MHz [25]. Here fractional bandwidth is given as:

$$FB = 2 \left( \frac{f_h - f_l}{f_h + f_l} \right) \quad (2.1)$$

where  $f_h$  is the upper -10dB cut off frequency and  $f_l$  is the lower -10dB cut off frequency. Antenna plays a vital role in wireless communication systems. As a significant part of the UWB technology, the UWB system must be compact and have large impedance bandwidth. The ever-developing UWB system and the short-range civil applications, working in the from 3.1–10.6 GHz created the demand for a compact transmitter and receiver module. The size of the transmitter and receiver can be made compact by the small size of the antenna [26]. In this

perspective, it has become essential to study the electrical characteristics and radiation pattern of small, compact, and low profile UWB antenna [27]. The effective antenna size, operating frequency, and -10 dB bandwidth decide its wireless application. Compact antenna design for UWB applications still faces a problem of interference from the existing narrowband wireless communication systems.

## 2.2 Monopole Antennas

The most popular antennas such as the dipole, patch antenna, and monopole antenna are engaged in current wireless communication systems. A monopole antenna usually comprises a vertical wire, tube, or helical whip which is mounted perpendicularly on a conducting surface called a ground plane (e.g. earth ground)[28]. The first monopole was invented by Guglielmo Marconi, an Italian inventor, and engineer in 1895 [29]. Incorporating the earlier work of Heinrich R. Hertz, he attained a propagation space of 2.5 km by using both Marconi transmitter and Marconi receiver [5] and in 1901 he successfully sent wireless signals across the Atlantic Ocean between Poldhu (see Figure 2.1), Cornwall, England, and St. John's, Newfoundland, USA, a space of 2100 miles [30].

A monopole antenna can be considered as having a dipole like radiation pattern as the reflected wave from the ground plane seems to be generated from its image (image theory [31]) under the ground plane surface which can be identified as the missing half of the equivalent dipole. Figure 2.2 shows the monopole antenna on a ground plane compared with an equivalent dipole. Same as dipole antennas, the dimension of a monopole antenna is a function of the wavelength of its resonant frequency with is typically around  $\lambda/4$ . A  $\lambda/4$  monopole placed on a very big ground surface has the same field expressions as those of a  $\lambda/2$  dipole. The radiation plot of the monopole is related to a dipole but is only present on the hemisphere overhead the ground, which is half the space a dipole antenna can radiate in. As a result, the gain of a monopole antenna will be double the gain of an alike dipole antenna. Furthermore, its radiation resistance will be half that of a dipole [32]. However, in practice, monopoles employ finite ground plane sizes and the radiation pattern is dependent on this size and shape. Ideally, a ground plane should be better as compared to the quarter wavelength around the monopole base. An electrically small ground plane will cause the maximum

radiation pattern direction. to shift to higher elevation angles. Generally, as the dimension of the ground surface increases towards infinity, the point of view of concentrated radiation will be closer to the horizontal plane (ground plane). Monopole antennas exhibit wide -10dB bandwidths that can be prolonged by varying the diameter of the structure. [33].

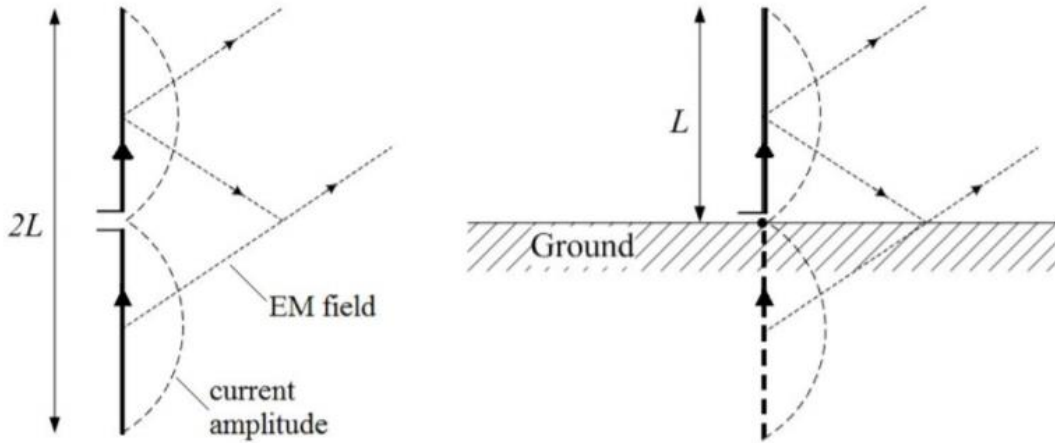


**Figure 2.1:** Monopole antenna [33]

As they have completely omnidirectional radiation patterns, vertical monopoles are extensively used for omnidirectional radio communications, such as radio broadcast and base-station antennas in mobile communications. Besides, vertically-polarized waves propagate with less loss close to the surface of the earth as the electric field of a horizontally-polarized wave becomes short-circuited because of the conductivity of the earth [34].

### 2.2.1 Feeding Techniques

Various techniques are used to feed the radiating elements. It can be broadly categorized into contacting and non-contacting methods. In the contacting technique, a stripline is used to straighten feed the metallic patch with RF power. In the non-contacting method, the process of em coupling is used to deliver power to a radiating patch of the microstrip antenna [35-40].

#### 2.2.1.1 Microstrip Line

This is a contacting method to feed the antenna element. A narrow stripe is straight connected to the end patch. The dimension of the metallic stripe is small as compared to the microstrip patch. This gives the advantage of attaining a planar structure as the strip can be inserted on

the identical surface where the patch is present. The small square is cut in the patch to adjust the characteristic impedance of feed to input impedance the patch lacking the use of any extra circuit [41]. So the location of the inset cut be adjusted accordingly

#### **Advantages**

- Planar structure.
- No additional matching circuit is required so its design is simple.
- Ease of fabrication.

#### 2.2.1.2 Coaxial Probe

It is a form of a contacting method as the power delivered is via direct connection with the microstrip patch. It consists of two interior and exterior conductors. The interior conducting wire of the SMA connector prolongs by the substrate and gets connected to the patch plane. The exterior conductor on the former side connects the ground [42-45].

#### **Advantages**

- The coaxial conductor can be placed anywhere inside the microstrip patch to match the impedance patch.
- Easy to fabricate.
- Low spurious radiations

#### **Disadvantages**

- Modeling is difficult as a hole must be punctured into the substrate and the SMA connector prolongs from the ground surface, thereby making the structure nonplanar for heavy substrates narrow bandwidth.
- In the case of thicker substrates, the matching problem takes place due to an increase in the length of the probe which makes input impedance more inductive.

#### 2.2.1.3 Aperture Coupling

This is a non-contacting method of feeding which involves the usage of two substrates which are disconnected by the ground surface. A slit is removed on the ground surface to deliver coupling amid the patch and feed line. The dimension, location, and shape of the slot indicate the amount of coupling between the two. To get optimum radiations, the less permittivity

value is used for the upper substrate and the high permittivity value is used for the bottom surface [45-50]

### Advantages

- The symmetry of configuration is acquired in the existence of a coupling slot under the microstrip antenna which limits lower cross-polarization.
- In the manifestation of the ground plane between the two substrates, spurious radiations are reduced

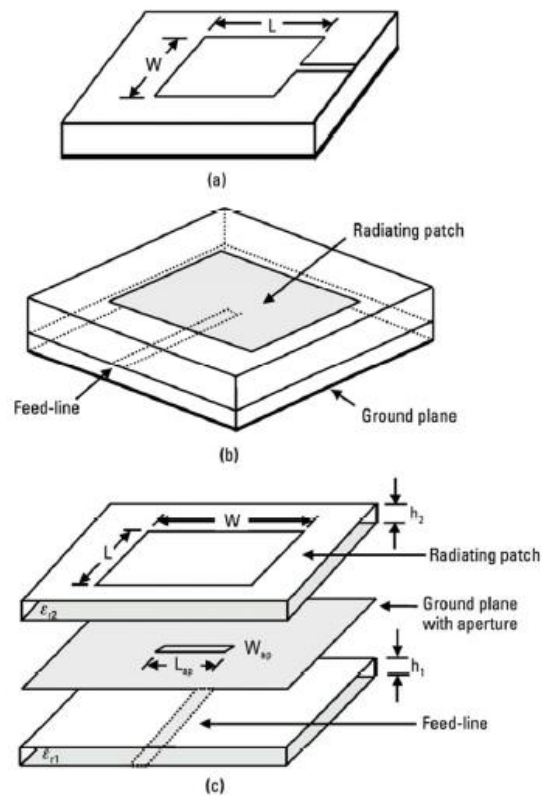


**Figure 2.2:** Microstrip patch antenna with different feeds by (a) Microstrip feedline, (b) Proximity coupling, (c) aperture coupling [52]

### Disadvantages

- Multiple layers lead to an increase in thickness.
- Fabrication is difficult and narrow bandwidth

#### 2.2.1.4 Proximity Coupling

This is also known as the electromagnetic coupling method and is a non-contacting type. In this method, two substrates are placed one above another where a strip line amid them, and the upper dielectric contains the patch. Impedance matching is attained by governing by varying the measurements of length and width of the feed line [51-53].

##### **Advantages**

- High bandwidth.
- No spurious feed radiation because of the thinness of the substrate.

##### **Disadvantages**

- Increase in thickness of antenna.
- Since two dielectric substrates require proper alignment, fabrication is difficult.

#### 2.2.2 Analytical Modelling of PMAs: Related Issues

To understand the physical phenomena and their corresponding characteristics of printed antennas, especially the microstrip antenna, various analytical and numerical methods have been developed. The available approaches for the study of microstrip antenna are as follows:

##### 2.2.2.1 Cavity Model Analysis

In this model analysis, the patch structure is demonstrated as a lossy cavity. The cavity is formed enclosing a dielectric region by electric conductors at the upper and end while by magnetic walls along the boundary of the element. The EM field within the model is conveyed as the addition of the fields of several resonant modes while far fields are calculated from the magnetic currents [55]. The cavity model can take into account the higher-order resonant modes and the feed inductance. It offers a simple yet clear physical understanding of the resonant behavior of microstrip patch antennas. Though, this model applies only to irregular patch shapes [56].

##### 2.2.2.2 Transmission Line Analysis

Microstrip antenna was first analyzed by Munson in 1974 using the transmission line model [57]. In the model of a patch antenna, two radiating slots (which accounts for the fringing

fields) detached by a distance equal to the dimension of the patch accounts for the radiation from the patch. Since these slots are in the surrounding area of the ground, image theory is made use of to compute the radiated fields. Further, each of the radiating slots is equivalent to parallel admittance comprise of conductance and susceptance. The mutual coupling effect between the radiating edges using the transmission line method is talk over in [58]. The transmission line model usually applies to only a rectangular patch. But this limitation can be avoided to a great extent by modeling through generalized transmission line theory. In this method, the circular, annular sector, ring-shaped structures can be modeled [59–61]. In another method, using the transmission line approach proposed by Jackson and Alex- opoulous in which substrate is considered as a transmission line and combining with reciprocity theorem, far-field components of printed antennas are derived analytically [62].

#### 2.2.2.3 Full-Wave Analysis

Cavity model and transmission line model analysis works well with thin substrates only. It is difficult to model different feed configuration patches with the anisotropic substrate and cross-polarization can't be predicted because of single-mode analysis. Most of the drawbacks are overcome by using full-wave analysis. In this method, the dielectric and ground surface is assumed to be infinite. The effect of dielectric and its corresponding thickness is accounted for by Green's function evaluated by imposing boundary conditions at the interfaces. The evaluated Green's function is further employed in an integral equation method such as Electric Field Integral Equation (EFIE) [2, 63, 64], in which the current distribution over the metallic patch is calculated using Method of Moment (MoM). This method provides accurate results for impedance and radiation characteristics of printed antennas. It is possible to analyze arbitrarily shaped structures, it can account for surface wave, dielectric and radiation losses. Apart from these, this technique is also able to analyze patch antenna on anisotropic substrates. Apart from MoM, the FDTD technique [65, 66] is also a full-wave technique with the difference that it computes in the time domain and the derivation of Green's function is not required. Due to volumetric discretization employed in FDTD, MoM is a better choice that uses surface discretization. Besides, in FDTD, to truncate the infinite simulation domain, a proper absorbing boundary condition is necessitated.

## 2.3 UWB Antennas

The antenna is a key component of any wireless communication system, the device that transforms the EM energy guided via a transmission line to radiated EM energy from the transmitting side and vice versa at the receiving side. Antennas have different applications in various regions of the electromagnetic spectrum. Therefore, for these applications, different antennas can be designed such as patch antenna, lens antenna, wire antennas, etc. In practice, the performance and characteristics of different antennas are described by usually known antenna factors such as BW, radiation plots, efficiency, gain, time-domain characteristic, and so on. The need for larger bandwidth and smaller dimensions in the modern telecommunication system has initiated the antenna research towards the UWB planar antennas [67].

### 2.3.1 Advantages

The ultra-wideband antennas have several advantages over the narrowband antennas as given below:

1. Multiband performance - A single antenna can be used for multi-band operation due to its large bandwidth. Many lower and higher frequency bands such as Bluetooth band, GSM band, GPS band, Ku band, etc. can also be integrated with UWB antennas to enhance the utility [68].
2. Channel capacity -UWB has an ultra-wide BW, it can attain a great data rate of a few Gbps and within distances of 1 to 10 m. The channel capacity of the scheme can be expressed using Shannon's capacity as given [69]:

$$C = B \log \left( 1 + \frac{S}{N} \right) \quad (2.2)$$

Where, C, B, and S/N refers to capacity, bandwidth, signal power, and noise power.

3. Superior performance- The printed monopole UWB antennas have enhanced performance due to omnidirectional radiation plots and great gain and efficiency.

4. Low fabrication cost - The printed monopole UWB antennas are very easy to fabricate.

Therefore, the cost of fabrication is very less.

5. Stability -Parameters of UWB antennas are more constant than multi-band antennas, recuperating pulse, and non-pulse performance.
6. Minimal pulse distortion- A linear phase response of UWB antennas guarantees the low Signal deformation [70].

## **2.4 Multiple-Input-Multiple-Output Communication systems**

### *2.4.1 MIMO system*

In a traditional method, one antenna is placed on both the transmitter and the receiver side. This type of arrangement is stated as a SISO method. According to the Shannon-Nyquist criterion, the capacity of SISO systems is limited. The SISO systems capacity needs to increase to achieve growing demands for good-speed data rates with a wider bandwidth. Though, it is now not a possible solution as mentioned earlier. Without increasing the transmission strength, MIMO systems amplify the capacity in the wireless communication system [71, 92]. In traditional systems, the main problem is Rayleigh fading due to the multipath environment system. Nevertheless, to enhanced capacity, MIMO systems take advantage of multipath rather than mitigating it.

1. **Array Gain:** It helps in the improvement of signal strength. The receiver side of the SNR value increases utilizing merging coherent signals acquired at every antenna element in the MIMO system [73].
2. **Diversity Gain:** DG is a significant method to diminish multipath fading. Diversity methods are determined by transferring the signal over more than one independently fading path [74]. The signal at the receiving side is a combination of coherent signals to yield higher SNR.
3. **Spatial Multiplexing Gain:** The MIMO system provide enhanced capacity without additional energy or bandwidth expenditure. This gain is achieved by transferring unbiased signals from the single antennas. Further good channel circumstances, for example, rich scattering, enhanced capacity can be achieved [75].

### *2.4.2 MIMO Channel Model*

The MIMO system proceeds the benefit of a multipath environment. A MIMO channel with

$x$  transmitted signal and  $y$  received signal is given below:

$$y = Hx + n \quad (2.3)$$

Figure 3.1 presented the MIMO channel, it is required to understand the channel model. For a scheme with  $m$  transmitters and  $n$  receivers, the MIMO channel matrix has been signified by the  $m \times n$  matrix. The MIMO system is categorized into several forms of reliable. MIMO is mainly a mixture of all the many antenna arrangements for example SISO, SIMO, and MISO. Dual ability to merge the SIMO and MISO systems. And additionally, expand capacity by the use of Spatial Multiplexing. The signal fading is considerably removed with the aid of spatial diversity; low power is mandatorily equated to dissimilar methods in MIMO [78].

#### 2.4.2.1 Spatial multiplexing:

Parallel data transmission amid the transmitter and receiver antennas is achieved by the mean of multiple antenna systems can make. Capacity or data transfer of the system can be increased by spatial multiplexing is done. The data stream that is communicated is spitted into several data epochs [79]. These epochs are then sent using dissimilar antennas simultaneously. Meanwhile, several transmitting and receiving antennas are in use, the data rate will rise as the number of antennas increases. In a multipath environment, the signal reserved at the receiving antenna is a mish-mash of all single epochs. Each one of them is alienated at the receiver and combined coherently to attain higher SNR [80].

#### 2.4.2.2 Mutual Coupling and Isolation:

The pulse communicated by the MIMO antenna is considered uncorrelated. But, the current induced on a single element generates the voltage at the close elements, called mutual coupling [81]. Though the mutual coupling should be low for MIMO application. In a self-contradictory way, it is also considered that the lower the mutual coupling, less will be the similarity between the different radiation plots of different elements of the MIMO antenna. The mutual coupling is defined as the distribution of current and voltage among the different ports of the MIMO antenna. It is symbolized by  $|S_{21}|$  factor. In this system, to achieve the best performance of the antenna, it should be confirmed that an insignificant quantity of transferred power is lost into the ports of the multiport antenna. As mutual coupling is directly linked to

the antenna efficiency so it is essential to minimize the  $|S_{21}|$  as low value as possible. Many authors have a lot of research to diminish the mutual coupling. Though in [82], it is indicated isolation is not the precise illustration  $|S_{21}|$ , there is a possibility that there is great isolation but it is not compulsory that mutual coupling will also low. Therefore, to determine the  $|S_{21}|$ , it is good to perceive the current spreading on the non-excited patch element, while the closely placed patch is excited.

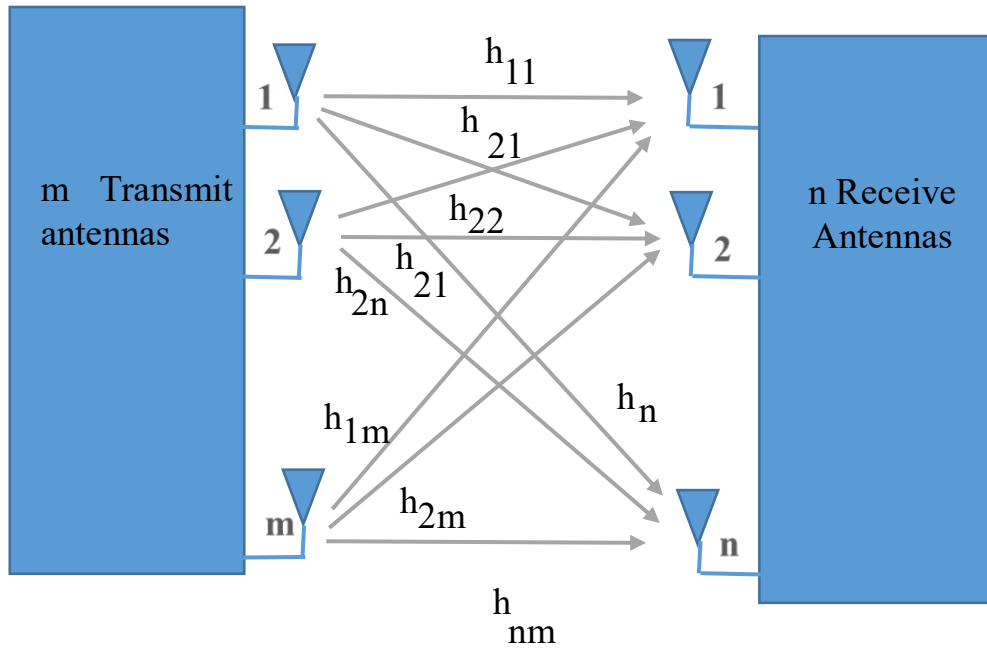


Figure 2.3: MIMO Channel Model.

#### 2.4.2.3 Mean Effective Gain

It is a significant parameter that is used to also characterize the performance of MIMO systems. The MEG is fraction received power to imping power. The formula has given in equation as in [83] where XPR signifies the cross-polarization gain. The MEG is a fraction of the total efficiency of the antenna by two [84] and it does not depend on the radiation patterns of the antenna. To attain decent DG, the fraction of the MEG among the elements would nearly unity [85].

$$MEG_i = 0.5 \left[ 1 - \sum_{j=1}^N |S_{ij}|^2 \right] < -3dB \quad (2.4)$$

$$\text{Also, } |MEG_i - MEG_j| < 3dB \quad (2.5)$$

$$MEG_i = 0.5 \left[ 1 - |S_{11}|^2 - |S_{12}|^2 \right] \quad (2.6)$$

$$MEG_j = 0.5 \left[ 1 - |S_{21}|^2 - |S_{22}|^2 \right] \quad (2.7)$$

#### 2.4.2.4 Envelope Correlation Coefficient

The correlation coefficient is another important that is related to diversity gain. It is an accurate and arithmetical means that checks the resemblance between the radiation plots of the two elements antenna. It ranges from 0 to 1. In an ideal case, the correlation coefficient of 0. Commonly, the correlation is obtainable to determine the diversity performance of multiple antenna systems [86]. The Correlation Coefficient is a real value and it tells the similarity between amplitudes of the signals. The formula of envelope correlation for the Rayleigh fading channel is shown below. In literature it is given that correlation is intended using 3D radiation patterns but it is complex to determine. Though, supposing that the diversity system will work in an unvarying multipath situation, the envelope correlation can be intended in the equation in [87]

$$ECC = \frac{\left| \int_{\Omega} \left[ XPR \cdot E_{\theta_i} E_{\theta_j}^* P_{\theta} + E_{\phi_i} E_{\phi_j}^* P_{\phi} \right] d\Omega \right|^2}{\int_{\Omega} \left[ XPR \cdot E_{\theta_i} E_{\theta_i}^* P_{\theta} + E_{\phi_i} E_{\phi_i}^* P_{\phi} \right] d\Omega \int_{\Omega} \left[ XPR \cdot E_{\theta_j} E_{\theta_j}^* P_{\theta} + E_{\phi_j} E_{\phi_j}^* P_{\phi} \right] d\Omega} \quad (2.8)$$

$$XPR = \frac{P_V}{P_H} \quad (2.9)$$

where  $P_V$  and  $P_H$  are the power laterally elevation( $\theta$ ) and azimuthal angle( $\Phi$ ).ECC [88] is also related to S parameters given below

$$ECC = \frac{|S_{11}^* S_{12} + S_{21}^* S_{22}|^2}{(1 - |S_{11}|^2 - |S_{21}|^2)(1 - |S_{22}|^2 - |S_{12}|^2)} \quad (2.10)$$

Where  $S_{11}$  and  $S_{22}$  is the reflection coefficient.  $S_{12}$  and  $S_{21}$  are coupling among the different ports. This equation is rigorously effective when the below mention assumptions are satisfied [89]:

- High efficiency and good isolation among the antenna elements.

- Antenna is placed in an unvarying multipath situation that is different in actual atmospheres.

#### 2.4.2.5 Diversity Gain

DG is an efficient factor to measure the enactment of diversity systems. DG is defined as the fraction of the received SNR in a combined diversity system to the received SNR in a single diversity system. It means the growth of the SNR value at a specified probability, The DG can be intended by using [90]

$$DG = \frac{(SNR)_c}{(SNR)_r} \quad (2.11)$$

where “c” and “r” are referred to as combined and the reference. The DG is directly linked to the envelope correlation coefficient. The relationship between DG and ECC can be given in equation [91]

$$DG = 10\sqrt{1 - ECC^2} \quad (2.12)$$

From the equation, it is observed that the less ECC the higher will be the DG. Hence, the low mutual coupling is necessary among the radiating elements otherwise the DG will below. Further, in the diversity scheme at the receiver side various merging scheme, the thoroughgoing DG is attained when the ECC is zero.

#### 2.4.2.6 Total Active Reflection Coefficient

The RE and BW of a MIMO antenna are not accurately characterized by return loss. So, rather than using return loss, TARC is a parameter that considers mutual coupling between the antenna elements and signal arrangement. Thus, TARC delivers a significant degree of MIMO efficiency. TARC is a fraction of the square root of backward traveling power and toward traveling power [92]

$$TARC = \frac{\sqrt{\sum_{i=1}^N |b_i|^2}}{\sqrt{\sum_{i=1}^N |a_i|^2}} \quad (2.13)$$

Where  $a_i$  and  $b_i$  is the frontward moving signal and retrograde moving signal respectively. For the two-port antenna, the TARC is given by [93]

$$TARC = \sqrt{\frac{(S_{11} + S_{12})^2 + (S_{21} + S_{22})^2}{2}} \quad (2.14)$$

The TARC is intended by the addition of dissimilar excitation signals to each port. The value of TARC is a real number that varies from 0 to 1. When TARC is 0, that means all the total forward-moving signal is radiated into space and when the value is 1, all the forward-moving signal is either retrograde.

#### 2.4.2.7 Channel capacity loss (CCL)

Channel capacity loss is a very vital parameter for the MIMO antenna; it measures the capacity loss in the channel at a certain frequency per unit time. The unit of (CCL) is bit/sec/Hz. The CCL is specified by [94]

$$C_{loss} = -\log_2 \det(\beta^R) \quad (2.15)$$

where,

$$\beta^R = \begin{bmatrix} \beta_{ii} & \beta_{ij} \\ \beta_{ji} & \beta_{jj} \end{bmatrix} \quad (2.16)$$

$$\beta_{ii} = 1 - \left( \sum_{j=1}^N |S_{ij}|^2 \right) \quad (2.17)$$

$$\beta_{ij} = -(S_{ii}^* S_{ij} + S_{ji}^* S_{ij}) \quad (2.18)$$

## 2.5. UWB MIMO Antenna characteristics

In wireless communication systems, the demand to improve the bit rate is increased. In rich scattering environments to implement diversity techniques in the system, two antennas are required to increase the data rate and consistency devoid of losing additional spectrum or transmitted power [95]. As compared to traditional MIMO systems, the UWB MIMO system expands additional channel capacity for narrowband applications. To resolve the signal fading issue in the system, the diversity antenna system is a capable applicant.

### 2.5.1 Challenges in designing UWB MIMO systems

1. Mutual coupling: In MIMO system isolation is a major problem among the antenna elements. High isolation affects the antenna efficiency as well as the correlation of the MIMO system. For good enactment, the value of  $|S_{12}|$  must be below -15 dB for the entire operating range [96].
2. Bandwidth: In an antenna, operating bandwidth is determined using Return loss. The impedance bandwidth of less than -10 dB works in the complete range from 3.1 to 10.6 GHz. Mutual coupling and bandwidth are the two difficult challenges that cause the problem MIMO system [97].
3. Size: MIMO systems are used in various mobile applications, which use numerous wireless systems for example UWB WLAN, WIMAX, and WCDMA, to get great data communication. It is another hardest challenges to achieve both compact UWB MIMO antenna with good channel capacity.

## 2.6 Polarization

Polarization of a uniform plane wave is the orientation that the slope of the E field vector as it oscillates in time at a specified point in space. An electric wave vector can be considered as having two components that are perpendicular to each other [98-102]. At a fixed point in space, as the time varies, the shape that the vector sum of the two components will describe can be a line, an ellipse, or a circle depending on the ratio of the magnitude of vector components and the phase difference between them. In general, the instantaneous total electric vector can be written as

$$E_t = \hat{x}E_x + \hat{y}E_y \quad (2.19)$$

Where

$E_x = E_1 \cos(\omega t - \beta z)$  is the horizontal component with amplitude  $E_1$ ,

$E_y = E_2 \cos(\omega t - \beta z \pm \delta)$  is the vertical component with amplitude  $E_2$  and a phase difference  $\delta$  by which  $E_y$  leads/ lags  $E_x$ .

### 1. Linear polarization

A traveling wave is said to be linearly-polarized if the two orthogonal components of the wave vector have no phase difference i.e.  $\delta=0^\circ$ [103]. Then depending on the component magnitudes, a linearly-polarized wave will be generated in the horizontal, vertical, or any plane between them e.g. if  $E_1=0$  then it is vertical linear-polarization and it will have a  $45^\circ$  slanted linear-polarization when  $E_1= E_2$ .

### 2. Circular polarization:

A wave has a circular-polarization when  $E_1= E_2$  and  $\delta = \pm 90^\circ$ . When  $\delta = -90^\circ$  the wave is right-hand circularly-polarized and it has left-hand circular polarization when  $\delta = \pm 90^\circ$ . Figure 2.6 shows two orthogonal waves, a sine (XZ plane) and a cosine (YZ plane) which have a phase difference  $\delta = \pm 90^\circ$ , generate an RHCP in the Z direction as time progresses [104].

### 3. Elliptical polarization

A wave is said to have elliptical-polarization when  $E_1 \neq E_2$  and  $\delta \neq 0^\circ$ . Like circular polarization, elliptical-polarization can be right-hand (clockwise) (Figure 2.7) or left-hand (anti-clockwise.)

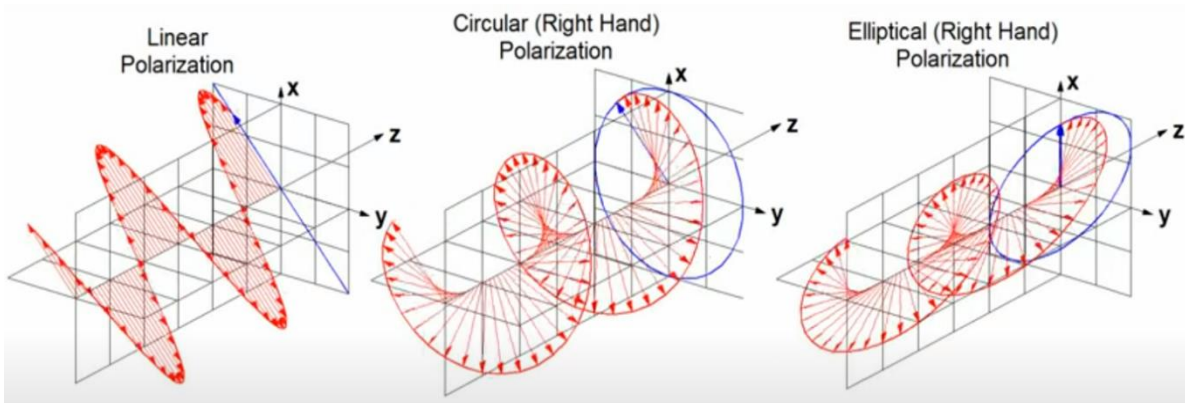


**Figure 2.4:** Different type of polarization [105]

#### 2.6.1 Axial ratio and Polarization ellipse

An antenna is intended to have only one sense of polarization in a certain direction. However,

no antenna works perfectly in reality so there is always an orthogonal polarization (cross-polar component) to that of the main intended one (co-polar component). The E field can be termed as the summation of two orthogonal components that are amplitudes and the phase amid them. The angle of the E vector of a polarized wave traces out a regular pattern when observed from the direction of propagation, which is generally an ellipse called the polarization ellipse. A circular-polarization can be considered as two electric vector components, RHCP and LHCP. The ratio between the intended polarization (e.g. RHCP) and unwanted cross-polar component (e.g. LHCP) is defined as polarization ratio ( $r_c$ ) [105]:

$$r_c = \frac{E_{RHCP}}{E_{LHCP}} \quad (2.20)$$

The polarization ratio or the cross-polar level is of particular interest in circular polarization as the AR is expressed as [106]:

$$AR = \frac{r_c + 1}{r_c - 1} = \frac{E_{RHCP} + E_{LHCP}}{E_{RHCP} - E_{LHCP}} \quad (2.21)$$

It can be seen that the polarization ellipse becomes a circle when AR=1 i.e. no unwanted polarization (LHCP=0) and it becomes a line when AR= 0 i.e. the cross and co-polar are of the same magnitude. This means that the antenna radiates both RHCP and LHCP in the same direction with equal magnitude. This indicates a fact that an LP wave can be considered a summation of two CP wave vectors with equal magnitude. Furthermore, an antenna is purely CP if AR=1 but as it is not the case for most antennas, an AR of < 3 dB is considered CP in antenna measurements [107].

### 2.6.2 Antenna polarization loss factor (PLF)

The sense of rotation determines the polarization of an antenna in the far-field. Suppose the transmitter and receiver are linearly polarized, the orientation of both antenna are different will give polarization mismatch loss which is given as [108]:

$$PLF = \cos^2(\psi_p) \quad (2.22)$$

Where  $\psi_p$  is the misalignment angle between the two antennas (Figure 2.8). The polarization mismatch increases as  $\psi_p$  increases. For two antennas with linear polarization, a perfect

match occurs when  $PLF = 1$  (antennas are perfectly aligned,  $\psi_p = 0^\circ$ ) and a complete mismatch occurs  $PLF=0$  when (antennas are orthogonal,  $\psi_p = 90^\circ$ ). It is assumed that there is always a 3 dB polarization mismatch loss among a linearly and a CP antenna. This is only true if the CP antenna has an AR of 0 dB. Given transmit and receive antennas AR and alignment angle,  $\theta$  between the major axis of the two polarization ellipses, the Polarization loss can be intended utilizing the subsequent Equation[109]

$$Mismatch(dB) = \frac{1 + r_t^2 r_r^2 + 2r_t r_r \cos(2\theta)}{(1 + r_t^2)(1 + r_r^2)} \quad (2.23)$$

Where

$$r_t = \frac{AR_t + 1}{AR_t - 1} \quad (2.24)$$

$$r_r = \frac{AR_r + 1}{AR_r - 1} \quad (2.25)$$

are the polarization ratios of the transmit and the receive antennas, respectively.

### 2.6.3 Advantages of circular polarization

#### 2.6.3.1. Immunity to Faraday rotation

Faraday rotation effect (Figure 2.11) arises in the presence of magnetic flux density that rotates the plane of polarization. It normally occurs in the ionosphere when a linearly-polarized signal passes the Earth's magnetic field, its plane of polarization is rotated. The amount of rotation is related to the magnetic flux density in the propagation path. This Faraday rotation effect is more pronounced in higher altitudes where stronger magnetic fields are found in extremely ionized plasma [110]. The magnitude of the effect varies since the density of electrons in the ionosphere varies greatly daily. However, the amount of rotation of the polarization angle is always contrariwise relative to the square of the frequency. As a result of the Faraday Effect, there is a polarization mismatch for linearly-polarized antennas. On the other hand, circular-polarization is immune as it has two equal orthogonal components and any rotation will be on both components equally, therefore, the wave will still be circularly-polarized [111].

### 2.6.3.2 Mitigation of multipath propagation

When a CP wave is reflected from the ground the sense of the polarization changes i.e. RHCP becomes LHCP and vice versa. As a result, the receiving antenna will not receive the reflected waves, hence, no interference between the direct and reflected waves occurs. This means that in a multipath environment such as indoor scenarios the multipath interference can be greatly reduced by using circularly-polarized antennas [111].

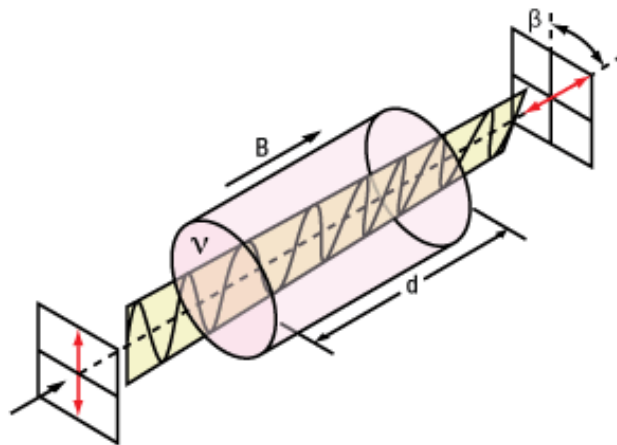


**Figure 2.5:** Faraday rotation effect [110]

### 2.6.3.3 Polarization mismatch loss

The polarization mismatch occurs due to the different orientation of both side antennas. For linearly-polarized antennas, the transmit and receive antennas must be line up to avoid polarization losses. However, a linearly-polarized antenna will receive a CP wave whatever its orientation is [112]. This is because a CP wave propagates in both horizontal and vertical planes and the planes in between so for an arbitrarily oriented LP antenna, there will always be a component of the CP wave that will be aligned with it.

## 2.7 Application of UWB MIMO antenna system

### 2.7.1 RFID Radio Frequency Identification (RFID)

RFID is used to set the automatic identification of objects or people through the storage and

retrieval of data when exposed to electromagnetic waves. EM waves are transmitted to an integrated well-suited radio frequencies circuit, called RFID tag, and consequently, data is read by an RFID reader [113-115]. In 1948, the RFID system is used after the 2nd World War, and in 1980 it is used in many commercial applications. There are three different ways i.e., capacitive, inductive, and radiative to begin communication between the RFID Tag and RFID readers. The way these components couple can determine the read range and frequency of the system. Close coupling uses EM coupling, dependent on the reader and tag. Readers are used E coupling to communicate in between 0.1 and 1 cm. Systems can use the H field to the couple, which is called capacitive coupling. This coupling is only in effect on a distance range of 1-2 cm and this type of coupling is used in Low-frequency communications. Inductive coupling relies on the H field of the reader that means coupling occurs in the near-field up to 1cm up to 1m. Inductive coupling is present in LF, HF, and UHF applications. More or fewer applications include any UHF application within 1 meter of distance. Radiative Coupling among readers and tags is a communication technique containing EM waves. This coupling type is used by most of the UHF systems. Radiative Coupling type allows RFID reader/tag transfer from 1 to 4 meters [116].

### *2.7.2 Precision asset location (PAL) system*

The UWB deals with communication and identification of the exact position in one technology. The exact place measurement and its utilization in the strength system are major applications of the UWB system and it will be a significant market makes in the upcoming years [117]. The position can control vehicular robots in indoor environments, inventory items, locate personnel. [118]. The PAL organization uses the UWB position capability of the UWB system to work on the time difference of arrival (TDOA) technique. The evaluated precision of a couple of feet in open load situations with holders has been accomplished. Examinations on PAL statement that the framework functions admirably in open and incompletely stacked freight spaces. Unlike narrowband RFID systems, UWB seemed to enter extensive splits between compartments, keeping up confinement capacity amid blockage tests. In Navy ships, very narrowband radio frequency identification (RFID) tags have not able to work properly due to excessive multipath (i.e. large delay spreads) and

limited precision. To overcome these obstacles further the UWB PAL system was developed recently. The PAL system demonstrates the promise of UWB communications and ranging applications since short pulses can give to a great degree precise results, even in outrageous multipath environments. It was concluded for this specific application that UWB tags replace the current narrowband RFID tags. The significant developments and examination of a UWB PAL.

### 2.7.3 *Communication*

Two types of UWB applications are as follows [118]:

- Short distance with great data rate applications.
- Long-distance with less data rate applications.

The channel capacity of the antenna can be enlarged by varying the channel BW or SNR or both according to Shannon-Hartley theorem [119]. To attain a better data rate, UWB is used due to its wide bandwidth. Though, FCC allowed low power emission for the wide UWB range [120]. This results in short distance communication and therefore, UWB is the best candidate for great data rate, short distance devices. Applications like USB, multi-, device-to-device transfer, etc. UWB also delivers trade BW with range, security, multiuser setup, etc. Various applications like these wireless sensor networks (WSNs) can use the UWB. This pulse has remarkable transmission features as it can transmit through walls and bad situations, the perfect applicant for examination and rescue application.

### 2.7.4 *Medicine*

UWB pulse is useful for biomedical applications due to its noise-like behavior with exceptionally small ERIP. In medical imaging and medical sensing, the UWB pulse is normally used. Blood pressure, observing cardiac gesture, the respiratory system, are the approximately medical system that uses UWB antenna. Obstetrics imaging and breast cancer detection are distinctive imaging system. It is also used in ear-nose-throat (ENT) organs [121], in rigorous care units to monitor coma patients and indoor localization.

### 2.7.5 Commercial UWB systems

Ubisense (5.8–7.2GHz) and Zebra Enterprise Solutions (5.94-7.12GHz) are non-standard system and localization solutions [122] that was used in commercial UWB technology. The transmitter tags which need localization are mounted on the targets such as a person, object, sensor, etc. [123].

## 2.8 Metamaterial

In 1898, artificial chiral structures is discovered by Jagdish Chandra Bose [24]. The author in [125-127] prepared their efforts to hollowly adapt the refractive index. Far along, the non-natural materials that show some novel responses in the unceasing examination. Metamaterials are non-natural provisions meant to work together govern EM signals. If any EM wave intermingles with the compound medium it makes E and H moments in that way that considerably disconcerting the permittivity and permeability. A metamaterial depends on positions of shape, structure, dimension, thickness, procedure, and placement of combinations. Materials comprise a different class with negative values of  $\epsilon$  and  $\mu$ . In [128] plain wave propagation in a medium where both  $\epsilon$  and  $\mu$  are negative. Many terms are used for example negative refractive index, retrograde wave media, double negative type metamaterials, and left-handed media.

The imping EM waves are mostly evaluated by the features of materials elaborate. These issues are categorized commonly by two factors  $\epsilon$  and  $\mu$ . In a medium where  $\epsilon$  and  $\mu$  positive is called as DPS Medium. Maximum dielectrics are DPS materials. ENG medium has negative  $\epsilon$  values and positive  $\mu$  values. The proper instances in this class embrace like silver and gold. MNG medium has positive  $\epsilon$  and negative  $\mu$ . One example is MNG is gyrotropic materials. DNG medium has negative  $\epsilon$  and  $\mu$  [129]. The features of the DNG medium found in non-natural materials[130-132], Left-handed media, and BWM [133] are commonly related to DNG materials [134]. Left-handed materials are generally related to negative refraction. H fields of an electromagnetic wave are smaller than E fields by an important parameter known as intrinsic impedance ( $\eta$ ). In the E field, electron movement around the nucleus results in susceptibility and hence its permeability. In [135] metallic wires and SRR presented showed the presence of negative refractive index metallic wires helps in attaining

negative  $\epsilon$  and negative  $\mu$  is attained by SRR. Metamaterials can be used in various applications [136-139]. Moreover, fascinating unique assets are attained by combining two different metamaterials with different signed metamaterials like DNG combined with DPS and ENG combined with MNG. Investigational classifications of SNG medium and DNG are performed [140-142] in a scattering chamber. It is enclosed by an EM wave absorber and limited in a metallic box. Standing waves will not excite in a chamber if TE mode is launched.

### *2.8.1 Electromagnetic Band Gap (EBG) Structures*

The furthestmost proceeding materials are the EBG structure. EBG structure can encourage the transmission of em propagation to a level that was not possible earlier [142]. EBG structures have different types of structures that attract the attention of various researchers. The main aim of the discovery of real applications with detailed modeling. Because of the unique feature EBG unit cell, it can be used in various applications. New firms started to track to exploit the commercial potential of this system [143]. Normally, EBG structures are non-natural material that obviates or supports the transmission of em waves in a particular frequency band [144]. By integrating EBG structures with the antenna to achieve better good radiation/gain curves and to suppress the noise /losses in propagation. It is known as a high impedance surface because it eliminates the surface current propagation in the bandgap of the EBG unit cell. Recently, speedy growth EBG structure is seen in the antenna community [144] [145]. This unit cell work on the principle of total internal reflection [146]. These unit cell are commonly recognized as photonic crystals that are artificially synthesized crystals which control light completely [147].

### *2.8.2 EBG Structure and characterization*

The bandgap EBG structure elevated using three different methods that are dispersion diagram, reflection phase characteristics, and the suspended transmission characteristics. The dispersion diagram is plotted between wavenumber and frequency.

### 2.8.2.1 Mushroom like EBG Structure

The EBG structure [7] contains three planes: a metallic patches plane, a ground plane, and a dielectric substrate plane with vias to connect the patch to the ground plane. The EBG structure behaviors as a stop-band filter for surface-wave. This EBG structure mechanism can be described by an LC filter circuit[8]. The unit cell of the mushroom-like EBG structure is depicted in Figure1(a,b). In equation (1),  $L$  indicates the inductor which is due to the current passing through the vias, and in equation (2),  $C$  indicates the capacitor results from the gap among the neighboring patches. the inductor  $L$  and capacitor  $C$  are evaluated using [7, 8]:

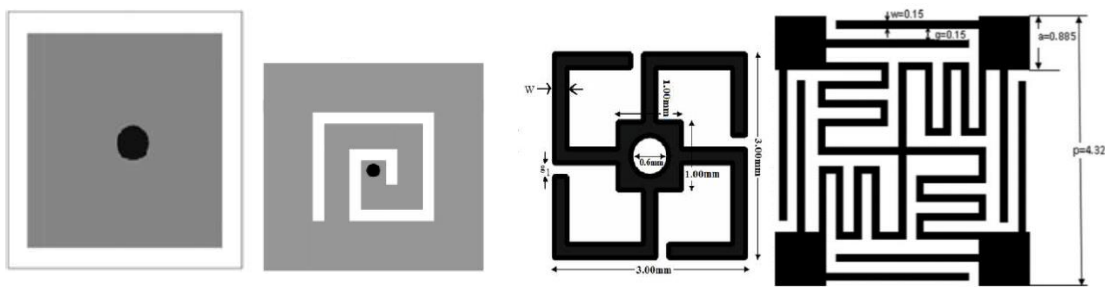
$$L = \mu_0 h \quad (2.25)$$

$$C = \frac{W \varepsilon_0 (1 + \varepsilon_0)}{\pi} \cosh \frac{(2W + g)}{g} \quad (2.26)$$

Where,  $W$ ,  $g$ ,  $h$ ,  $\mu_0$ , and  $\varepsilon_0$  is patch width, gap width, and substrate thickness, the permeability of free space and permittivity.

### 2.8.2.2 Uniplanar EBG Structure

The unit cell of the Uniplanar EBG unit cell is depicted in Figure 2.6(d). Unipolar EBG structure is similar to mushroom-like EBG unit cell but it does not contain via in between the patch and ground plane. Uniplanar EBG structure is easy to fabricate because it does not contain Via. In Figure 2.6 various EBG structures are shown. Figure 2.6(d) contains straight lines that are used to increase the capacitance and zig-zag lines in the center increase the inductance.[159]



(a) Mushroom EBG[155] (b) Spiral EBG[156] (c) Swastika EBG [157] (d) Modified uniplanar EBG [159]

**Figure 2.6:** Various EBG unit cell geometries

### 2.8.3 Band Gap Determination Methods of EBG Structures

The bandgap of the EBG unit cell can be evaluated using various methods such as the reflection phase, the dispersion diagram, and the transmission characteristics. The EM behavior of a propagating wave is foreseeable from the reflection phase method, in such a way  $180^\circ$  reflection phase implies a PEC plane and a  $0^\circ$  reflection phase be similar to a PMC plane. Uncertainty a plane wave impinges on PEC, the reflected wave and the incident wave are opposite signs, which results in  $-1$  reflection coefficient. Similarly, a plane wave impinges on PMC, the reflected wave and the impinging wave have the identical signs. The value of the reflection coefficient is  $+1$ , and the resultant reflection phase is  $0^\circ$  [159]. Though, the PMC material is artificial material and does not exist in nature. With the increase in frequency, the reflection phase varies from  $+180^\circ$  to  $-180^\circ$  [160], and the resonant bandgap ranges from  $+90^\circ$  and  $-90^\circ$  as shown in Figure 2.7 (a). Secondly, the gap of the EBG array structure is intended from the dispersion diagram [161]. The dispersion diagram is plotted between phase constant and resonant frequency [162] as shown in Figure 2.7(b). It is observed that the gray area in Figure 2.7 (b) band gap for a structure. The third method is the transmission characteristic of an EBG structure is obtainable through the suspended microstrip line method. In this method, the bandgap is determined using the EBG periodic structure as a ground plane which is suspended above the array [163]. As shown in Figure 2.7(c), the attenuation losses of less than  $-10$  dB or  $-20$  dB are commonly termed as the bandgap [164]-[165]. The EBG design particularly for antenna applications, the reflection phase, and the transmission responses are enough for exploring the bandgap features. From the reflection phase diagram, the artificial magnetic conductor point ( $0^\circ$ ), of the surface wave can be easily identified. As compared to the dispersion diagram would give extra information on the bandgap, but it needs much greater time and memory allocation. The time and memory allocation necessities rise with operational complexity.

### 2.8.4 EBG Structure Miniaturization

Recently, compact devices and antennas have come to be progressively increased. Current technology needs compact devices that give high-data-rate communication system systems.

In the literature, various Miniaturization methods are discussed. In [166] Sivenpiper explained that varying the capacitor and inductor in the HIS surface can be achieved with a reduced dimension of EBG structure. In [167] Feresidis presented the idea of Metallo dielectric EBG cell and 2-D double layer dipole arrays. He also explained that outside the HIS surface, surface waves can propagate. These possessions can be exploited for the miniaturization of microwave elements, [168]. Fractal-type structures are used for multiband AMC designs [170].

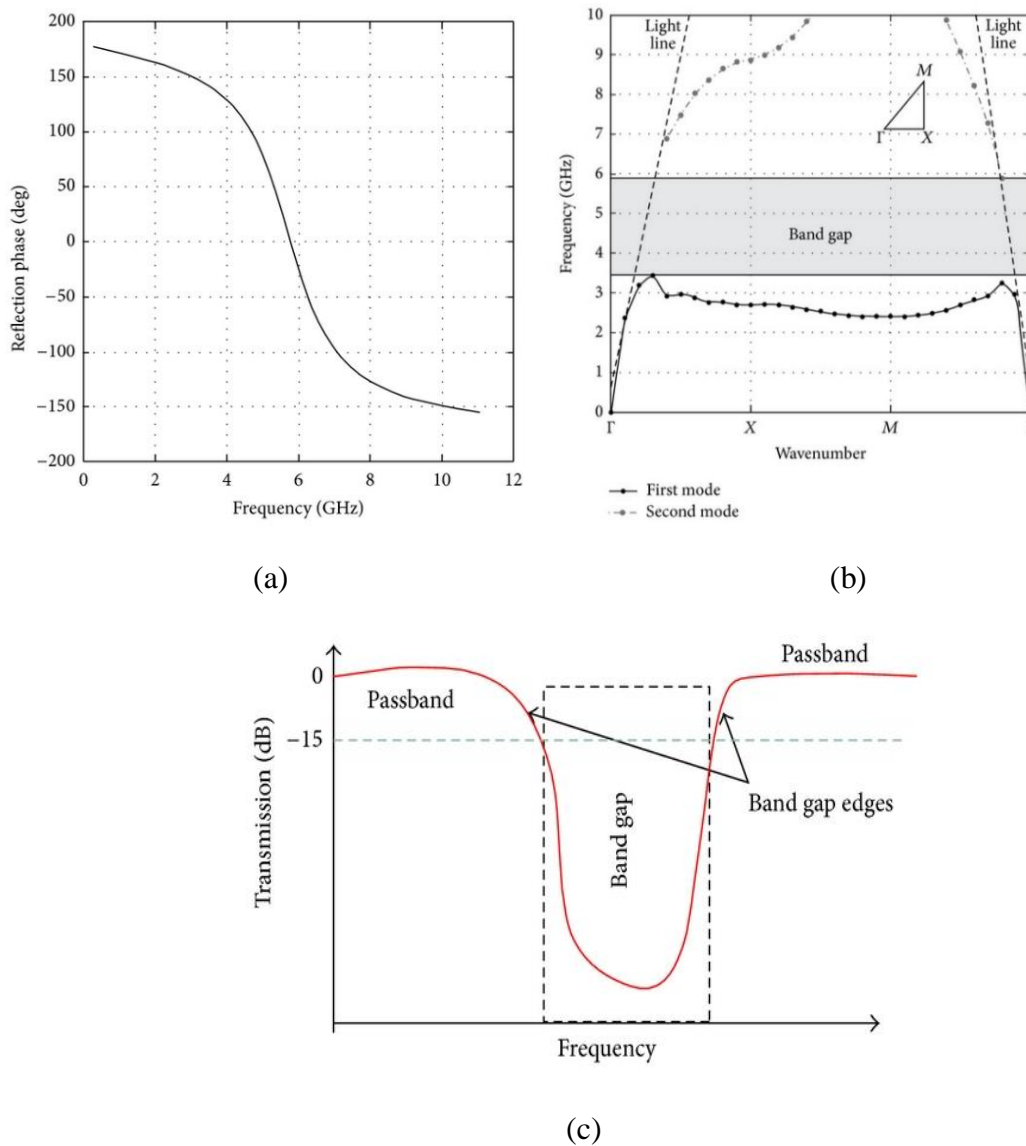


**Figure 2.7:** Different Analysis Methods for EBGs [165]

## 2.9 Band notch operation in patch antenna using EBG Structures

In April 2002, FCC unbinds the frequency range that lies from 3.1 to 10.6 GHz and this band is termed as UWB. Some narrowband communication systems (WiMAX, WLAN, and X Band) also work within this range, which produces interference. Many different design methods have been presented in the literature to deal with to avoid interference. The methods like etching slots, stubs, resonators like the CLL, electric ring disturb the radiation pattern because of discontinuity in patch element. This issue can be resolved by using the band rejection features of EBG structures. By inserting the EBG unit cell close to the feed of the UWB antenna, interference of narrowband communication can be discarded [171]. In literature, the various design of the EBG structure is presented to obtain band-notch characteristics. A swastika-type EBG [63] is used to achieve single band notch characteristics with a bandgap of 7.5 GHz to 11.1 GHz band. In [172] by placing the EBG structures near the feedline, triple notches at WiMAX (3.5 GHz), and WLAN (5.2/5.8 GHz) bands are achieved. Mushroom EBG Structure via at center [173] and edge located Mushroom EBG [174]–[175] are some structures presented by the researchers. A uniplanar EBG and two mushroom EBG structure [176] is placed near the feedline of the monopole antenna to have triple-band rejection characteristics. A hexagonal shape with c slot mushroom EBG [177] is used to achieve a band notch function for the X band satellite communication system (6.7–7.7GHz). In [178] four EBG structures are placed close to the feed line to attain dual-band notch characteristics [179] presented in figure 2.7(a). The patch antenna and EBG structure are fabricated on a cheap FR-4 substrate with dimensions of  $58 \times 45 \times 1.6 \text{ mm}^3$ . Figure 2.7(b) indicates the VSWR of the UWB MIMO antenna. Another interesting study is performed [180] where the circular monopole antenna [181]–[182] with two mushrooms EBG unit cell is used to obtain band notch characteristics for WLAN and WiMAX. Moreover, 34% of compactness is also achieved by etching L shaped slot on the EBG surface. This modified EBG structure contains two L shaped slots with an edge-located via (ELV) that achieves dual notched bands. So, in this single EBG is used to obtain dual-band notch characteristics. Figure 2.8(a) shows a circular antenna with two changed EBG structure. A dual band-notched MIMO antenna obtains notches in the WiMAX band (3.3–3.6 GHz) and WLAN band (5–6

GHz) as presented in Figure 2.8(b). Figure 2.9 indicates the band-notched antenna. The designed antenna avoids the interference from WiMAX ranging from 3.3-3.6 GHz, WLAN ranging from 5-6 GHz, and the X band satellite communication system ranging from 7.2 -8.4 GHz. Another modified EBG structure connected with the feed line is used to reject the interfering narrowband Communication system [183]

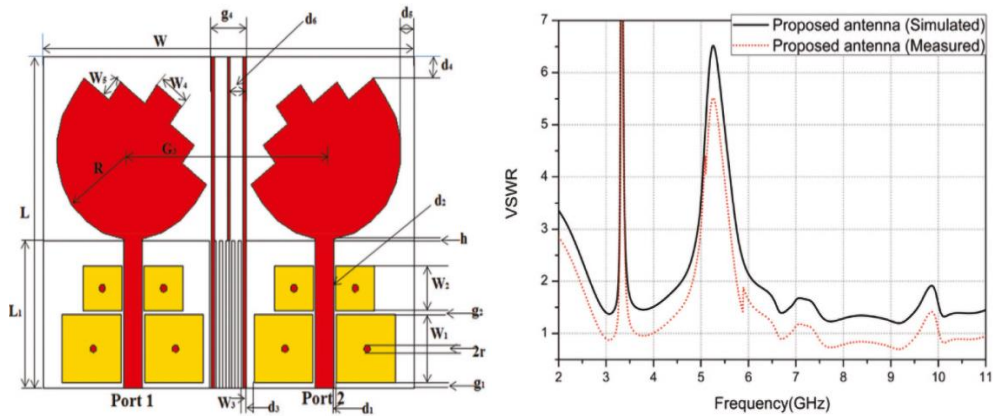


**Figure 2.8** a) Band-notched UWB MIMO Antenna (b) VSWR Plot [179]

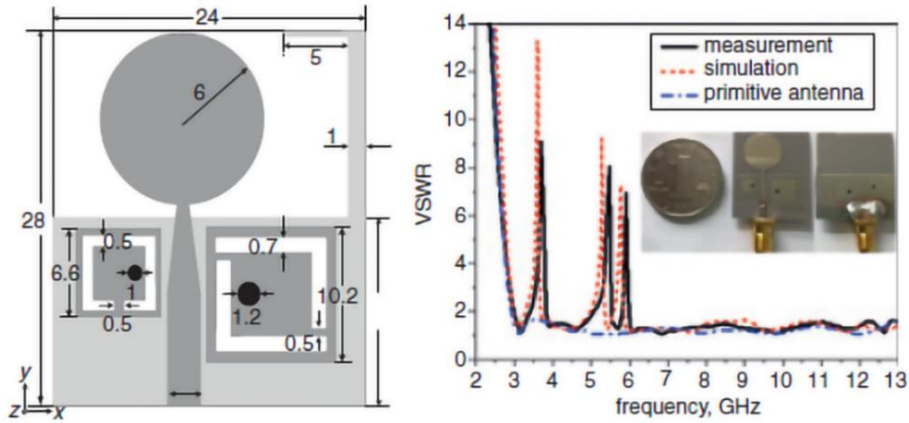


**Figure 2.9:** (a) Monopole UWB Antenna with triple band-notched (b) VSWR plot [180]

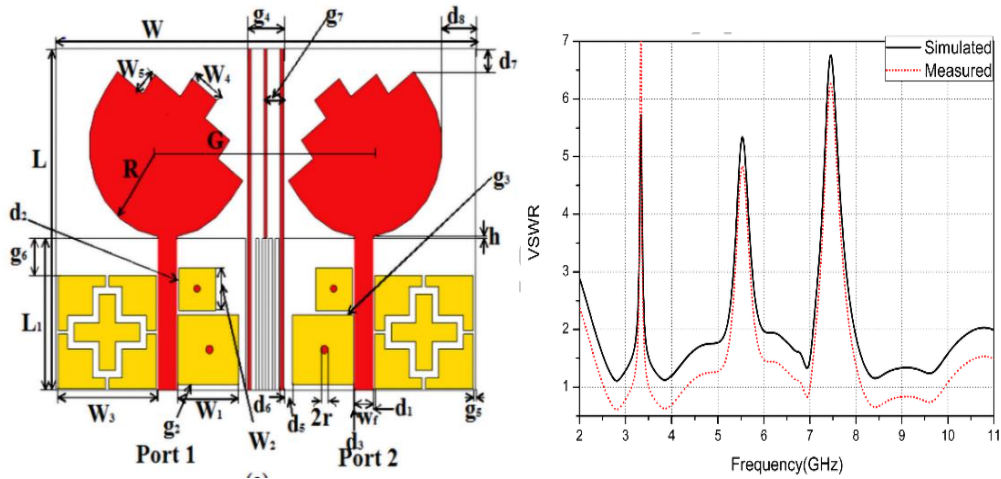


Figure 2. 10: (a) Triple band-notched UWB MIMO Antenna (b) VSWR plot[183].

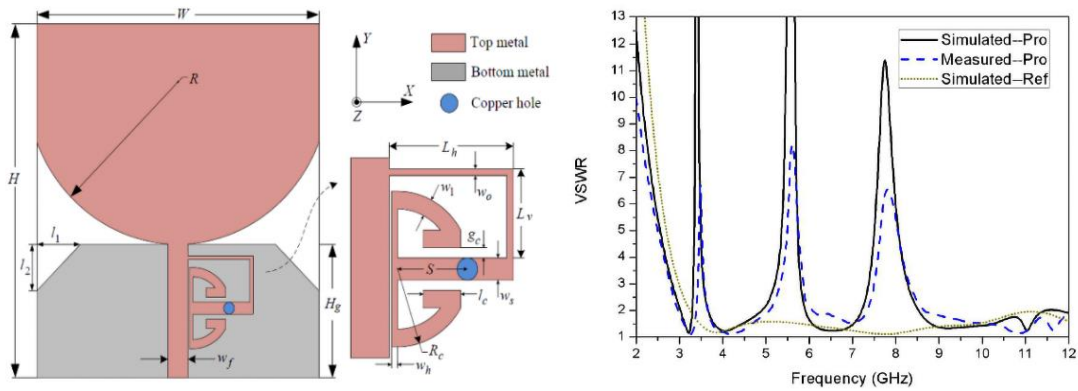


Figure 2. 11 : (a) Band-notched UWB Antenna (b) VSWR of triple band-notched UWB MIMO antenna [183]

This single EBG structure rejects are for WiMAX, WLAN, and X-band satellite communication systems. Figure 2.10 (a) displays the band-notched UWB antenna [183]. The antenna and EBG structure are designed using FR4 substrate with a height of 1 mm, the dielectric constant of 4.4 and with an overall dimension of  $30.5 \times 26 \times 1 \text{ mm}^3$  and  $8 \times 5.95 \text{ mm}^2$ , respectively. Pentagonal printed UWB monopole antenna having triple-band notches shown in Figure 2.11(a). Two slots are inserted in the EBG structure to attain multiple band rejection. The dimension of the EBG structure is  $9.4 \times 4.5 \text{ mm}^2$ . Figure 2.11 (b) indicate the VSWR of the band notch UWB antenna [184]

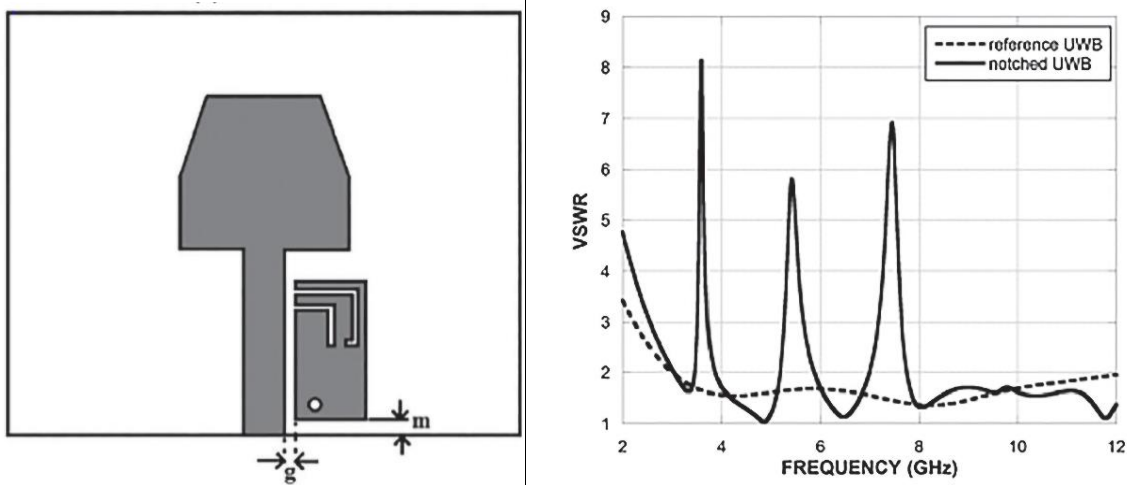


Figure 2. 12: (a) Pentagonal UWB monopole antenna (b) VSWR Plot [184].

## 2.10 Designing of different feeding methods in Microstrip Antenna

In this section, the microstrip antenna is designed with different feeding techniques. Different feeding techniques are designed and factors like return loss, directivity, gain, and radiation efficiency are analyzed.

### 2.10.1 Antenna Design and discussion

The layout of the suggested MPA with a dissimilar design that contains a metallic patch with FR4 epoxy with dielectric relative permittivity ( $\epsilon_r$ ) of 4.4 with a height of 1.6 mm. To achieve good antenna performance, a substrate with thick height is used because it is responsible for greater bandwidth and improved radiation [185]. The three patch antennas are designed using HFSS (v 13) software.

#### 2.10.1.1 MPA Design with Coaxial Feed technique

The patch antenna is intended at the resonant frequency of 2.4 GHz for Bluetooth application. The dimensions of the patch are intended using [186]

$$L = L_{eff} - 2\Delta L \quad (2.27)$$

$$L_{eff} = \frac{c}{f \sqrt{\epsilon_{eff}}} \quad (2.28)$$

$$W = \frac{c}{2f\sqrt{\epsilon_r + 1}} \quad (2.29)$$

$$\epsilon_{eff} = \frac{\epsilon_r + 1}{2} + \frac{\epsilon_r - 1}{2} \left( 1 + 12 \frac{h}{W} \right)^{-1/2} \quad (2.30)$$

where  $L$ ,  $L_{eff}$ ,  $f$ ,  $W$ ,  $h$ , and  $\epsilon_{eff}$  indicates the patch length, effective length, resonant frequency, patch width, substrate height, and effective dielectric constant, respectively. The effect length is intended using [187]

$$\Delta L = 0.412h \frac{(\epsilon_{eff} + 0.3) \left( \frac{W}{h} + 0.264 \right)}{(\epsilon_{eff} - 0.258) \left( \frac{W}{h} + 0.8 \right)} \quad (2.31)$$

The intended effective dielectric  $\epsilon_{eff}$  is equal to 4.04. So, the patch length is 1.116 mm. Additionally, the intended dimension of the patch is presented in Table 2.1. The intended effective dielectric  $\epsilon_{eff}$  is equal to 4.04.

**Table 2.1:** Parameters of inset feed MPA Design

S. No	Parameters	Values (mm)
1.	Width of patch( $W_{P2}$ )	29.44
2.	Length of patch( $L_{P2}$ )	38.04
3.	Width of the substrate( $W_{S2}$ )	49.75
4.	Length of the substrate( $L_{S2}$ )	50
5.	Slot width ( $C_W$ )	2.4
6.	Slot Depth ( $C_D$ )	5
7.	Feed Length( $f_l$ )	20
8.	Feed width( $f_w$ )	1.6

### 2.10.1.2 Simulated Results of MPA

Figure .2.13 indicates the return loss of the MPA. If the value of return loss less than  $-10$  dB, this means that 90% of the incident power is transmitted to the antenna [188]. The attained BW for coaxial feed is 50 MHz. The return loss and bandwidth ( $BW$ ) are as [189]

$$RL = -20\log(\Gamma) \quad (2.32)$$

$$BW = \frac{(f_h - f_l)}{f_c} * 100 \quad (2.33)$$

**Table 2. 2:** Parameters of Coaxial feed MPA Design

S. No	Parameters	Values (mm)
1.	Width of patch( $W_{P1}$ )	30
2.	Length of patch( $L_{P1}$ )	39.5
3.	Width of the substrate ( $W_{S1}$ )	90
4.	Length of the substrate ( $L_{S1}$ )	100
5.	Feeding point( $Y_0$ )	4.3
6.	The radius of the internal conductor	0.7
7.	The radius of the external conductor	1.7

Ideally, the value of return loss is zero or 0 dB for the perfectly matched condition. Practically the value of return loss ranges from 1 to 2 dB. Figure 2.16 shows the radiation plot.

### 2.10.1.3 MPA with inset Feed

Inset Feed is used to match the impedance of the feedline to the patch to attain decent antenna efficiency. The inset feed is designed by the intended given formula as [188]

$$R_m(C_D) = \frac{1}{2(G_1 + G_{i2})} \cos^2\left(\frac{\pi}{L} C_D\right) \quad (2.34)$$

$$G_1 = \begin{cases} \frac{1}{90} \left( \frac{W}{\lambda} \right)^2 & W \ll \lambda \\ \frac{1}{120} \left( \frac{W}{\lambda} \right) & W \gg \lambda \end{cases} \quad (2.35)$$

$$G_{12} = \frac{1}{120\pi^2} \int_0^\pi \left[ \frac{\sin^2 \left( \frac{k_0 W}{2} \right)}{\cos \theta} \right] J_0(k_0 \sin \theta) \sin^3 \theta d\theta \quad (2.36)$$

$$R_{in}(C_D) = \frac{1}{2(G_1 + G_{12})} \cos^2 \left( \frac{\pi}{L} C_D \right) \quad (2.37)$$

Where  $R_{in}(C_D)$  is the input impedance at point C

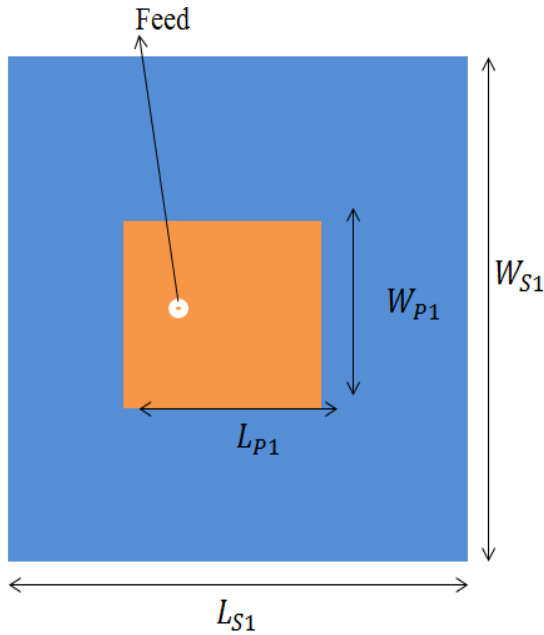


**Figure 2.13:** layout MPA with Coaxial probe feed

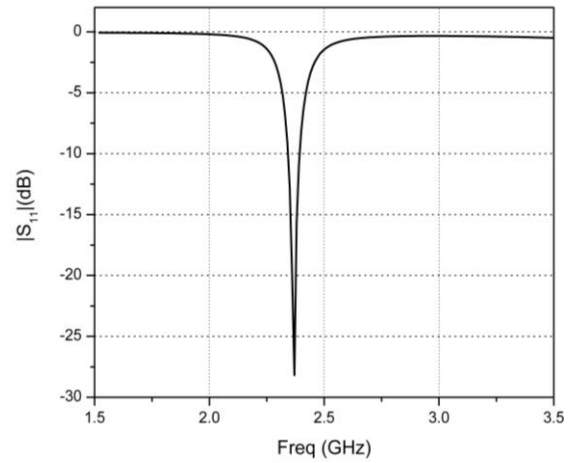


**Figure 2.14:** Return loss of inset feed

#### 2.10.1.4 Simulated results of MPA with Inset feed

Figure 2.16 displays the return loss. The intended parameters of MPA with inset is presented in Table 2.2. Figure 2.17 indicates the H plane and E plane curves of rectangular MPA with inset feed at 2.4 GHz center frequency. [18]

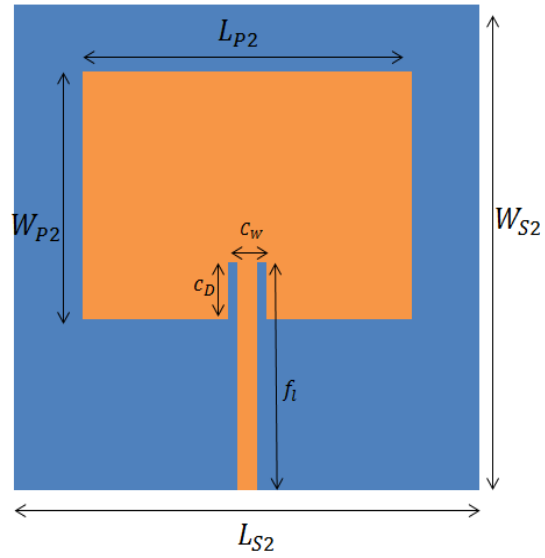


**Figure 2. 15:** Layout of MPA with inset feed

**Table 2.3:** Parameters of Quarter wavelength feed MPA Design

S No.	Parameters	Values (mm)
1.	Width of patch( $W_{P3}$ )	29.26
2.	Length of patch( $L_{P3}$ )	36.26
3.	Width of substrate ( $W_{S3}$ )	45
4.	Length of substrate ( $L_{S2}$ )	60.94
5.	Feed length ( $f_{l1}$ )	5
6.	Feed length ( $f_{l2}$ )	15
7.	Feed width( $w_{l1}$ )	0.62
8.	Feed width( $w_{l2}$ )	3.05

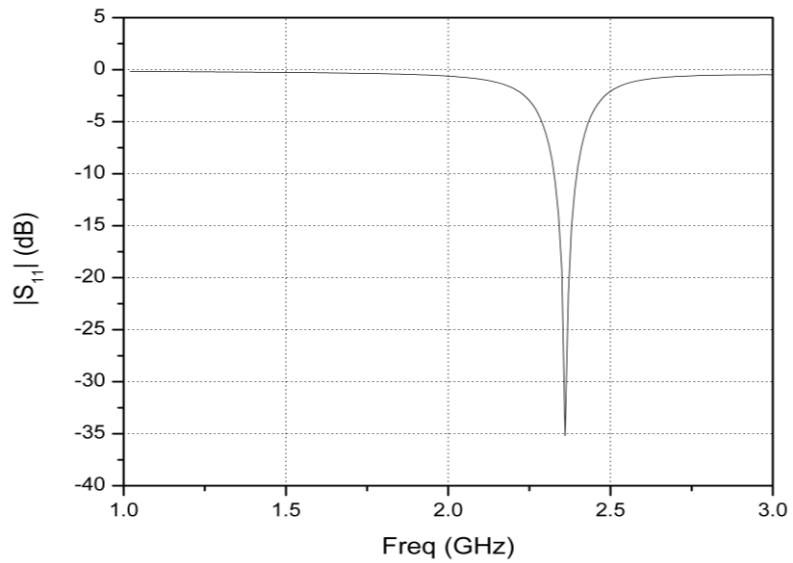


**Figure 2. 16:** Return loss of MPA

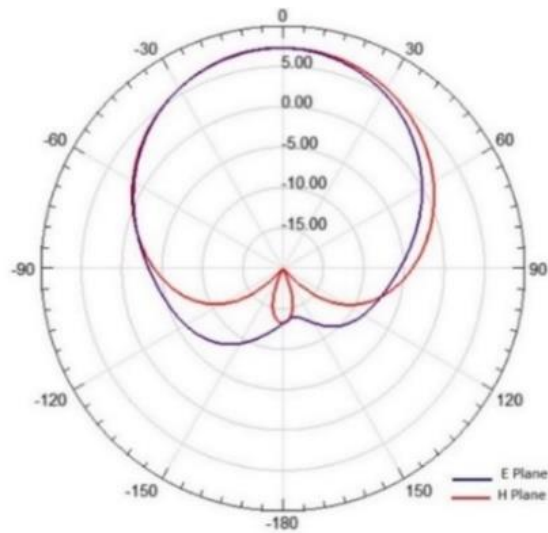


**Figure 2. 17:** Radiation curves of coaxial feed MPA

#### 2.10.1.5 Simulated results of MPA with Quarter wavelength Feed

Figure 2.18 indicates the return loss. It is observed from Figure 2.18 that the BW attained is 80 MHz. The radiation curves of rectangular MPA with Quarter wavelength feed at 2.4 GHz center frequency presented in Figure 2.19.

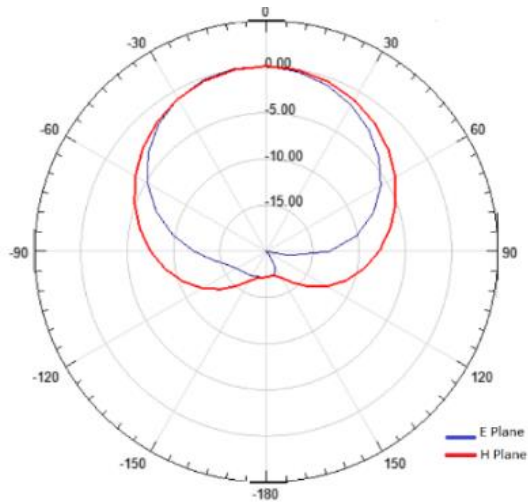


**Figure 2. 18:** Radiation curves of inset feed MPA

### 2.10.1.6 Comparison between three different feeding techniques

The comprehensive comparison of all feeding methods is presented in table 2.3. These feeding methods are Microstrip inset Line, Quarter wavelength, and Co-axial probe feed which define the contrast of dissimilar parameters like directivity and gain [189-191], etc.

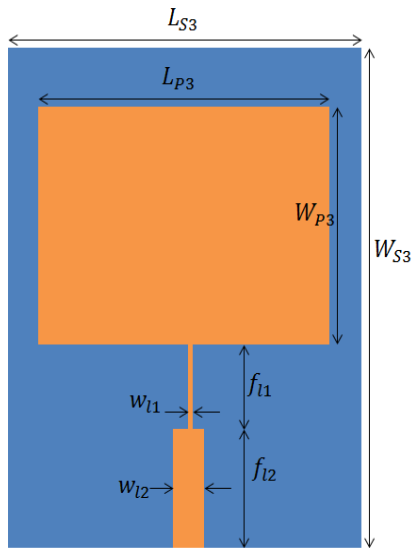


**Figure 2. 20:** MPA with Quarter wavelength feed

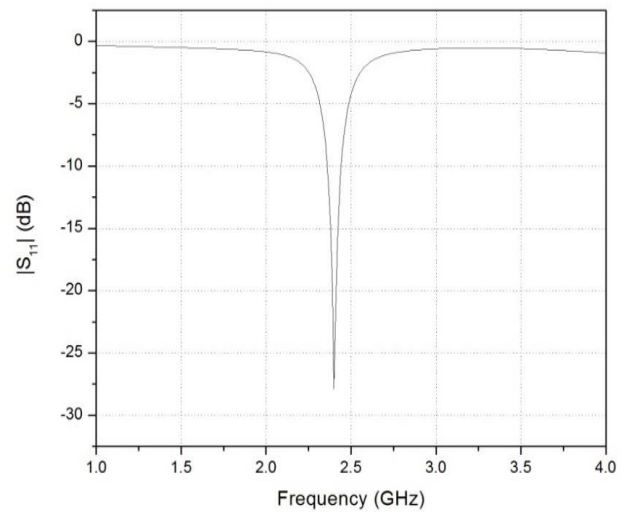


**Figure 2. 19** Return loss

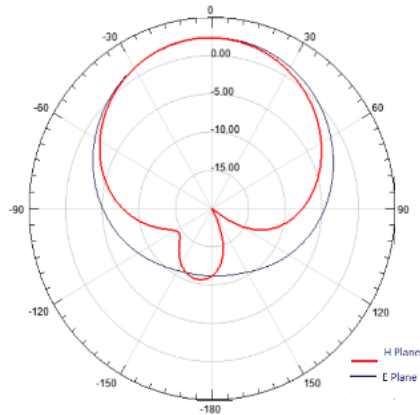


**Figure 2. 21:** Radiation curve

**Table 2.4:** Comparison of numerous feeding methods

S No.	Parameters	Coaxial Feed	Inset Feed	Quarter Wavelength Feed
1.	Return loss (dB)	-26	-35	-27
2.	Frequency (GHz)	2.4	2.4	2.4
3.	Max U(W/sr)	0.0036528	0.070014	0.13607
4.	Bandwidth(MHz)	50	10	80
5.	Peak Gain(dB)	5.3308	1.2	1.7167
6.	Radiated Power (W)	0.0084524	0.047574	0.54238
7.	Peak Directivity(dBi)	5.4309	1.8494	3.152
8.	Accepted power(W)	0.008611	0.86261	0.99607
9.	Incident Power (W)	0.010122	0.0094294	1
10.	Radiation Efficiency	0.98157	0.5515	0.5452
11.	Front to Back Ratio	113.48	56.188	25.795

## 2.11 Summery

In this chapter the introduction and literature review of band-notched UWB MIMO antenna using EBG Structure are discussed. This chapter starts with the historical background of

monopole antennas with feeding techniques and their advantages, disadvantages are discussed. Then an introduction to MIMO antenna with challenges faced to design MIMO antenna is also discussed., Introduction to metamaterials with classifications like ENG, DNG, DPS, and MNG are discussed. Then an introduction to EBGs starts with their systematic evolutions through DGS, PBG, and FSS, etc. Different band gap methods used in this thesis like the dispersion diagram method, reflection phase method with basics are discussed. Introduction of polarization, different type polarization, Antenna polarization loss factor, and advantages of polarization is also discussed. Then an application of the UWB MIMO antenna system with the literature review of EBGs to achieve band rejected features discussed. After this, some popular notched UWB antennas with single double and triple notches are introduced. It is understood from Table 2.4 that different feeding technique of the MPA provides dissimilar results for the same parameters. Feed pickup is an important choice since it interrupts the performance of the system. Different excitation methods provide unlike bandwidth, directivity, gain, and different efficiency, etc. From Table 4 it is observed that coaxial feed achieved improved gain and directivity that is 5.43 dB and 5.33 dB respectively.

**CHAPTER 3**

**COMPACT BAND NOTCHED UWB  
MIMO ANTENNA USING QUARTER  
WAVELENGTH SLOTS**

## CHAPTER 3

# Compact Band notched UWB MIMO Antenna using Quarter wavelength slots

### 3.1 Introduction

In April 2002, the FCC permitted UWB that ranges from 3.1-10.6 GHz for profitable use. A promising method for refining the data rate is UWB technology. UWB technology has fascinated significant consideration due to its features like extremely less power consumption, increased data rate, and low spectral density. It is used in many applications such as high accuracy radar, sensor data collection, imaging, and indoor position systems. UWB is a popular system for a small distance and less power communication. However, some narrowband applications cause interference in the UWB frequency range. To minimize this interference, the antenna with multiple band elimination is needed. Band rejection characteristics can be realized in UWB antennas by using dissimilar shapes of slots. These slits are inserted in radiating patch to generate band elimination for the suppression of interference, for example, an arc-shaped slot, multiple fractal-shaped slots, vertical H-shaped slot, half wavelength slot in the antenna element [192], three semi-circle half-wavelength slots, and three straight rectangular strips with open-ends. Further, to attain notches an arc slit on the ground and a fractal arc slit on the radiating patch can be used. Different shapes of stubs like fork-shaped or short stub [193] on the radiator, by using Electromagnetic Band Gap (EBG) structures, can also discard the interfering band. Band rejection resonators like CLL [194] and electric concentric ring [195] are also reported in the literature.

Signal fading is the major problem because of the multipath atmosphere. This problem is solved by the UWB MIMO antenna which delivers better channel capacity. UWB MIMO antennas have a problem of isolation between the radiating patch. EM coupling between the elements disturbs antenna performance. Isolation can be reduced by Defective Ground Structures (DGS)[196] for example in] and U-shape[197]. Another method to achieve better isolation is to extend the ground like a T-shaped strip [198]. Various researchers have discussed dual and triple notched band characteristics of MIMO antenna. After surveying

different techniques, it is realized that achieving a compact size remains a challenge. A miniaturized triple band-notched UWB MIMO antenna is proposed in this work. An I-shaped stub is used to increase the isolation. Open-end quarter wavelength slits are used to attain band rejected notches in interfering bands. The presented antenna has tremendous low isolation and impedance matching.

## 3.2 Proposed UWB MIMO Antenna with triple notches

### 3.2.1 Antenna Design and Analysis

Figure 3.1 displays the dimensions of the structure with an overall size of  $23 \times 40 \times 1.6\text{mm}^3$ . An I-formed stub is connected with a ground plane to increase isolation. FR-4 substrate has relative permittivity ( $\epsilon_r$ ) is 4.4, the thickness of the substrate is 1.6 mm with a loss tangent of 0.02. Further, three open-end quarter wavelength slots denoted as twisted quarter wavelength open-end slot (slot-1), inverted L-shaped open-end slot (slot-2), and rectangular slot (Slot-3) are inserted on the radiator. Slot 1 and slot 2 are twisted to achieve miniaturization in antenna size. Figure 3.2 illustrates the stepwise design of the suggested antenna. Antenna A is a UWB antenna without any notch. Once the UWB antenna is achieved, it is further modified to Antenna B using slot 1 to eliminate interference from the WiMAX/C band. Slot 2 and slot 3 are inserted into the radiating surface to suppress intrusion from WLAN Band and X Band, respectively. The dimension of the presented structure is given in Table 3.1.

**Table 3.1** Augmented dimensions of the Ultra-Wideband antenna

<b>Parameters</b>	$L_S$	$W_S$	$L_g$	$L_f$	$W_f$	$L_{wm1}$	$L_{wm3}$
<b>Unit(mm)</b>	23	40	9.3	9.7	2.6	8	2
<b>Parameters</b>	$L_{wl2}$	$w_g$	$L_x$	$w_s$	$G_A$	$G_F$	$L_G$
<b>Unit(mm)</b>	1.3	0.2	6	0.5	19.7	8.9	11.5
<b>Parameters</b>	$G_H$	$W_{F1}$	$W_{F2}$	$G_P$	$L_{wl1}$	$G_W$	$L_P$
<b>Unit(mm)</b>	6	26	16	2	7	0.7	7.5

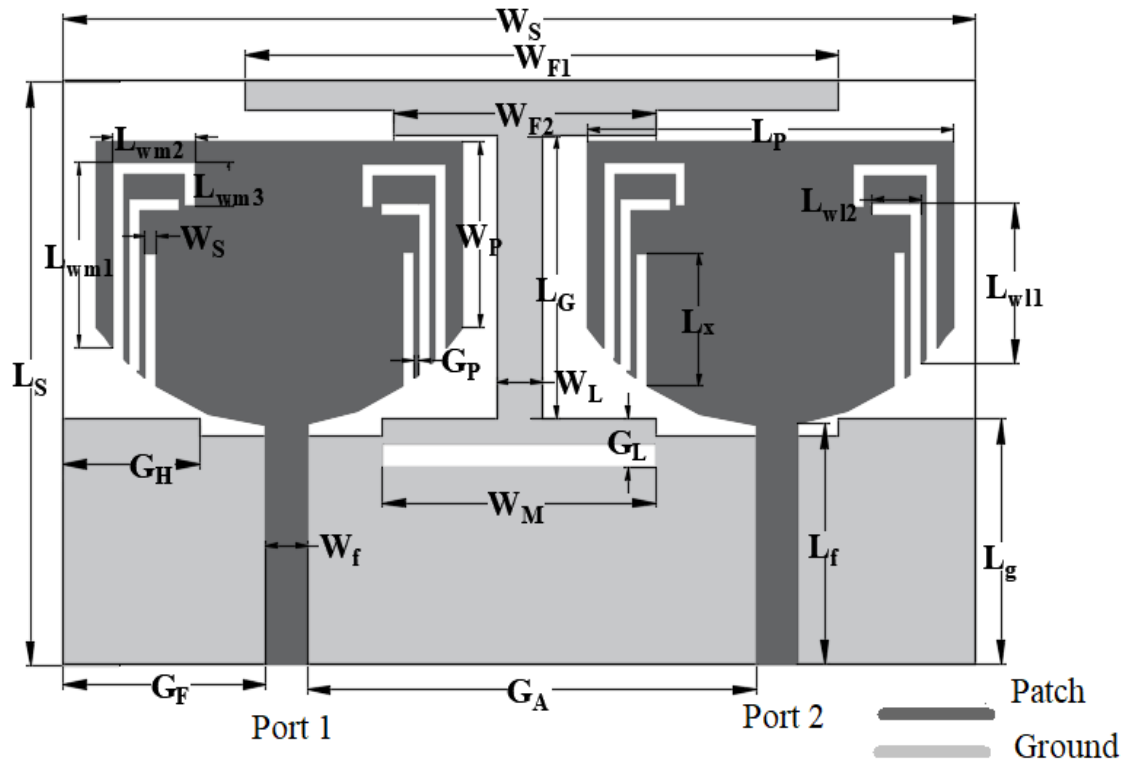


Figure 3.1: Design of Ultra wideband antenna with three quarter wavelength slots

### 3.3 Parametric study

#### 3.3.1 Variation of Slot length

In Figure 3.3, VSWR deviations of all in-between antennas along with the suggested antenna are observed. By inserting open-end slots in the radiator, triple band-notches are achieved. These open-end quarter wavelength slots introduce impedance mismatch. By varying the dimension of the slots, one can adjust notch bands. It is shown that each slot is accountable for rejection production in its frequency range. The total length ( $L_{Wi\max}$ ) of slot-1 is given as [199]

$$L_{Wi\max} = L_{wm1} + L_{wm2} + L_{wm3} \quad (3.1)$$

$$L_{wlan} = L_{wl1} + L_{wl2} \quad (3.2)$$

$$L_{xband} = L_x \quad (3.3)$$

$$L_{slot} = \frac{c}{4f\sqrt{\epsilon_{eff}}} \quad (3.4)$$

$$\epsilon_{eff} = \frac{\epsilon_r + 1}{2} \quad (3.5)$$

Where  $\epsilon_{eff}$  represents the effective dielectric constant. Slot-2 is inserted in the patch to get a band-notch function at the WLAN band. The total length ( $L_{wlan}$ ) of the slot can be given in equation 3.2. The Slot-3 is inserted in the patch that to attain a notch characteristic at the X Band. The entire length ( $L_{xband}$ ) of the slot can be given in equation 3.3. The calculated  $\epsilon_{eff}$  is 2.7. Therefore, the length of slot 1 ( $L_{wimax}$ ) is 13 mm. Figure 3.4 indicates the VSWR for the change of length  $L_{wimax}$  while keeping parameters constant. It is observed from Figure 3.5 that the notched frequency shifts towards 3.8GHz from 4.3GHz, as the length increases from 11mm to 14 mm. The intended length of slot 2 ( $L_{wlan}$ ) for the WLAN band is 8.3 mm. Figure 3.7 indicates the VSWR with the change of length  $L_{wlan}$  while keeping other parameters constant. As the length increases from 5mm to 8 mm, the center notched frequency shifts from 6.2 GHz to 5.5 GHz

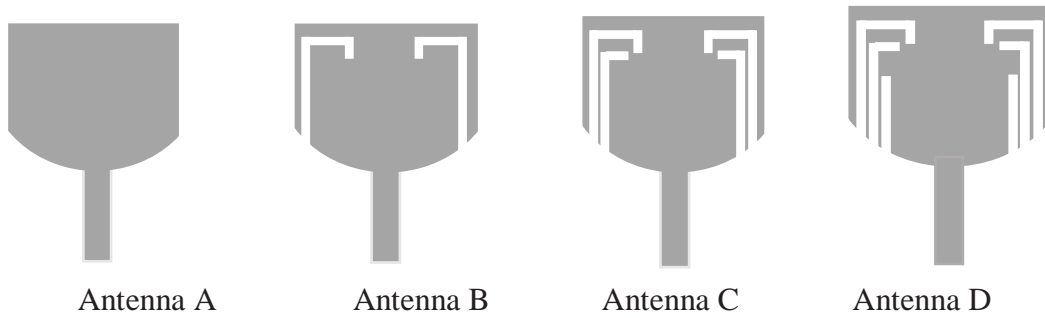


**Figure 3. 2:** Stepwise expansion

For the X band, the calculated length of slot 3 ( $L_{xband}$ ) is 6mm. Figure 3.6 illustrates the VSWR for the change of length  $L_x$  while keeping other parameters constant. By varying the length from 6 mm to 9mm, the center notched frequency changes 8 GHz to 6.9 GHz. It can be

observed from Figure 3.4 3.5, and 3.6 that tuning a particular slot length does not disturb the other notch frequency. Therefore, coupling among slots is very little and can be tuned individually.

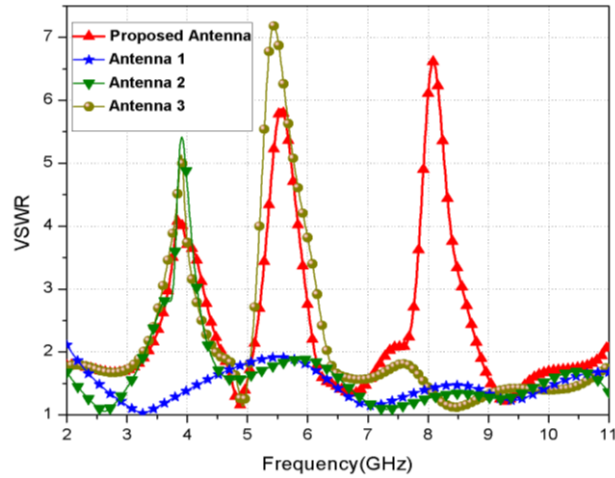


**Figure 3.3:** Variation of different antenna structure

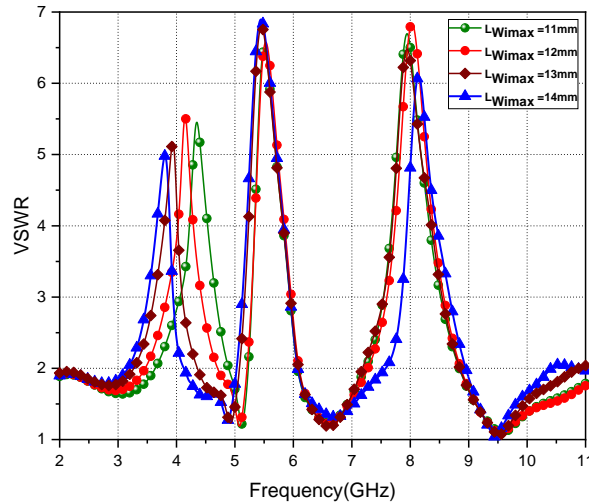


**Figure 3.4:** Variation of WiMAX Length

### 3.3.2 Effect of Variation of Ground Plane

The antenna performance also depends on the ground plane. Due to the modified ground plane, the isolation is enhanced. Figure 3.7 illustrates the stepwise expansion of the UWB MIMO antenna ground plane design. Antenna D in Figure 3.7 is selected for the presented MIMO antenna design to have triple-band notches. Further, Figure 3.8 shows mutual coupling

deviations with different ground plane shapes. It is observed from Figure 3.8 that the finest performance can be attained using ground plane D.

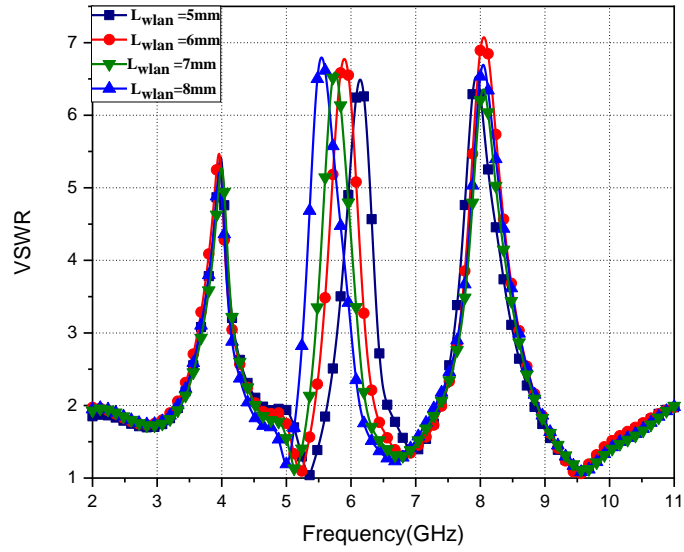


Figure 3.5: Variation of WLAN Length

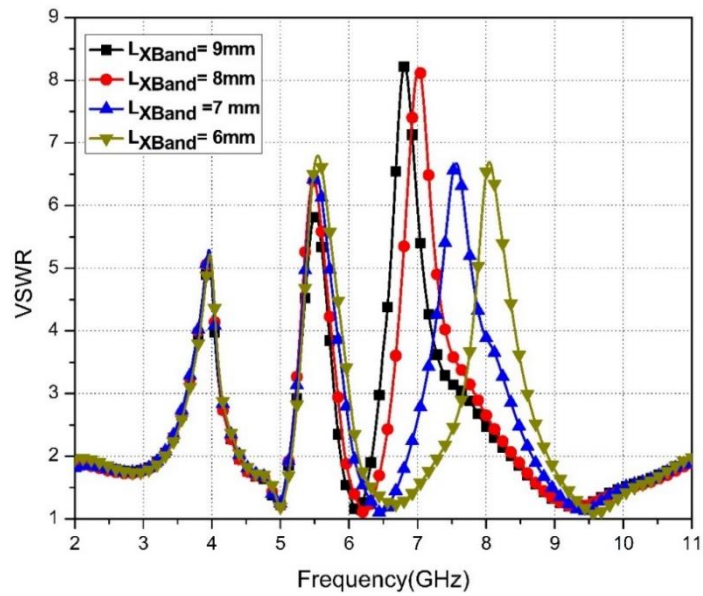
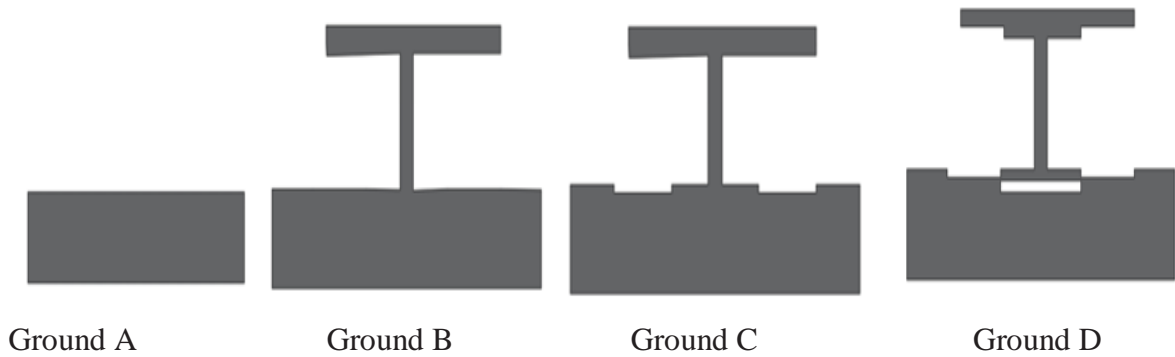
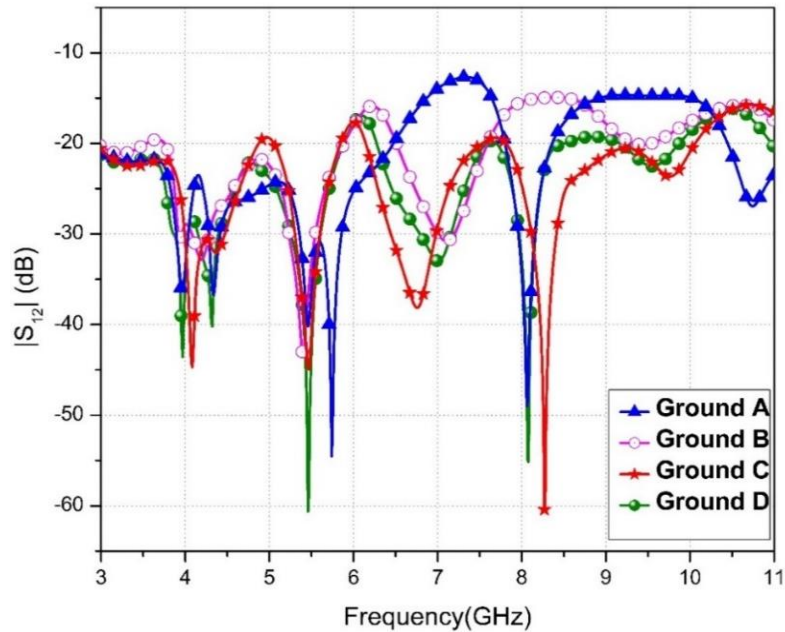


Figure 3.6 Variation of X Band Length



**Figure 3. 7:** Extension of the metallic ground surface



**Figure 3. 8:** Variation of mutual coupling in the different ground plane

### 3.3.3 Current Distribution Analysis

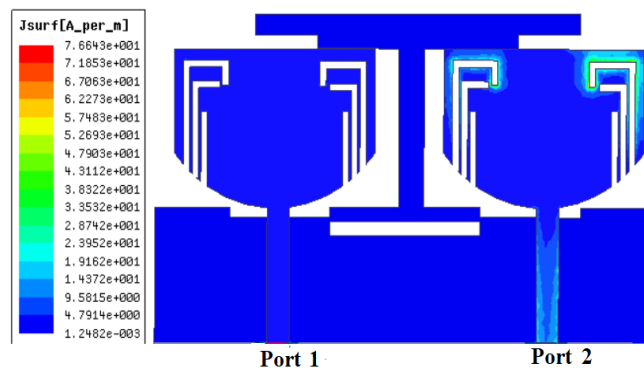
Figure 3.9 depicts the current is focused on slot 1, slot 2, and slot 3 of the radiator, respectively. Here, in all three cases, the current is concentrated along the slot are in the opposite direction. Therefore, VSWR is greater than 2 at these frequency bands. The surface current is evenly disseminated on the patch and ground plane in all three cases at the former frequency.

### 3.4 Fabrication and Experimental demonstration

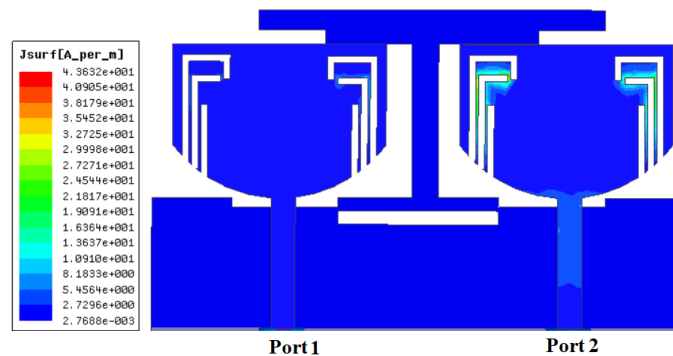
#### 3.4.1. Measured Scattering Parameters and radiation pattern

To validate the simulated curve, the presented structure is made-up using the Ever Precision machine. Scattering parameters and radiation plot and gain of the structure are tested with a vector network analyzer (9 kHz to 13.6 GHz) and an anechoic chamber. The archetype of the presented structure is demonstrated in Figure 3.10. After calibration with the network analyzer, both a return loss and mutual coupling have been measured as shown in Figure 3.11 and 3.12.

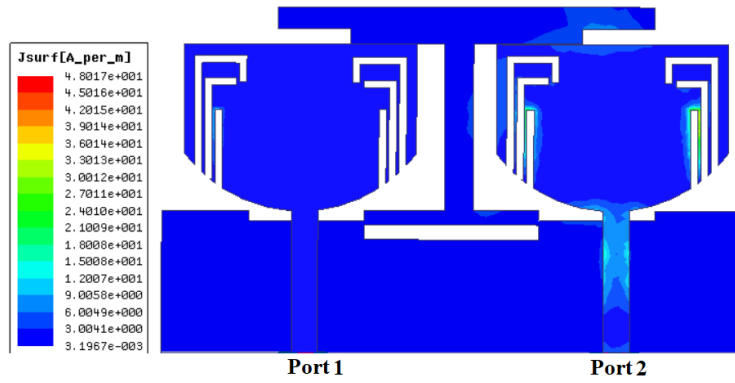
Figure 3.13 displays the simulated and tested VSWR variations. The fabricated presented antenna has -10 dB bandwidth ranges from 2 to 11 GHz range. Another important parameter is mutual coupling presented in Figure 3.14 that is less than -17dB for the entire range of the UWB system. Figure 3.15 displays the measurement set up for the presented triple-band notch fabricated prototype antenna in an anechoic chamber.



(a)

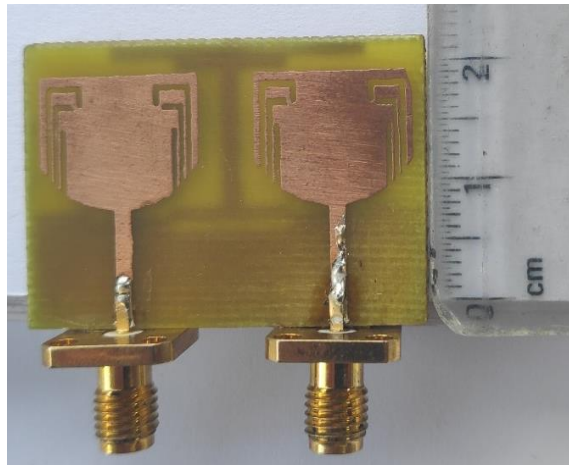


(b)

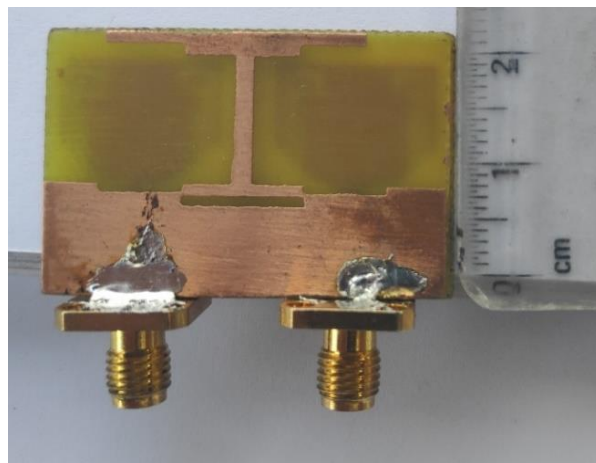


(c)

**Figure 3. 9:** Current distribution of the suggested antenna at notched frequencies



(a)



(b)

**Figure 3. 10** a) Upper sight b) Foot sight of fabricated Suggested antenna

The anechoic chamber is a specially designed room that completely absorbs the reflection of electromagnetic and sound waves [200-205]. A pyramidal horn antenna is used as a receiver antenna with an operating frequency of 700 MHz to 40 GHz. Figure 3.16 (a, b and c) depicts the radiation pattern plot of E Plot and H Plot for both simulated and measured results at different frequencies.

### 3.4.2 MIMO performances:

The diversity characteristics of the MIMO system can be determined using the Envelope correlation coefficient (ECC) and diversity gain (DG) [206]. Correlation is generally used to calculate the resemblances among two radiation plots. ECC and DG in the MIMO system can be evaluated in two possible ways such as by using the scattering parameter and from 3-D radiation pattern [208]. The mathematical relation of ECC for two antenna system using S - parameter is given by [209]

$$ECC = \frac{|S_{11}^* S_{12} + S_{21}^* S_{22}|^2}{(1 - |S_{11}|^2 - |S_{21}|^2)(1 - |S_{22}|^2 - |S_{12}|^2)} \quad (3.6)$$



**Figure 3. 11:** Photograph of the VSWR of the proposed antennas measured using a VNA

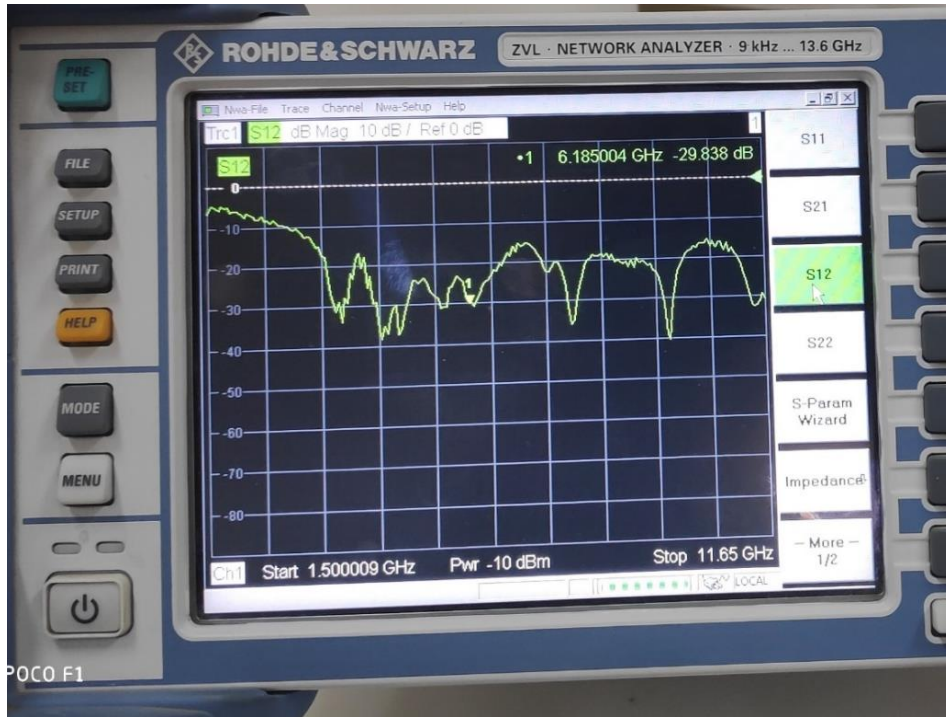


**Figure 3. 12:** Photograph of the mutual coupling of the proposed antennas measured using a VNA

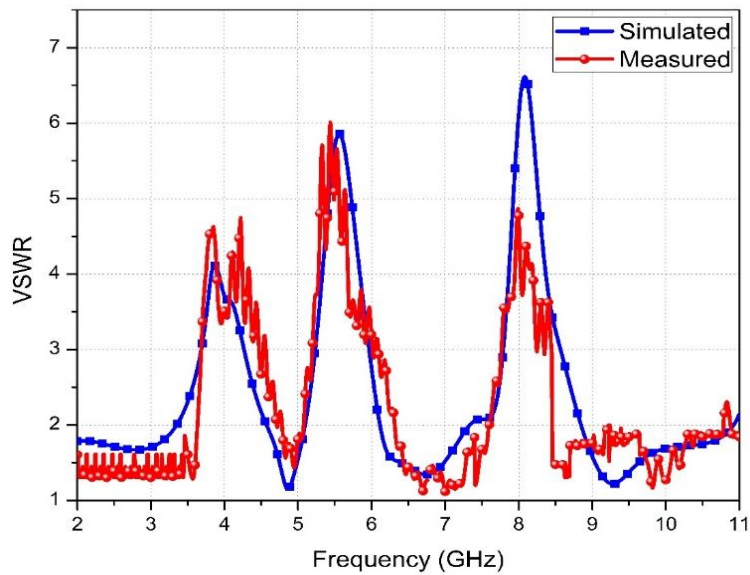


**Figure 3. 13** Measures and simulated VSWR

Ideally, the value of ECC is zero for uncorrelated radiation patterns, but its practical value is less than 0.5. The measured and simulated deviation of ECC and DG with frequency is shown

in Figure 3.17. In the MIMO system, the effect of nearby antenna elements is visible in terms of mutual coupling [209]. As return loss is used to account for the performance of a single antenna element, similarly TARC accounts for the overall system performance. TARC is conveyed as given below [210]:

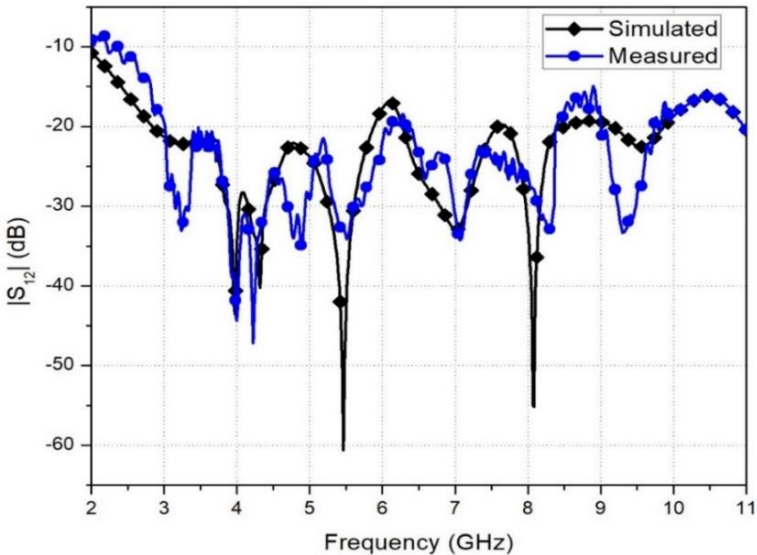
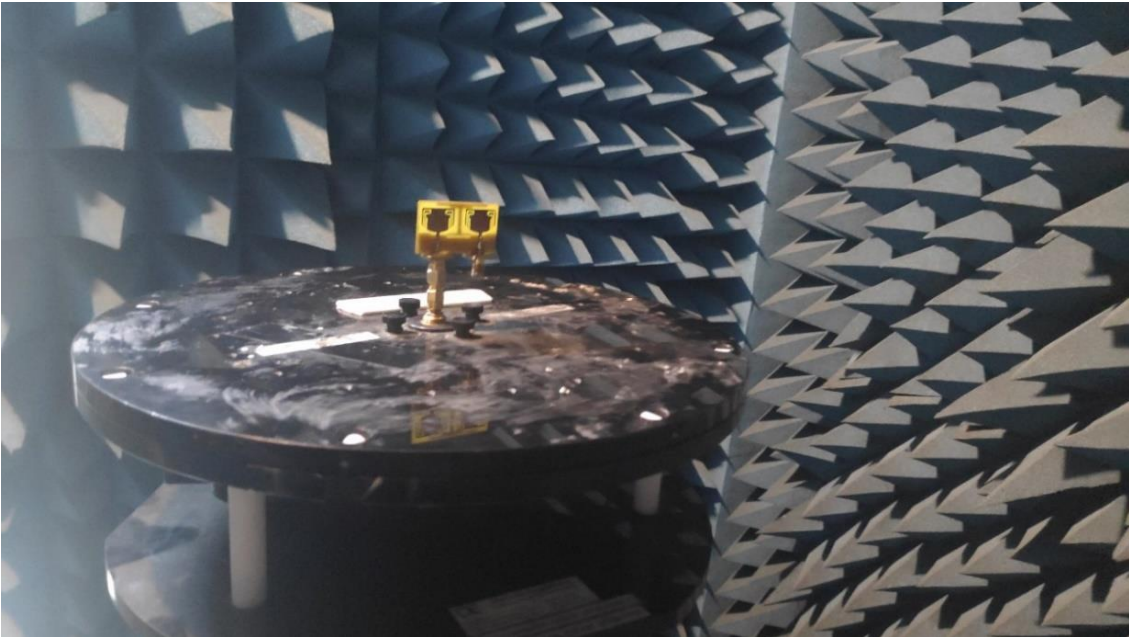
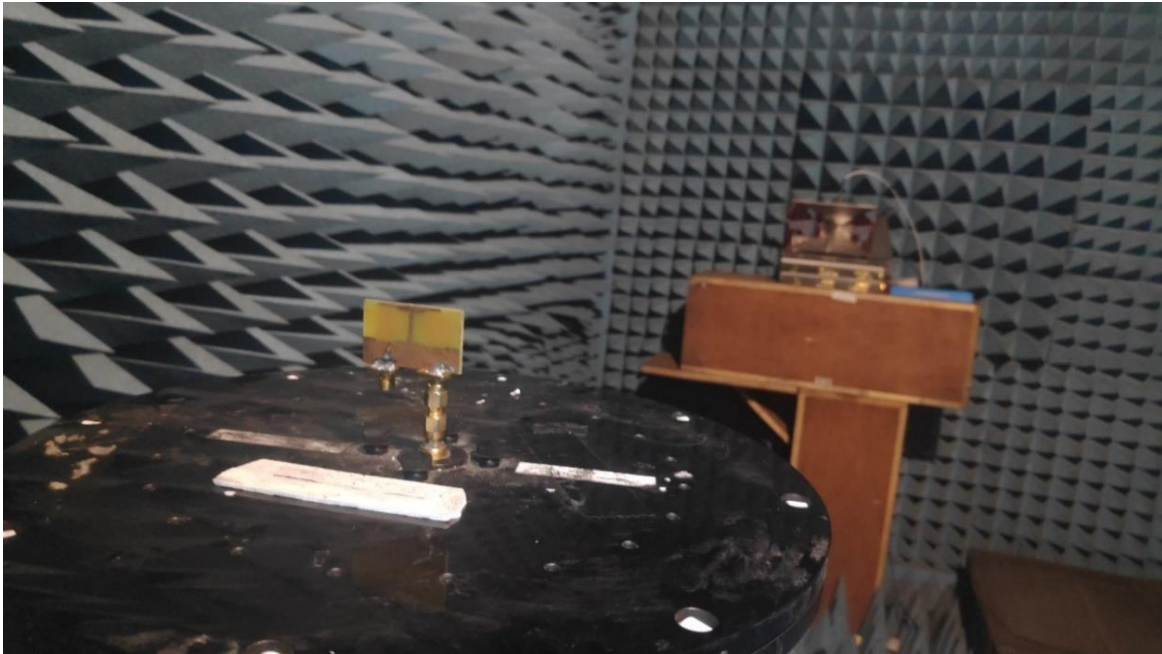


Figure 3. 14: Measures and simulated isolation

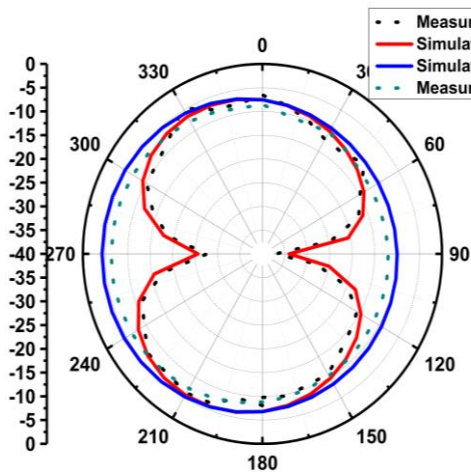


(a)

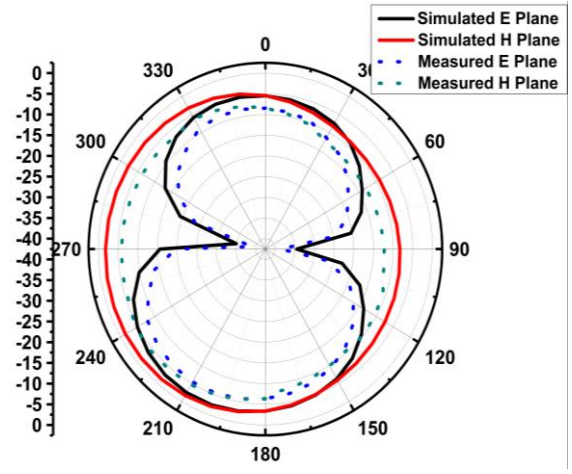


(b)

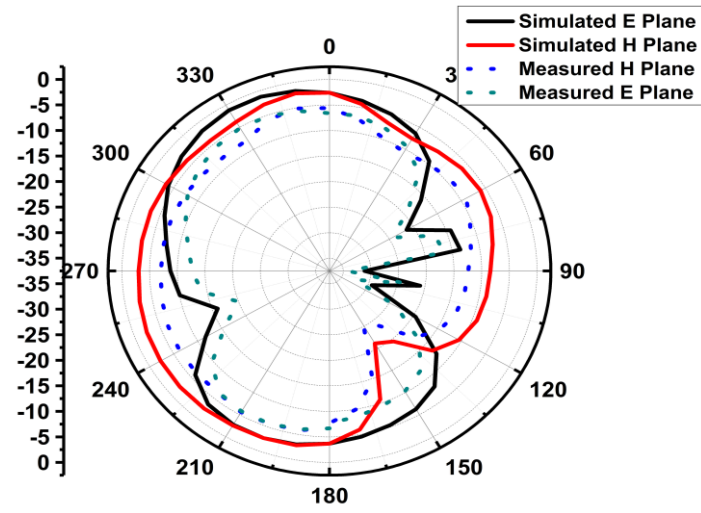
Figure 3.15 Photograph of the measurement of radiation pattern and gain in the anechoic chamber



(a)



(b)



(c)

**Figure 3. 16:** Radiation plot of the suggested antenna (a) 3GHz (b) 5GHz and (c) 9.5GHz

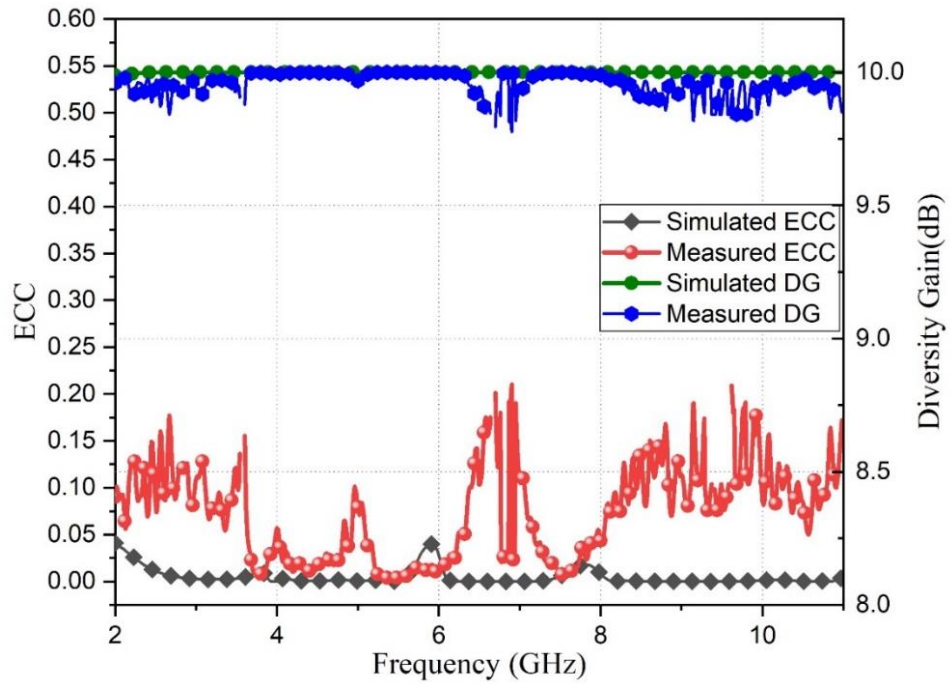


**Figure 3. 17:** Difference between measured and simulated ECC and DG

$$TARC = \sqrt{\frac{(S_{11} + S_{12})^2 + (S_{21} + S_{22})^2}{2}} \quad (3.7)$$

For Multiple antennae, the value should be less than 0 dB. Figure 3.18. presented the difference amid the simulated and tested curve of TARC. It is below -10 dB. Diversity Gain [211-215] is intended as:

$$DG = 10\sqrt{1 - ECC^2} \quad (3.8)$$

Figure 3.19 indicates the radiation efficiency of the suggested structure. With the small dimension and improved mutual coupling, radiation efficiency for the suggested structure is nearly 80% in the functional band.

The MEGs are the fraction of received power (PREC) to the incident power (PINC) of the UWB MIMO Antenna. To calculated UWB MIMO MEG's, the following expression is given as [217]

$$MEG_i = 0.5 \left[ 1 - \sum_{j=1}^N |S_{ij}|^2 \right] \quad (3.9)$$

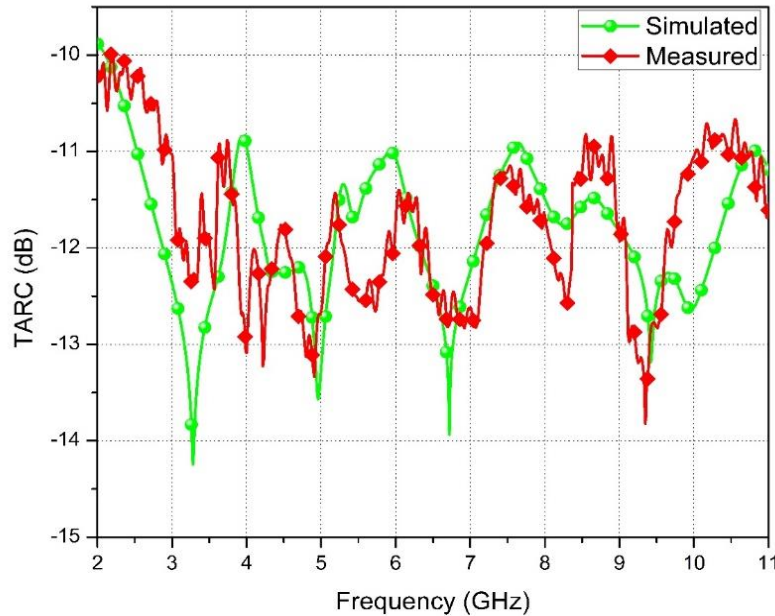


**Figure 3. 18:** TARC variation with frequency

The mean effective gain [219] is calculated using the following equation. So,  $MEG_i$  and  $MEG_j$  is intended as

$$MEG_i = 0.5 \left[ 1 - |S_{11}|^2 - |S_{12}|^2 \right] \quad (3.12)$$

$$MEG_i = \frac{P_{REC}}{P_{INC}} = \oint \left[ \frac{XPR \cdot G_{\theta i} \cdot P_{\theta}(\Omega) + G_{\phi i}(\Omega) \cdot P_{\phi}(\Omega)}{1 + XPR} \right] d\Omega \quad (3.10)$$

On simplifying [218]

$$MEG_i = \frac{e_{tot}^i}{2} \quad (3.11)$$

Here,  $e_{tot}^i$  is the overall efficiency of ith antenna elements

$$MEG_j = 0.5 \left[ 1 - |S_{21}|^2 - |S_{22}|^2 \right] \quad (3.13)$$

Where, i is antenna element 1 and j is antenna element 2. Figure 3.20 indicates the difference MEG's for the suggested structure, we can see that MEG is in between the desired limit [220] for the whole range of the UWB system.

$$\left| MEG_i - MEG_j \right| < 3dB \quad (3.14)$$

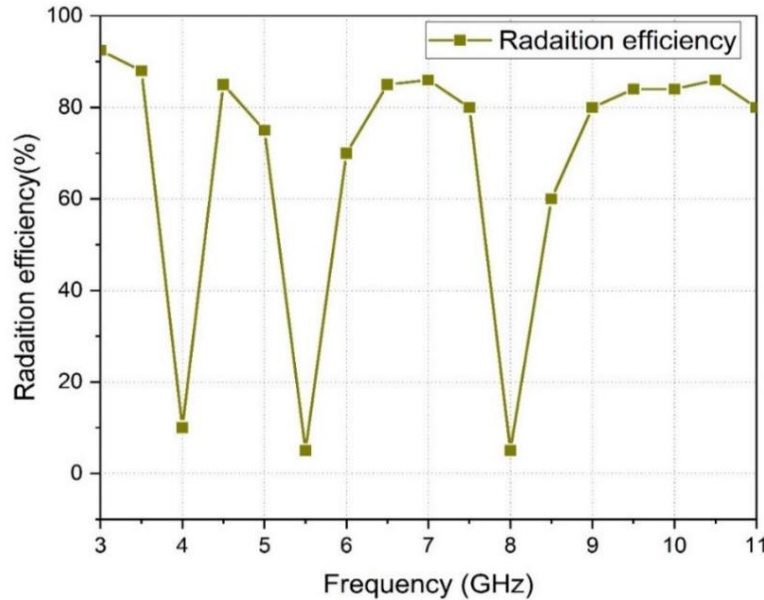


Figure 3.19: Radiation Efficiency plot of Suggested Antenna

**Table 3.2** Evaluation of designed Antenna with existing antenna design

Reference	Dimensions (mm <sup>2</sup> )	Notched band(GHz)	No. of Notches	Bandwidth (GHz)	Isolation (dB)	Radiation Efficiency
[220]	18 x 21	3.3-3.7, 5.15-6 & 7.8-8.4	3	2.9-20	-22	75%-85%
[221]	64×45	3.3-3.6,5-6&7.1-7.9	3	2-10.6	-17	80%
[222]	58×45	3.3-3.6&5-6	2	2.3-10.6	-15	-
[223]	50×50	3.3-3.6,5.15-5.35 &5.725-5.825	3	2.76-10.75	-15	Better than 68%
[224]	48×48	5.1-6.0	1	2.5-12	-18	-
[225]	38.5×38.5	5.03-5.97	1	3.08-11.8	-15	Above 75%
[226]	30×60	3.3-3.8,5.25-5.825&7.7-8.5	3	2.8-11	-20	80%
[227]	40×40	5.1-5.8&7.9-8.4	2	3.4-12	-15	-
[228]	34×49	5.1-5.8	1	3.1-10.6	-18	-
[229]	26.75×41.5	3.3-3.7, 3.7-4.2, & 5.15-5.85	3	3.1 -11.5	-15	75%
[230]	22x26	5.4-5.86 & 7.6-8.4	2	3.1-11.8	-20	85%
<b>Suggested Antenna</b>	<b>23×40</b>	<b>3.3-4.2,5-6&amp;7.2-8.6</b>	<b>3</b>	<b>2-11</b>	<b>-17</b>	<b>Around 80%</b>

Figure 3.21 represents the tested gain and it is noticed that the value of the gain reduces at the notched bands. Many MIMO antennae have been discussed in the literature with band notch

attributes. The suggested structure has a compact dimension than all other antennas mentioned as presented in Table 3.2.

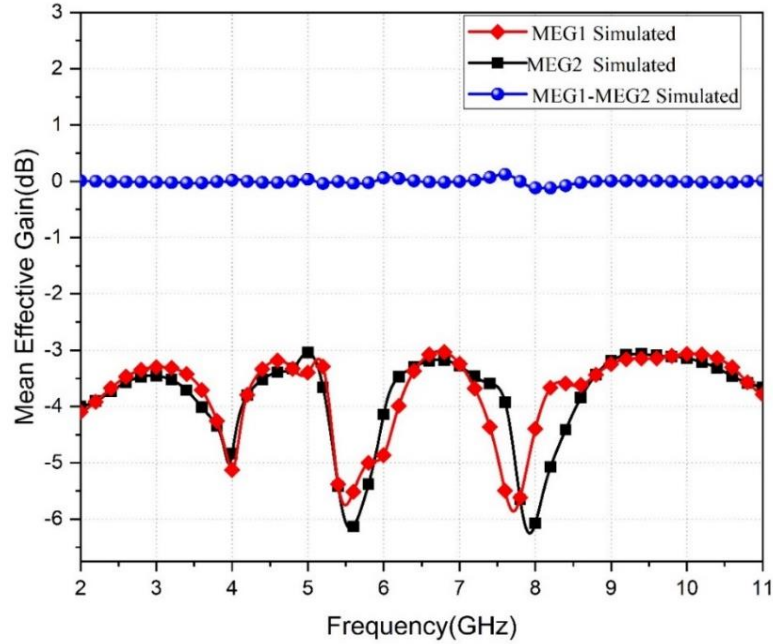


Figure 3.20: MEGs of two Antenna elements

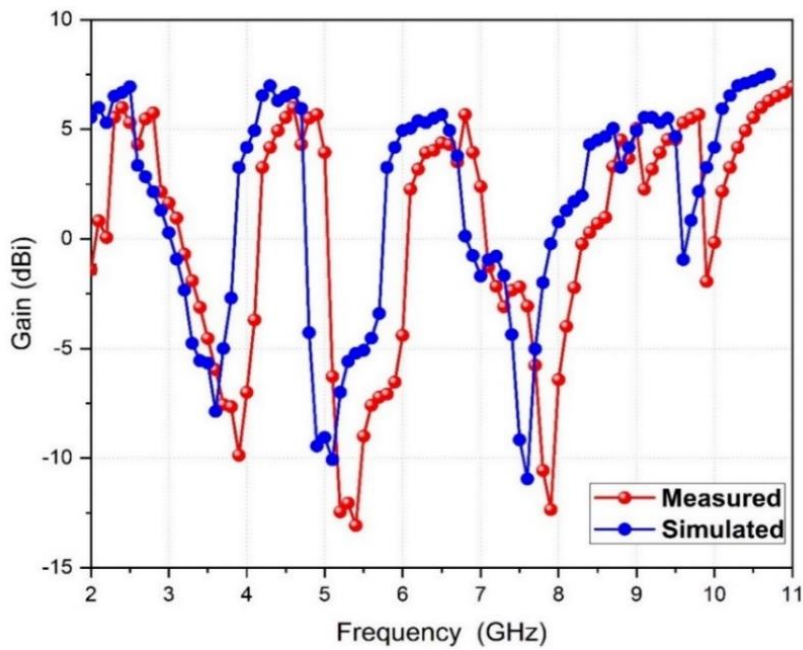


Figure 3. 21: Deviation of Gain with frequency

### **3.5 Summery**

Many band-notched antennas are presented in the works have stated excellent designs with a wideband operation. However, some of these UWB structures suffer from the large size, high profile, interferences in the operation band, utilization of complicated decoupling methods that can affect the fabrication cost, and/or increase antenna complexity. In this chapter, the above issues have been tackled through the proposal of a twisted quarter wavelength to avoid interference from narrowband applications. A multiple band-notched UWB MIMO antenna designed and fabricated having a compact size and high efficiency. The suggested antenna has a functioning impedance bandwidth from 2 to 11GHz ( $VSWR \leq 2$ ) excluding three notch bands: 3.3-4.2 GHz, 5-6 GHz, and 7.2-8.6 GHz. The presented structure indicates the decent MIMO enactment with  $ECC < 0.2$ , the ratio of MEG is in between the desired limits,  $TARC < -10.5$  dB, and radiation efficiency is nearby 80%.The measured result shows respectable similarity

**CHAPTER 4**  
**BAND REJECTED UWB**  
**MIMO/DIVERSITY ANTENNA**  
**WITH TVC EBG STRUCTURE**

## CHAPTER 4

# Band rejected UWB MIMO/DIVERSITY antenna with TVC EBG Structure

### 4.1 Introduction

In the last twenty years, with the growth of the wired network and mobile communication system, numerous wireless access technologies have been progressed. Latterly, with the growth of Smart gadgets like the Home Digital Entertainment Centre, the need for a high transmission rate in wireless technology has fascinated extensive attention. It has been proved that attain improved data rates by combining UWB with the MIMO system[231]. The UWB systems operate from 3.1 to 10.6 GHz comprise channel capacity, eliminate the fading effect, etc. So, by employing the UWB MIMO system, the fading effect and data rate can be further improved without the passive element. Presently, many researchers mainly focus on miniaturization, broadband, high isolation that improve the enactment of the UWB-MIMO antennas. Numerous methods developed in the literature to have enhanced impedance matching with compact size. These techniques are multi-section transformers, tapered lines, and distributed impedance matching[231]. The multi-section transformers method is the modified version of the quarter-wave transformer, employing multiple segments of  $\lambda/4$  transmission lines linked together[232]. The disadvantage of this technique is that it makes the system complex. In the tapered line technique, the feed line width is exponentially increased or decreased for the impedance matching purpose. Another technique is distributed impedance matching where the structure is modified itself without using any passive element for widening the impedance bandwidth. Other than impedance bandwidth, the UWB system requires a band-notched filter to suppress the interference from the narrowband system, therefore, the UWB system doesn't cause any interference to the other existing narrowband system[233]. Numerous designs are discussed in the literature such as etch slots of different shapes such as open-end quarter wavelength rectangular slot [233], arc [234], meandered-[235] in the patch surface or on the ground surface. Another method to achieve band notch characteristics is by adding stub[236] and parasitic elements beside the feed line and rejection

resonators like capacitively-loaded loop[237]. The above-discussed method produces poor radiation patterns due to perturbation in the radiating surface or on the ground plane. Lately, multiple band notches are attained by using a single EBG unit cell. In [238], three bands are excluded by three different EBG Structures. In [239] two EBG structure obtains three rejected bands at three interfering narrow bands. Further in [240], a single EBG structure obtains the triple notches with a size of  $9.4 \times 4.5 \text{ mm}^2$ .

In this editorial, a miniaturized two-element and four elements UWB MIMO antenna with three rejection bands is generated using a one EBG structure. Rather than using multiple EBG cells, a modified EBG cell with C slots is used to attained triple-band notches. Decoupling strips are used to enhance the isolation in radiating elements. MIMO characterizes of the proposed structure are also studied. To validate, the suggested antenna is made-up and tested. Further simulated and tested results show good resembles.

## 4.2 Suggested TVC- EBG unit cell

### 4.2.1. TVC- EBG Structure Design

EBG structure behaves as an LC circuit when the size of the EBG structure is small than the operating wavelength [241]. It acts as a stop-band filter in a particular frequency range. EBG structures have a high impedance in operating frequency which help to eliminate the spread of surface wave. The mushroom EBG structure is consists of the patch, ground, dielectric material, and via. The following formulas can be used to calculate the bandgap frequency of EBG structures [242].

$$L = \mu_0 h \quad (4.1)$$

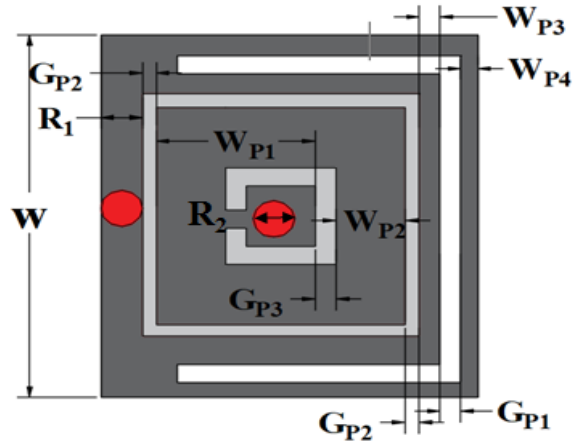
$$C = \frac{w \epsilon_0 (\epsilon_r + 1)}{\pi} \text{Cos}^{-1} \left\{ \frac{2w + g}{g} \right\} \quad (4.2)$$

$$Z_s = \frac{j\omega L}{1 - \omega^2 LC} \quad (4.3)$$

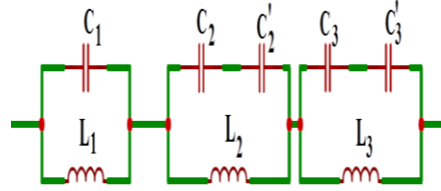
$$f_c = \frac{1}{2\pi\sqrt{LC}} \quad (4.4)$$

$$BW = \frac{\Delta\omega}{\omega} \quad (4.5)$$

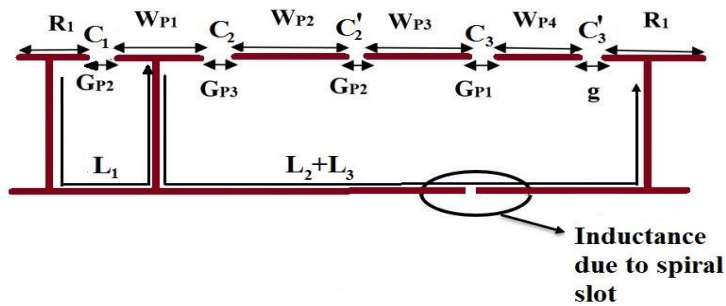
Where  $\epsilon_0$  and  $\mu_0$  are permittivity and permeability,  $\epsilon_r$  is the dielectric substrate,  $Z_s$  is surface impedance,  $f_c$  is the center frequency of bandgap and  $BW$  is the bandgap bandwidth. To obtain size EBG Structure the capacitance( $C$ ) and inductance ( $L$ ) required to be increased. The capacitance can be increased by inserting slots on the EBG patch and inductance can be increased by adding one more via.



(a)



(b)



(c)

**Figure 4. 1** (a) Geometry of the TVC-EBG unit cell (b) Circuit model (c) of TVC-EBG unit cell

Figure 4.1(a) shows the suggested TVC-EBG unit cell. The EBG cell is equal to a three operating circuit demonstrated in Figure 4.1(b). Figure 4.1(c) displays the lateral sight, here  $C_1$  is because of the square slot and  $L_1$  is because of current passing through the edge located via. The three nosey bands  $f_{c1}$ ,  $f_{c2}$  and  $f_{c3}$  [243].

$$f_{c1} = \frac{1}{2\pi\sqrt{L_1C_1}} \quad (4.6)$$

$$f_{c2} = \frac{1}{2\pi\sqrt{L_2C_{2eq}}} \quad (4.7)$$

$$f_{c3} = \frac{1}{2\pi\sqrt{L_3C_{3eq}}} \quad (4.8)$$

$$C_{2eq} = \frac{C_2C'_2}{C_2 + C'_2} \quad (4.9)$$

$$C_{3eq} = \frac{C_3C'_3}{C_3 + C'_3} \quad (4.10)$$

Figure 4.2 demonstrates the incremental extension of the suggested cell. The suggested cell is presented in Figure 4.2(e) realizes three rejected bands.

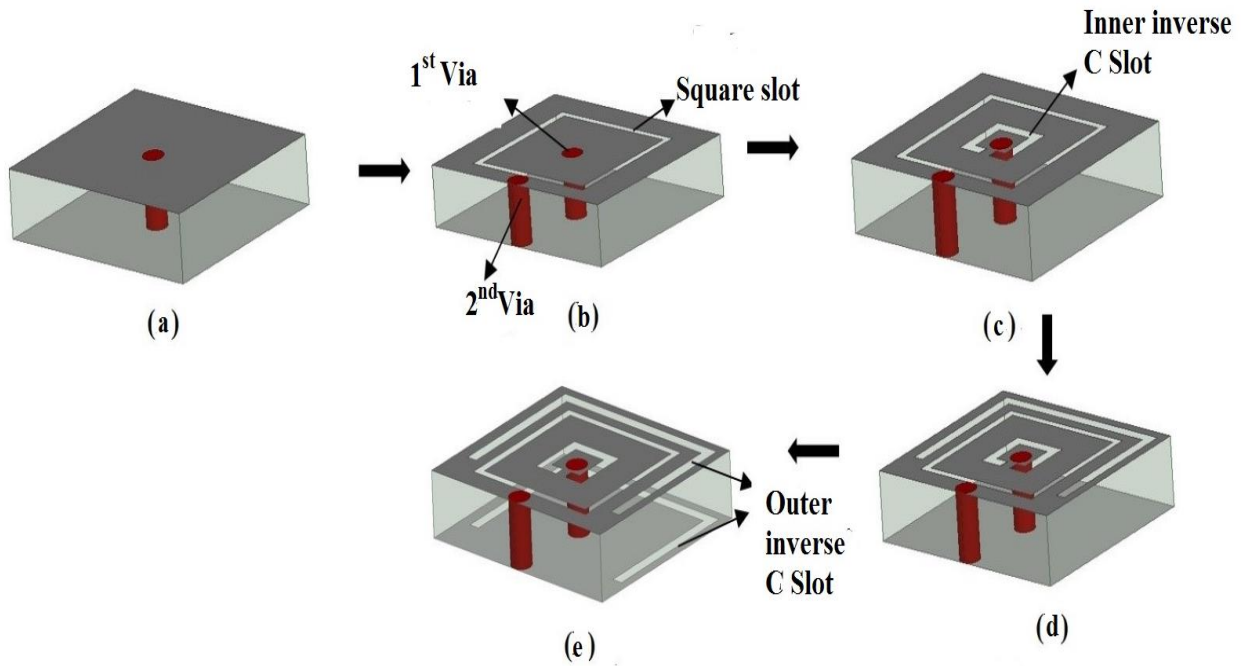


**Figure 4. 2** Extension of the TVC-EBG unit cell

### 4.3. Suggested UWB MIMO/DIVERSITY antenna with TVC-EBG unit cell

Figure 4.3. shows the geometric arrangement of the presented structure. The total size of the presented structure is  $21 \times 36 \times 1.6 \text{ mm}^3$ . Figure 4.4 indicates the VSWR of the presented structure. The bandwidth of the presented structure ranges from 2 to 11 GHz. Whereas with TVC-EBG the UWB MIMO antenna has band rejection.

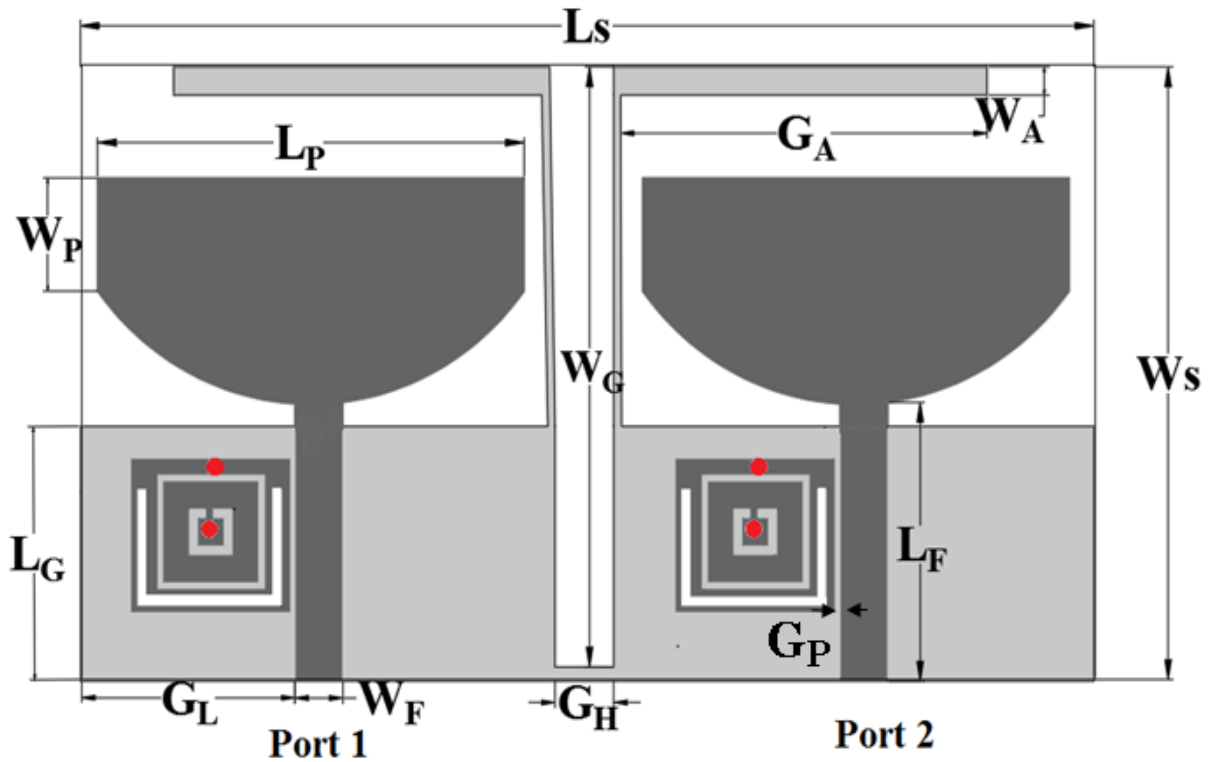


Figure 4. 3 UWB MIMO structure with TVC-EBG cell

## 4.4 Experimental Results and Discussion

### 4.4.1 Measured scattering parameters

Figure 4.5. represents the geometry of two elements UWB MIMO antenna. Figure 4.6 displays the measurement set up for the presented triple-band notch fabricated prototype antenna in a microwave shield chamber Figure 4.6 indicates the simulated and tested the VSWR of the band-rejected presented antenna. The isolation between the patch is ominously

improved by inserting converse L formed stumps on the ground plane. Moreover, to reduce the mutual coupling, a slot is etched on the ground plane. The mutual coupling of the presented structure is illustrated in Figure 4.8. It is perceived that isolation is below than -15 dB from 7 to 10.5 GHz and, and below than -20 dB at other frequencies range. Measured curves confirm good similarity with simulated curves. The insignificant difference among measured and simulated curves is due to losses because of the inaccuracy in the manufacture, solder connectors, and testing process.

#### 4.4.2 Radiation patterns characteristics

Figure 4.9. Indicates the measured and simulated radiation plot of different frequencies. Far-field curves are tested in a shielded chamber. Testing is completed with pretentious that Port 1 is excited, despite the fact Port 2 is closed with 50  $\Omega$ . The plot is the nearly spherical shape in the H plane and dumbbell formed in the E plane.

**Table 4. 1** Augmented dimensions of the presented antenna

<b>Parameters</b>	<b>L<sub>S</sub></b>	<b>W<sub>S</sub></b>	<b>W<sub>A</sub></b>	<b>W<sub>P</sub></b>	<b>L<sub>F</sub></b>	<b>L<sub>G2</sub></b>	<b>G<sub>L</sub></b>
<b>Unit(mm)</b>	36	21	1	4	9	7.8	8.2
<b>Parameters</b>	<b>W<sub>G</sub></b>	<b>R<sub>1</sub></b>	<b>R<sub>2</sub></b>	<b>G<sub>P1</sub></b>	<b>G<sub>P2</sub></b>	<b>W<sub>P1</sub></b>	<b>W<sub>P2</sub></b>
<b>Unit(mm)</b>	21	0.6	0.6	0.4	0.25	2.3	1.3
<b>Parameters</b>	<b>G<sub>P3</sub></b>	<b>W<sub>P4</sub></b>	<b>G<sub>H</sub></b>	<b>G<sub>P</sub></b>	<b>L<sub>wl1</sub></b>	<b>G<sub>w</sub></b>	<b>W<sub>A</sub></b>
<b>Unit(mm)</b>	0.3	0.3	2.2	0.2	7	0.7	1

#### 4.4.3 MIMO Characteristics

The presented structure enactment parameters can be intended using the ECC, DG, TARC, and RE. ECC can be evaluated using S-parameters [244-245].

$$ECC = \frac{|S_{11}^* S_{12} + S_{21}^* S_{22}|^2}{(1 - |S_{11}|^2 - |S_{21}|^2)(1 - |S_{22}|^2 - |S_{12}|^2)} \quad (4.12)$$

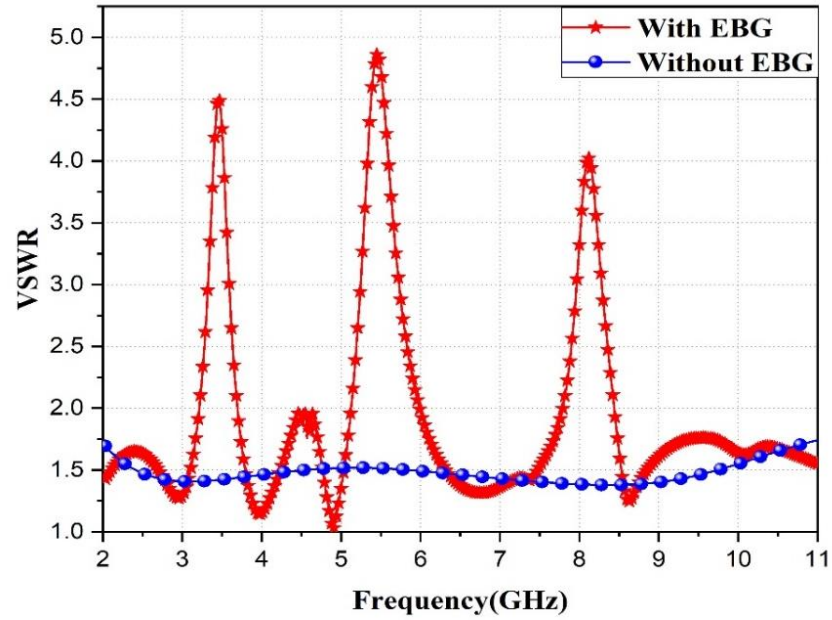
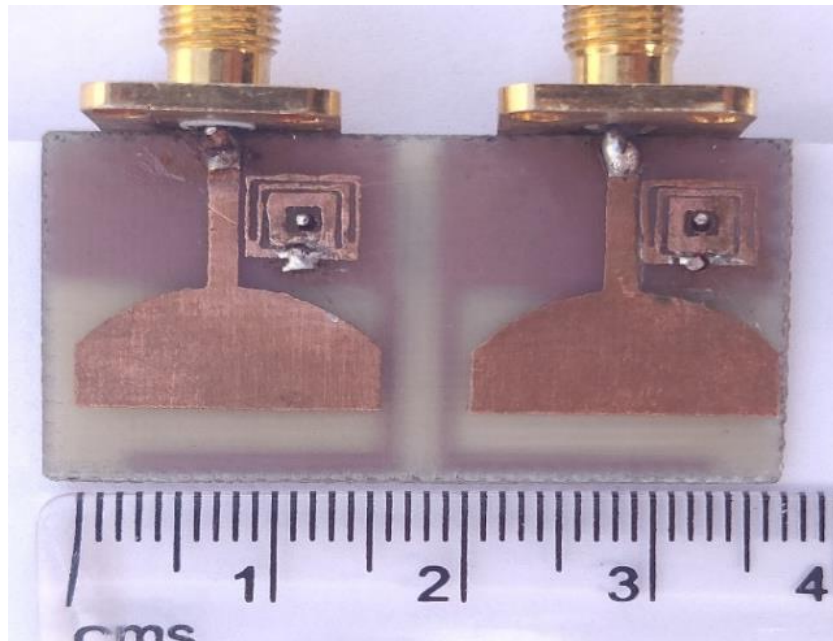
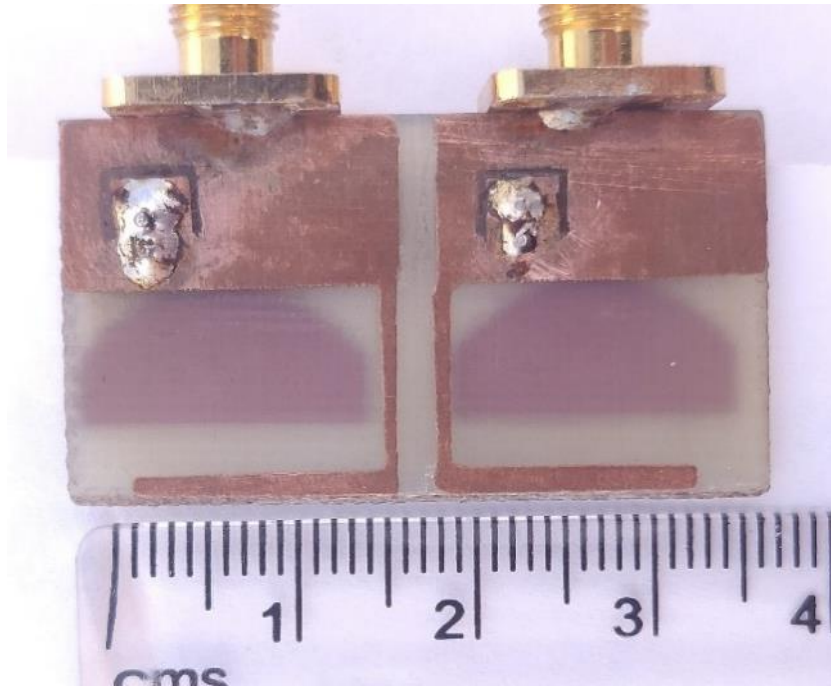


Figure 4. 4 VSWR of the presented structure

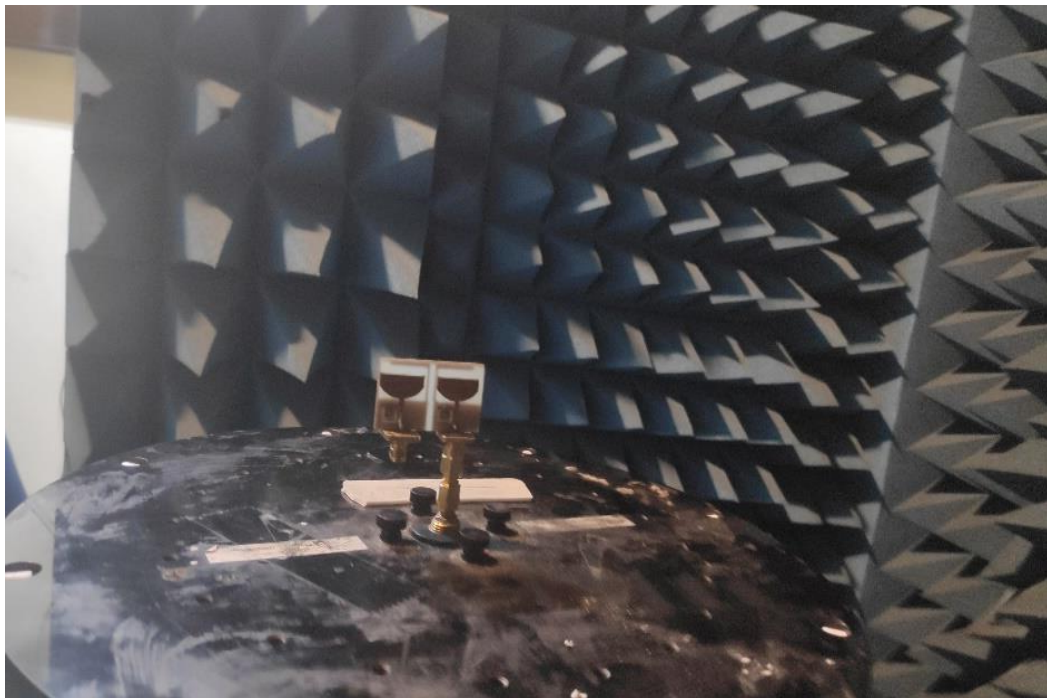


(a)

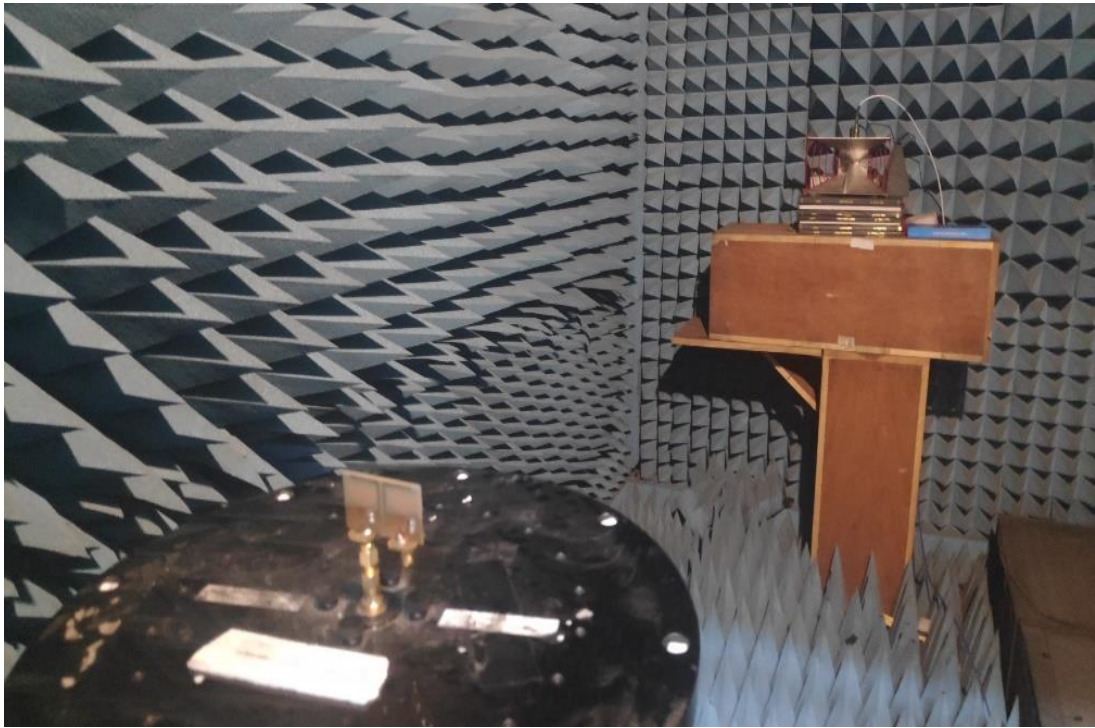


(b)

**Figure 4. 5** a) Upper sight b) Foot sight



(a)



(b)

Figure 4. 6 Measurement set up for proposed dual notch fabricated prototype antenna in the anechoic chamber

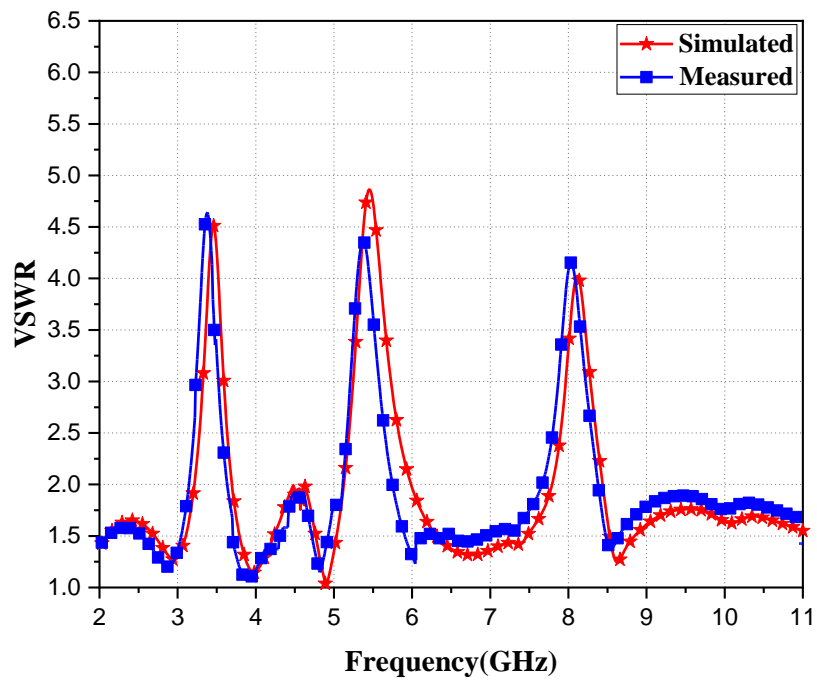
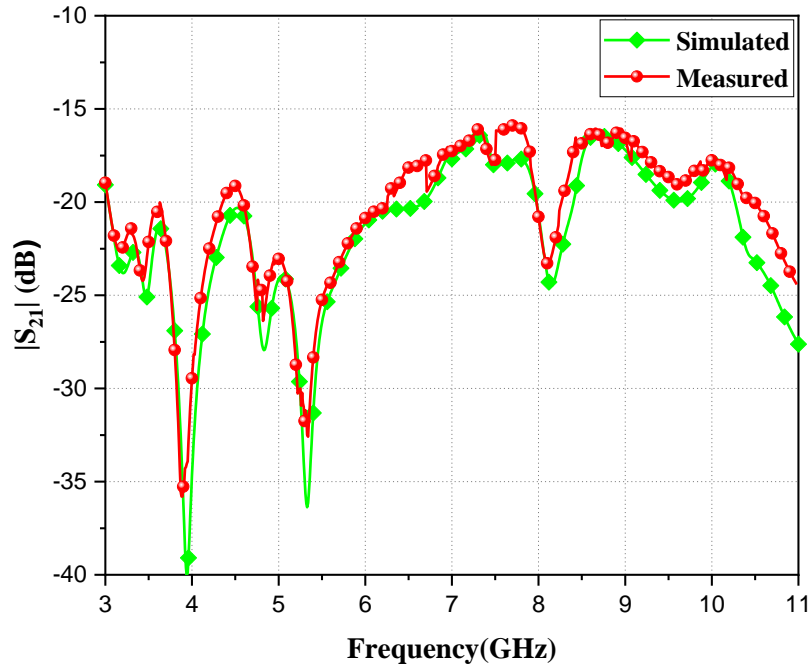


Figure 4. 7 VSWR of the fabricated prototype

Figure 4.10 represents the measured and simulated ECC and DG. The similarity of the presented structure is below 0.005 for the whole range eliminating the intrusive bands. ECC increases to 0.15. DG [246] of the suggested structure is correlated to the ECC which is specified as

$$DG = 10\sqrt{1 - ECC^2} \quad (4.13)$$

Figure 4.10 states that the DG is about 9.98 dB for the complete working bands.



**Figure 4. 8** Mutual couplings of the presented structure

TARC for the presented structure is specified as [247]:

$$TARC = \sqrt{\frac{(S_{11} + S_{12})^2 + (S_{21} + S_{22})^2}{2}} \quad (4.14)$$

Figure 4.11 indicates the simulated and measured curves of TARC. The achieved value of TARC is below -15 dB for the whole for the operating band, eliminating the rejected bands where TARC rises to -10 dB. Another important parameter is gain that has the ability of the antenna to communicate electromagnetic waves in a specific direction. Figure 4.12 demonstrates the deviation of gain and radiation efficiency.

#### 4.4.3 Comparison of the proposed antenna with published work

A relative study of dissimilar EBG structures is done in Table 4.2. In Ref. [248-252]. EBG unit cell operates at a single frequency. Though unit cell in ref. [253] operates at dissimilar frequencies, however, the suggested structure has a small size and specific. Table 4.3 indicates a valuation of the proposed structure with the available structure in the work.

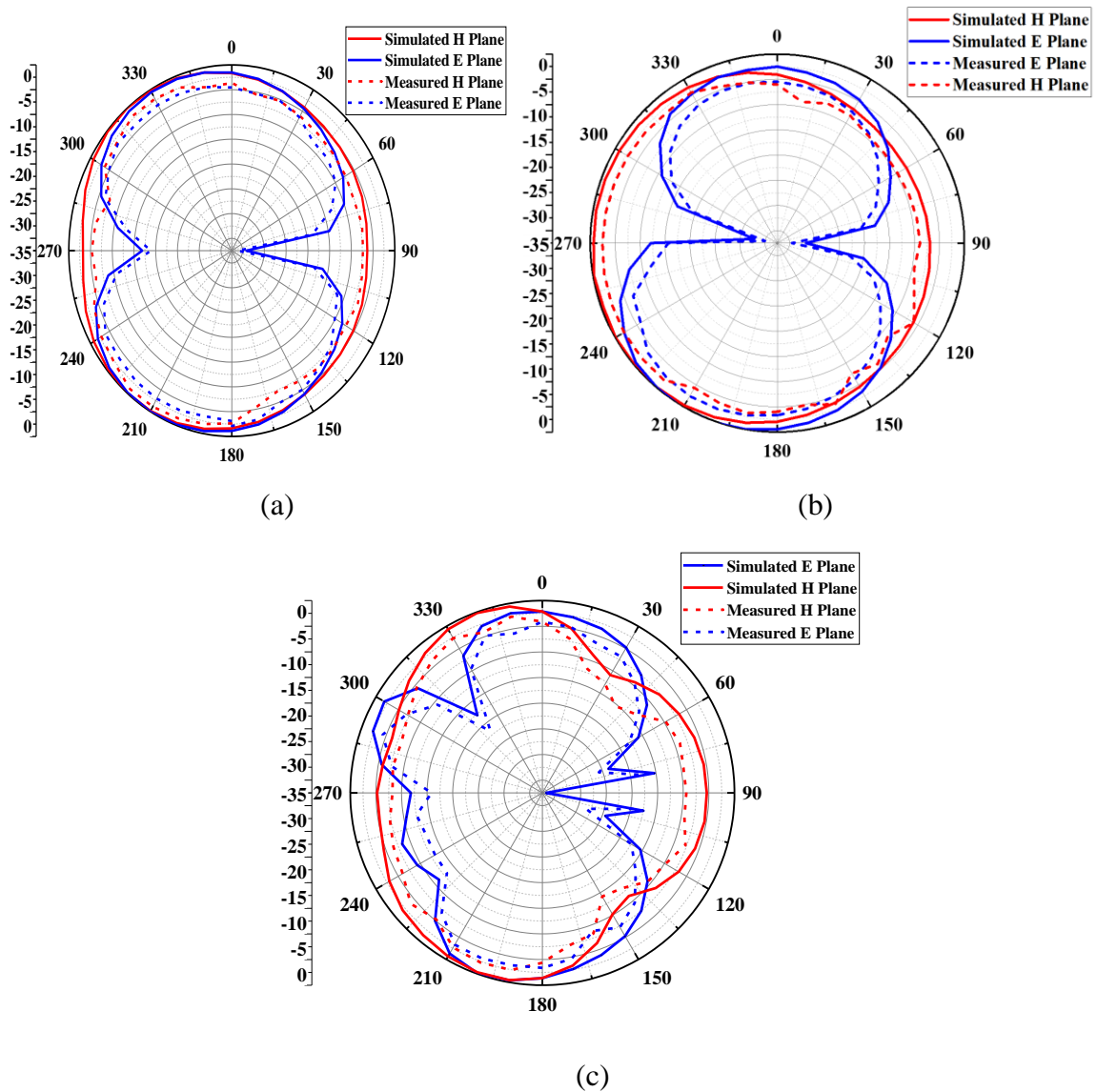


**Figure 4. 9** Radiation plots of the presented structure (a) 3 GHz (b) 5 GHz and (c) 10 GHz

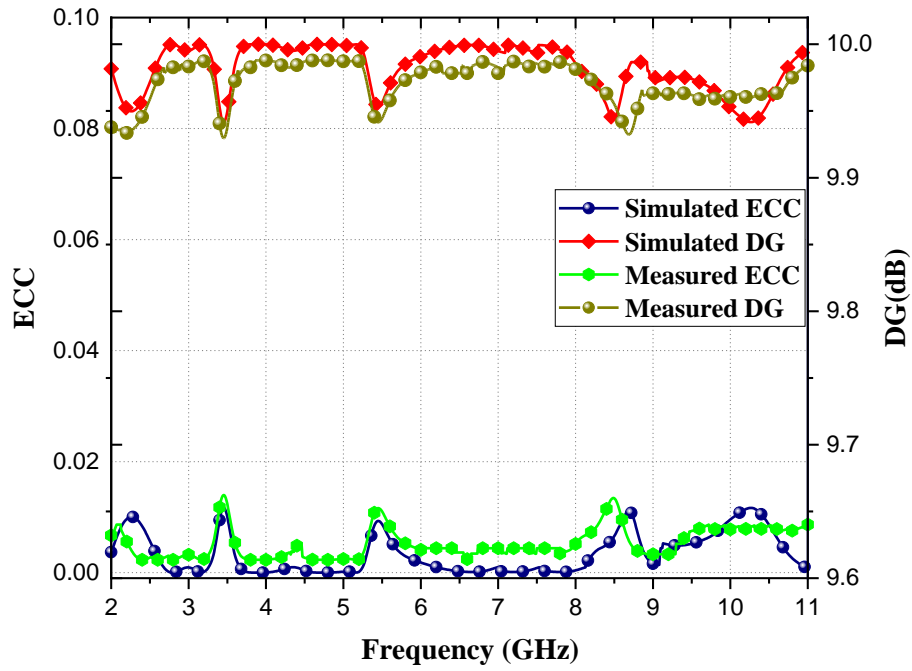


Figure 4. 10 ECC and DG with frequency

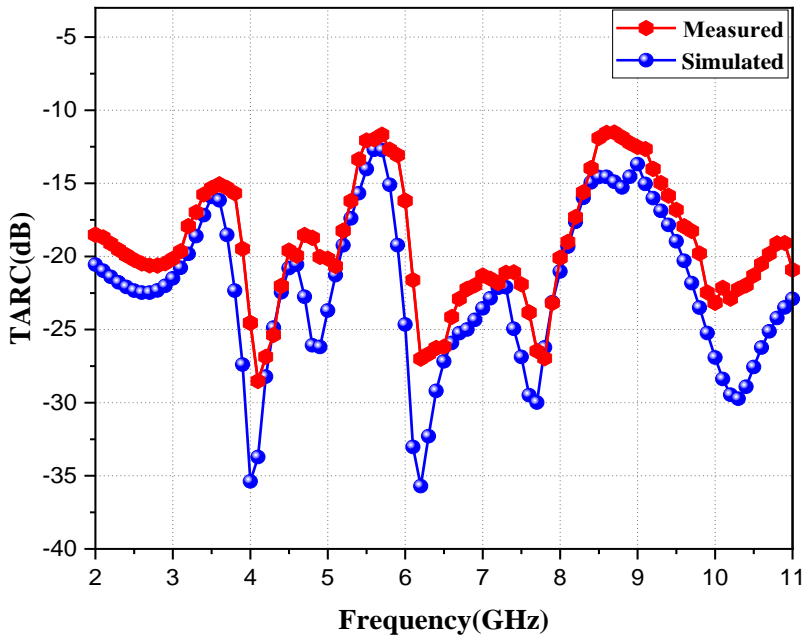


Figure 4. 11 Variation of TARC with frequency

It is perceived that the antenna in [252, 253-264] inhabits the dimension greater than the presented structure; therefore, the suggested structure rejects three bands using only EBG unit cell.

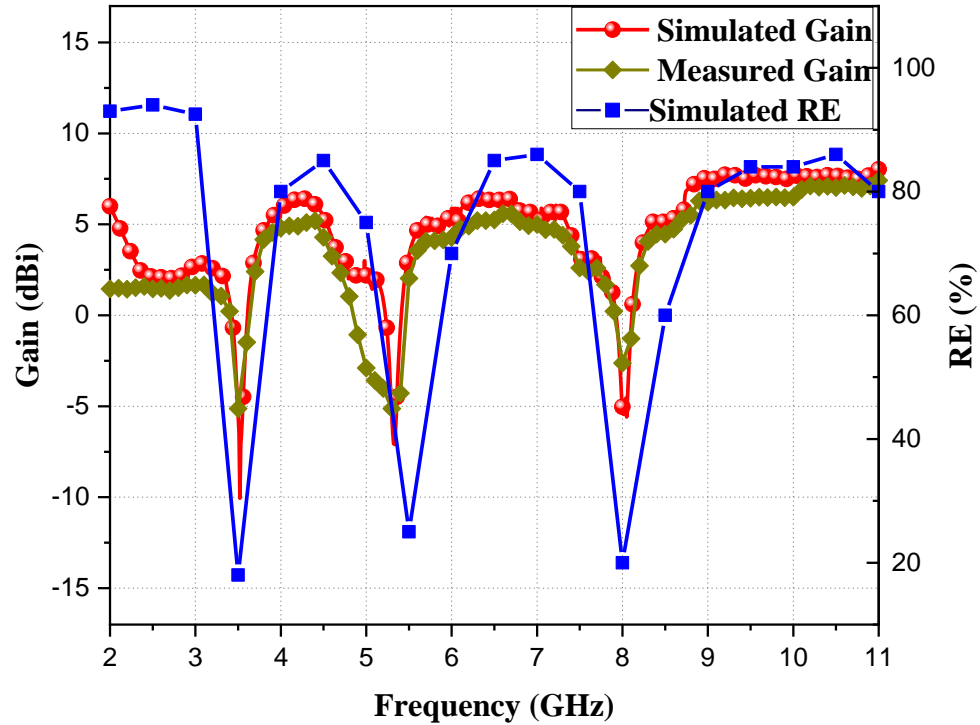


Figure 4. 12 Deviation of gain and radiation efficiency

## 4.5 Four elements band-notched UWB MIMO antenna

### 4.5.1 Antenna Design

The final prototype of the structure is depicted in Figure 4.13 and the adjusted parameters of the suggested antenna are presented in Table 4.4. This four-element UWB antenna is designed using FR-4 having  $\epsilon_r$  is 4.4 and has a compact size of  $38 \times 43 \times 1.6 \text{ mm}^3$ . Figure 2 signifies the prototype of the suggested UWB MIMO antenna.

The S-parameters are measured using the Agilent N5230C vector network analyzer and gain and radiation patterns are tested using the microwave shield anechoic chamber respectively. The values of SL, SW, WP, LP, and LT are varied to get a wider bandwidth of 9 GHz (2 - 11GHz), which covers the entire frequency range

### 4.5.1 Bandgap determination

To further validate the bandgap characteristic of EBG structure the proposed EBG structure  $5 \times 4$  lattice of EBG structure is simulated. The bandgap of the EBG unit cell is intended by

the transmission line technique presented in Figure 4.14. In the existence of the EBG periodic structure, the  $S_{21}$  amid the ports is analyzed to attained the bandgap properties. Figure 4.15 shows three-band gaps are 0.4 GHz (3.3–3.7 GHz) and 1GHz (5.15-5.85 GHz), and 1.4 GHz (7.2 -8.6 GHz), the minimum  $S_{21}$  value is about  $-37$  dB for the triple band gaps.

**Table 4. 2** Assessment of suggested EBG unit cell Designs

Ref.	Type of EBG	Number of EBG cell	Number of band-notched	Notched Band (GHz)	Dimensions (mm×mm)	$\epsilon_r/h$ (mm)
[248]	CMT-EBG	1	Single	5-6	8.5×8.5	4.4/1.6
[249]	ELV-EBG	1	Single	5.2-5.8	5.3×5.3	4.5/1
[250]	U shaped EBG	2	Dual	3.3-4.0&5–5.90	6.6×5	3.38 /0.8
[251]	SPRIAL EBG	2	Dual	5.15–5.35&5.725– 5.825	5.6×5.6	3.66/0.762
[252]	DG-EBG	3	Triple	3.3-3.6,5-6 &7.2-8.4	1.7×1.7,3×3 5×5	4.4/1.6
[253]	MSS-EBG	1	Triple	5.15–5.72,7.25–7.75 & 7.9–8.395	9.4×4.5	4.4/1.6
<b>Proposed EBG Structure</b>	<b>TVC-EBG</b>	<b>1</b>	<b>Triple</b>	<b>3.3-3.7 5-6 7.9-8.4</b>	<b>6×6</b>	<b>4.4/1.6</b>

#### 4.5.2 Equivalent circuit Model

The equivalent circuit of the suggested structure is depicted in Figure 4.16. The arrangement of inductor (L) capacitor (C) and resistance (R) is used to demonstrate the port of  $50 \Omega$  load, feed line, and radiating patch. The fed lines and radiating patch are symbolized by the series and parallel arrangement of  $L_1, C_1, R_1,$  and  $L_7, C_7, \dots, L_N, C_N$  respectively.

**Table 4. 3** Evaluation of Proposed structure with different antenna

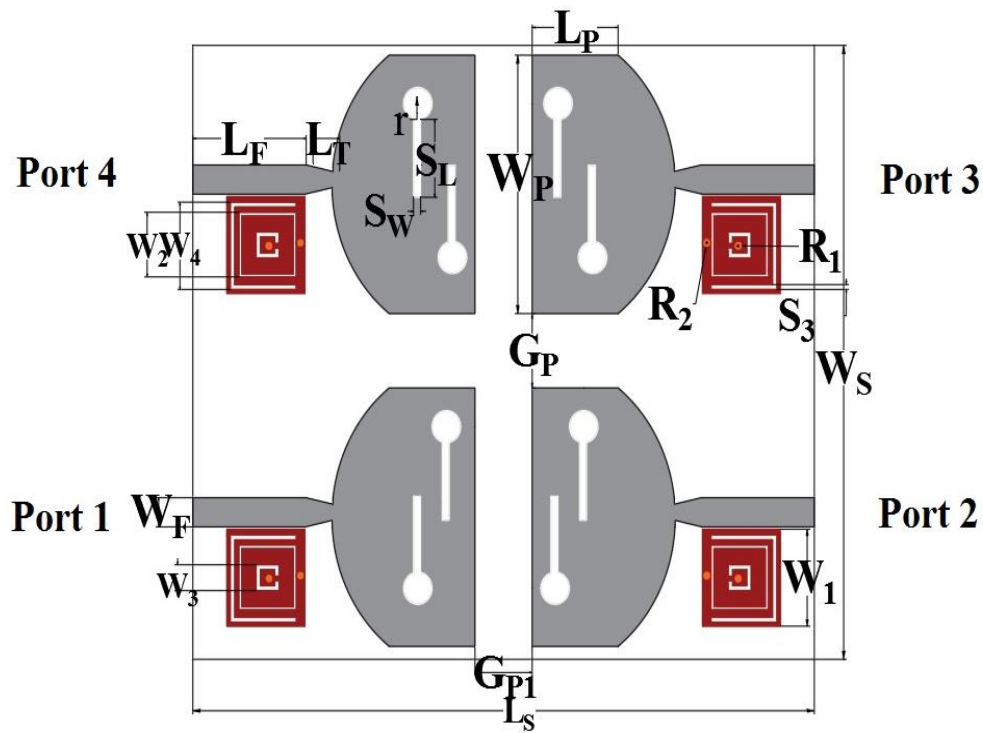
Ref.	Size (mm <sup>2</sup> )	Notched band (GHz)	No. of Notched band	BW (GHz)	DG (dB)	ECC	TAR C (dB)	Port number	Number of EBG	Gain (dBi)
[254]	22×32	5.1-6	1	3-11	NA	NA	NA	1	1	0.0-7.0
[255]	64×45	3.3-3.6,5-6&7.1-7.9	3	2-10.6	NA	0.02	NA	2	3	0.0-6.0
[256]	58×45	3.3-3.6&5-6	2	2.3-10.6	NA	0.01	NA	2	2	0.0-10
[257]	58 × 45	3.3-3.6, 5-6,7.2-8.4	3	2.76-10.75	NA	0.01	NA	2	3	3.0-12
[258]	42×50	3.3-3.8	3	2-11	NA	0.03	NA	2	2	NA
[259]	39×39	3.3-3.7, 5.15-5.875 & 7.1-7.9	3	2.3-13.75	NA	0.02	-10	2	NA	1.4-4.9
[260]	30×30	4.98 -5.96	1	3.1-11	NA	0.02	-10	4	NA	2.0-5.0
[261]	34×18	5.1-5.8&6.7-7.1	2	2.93-20	9.95	0.01	-20	2	NA	0.0-7.0
[262]	26 × 28	5.05-5.86 & 6.68-7.43	2	2.90-10.8	9.5	0.08	-12	2	NA	1.6-4.0
[263]	42×30	4.9 - 5.4	1	3-11	9.93	0.2.	NA	2	NA	2.0 -5.2
[264]	28×50	3.3 to 3.9	1	2.8 - 11.5	9	0.12	NA	2	NA	NA
<b>PA</b>	<b>21×36</b>	<b>3.3-4.4,5-6&amp;7.9-8.6</b>	<b>3</b>	<b>2-11</b>	<b>9.95</b>	<b>0.015</b>	<b>-10</b>	<b>2</b>	<b>1</b>	<b>0.0-7.1</b>

The parallel arrangement of L6 and C6 use to denote the mutual coupling among ports 1-2, and ports 1-4. Similarly, the parallel arrangement of L5 and C5 is used to symbolize isolation

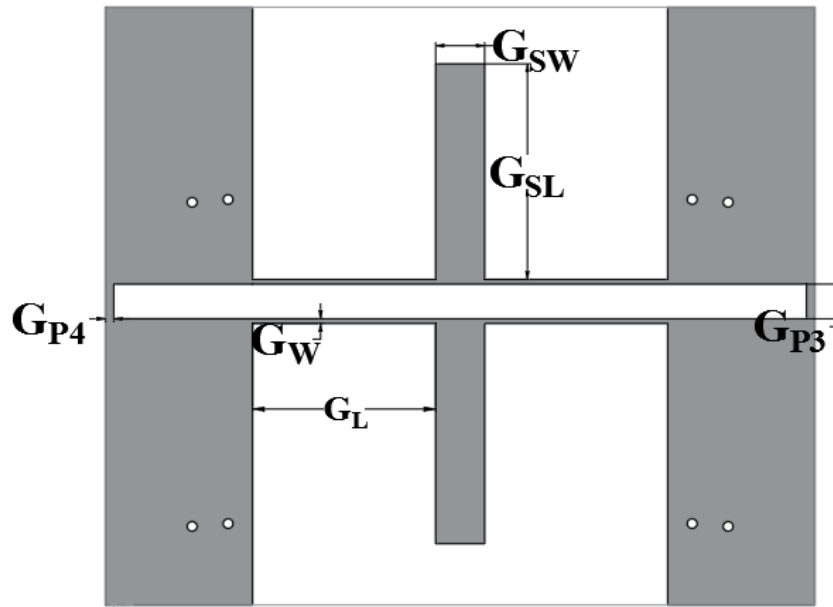
between ports 1–3. Modified EBG Structure is equivalent to three resonant circuits denoted by parallel combination L2 and C2, L3 and C3, and L4 and C4.

#### 4.6 Experimental result and discussion

The archetype of the presented structure is demonstrated in Figure 4.17. Figure 4.18 illustrates the VSWR. From the simulated result, it can be seen that the UWB MIMO structure with EBG structure-function in the entire UWB range expects WIMAX, WLAN, and X Band. The VSWR factor of the suggested structure is illustrated in Figure 4.19 and that the VSWR value at rejecting bands is more than 2 therefore; it is clear that no radiation is taking place at the rejecting frequencies.



(a)



(b)

Figure 4. 13 Layout of 4 element suggested antenna

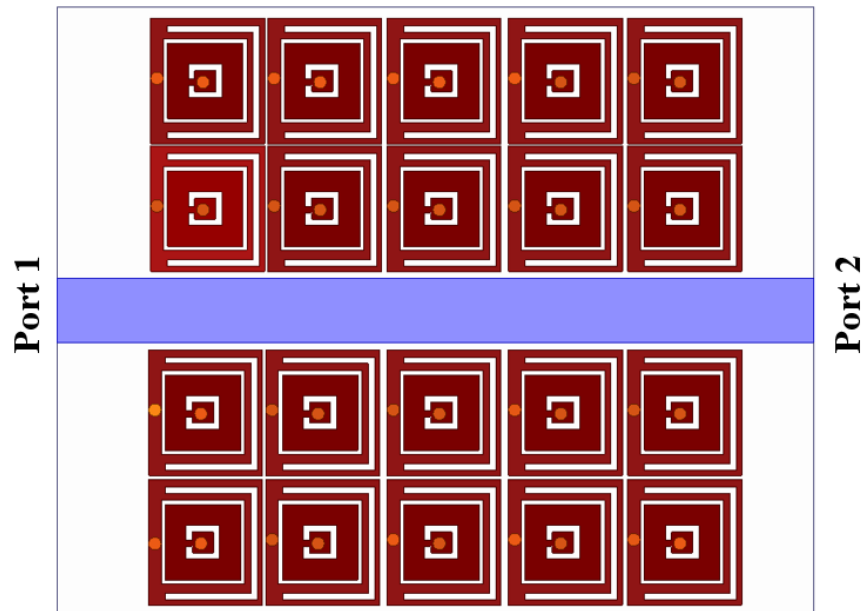
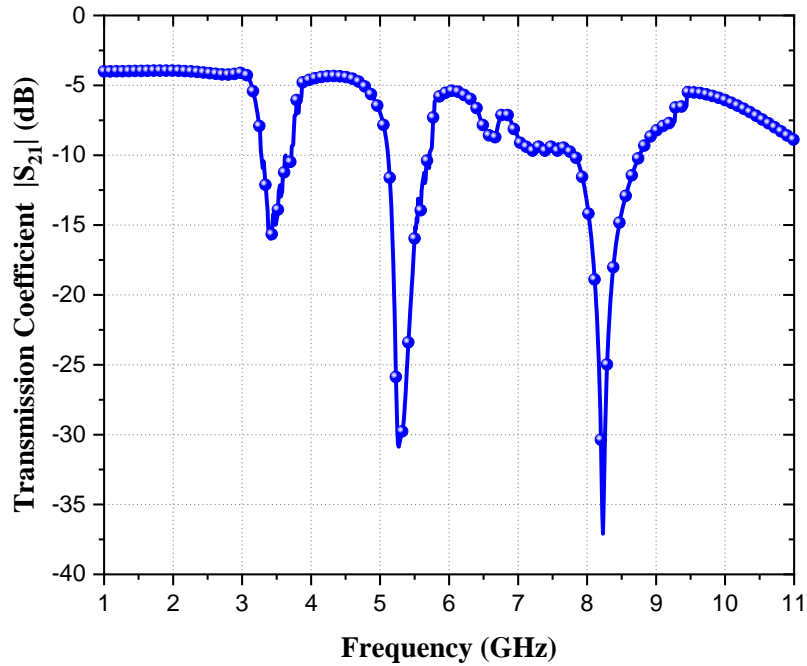


Figure 4. 14 Transmission line over modified EBG structure

**Table 4. 4** Parameters of four element UWB MIMO Antenna

Parameters	Value (mm)	Parameters	Value (mm)	Parameters	Value (mm)
$W_s$	38	$L_P$	6	$G_P$	4.6
$L_s$	45	$W_P$	16	$G_{P1}$	4
$L_1$	6	$S_3$	0.3	$R_1$	0.3
$W_1$	6	$S_2$	0.2	$S_L$	4.8
$S_w$	11	$L_F$	7.9	$W_3$	1.6
$L_T$	0.8	$W_2$	5.4	$W_4$	4
$W_2$	5.4	$W_F$	1.8	$G_{P4}$	0.52
$G_w$	0.3	$G_L$	11.2	$G_{P3}$	2.2
$G_{Sw}$	0.3	$R_2$	0.3	$r$	1



**Figure 4. 15:** Transmission coefficient for modified EBG structure

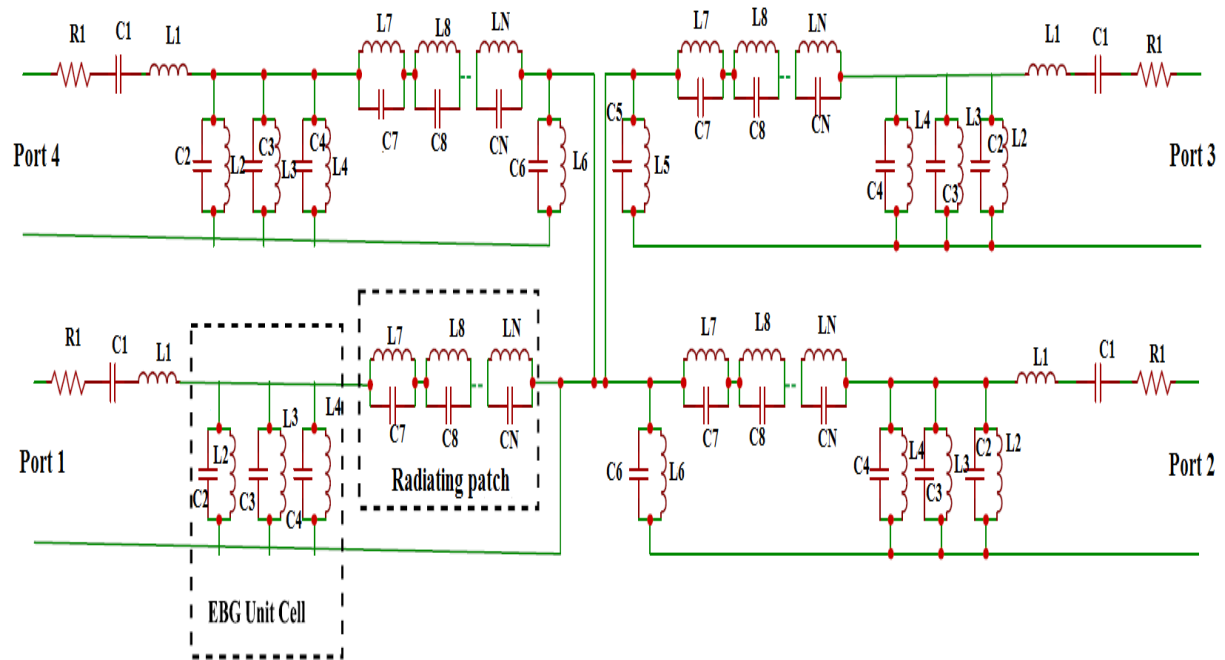
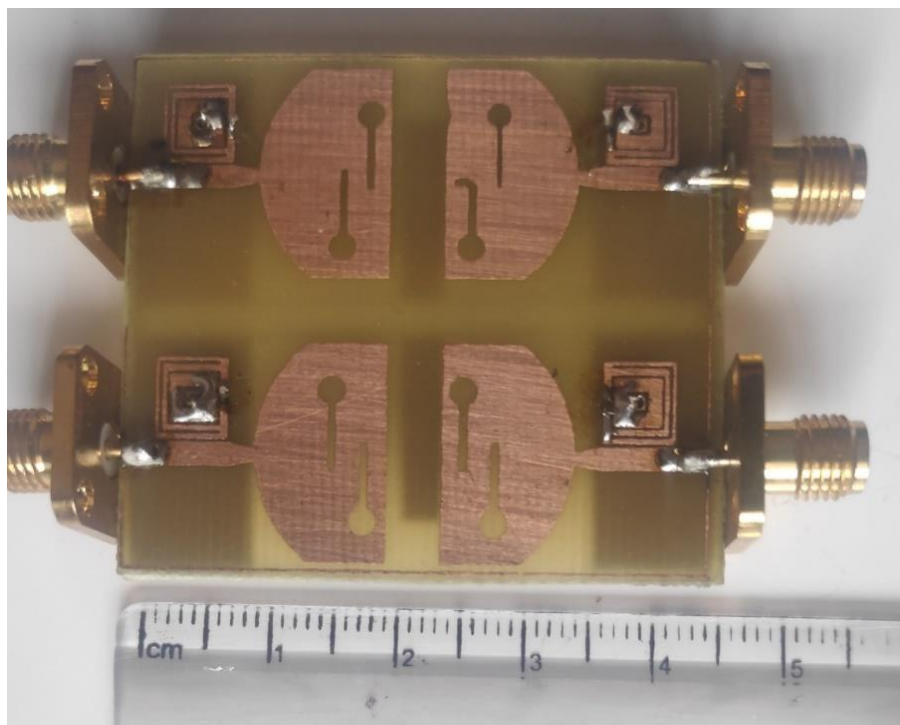
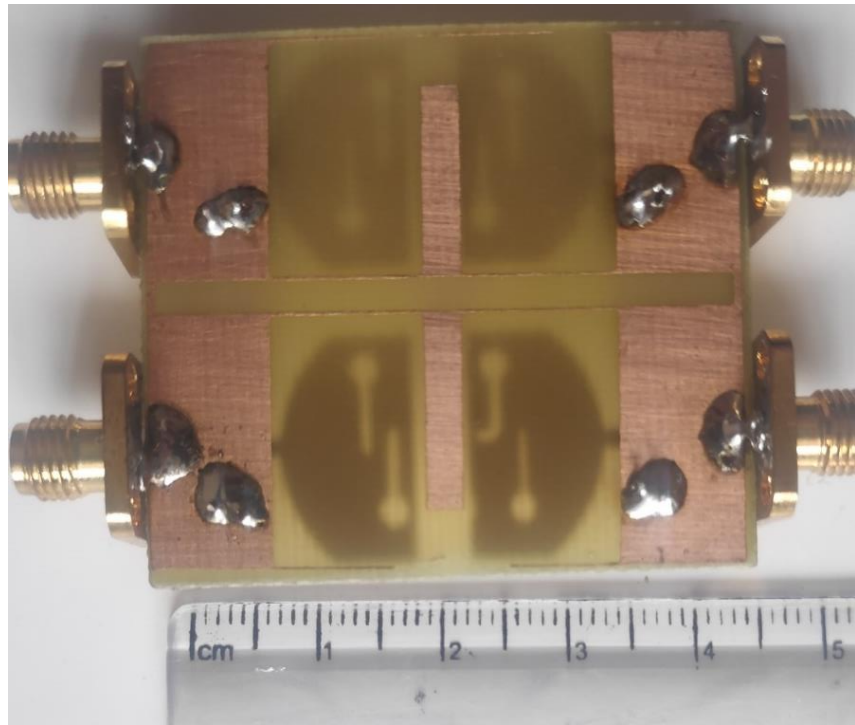


Figure 4. 16 Equivalent circuit Model



(a)



(b)

**Figure 4. 17** Prototype of proposed four element UWB MIMO antenna

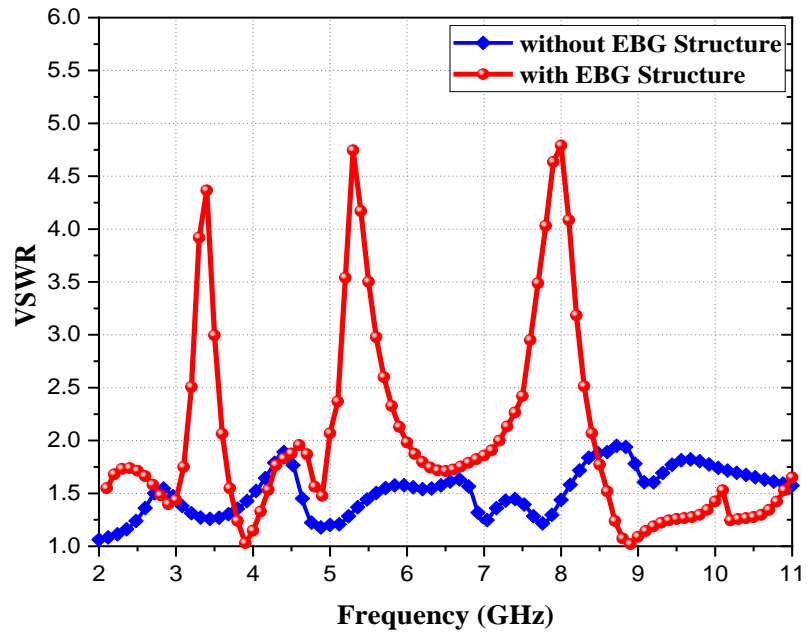


**Figure 4. 18:** Deviation of VSWR with frequency

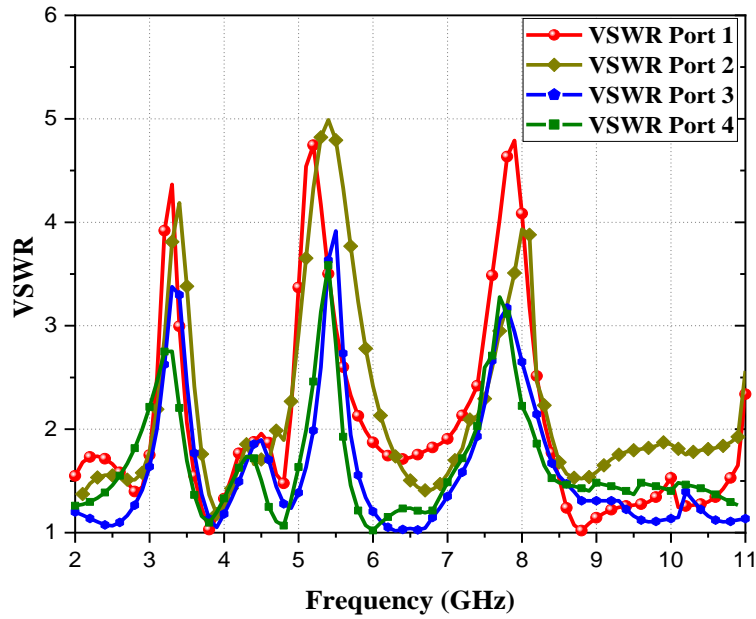


**Figure 4.19** Variation of VSWR with the frequency of different port

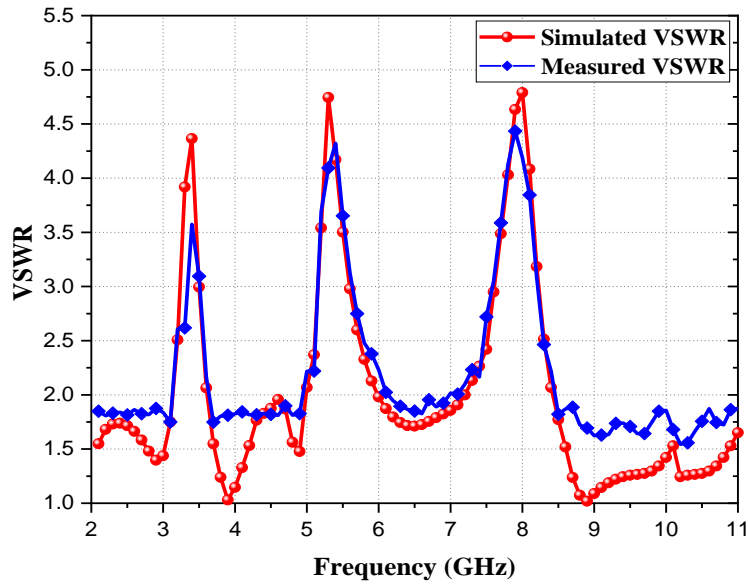


**Figure 4.20** Variation of Measured VSWR

#### 4.6.1 Numerical Results and discussion

However, Figure 4.20 specifies the tested and simulated VSWR curve of the structure. The difference in the tested result is because of the various losses like conduction loss, dielectric

loss, and orientation problems when the proposed structure is connected to the vector network analyzer. Figure 4.21 demonstrates the isolation of the suggested structure. The isolation amid the patch antenna is considerably minimized by using T formed stubs on the ground. A slot is removed to enhance the isolation. It can be observed from Figure 4.22 that isolation is below  $-15$  dB for the whole frequency band. The measured curves confirm a good resemblance with simulated curves.

#### 4.6.2 Radiation pattern plots and gain

Figure 4.23 indicates the radiation plot at 4, 6.3, and 7.6 GHz at both E Plane and H Plane. It is seen that the suggested structure shows a ring-shaped radiation pattern in H Plane and rotation symmetry at the E plane. Figure 4.24 illustrates the gain of the suggested antenna is varied  $-9.5$  to  $7.5$  dB for the entire UWB range.

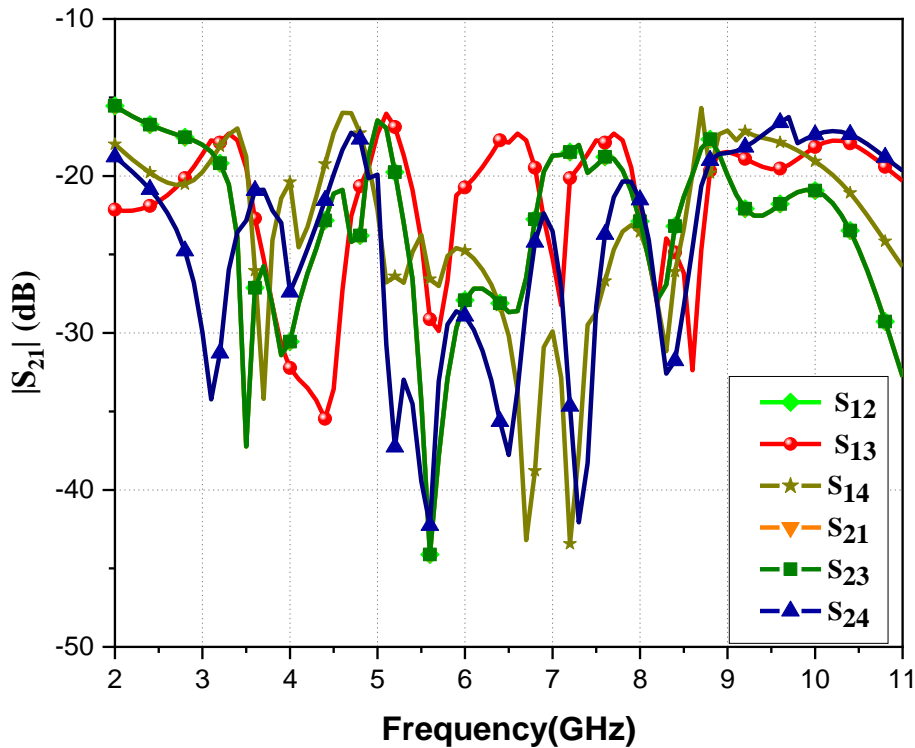


**Figure 4. 21** Deviation of mutual coupling with frequency

#### 4.6.3 MIMO characteristics

The significant factors to analyze and validate the MIMO characteristics are ECC, DG, TARC, and MEG. Correlation is commonly used to measure the difference between the radiation patterns. ECC and DG can be determined using s parameters and radiation patterns. The mathematical formula to evaluate the ECC in terms of scattering parameters and radiations pattern can be given by [265]

$$ECC(\rho_{ij}) = \frac{|S_{ii}^* S_{ij} + S_{ji}^* S_{jj}|^2}{(1 - |S_{ii}|^2 - |S_{jj}|^2)(1 - |S_{jj}|^2 - |S_{ij}|^2)} \quad (4.15)$$

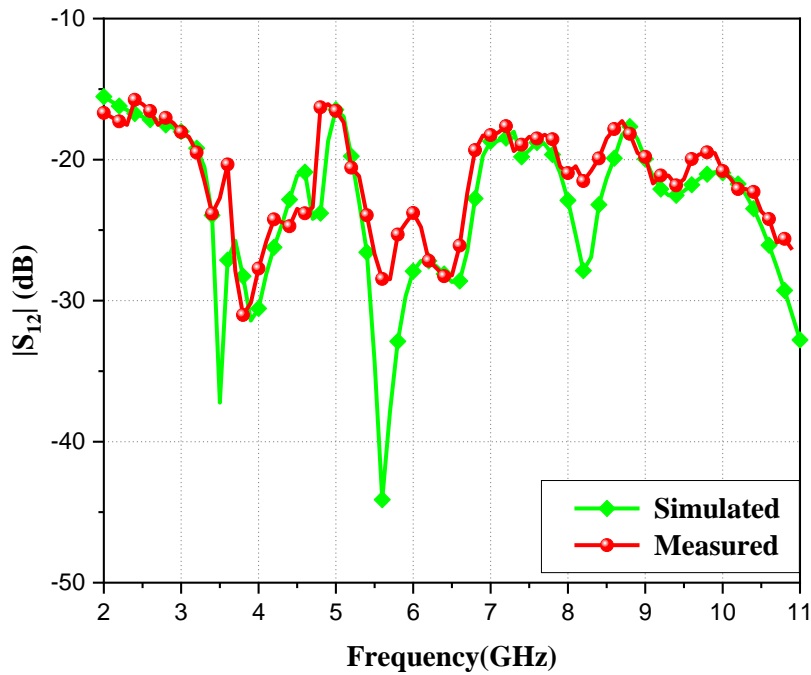


**Figure 4.22** Variation of mutual coupling with frequency

For 4 element,

$$ECC(\rho_{12}) = \frac{|S_{11}^* S_{12} + S_{21}^* S_{22}|^2}{(1 - |S_{11}|^2 - |S_{21}|^2)(1 - |S_{22}|^2 - |S_{12}|^2)} \quad (4.16)$$

$$ECC(\rho_{13}) = \frac{|S_{11}^* S_{13} + S_{31}^* S_{33}|^2}{(1 - |S_{11}|^2 - |S_{31}|^2)(1 - |S_{33}|^2 - |S_{13}|^2)} \quad (4.17)$$

$$ECC(\rho_{14}) = \frac{|S_{11}^* S_{14} + S_{41}^* S_{44}|^2}{(1 - |S_{11}|^2 - |S_{41}|^2)(1 - |S_{44}|^2 - |S_{14}|^2)} \quad (4.18)$$

$$ECC = \frac{\left| \int_{\Omega} [XPR.E_{\theta_i} E_{\theta_j}^* P_{\theta} + E_{\phi_i} E_{\phi_j}^* P_{\phi}] d\Omega \right|^2}{\int_{\Omega} [XPR.E_{\theta_i} E_{\theta_i}^* P_{\theta} + E_{\phi_i} E_{\phi_i}^* P_{\phi}] d\Omega \int_{\Omega} [XPR.E_{\theta_j} E_{\theta_j}^* P_{\theta} + E_{\phi_j} E_{\phi_j}^* P_{\phi}] d\Omega} \quad (4.19)$$

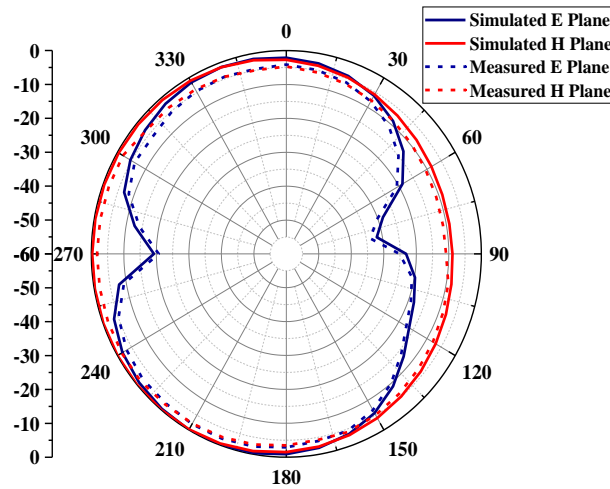
Diversity gain is one more key parameter that is related to ECC by the given below equation [266]

$$DG = 10\sqrt{1 - ECC^2} \quad (4.20)$$

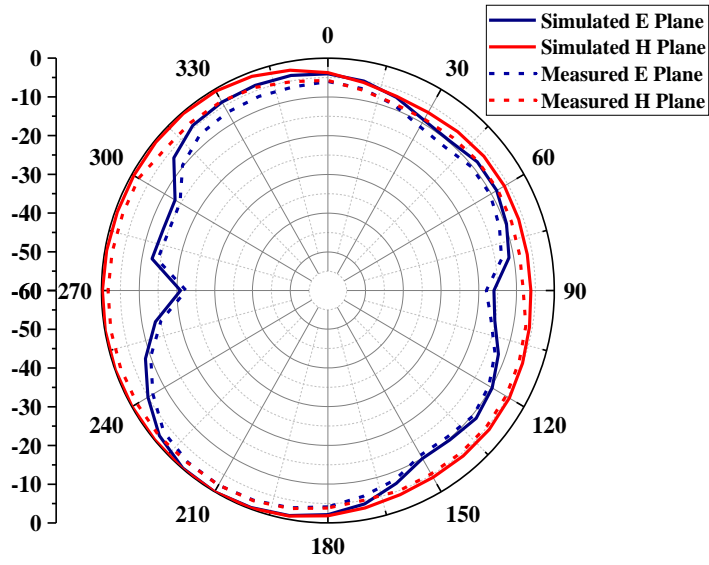
Figure 4.25 displays the ECC and DG measured using s parameters. Ideally, ECC must be 0 but practically it should be beneath 0.5 and DG must be around 10 dB. The ECC and DG for different antenna elements are within 0.02 and 9.92 dB respectively.

TARC is a significant factor that denotes the mutual coupling of the ports. For a four-port UWB MIMO antenna, the TARC can be calculated using [267]

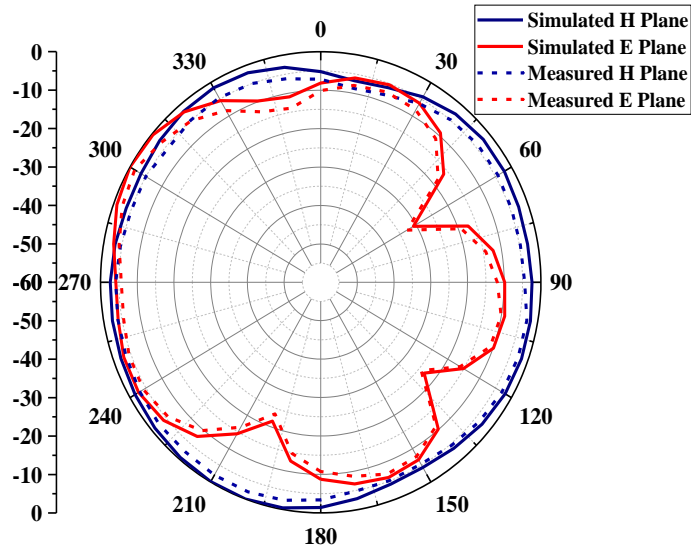
$$TARC = \sqrt{\frac{(S_{11} + S_{12} + S_{13} + S_{14})^2 + (S_{21} + S_{22} + S_{23} + S_{24})^2 + (S_{31} + S_{32} + S_{33} + S_{34})^2 + (S_{41} + S_{42} + S_{43} + S_{44})^2}{4}} \quad (4.21)$$



(a)



(b)



(c)

**Figure 4. 23 .** Normalized radiation plot at (a) 4 GHz (b) 6.3 GHz and (c) 7.6 GHz

Figure 4.26. Illustrates the TARC of the suggested antenna. Ideally, for a MIMO system, the TARC should be less than 0 dB. It can be seen from Figure 4.27 that the TARC is below than  $-2.5$  dB for the complete band with the triple rejected bands. Mean effective gain (MEG) is one of the significant factors and it is defined as the relation given [268]

$$MEG_i = 0.5\mu_{irad} = 0.5 \left( 1 - \sum_{j=1}^N |S_{ij}|^2 \right) \quad (4.22)$$

Where N is the number of patches and  $\mu_{irad}$  is the efficiency. In this case N=4.

$$MEG_1 = 0.5 \left[ 1 - |S_{11}|^2 - |S_{12}|^2 - |S_{13}|^2 - |S_{14}|^2 \right] \quad (4.23)$$

$$MEG_2 = 0.5 \left[ 1 - |S_{21}|^2 - |S_{22}|^2 - |S_{23}|^2 - |S_{24}|^2 \right] \quad (4.24)$$

$$MEG_3 = 0.5 \left[ 1 - |S_{31}|^2 - |S_{32}|^2 - |S_{33}|^2 - |S_{34}|^2 \right] \quad (4.25)$$

$$MEG_4 = 0.5 \left[ 1 - |S_{41}|^2 - |S_{42}|^2 - |S_{43}|^2 - |S_{44}|^2 \right] \quad (4.26)$$

For better diversity performance the range of MEG should be  $|MEG_i - MEG_j| < -3dB$ . The simulated MEG of the suggested four-port antenna is presented in Figure 4.27. The value of MEG's for all the four elements is within the desired limit. The performance evaluation of the presented structure with those recent antennas in the publication is presented in Table 4.5.

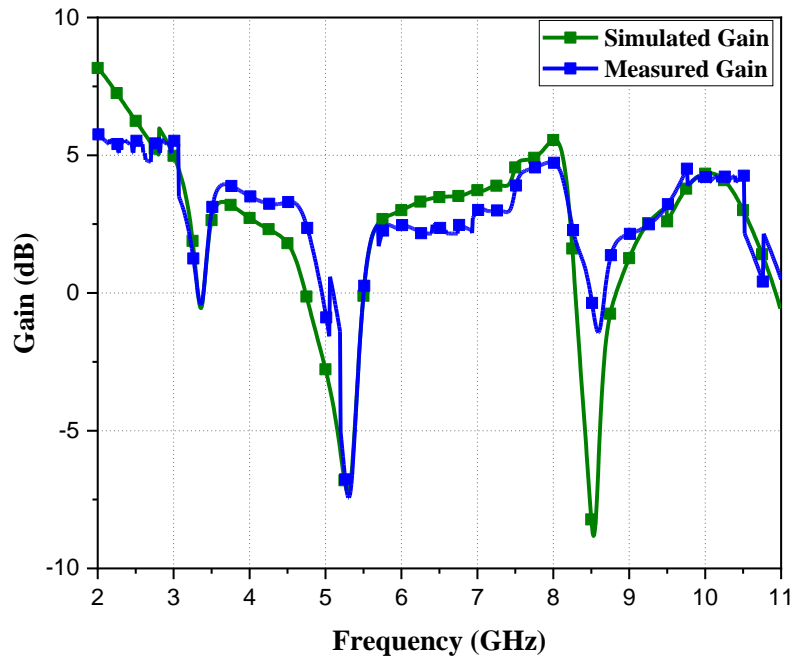


**Figure 4. 24** Deviation of gain with frequency

**Table 4. 5** Evaluation of proposed antenna with the existing structure

Ref	Dimensions (mm <sup>3</sup> )	Notched band (GHz)	No. of Notches	Radiating elements	BW (GHz)	Notch Technique
[269]	63×63×1.6	3.5,5.5,8.5	3	4	1.3-40	Complementary split-ring resonator(CSRR)
[270]	58×58×0.8	3.5,5.5	2	4	3-16	Hexagonal-shaped CSRR
[271]	52×52×1.6	3.5,5.5	2	4	2-40	L- and C-shaped resonator slits.
[272]	81 × 87 × 1.6	3.87-5.94, 7.04–8.7	2	4	1-14	L-shaped slot and rectangular stub
[273]	60×60×1.6	5.36-6.34	1	4	2.73-10.68	Mushroom-like EBG
[274]	60×60×1.6	5.1-5.6,7.3-9.1	2	4	3-16.2	Periodic EBG structure
[275]	44×44×1.6	5.10–5.95	1	4	2.95–10.8	Half-wavelength resonant stub
[276]	39×50×1.6	5.15-5.35, 5.75-5.825	2	4	2-12	LC band-stop resonator
<b>Proposed Antenna</b>	<b>38×45×1.6</b>	<b>3.3-3.7, 5.15-5.85, 7.9-8.6</b>	<b>3</b>	<b>4</b>	<b>2-11</b>	<b>Modified EBG structure</b>

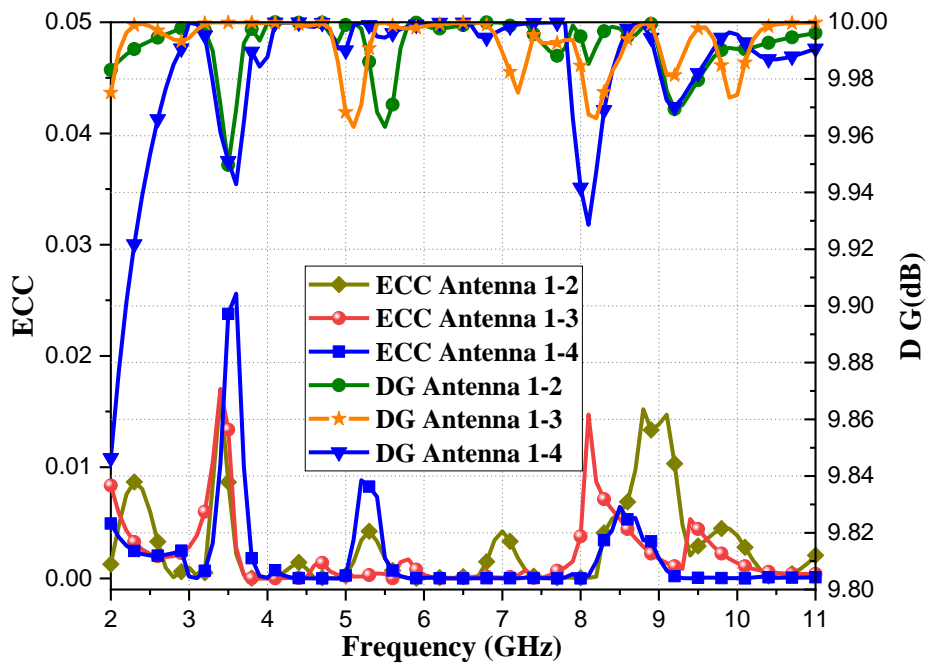


Figure 4. 25 Deviation of ECC and DG with frequency

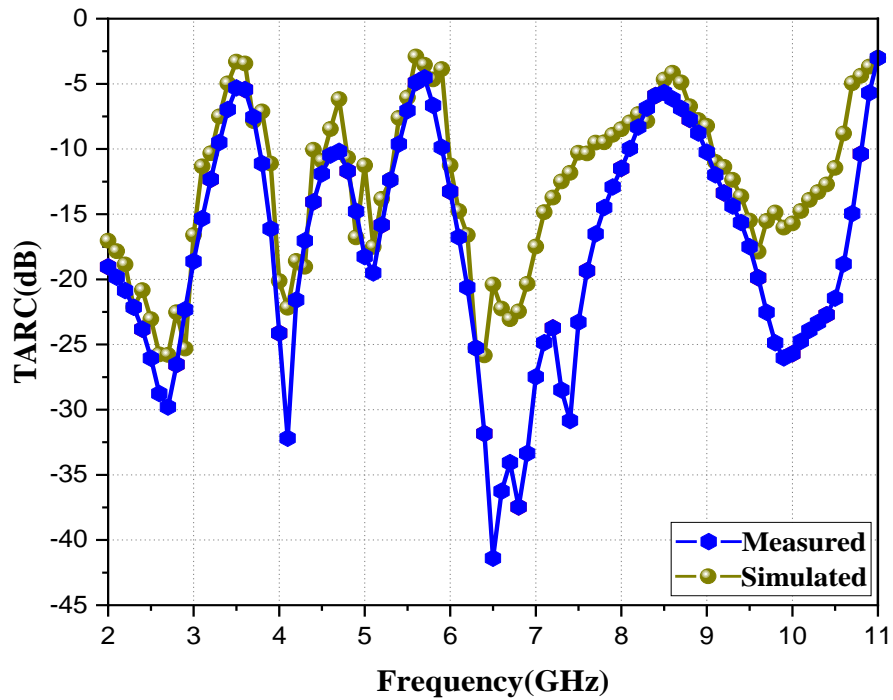


Figure 4. 26 Deviation of TARC

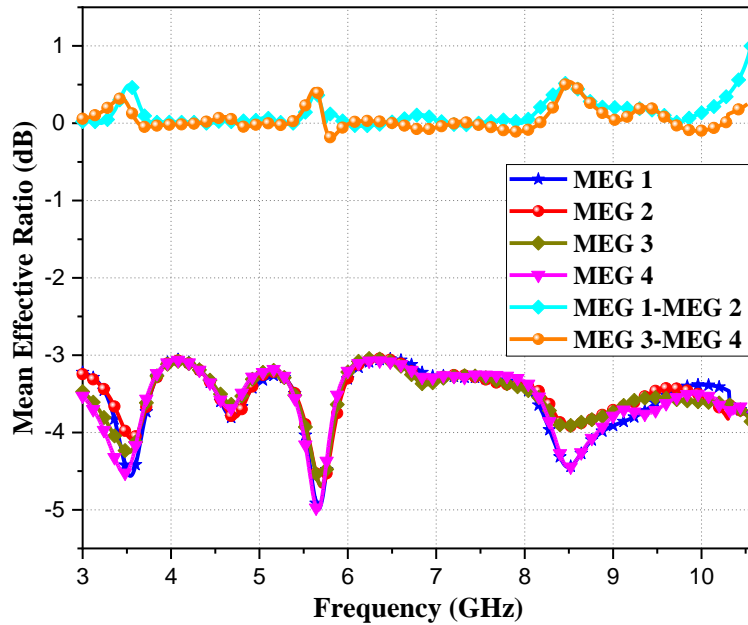


Figure 4. 27 Deviation of MEG

#### 4.7 Summery

In this chapter, we have presented a miniaturized two-element and four-element band rejected UWB MIMO antenna. A Modified EBG unit cell is used to acquire three band-eliminated characteristics. The novelty of this structure is that the three rejection bands are obtained by using only a modified compact EBG structure with C shaped slots on its surface.

A single EBG structure is used instead of using multiple EBG structure. The tested and simulated Scattering parameters, gain, mutual coupling, and radiation patterns were studied for both the antennas. The proposed two elements antenna and four elements antenna attains -10dB bandwidth from 2 to 11 GHz with three-band rejections. The four-element antenna attains decent MIMO performance with  $ECC < 0.015$ ,  $TARC < -10$  dB, and radiation efficiency is almost 80%.The decent diversity performance parameters with  $ECC < 0.02$ ,  $TARC < -7.5$  dB, and MEG is within desired limits. The measured result shows a good resemblance.

**CHAPTER 5**

**CIRCULARLY POLARIZED ULTRA-  
WIDEBAND MIMO/DIVERSITY  
ANTENNA**

## CHAPTER 5

### Circularly Polarized Ultra-Wideband MIMO/Diversity antenna

#### 5.1 Introduction

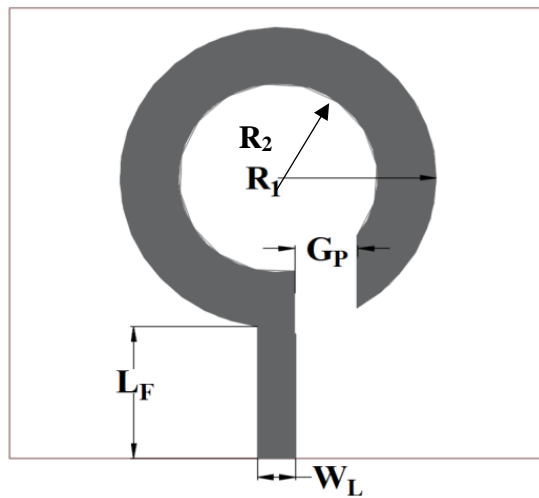
UWB system is used in most of the communication systems because of wide Impedance Bandwidth (IB), simple fabrication method, low power dissipation, higher transmission data rates, low cost, multipath cancellation. The UWB [277]- [278] ranges from 3.1 to 10.6 GHz is used for numerous wireless applications. The biggest challenge for wireless communication systems is the polarization mismatch loss between the transmitter and the receiver [279]. To overcome the polarization mismatch loss and multiple path interference it is essential to propose a with circular polarization (CP) features. In general, equated to the LP antenna, the CP antenna has many advantages such as eliminating polarization mismatch and reducing multipath interference [280]. Normally, CP wave in the UWB antenna can be produced by two orthogonally placed electric fields or magnetic fields with identical amplitude and 90° phase difference. Different techniques are used to generate the CP wave in the UWB antenna such as by employing couplers, phase shifters, or modified antenna structures. With the growing demand for the CP structure the ARBW of the CP antenna is required to be improved. A CP antenna can be obtained by using two feeding techniques: single feed and multi-feed. For ease, we have chosen a single fed monopole antenna. With the growing demand for CP UWB antenna for great data, the ARBW needs to enhance. Although the impedance bandwidth of the single fed monopole antenna is small due to the high Q factor of the antenna [281]. Therefore, to design an only fed monopole antenna with a wide axial ratio is a countless challenge. Further, to obtain wide ARBW different stub [282]and slots [283] is reported in the literature. Various CP Antenna with different patch shape, for example, S-model [284], arc- slot antenna [285] and X-shaped [285], meandered- [286], hook [287], modified circular ring [288] antenna has been also suggested with wide 3 dB ARBW. In this editorial, a ring-shaped planar antenna is suggested with wide ARBW. A slot is etched under the feed line and the strip is extended from the ground to obtain a wider AR. The presented structure has an impedance of 3-11GHz, whereas the ARBW is 4-9 GHz. Further, the entire ARBW is

coincided by impedance bandwidth, thus CP characteristics are satisfactory for the suggested antenna. In the interim, the suggested antenna has a simpler compact size with wider ARBW than the above-mentioned antenna. The design process and measured outcomes are analyzed and discussed in detail in the succeeding divisions.

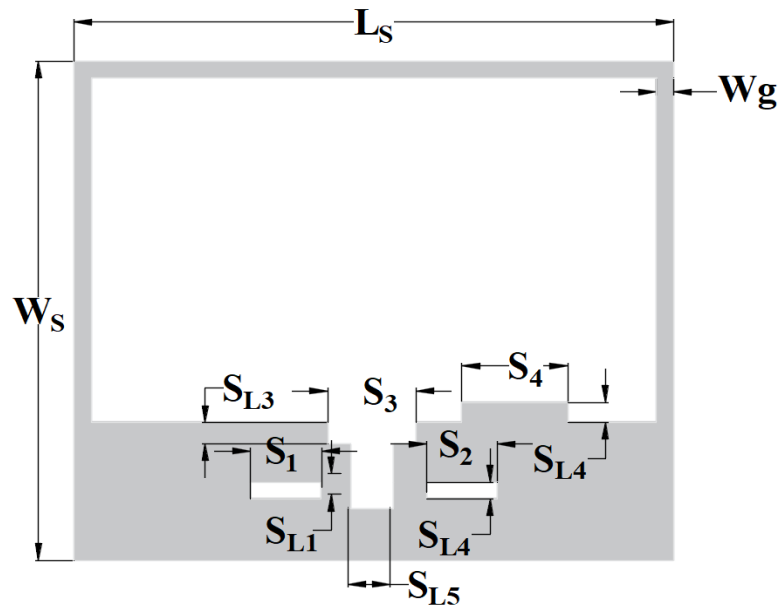
## 5.2 Circular Polarized UWB Antenna

### 5.2.1 Design and Analysis

Figure 5.1 depicts the prototype of the CP UWB antenna. The suggested structure comprises of a ring-shaped patch with the outer is  $R_1$  and the inner radius is  $R_2$ . Table 5.1 presents the dimension of the suggested CP UWB Antenna. A slot and stub are incorporated in the ground to enhance the ARBW. The structure is simulated and made-up using FR-4 dielectric material whose  $\epsilon_r$  is 4.4 and height ( $h$ ) is 1.6 mm. the suggested antenna is designed using Ansoft HFSS v.13 software. EP 2006 PCB Prototype machine is used to fabricated the suggested antenna. The antenna parameters like S parameters and radiation pattern are evaluated using the Agilent N5230C VNA and microwave shield chamber respectively. Figure 5.2 indicates the archetype of the CPUWB antenna. The measured and simulated VSWR is presented in Figure 5.3. Figure 5.4 displays the variation of the simulated and tested axial ratio with frequency. It can be seen that 3 dB ARBW of the suggested structure is 4-9 GHz coincided by 10-dB impedance bandwidth.

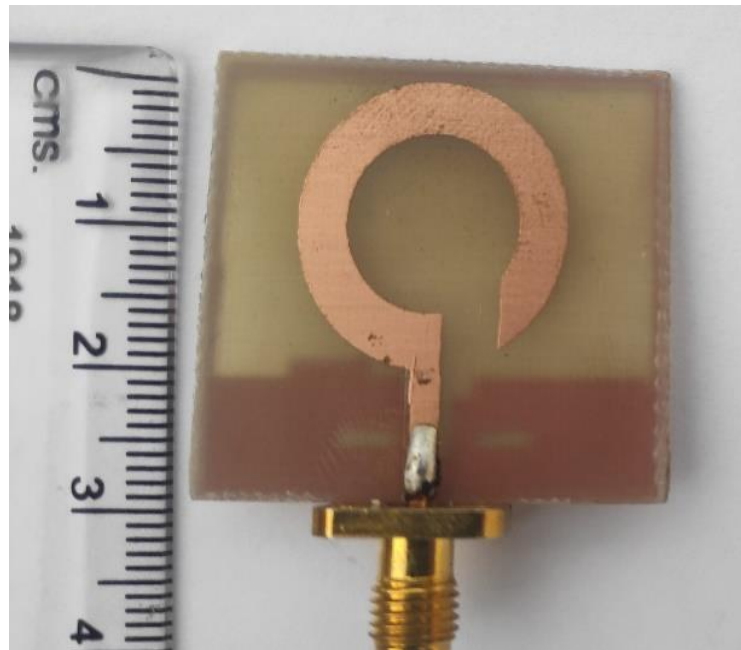


(a)



(b)

**Figure 5. 1:** Suggested UWB antenna with enhanced bandwidth



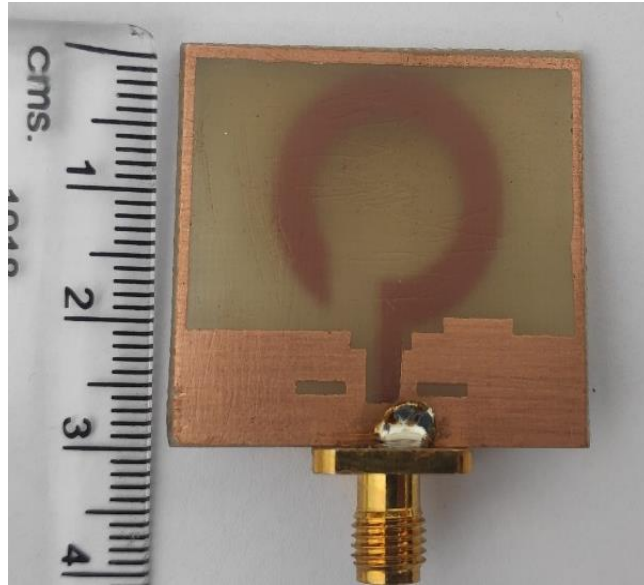
(a)

### 5. 3 Results and Parametric analysis

#### 5.3.1 Variations in the ring slot ( $G_p$ )

The deviation of the ring slot is a significant parameter that controls the axial ratio of the

proposed structure. The deviation of VSWR for different ring slot (GP) is explained in Figure 5.5. There is a marginal variation on impedance matching, as ring slot width is increased and the AR can be tuned to below 3 dB as displayed in Figure 5.6.



(b)

**Figure 5. 2:** (a) Uppermost view, (b) foot view

### 5.3.2 Variations in the ground slot ( $S_1$ )

Figures 5.7 and 5.8 depict the simulated VSWR and axial ratio for different values of  $S_1 = 2, 3,$  and  $4$  mm respectively. It is observed that there is a negligible variation on VSWR, whereas, in Figure 5. 8, significant variation is seen in the axial ratio for different ground slot length ( $S_1$ ). As the slot length increased from  $S_1 = 2$  mm to  $4$ mm, the lower band of the axial ratio moves from  $5.5$  GHz to  $4$  GHz, which improves overall ARBW. By varying  $S_2$  the same variation is observed in VSWR and the axial ratio of the suggested CP UWB antenna.

### 5.3.3 Variation of the slot length ( $S_3$ )

Figure 5.9. indicates the deviation of VSWR for different slot lengths ( $S_3$ ). It is seen that there is a little deviation on impedance matching, as slot length  $S_3$  increase from  $3$  mm to  $5$  mm. Figure 5.10. presents the variation of axial ratio with frequency. Two CP mode approaches

each other as  $S_3$  decrease to 5mm and the proposed structure shows the maximum bandwidth of AR. Thus, the two Circular Polarized modes get unite by varying the length of the slot.

### 5.3.4 Variations in the ground slot ( $S_4$ )

Figure 11. Indicates the deviation of VSWR with frequency for different ground slot lengths ( $S_4$ ). It is perceived that there is a minimal variation on VSWR, whereas, in Figure 5.12, significant variation is seen in the axial ratio for different ground slot length ( $S_4$ ). As the slot length increased from  $S_4 = 4$  mm to 6 mm, the upper band of the axial ratio moves from 8.3 GHz to 9.1 GHz, which improves the overall ARBW.

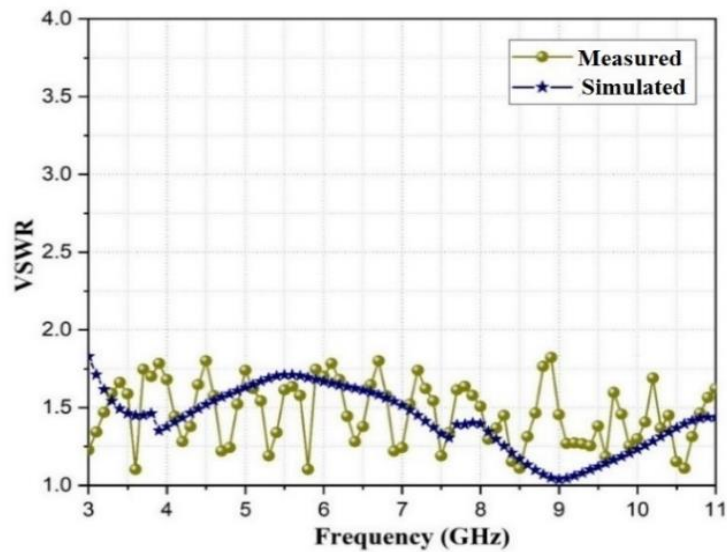


Figure 5.3: Tested and simulated VSWR

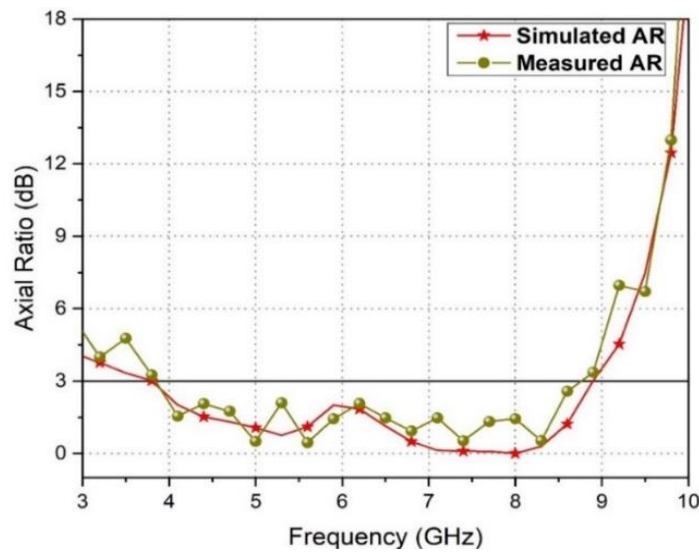


Figure 5.4: Tested and simulated axial ratio.

**Table 5. 1.:** Dimensions of Suggested Antenna

<b>Parameter</b>	<b>S<sub>3</sub></b>	<b>S<sub>L3</sub></b>	<b>S<sub>2</sub></b>
<b>Units(mm)</b>	5	1.3	4
<b>Parameter</b>	<b>S<sub>L2</sub></b>	<b>S<sub>1</sub></b>	<b>S<sub>L1</sub></b>
<b>Units(mm)</b>	1	1	4
<b>Parameter</b>	<b>S<sub>L4</sub></b>	<b>S<sub>4</sub></b>	<b>L<sub>G</sub></b>
<b>Units(mm)</b>	6	1.2	8.3
<b>Parameter</b>	<b>W<sub>g</sub></b>	<b>G<sub>P</sub></b>	<b>L<sub>F</sub></b>
<b>Units(mm)</b>	1	4	8.7
<b>Parameter</b>	<b>W<sub>s</sub></b>	<b>L<sub>s</sub></b>	<b>W<sub>L</sub></b>
<b>Units(mm)</b>	34	30	2.4
<b>Parameter</b>	<b>R<sub>1</sub></b>	<b>R<sub>2</sub></b>	<b>G<sub>P</sub></b>
<b>Units(mm)</b>	10	6.3	4

The current circulations of the proposed structure at 5.5 GHz at dissimilar time pause:  $w(t) = 0^\circ, 90^\circ, 180^\circ,$  and  $270^\circ$  is demonstrated in Figure 5.13. To understand the circular polarization mechanism the surface current distribution is analyzed with phase change from  $0^\circ$  to  $270^\circ$ . The predominant vector direction is in  $-Y$  direction for  $0^\circ$ , while for  $90^\circ$  the predominant vector direction is  $-X$  direction. For  $180^\circ$  and  $270^\circ$ , the predominant vector direction is reverse to  $0^\circ$  and  $90^\circ$ . It is observed from the Figure that as the phase increase from  $0^\circ$  to  $270^\circ$ , with the identical amplitude and  $90^\circ$  phase difference the current moves in the left-handed or clockwise direction, as observed from the  $+Z$  direction. Thus, it is noticed that the suggested circularly polarized UWB antenna can radiate left-hand CP (LHCP) wave as observed from  $+Z$  direction and right-hand CP (RHCP) from the  $-Z$  direction. Figure5.14 indicates the simulated and tested H plot and E plot at 5 GHz and 7 GHz. In  $+Z$  direction, the radiated wave is LHCP and in the  $-Z$  direction the radiated wave is RHCP. Figure5.15 illustrates radiation efficiency. Figure 5.16 indicates the gain variation with the frequency of the suggested antenna. Good constancy can be attained compared to replicated and tested results. The tested gain of the antenna varies between 4.5 to 7 dB for complete UWB.

Table 5.2 indicates the performance evaluation of the suggested structure with those recent antennas in the publication. It is noticed that the proposed structure has a small size with wider impedance bandwidth and ARBW than the existing antenna.

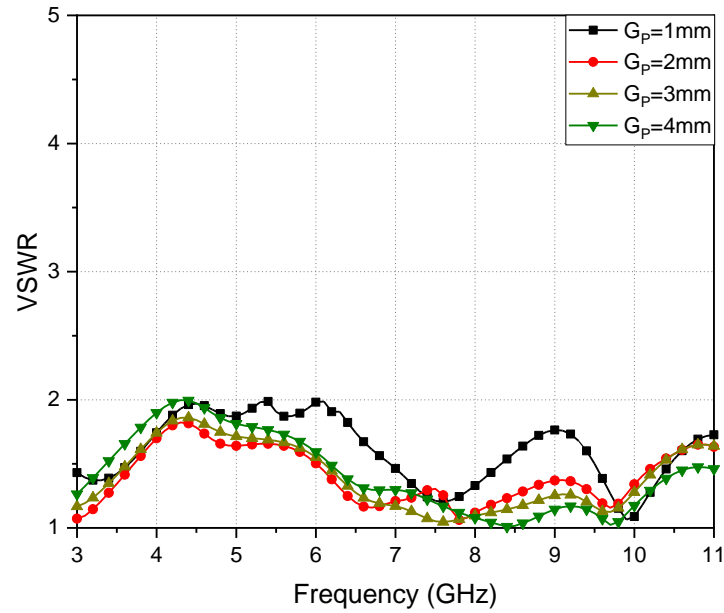


**Figure 5.5:** Variation of VSWR for different ring slot width

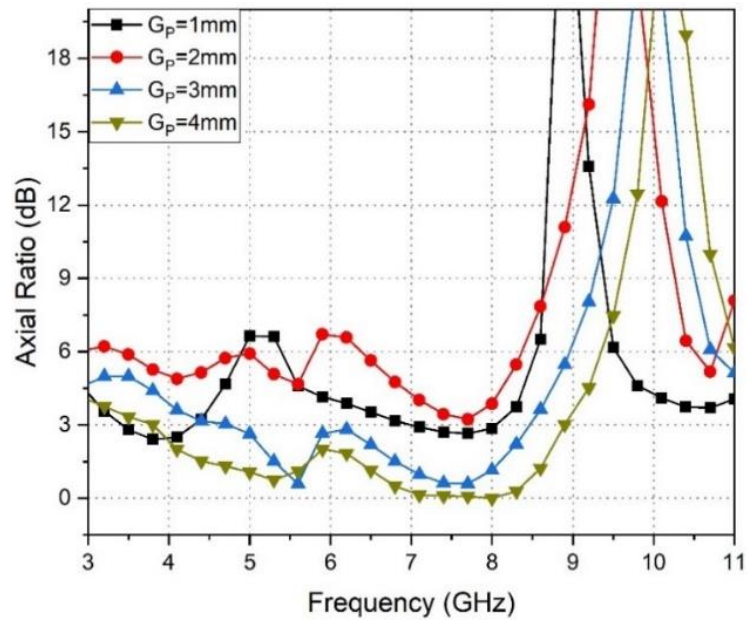


**Figure 5. 6:** Deviation of Axial ratio for different ring slot width.

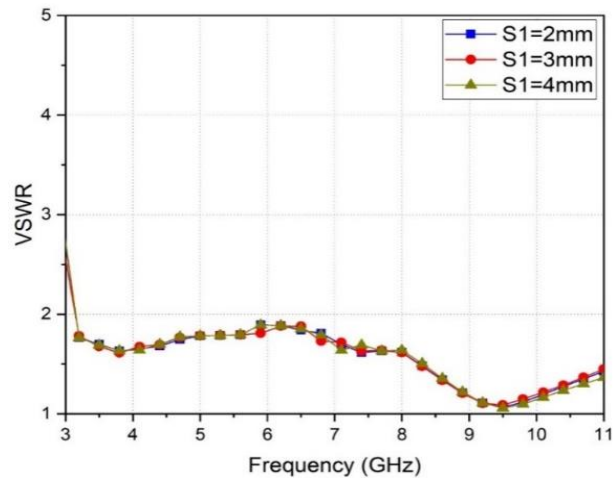


**Figure 5.7:** Deviation of VSWR for dissimilar ground slot length ( $S_1$ )

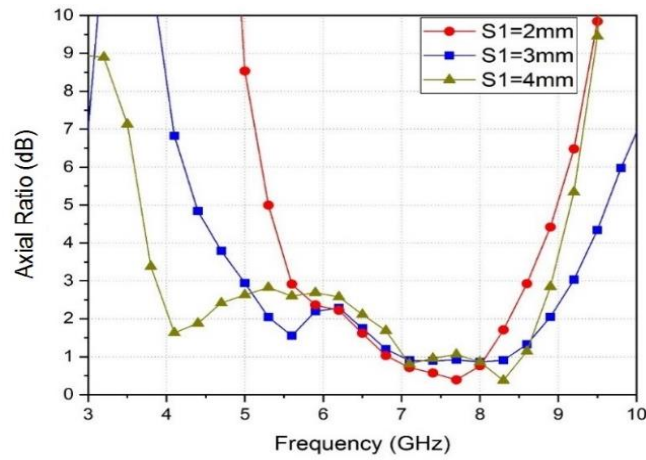


**Figure 5.8:** Deviation of Axial ratio for dissimilar ground slot length ( $S_1$ ).

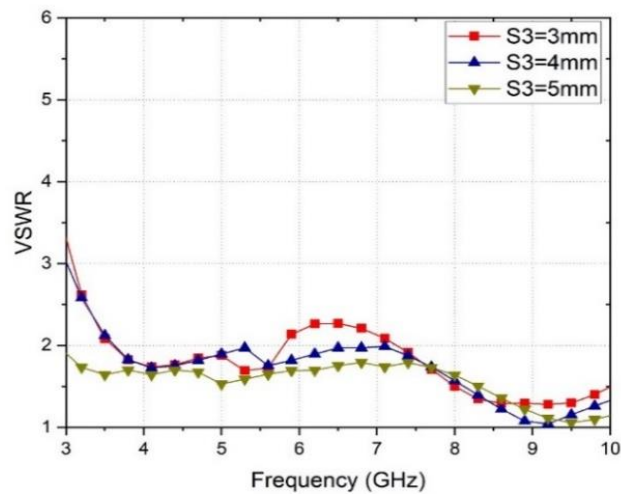


**Figure 5.9:** Deviation of VSWR for dissimilar the length of the slot ( $S_3$ )

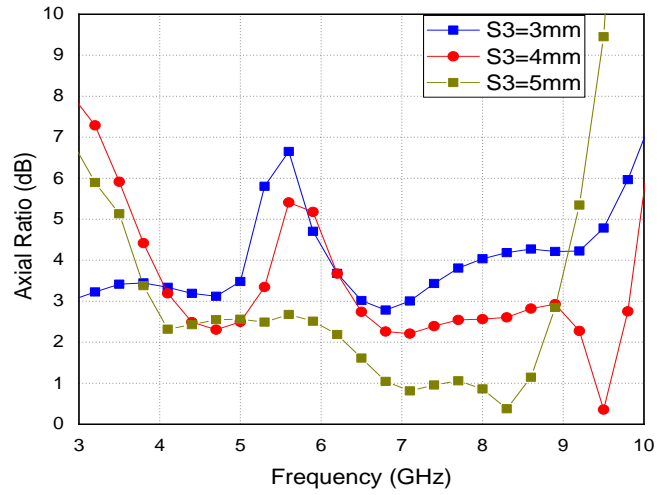


Figure 5.10: Deviation of Axial Ratio for dissimilar the length of the slot ( $S_3$ )

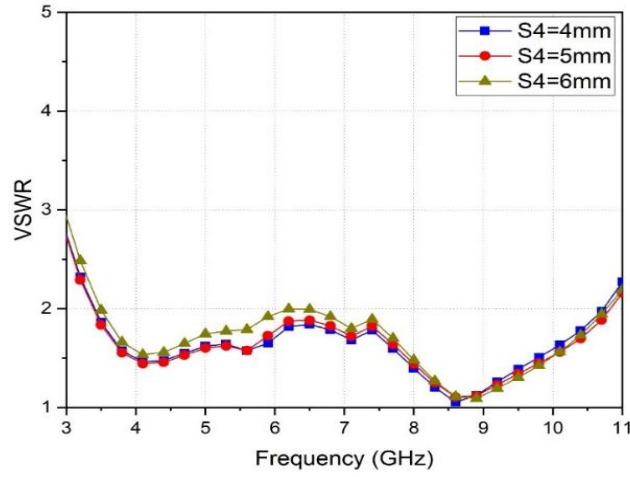


Figure 5.11: Deviation of VSWR for dissimilar ground slot length ( $S_4$ )

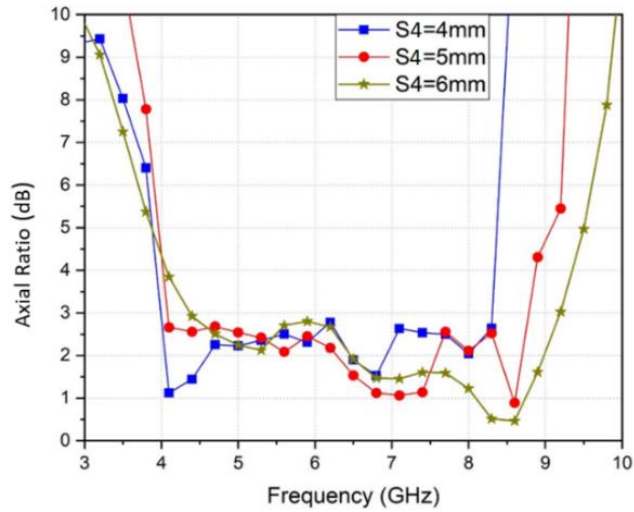


Figure 5. 12 Deviation of Axial ratio for dissimilar ground slot length (S4)

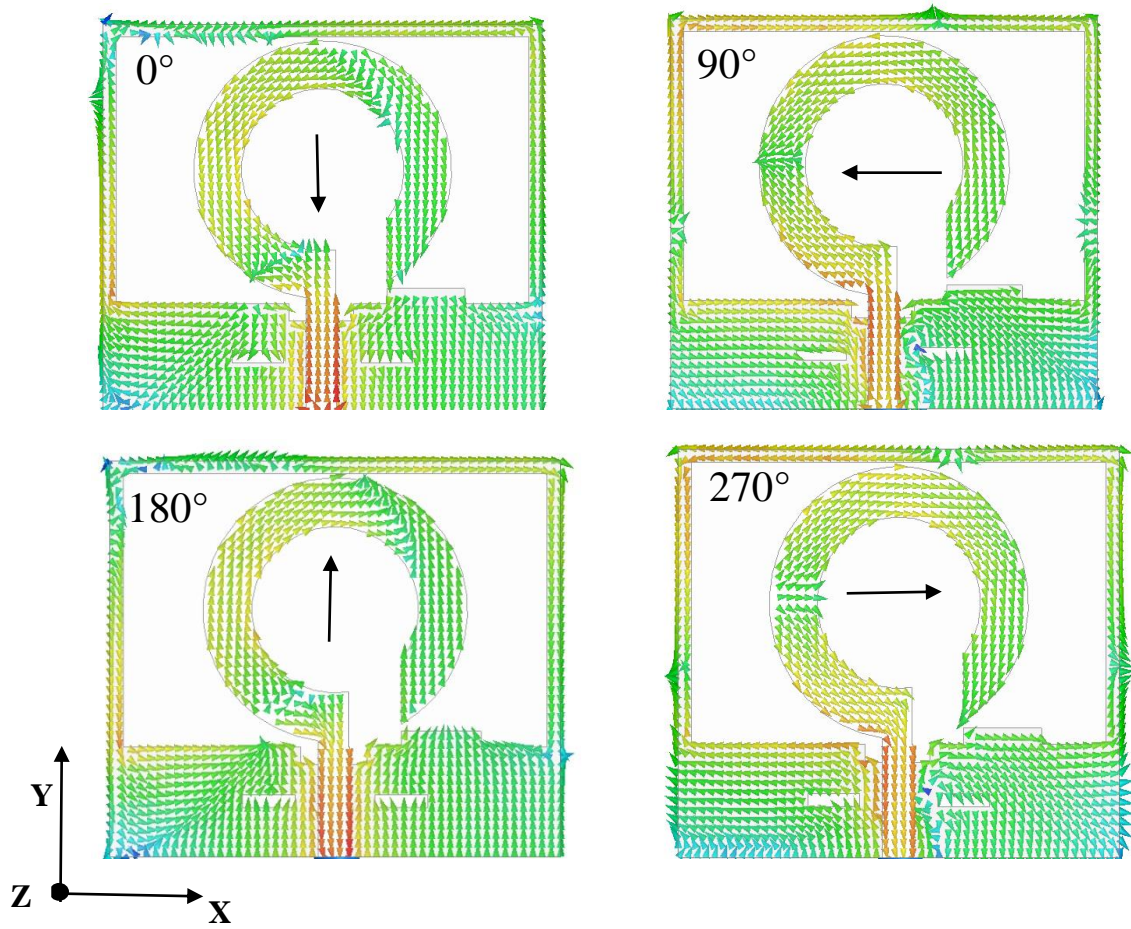
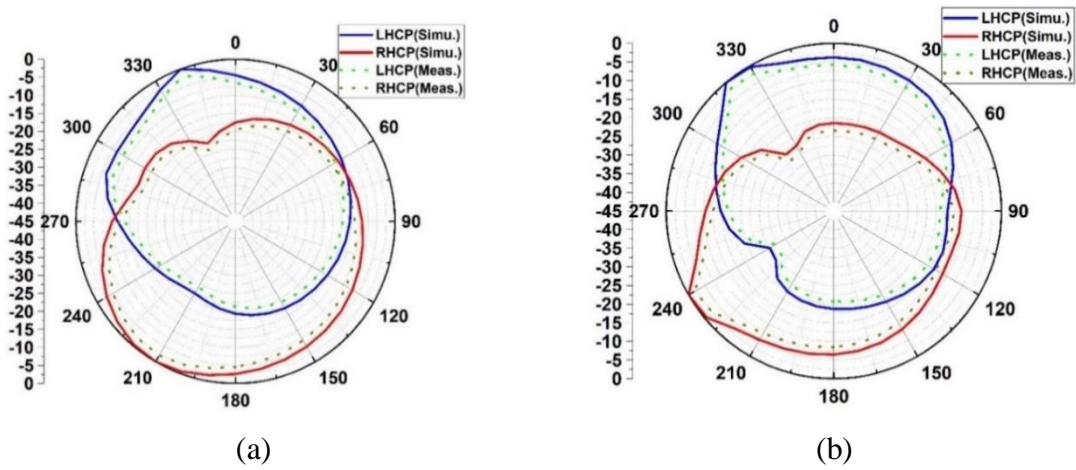


Figure 5. 13: Current density at 6 GHz with the dissimilar phase of 0°, 90°, 180°, and 270°.



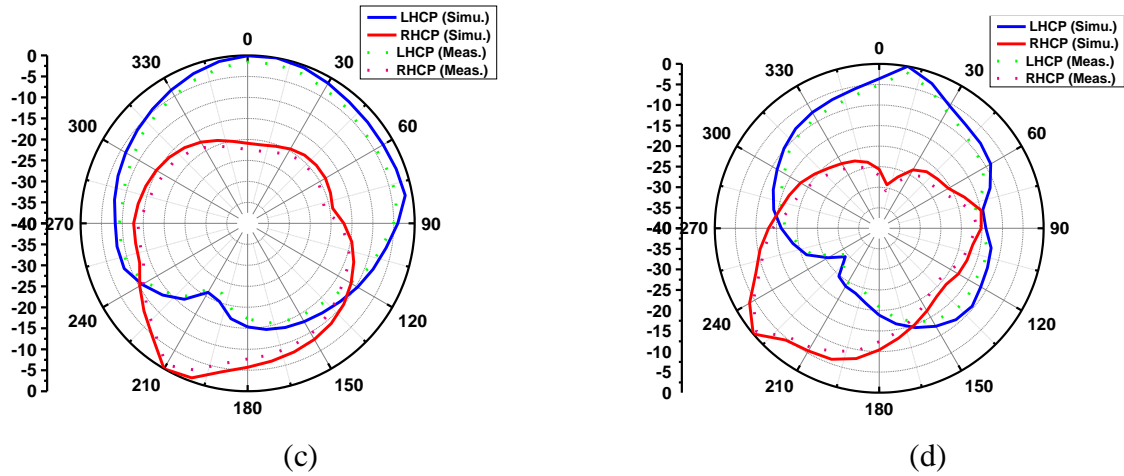


Figure 5. 14: Radiation plot (a) E -plane and (b) H-plane at 5 GHz c) E-plane and (d) H-plane at 7 GHz

### 5.4 Circular Polarized band-notched UWB MIMO Antenna

Circular polarization is more preferred as compared to linear polarization because it removes the need to bring into line alignment of the receiver and transmitter antennas thus reducing the polarization mismatch problem. It also minimizes the Faraday rotation effect and mitigates multipath interference [301]. In common, CP wave can be created by generating two orthogonally electric fields with identical amplitude and 90° phase difference [302].

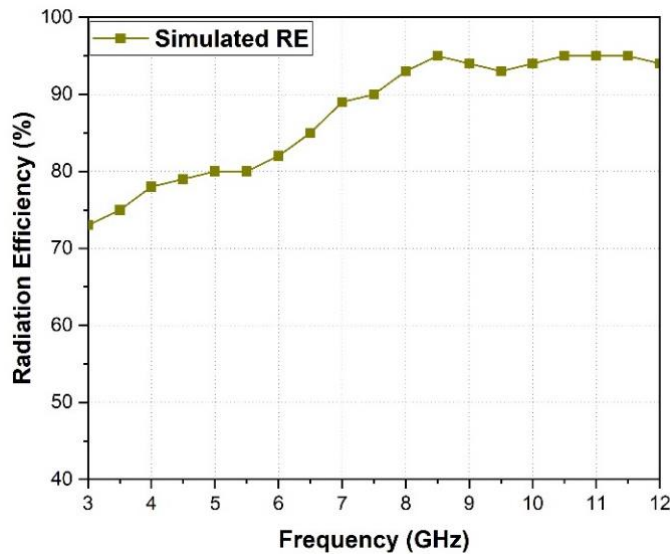


Figure 5. 15: The plot of radiation efficiency

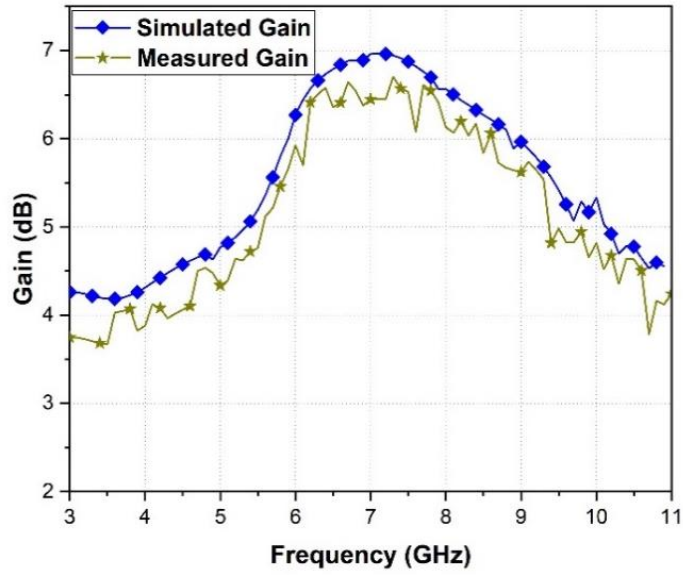
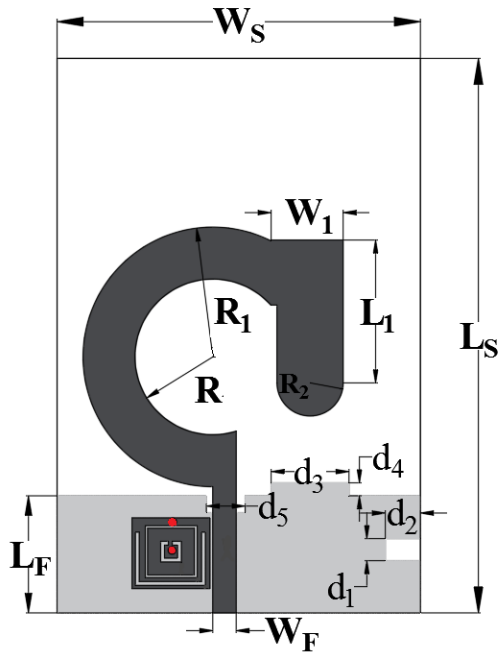


Figure 5. 16: The plot of radiation efficiency and Gain

Table 5. 2: Performance comparison of the suggested antenna

S. No.	Reference	IB (GHz)	Polarization	ARBW (GHz)	Size (mm <sup>2</sup> )
1.	<b>Proposed Antenna</b>	<b>3-11</b>	<b>LHCP</b>	<b>4-9</b>	<b>32×30</b>
2	[289]	3-11	LHCP	4-9.5	34×30
3.	[290]	2.25–7.35	LHCP	2.05–6.55	49 × 55
4.	[291]	2.4-14	LHCP	4.3-6.75	60 × 50
5.	[292]	2.67-13	LHCP	4.9-6.9	60 × 60
6.	[293]	4.56-8.5	RHCP	4.75-8.45	40 × 40
7.	[294]	5.02-10.84	LHCP	5.07-9.22	40 × 40
8.	[295]	2.08-3.75	LHCP	2.28-3.76	46.6 × 70
9.	[296]	1.84-2.43	LHCP	1.89-2.43	50 × 50
10.	[297]	1.48-4.24	RHCP	2.05-3.9	55×50
11.	[298]	0.85-4.15	LHCP	1.20-3.40	00 × 100
12.	[299]	1.78-5.64	RHCP	2.85-5.21	54×54
13.	[300]	2.4–7.4	LHCP	4.9–6.9	39×32



**Figure 5. 17:** Layout of the triple band-notched CP UWB antenna

The schematic of the band rejected CP UWB structure is illustrated in Figure 5.17. The design contains a modified ring-shaped CP UWB Antenna excited by microstrip feedline. To produce the triple band-notched characteristics, the TVC EBG unit cell is positioned close to the feed of the planar monopole UWB structure. A rectangular slot and stump are etched in the ground of the presented structure element to acquire wider axial ratio bandwidth. The band notched CP UWB antenna element size specifics are existing in Table 5.3.

The prototype of the presented structure is shown in Figure 5.18. Originally, a modified ring formed (Antenna-A) is intended, as demonstrated in Figure 5.18a.

The Axial ratio and VSWR of the design are displayed in Figure 5.19 and Figure 5.20. The shows VSWR of 3- 11 GHz and ARBW of 4-5 GHz for antenna A. In Figure 5.18b TVC-EBG unit cell is placed close to the feed (Antenna-B) to attain three rejection bands. Next, as illustrated in Figure 5.18c, stubs and slots are inserted in the ground plane (Antenna-C) to achieve a wider ARBW.

#### 5.4.1 Band notched CP UWB MIMO antenna

The symmetrical outline of the presented structure is shown in Figure 5.21, and Table 5.3. indicates the sizes of different factors. The ground plane of the structure is identical. The design considerations for obtaining UWB characteristics are considered, and the simulation and experimental results are presented. The made-up archetype of the structure is verified in Figure 5.22. The dimensions of the suggested structure are  $63 \times 63 \times 1.6 \text{ mm}^3$ .

**Table 5. 3.:** Optimized dimension of the proposed antenna

<b>Parameter</b>	$L_s$	$W_s$	$W_F$
<b>Units(mm)</b>	42.72	28	1.8
<b>Parameter</b>	$W_1$	$L_1$	$L_f$
<b>Units(mm)</b>	5.5	11	9
<b>Parameter</b>	$d_1$	$d_2$	$d_3$
<b>Units(mm)</b>	1.7	2.7	6
<b>Parameter</b>	$R$	$R_1$	$R_2$
<b>Units(mm)</b>	6	10	2.5
<b>Parameter</b>	$d_5$	$d_4$	$d_3$
<b>Units(mm)</b>	3	1	6

#### 5.4.2 Circular polarization phenomenon

The suggested band-notched CP UWB MIMO antenna is fabricated with polarization diversity rather than operating identical CP mode. As a result, RHCP or LHCP mode can be obtained with the same enactment of the MIMO antenna. The surface current circulations are used to evaluate the CP production of the suggested antenna. Figure 5.23 displays the simulated surface currents ( $J_s$ ) at different phase intervals  $0^\circ$ ,  $90^\circ$ ,  $180^\circ$ , and  $270^\circ$ . The surface currents are used to determine the Circular Polarized of the suggested antenna. Figure 5.23

displays the surface currents at dissimilar phase intervals  $0^\circ$ ,  $90^\circ$ ,  $180^\circ$ , and  $270^\circ$ . The predominant vector direction is in  $-Y$  direction for  $0^\circ$ , while for  $90^\circ$  the predominant vector direction is  $-X$  direction.

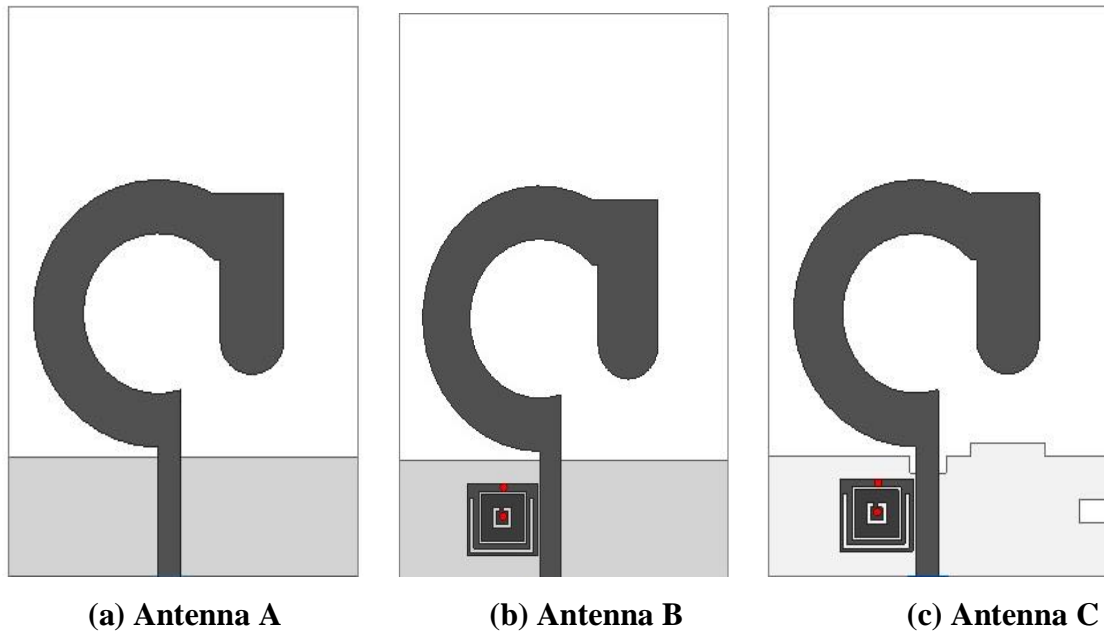


Figure 5.18: Stepwise expansion of the presented antenna.

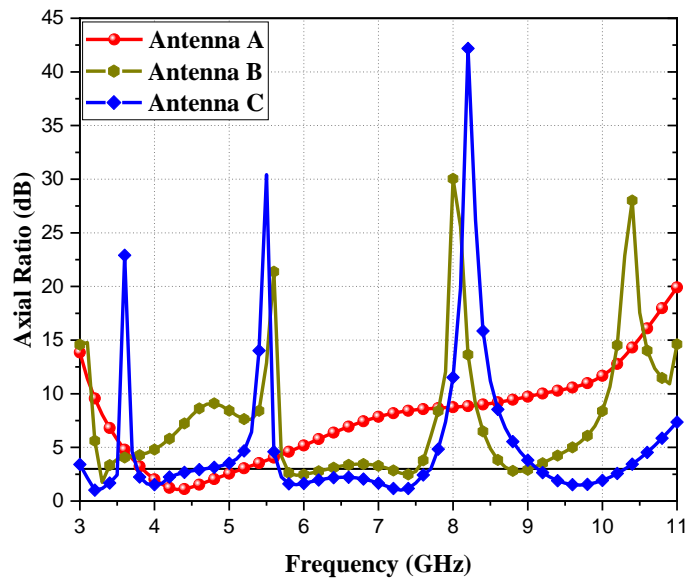


Figure 5.19: Axial ratio of different stages of the presented antenna.

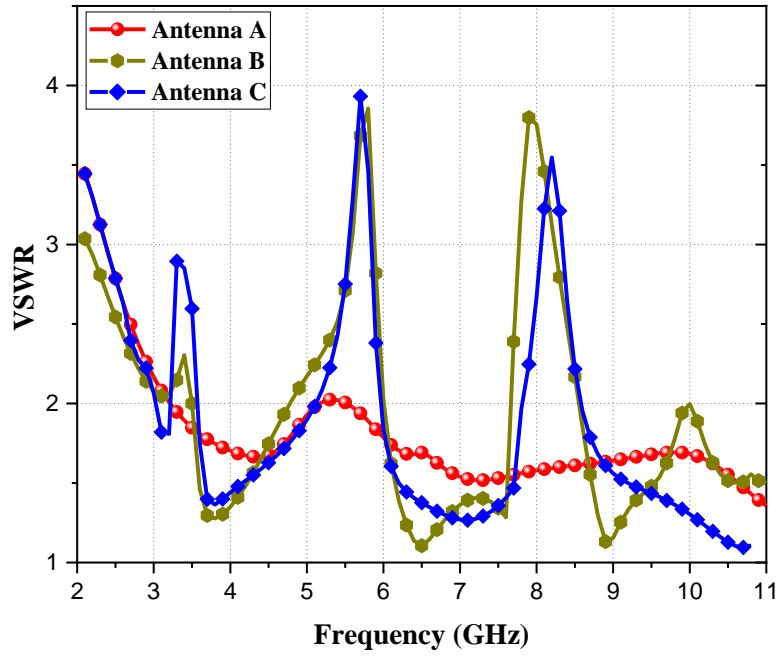


Figure 5.20: VSWR of different stages of triple band-notched CP UWB antenna.

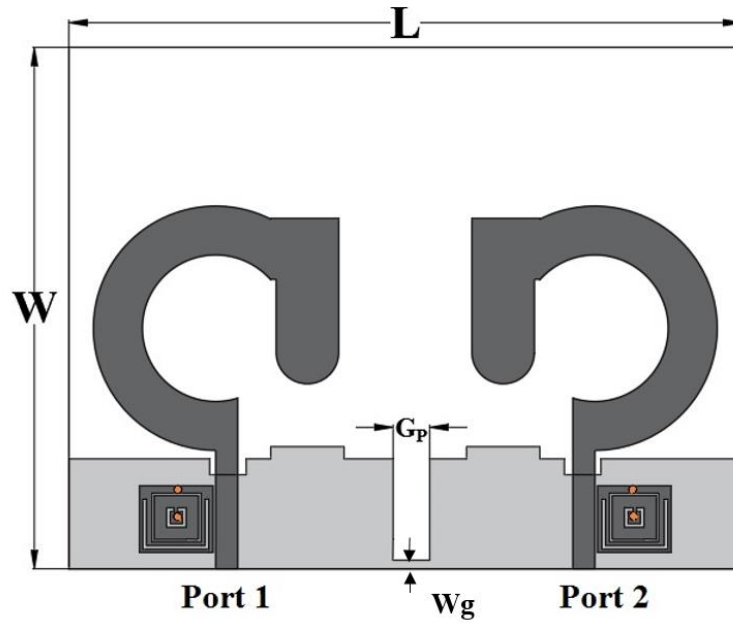
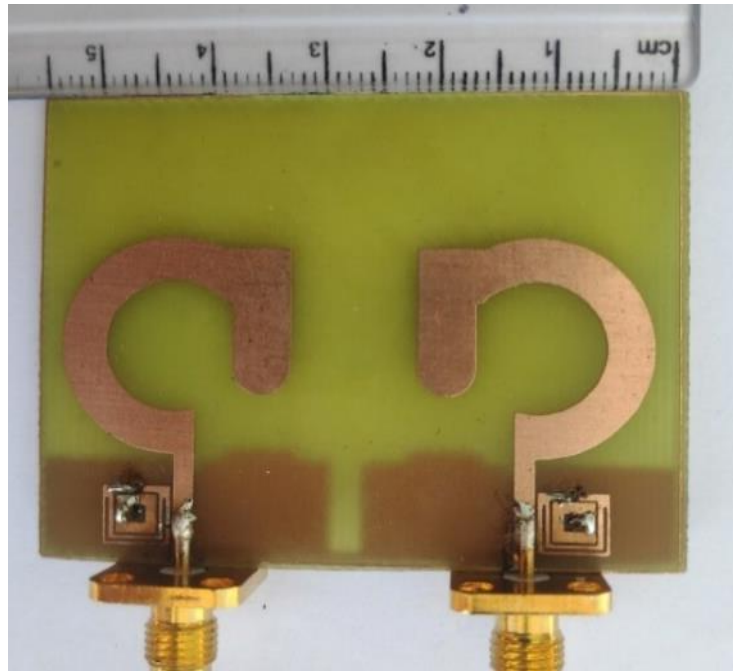


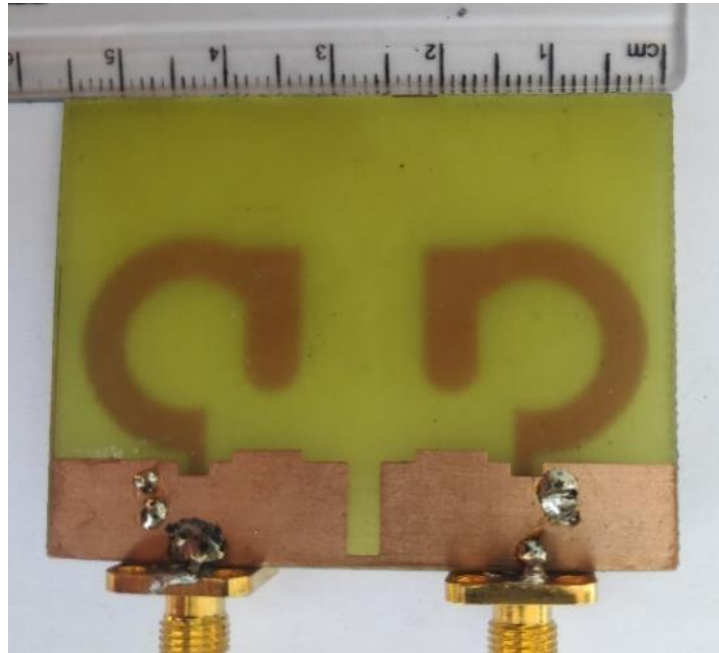
Figure 5.21: Geometric layout of the presented structure

**Table 5. 4** Circularly Polarized UWB MIMO Antenna Dimension

<b>Parameter</b>	<b><math>W</math></b>	<b><math>L</math></b>	<b><math>W_F</math></b>
<b>Units(mm)</b>	42.72	55	1.8
<b>Parameter</b>	<b><math>W_I</math></b>	<b><math>L_I</math></b>	<b><math>L_f</math></b>
<b>Units(mm)</b>	5.5	11	9
<b>Parameter</b>	<b><math>d_1</math></b>	<b><math>W_L</math></b>	<b><math>d_3</math></b>
<b>Units(mm)</b>	1.7	6	6
<b>Parameter</b>	<b><math>R</math></b>	<b><math>R_1</math></b>	<b><math>R_2</math></b>
<b>Units(mm)</b>	6	10	2.5
<b>Parameter</b>	<b><math>d_5</math></b>	<b><math>d_4</math></b>	<b><math>d_3</math></b>
<b>Units(mm)</b>	1.3	1	6



(a)



(b)

**Figure 5. 22:** Prototype of the made-up structure

For  $180^\circ$  and  $270^\circ$ , the predominant vector direction is reverse to  $0^\circ$  and  $90^\circ$ . It is observed from the Figure5.23 that as the left-handed or clockwise direction, as observed from the +Z direction. With Port 1 excitation the proposed antenna can operate as LHCP radiation of the antenna. Similarly, while Port 2 is excited, the surface current rotates in an anti-clockwise direction as the phase varies from 0 to  $270^\circ$ , which is opposite from the earlier event, as indicated in Figure5.24. This generates the RHCP radiation of the CP antenna.

## 5.5 Experimental results and validation

The simulated curves, authenticate when the layout of the suggested structure has been made-up, and tested curves like S parameters and radiation plot are attained from the VNA and anechoic chamber, respectively. Measured VSWR is presented in Figure5.25. The 3 dB ARBWs are 3 to 10.4 GHz excluding three interfering bands presented in Figure5.26. Figure5.27 displays the  $|S_{12}|$  is less than -15 dB for the entire range. Simulated and measured E-plot and H-plot radiation plots at 5 and 7 GHz are stated in Figure5.28. MIMO performance

has been calculated by calculating ECC, DG) and TARC. For two-port systems, ECC can be evaluated using:

$$ECC = \frac{|S_{11}^* S_{12} + S_{21}^* S_{22}|^2}{\left(1 - |S_{11}|^2 - |S_{21}|^2\right) \left(1 - |S_{22}|^2 - |S_{12}|^2\right)} \quad (5.1)$$

ECC shows the similarity between the radiation plots of the MIMO antenna. The DG is determined using

$$DG = 10\sqrt{1 - ECC^2} \quad (5.2)$$

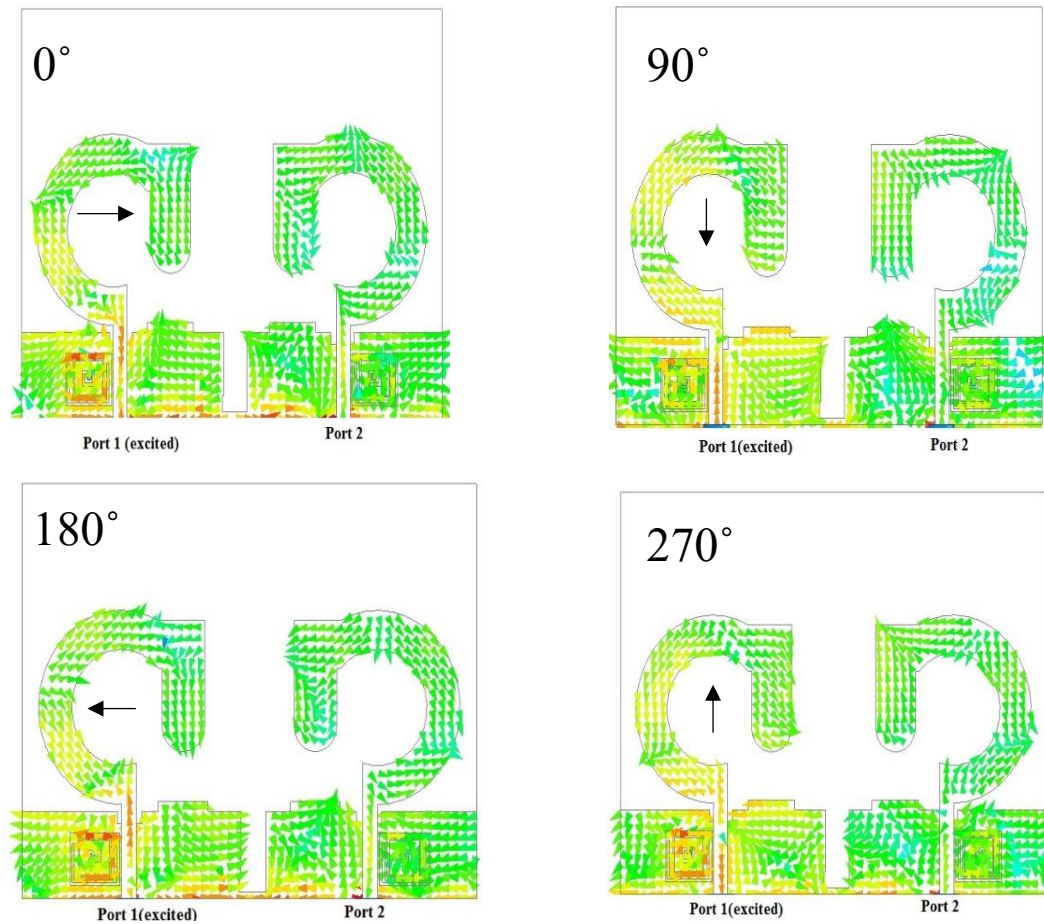


**Figure 5. 23:** Simulated surface currents with when port 1 is excited

The similarity of the two radiation plot is antenna is below than 0.005 for the whole frequency range, eliminating the interfering bands where ECC rise to 0.03. The TARC can be calculated

for MIMO antenna as return loss is calculated for single antenna elements, which is given as follows

$$TARC = \sqrt{\frac{(S_{11} + S_{12})^2 + (S_{21} + S_{22})^2}{2}} \quad (5.3)$$

.A TARC value of <, 0 dB is necessary for a MIMO system. Figure 5.29 is analyzed that the TARC value for the suggested structure is below than - 4 dB for the whole band. The DG is nearby 9.98 dB for the entire band, eliminating three interfering bands indicates in Figure 5.29.

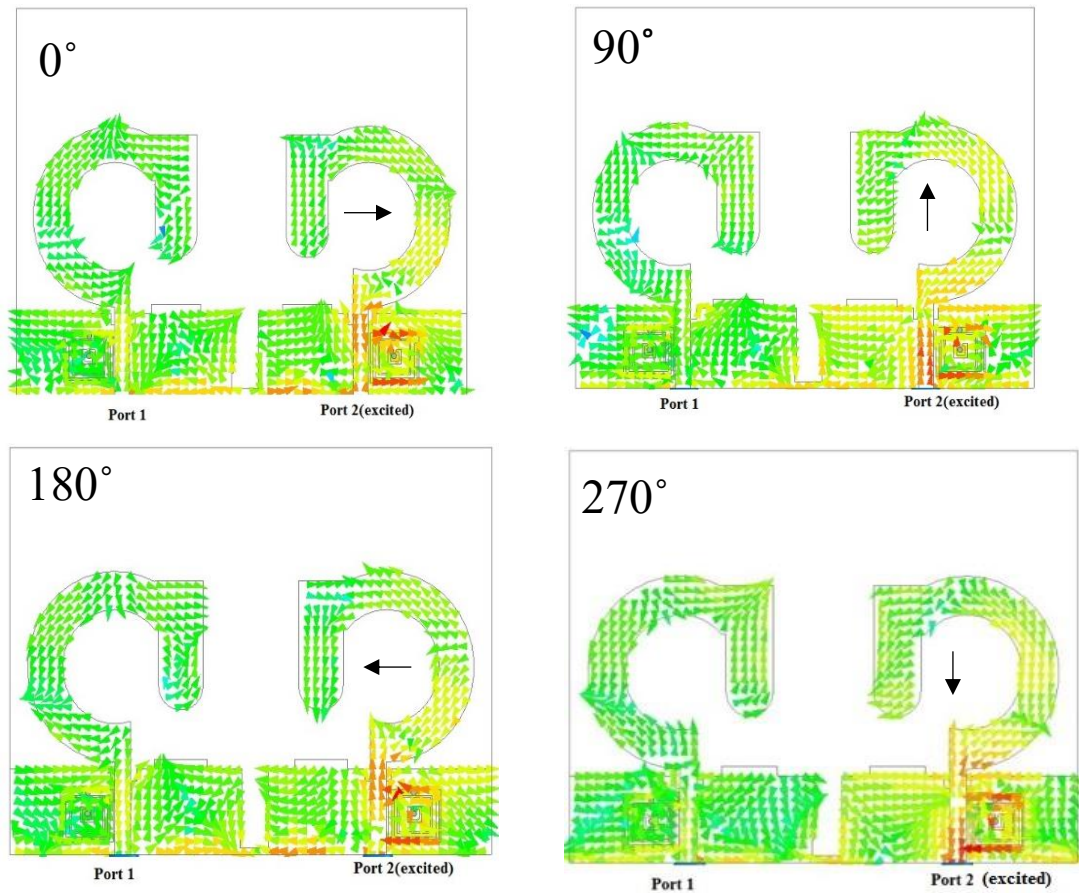


**Figure 5.24:** Simulated surface currents with when port 2 is excited

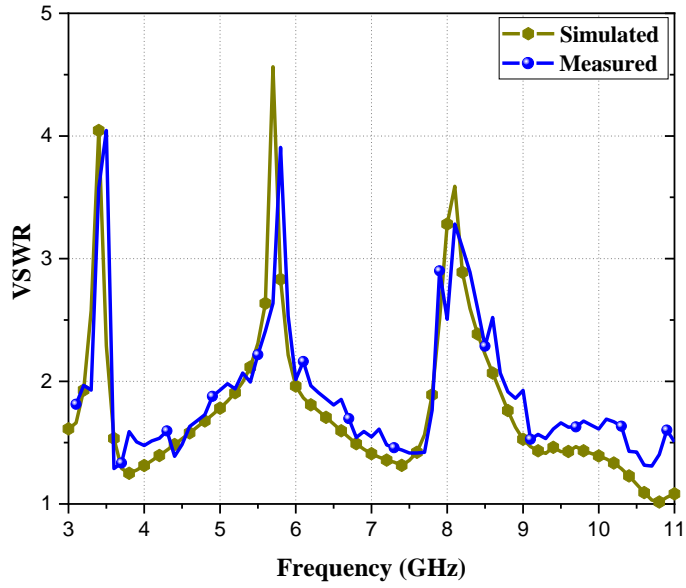


Figure 5. 25: VSWR of the presented structure.

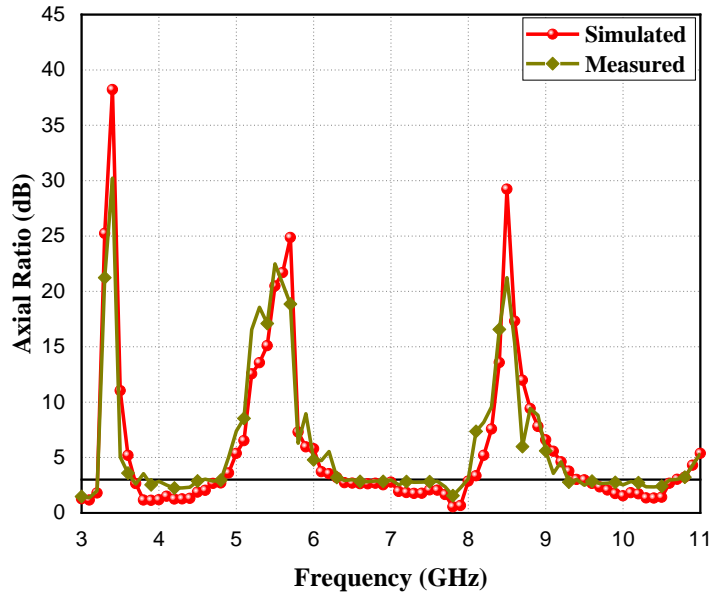
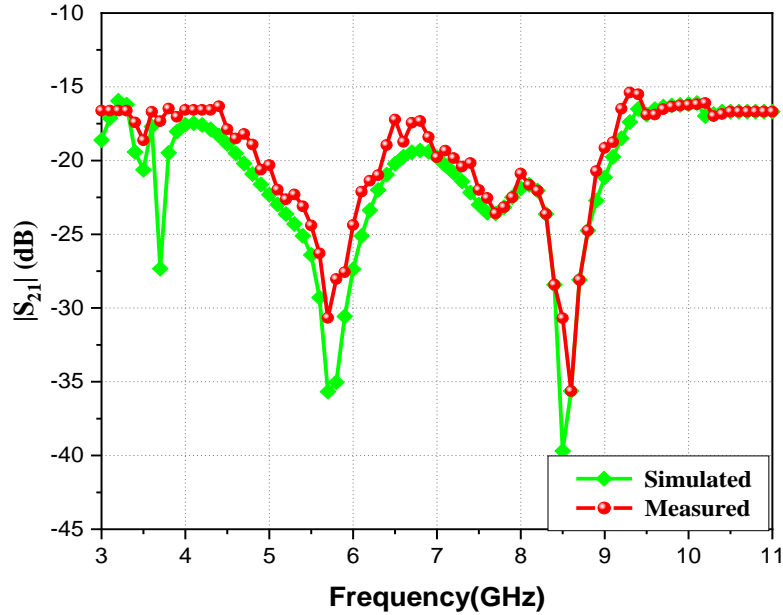


Figure 5. 26: A R of the presented structure

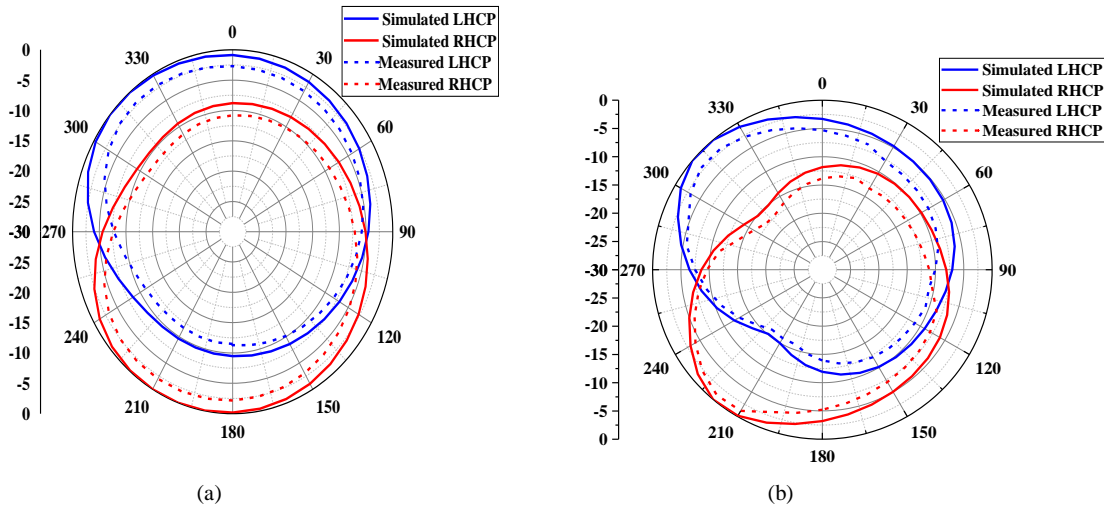
## 5.6 Comparison of different CP UWB MIMO Antenna

Table 5.5 comprises the comparative study of various CP UWB MIMO antenna with the proposed one. The size of the antenna, several notched bands, axial ratio bandwidth, and impedance bandwidth are some important parameters considered for the comparison. From the table, it is observed that ref. 9 obtain dual band-notched, whereas the proposed antenna

resonates at triple-band notched-. The proposed antenna has a compact size, as compared to the ref.9, 24-31 with wider axial ratio bandwidth of 3-10.4 GHz with excluding interfering bands. Figure 5.26 specifies the DG of the presented structure.



**Figure 5. 27:** Measured and simulated Mutual coupling of the band notched CP UWB MIMO antenna



## 5.7 Summery

In this chapter, a Circularly Polarized antenna is simulated and fabricated. The presented structure includes two monopole structures and they are placed facing each other to improve isolation. TVC-EBG unit cell attains three notches at interfering frequency bands. A wider -

10-dB bandwidth from 3 to 11 GHz with three rejected bands. Additionally, the MIMO antenna attains better diversity performances with mutual coupling  $< -15$  dB, ECC  $< 0.03$ , and TARC  $< -4$  dB. Therefore, the proposed antenna can be a good candidate for future UWB wireless Communication system

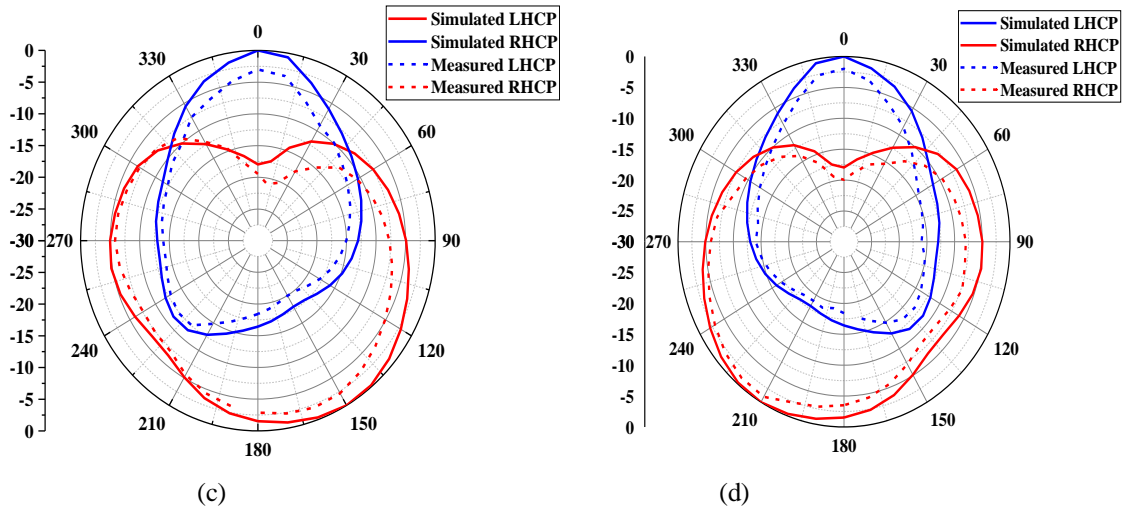


**Figure 5.28:** Tested and Simulated radiation plot with port 1 excitation (a) E-plane plot at 5 GHz (b) H-plane plot at 5 GHz c) E-plane plot at 7 GHz (d) H-plane plot at 7 GHz

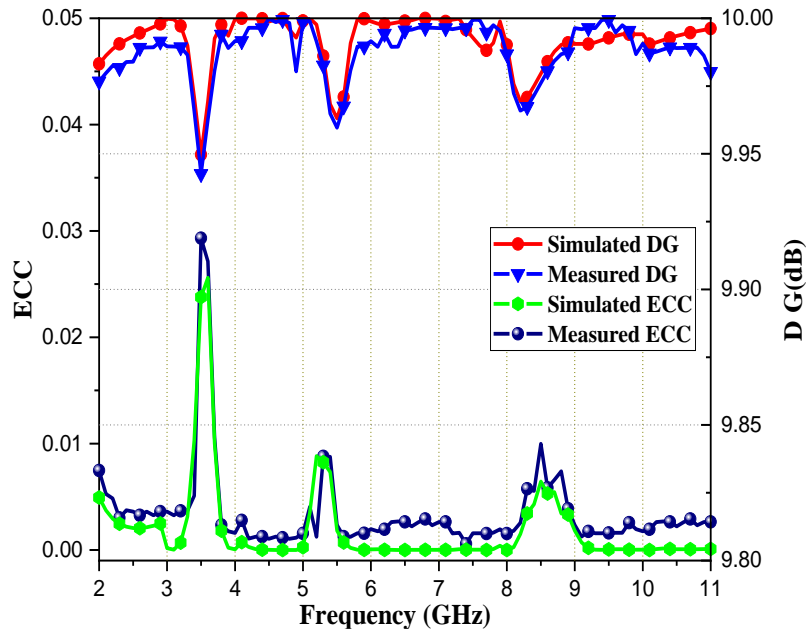


**Figure 5.29:** Measured and simulated ECC and DG

**Table 5. 5:** Evaluation of presented antenna with dissimilar antenna

<b>S. No.</b>	<b>Reference</b>	<b>IB (GHz)</b>	<b>ARBW (GHz)</b>	<b>No. of element</b>	<b>Band notches</b>	<b>No. of band notches</b>	<b>Size (mm×mm)</b>	<b>Isolation (dB)</b>
<b>1.</b>	<b>Proposed Antenna</b>	<b>3-11</b>	<b>3-10.4</b>	<b>2</b>	<b>3.5,5.5&amp;8.2</b>	<b>3</b>	<b>42.72×55</b>	<b>-15</b>
2	[303]	3.2 - 9.6	3.2-8.8	1	5.2 and 5.8	2	65×65	NA
3	[304]	5.10 - 5.85	5.10 - 5.85	2	NA	NA	56×32	-20
4	[305]	5.772–5.864	5.49–6.024	2	NA	NA	97× 26.72	-33
5	[306]	5.8	5.6-6	2	NA	NA	110×58	NA
	[307]	5.71–8.2	7.72–8.04	2	NA	NA	80 × 80	-15
7	[308]	4.56-8.5	4.75-8.45	1	NA	NA	40 × 40	NA
8	[309]	5.02-10.84	5.07-9.22	1	NA	NA	40 × 40	NA
9	[310]	2.08-3.75	2.28-3.76	1	NA	NA	46.6 × 70	NA
10	[311]	1.84-2.43	1.89-2.43	1	NA	NA	50 × 50	NA

**CHAPTER 6**

**COMPACT UWB MIMO ANTENNA**

**WITH ENHANCED BANDWIDTH**

## CHAPTER 6

### Compact UWB MIMO Antenna with Enhanced Bandwidth

#### 6.1 Introduction

UWB has a bandwidth from 3.1-10 GHz that provides various services for example WiMAX, WLAN, and X Band. To use GPS, GSM, ISM, Bluetooth, and WLAN application, an improved BW UWB planar structure is mandatory [312]. The existing UWB antenna supports the limited number of wireless communication services. To achieve UWB, many methods are given in the existing work. By etching the slots in the ground surface[313], [314]an additional resonance generated that couples to resonances of the antenna, which helps in bandwidth improvement[315], [316]. Dissimilar patch structure like Koch structure [317], U formed [318],lotus formed [319], binomial-curve[320] and inverted T-shaped [321] used to accomplish wider bandwidth. In literature to achieve wider impedance bandwidth electromagnetic bandgap [322] and parasitic elements [323]–[324] are also used.

The UWB system affronted the difficulty of signal fading [325] is one of the major challenges due to the multipath environment. To evade the affronted, UWB and MIMO systems are combined. The UWB MIMO antenna also delivers enhanced channel capacity. On the other hand, UWB MIMO has a concern about isolation among the patch elements. The overall parameters are disturbed due to high isolation amid the structure elements. To reduce the mutual coupling numerous methods such as DGS [326], meander line resonator [327],SSR [328],NL[329], [330] and strips [331] are used. In this chapter, an innovative formed small size UWB-MIMO antenna is introduced. Concentric Square slot and reverse L shaped are used to enhance isolation among patches. The complete size of the presented structure is  $27 \times 17 \times 1.6\text{mm}^3$ .

#### 6.2 UWB MIMO Antenna with Enhanced Bandwidth

##### 6.2.1. Antenna Design and Analysis

Figure 6.1 demonstrates the sizes of the presented structure and the design dimensions shown in Table 6.1. The designed structure is fabricated using cheap FR-4 dielectric material with

relative permittivity ( $\epsilon_r$ ) and dielectric height (h), of 4.4, and 1.6mm respectively. A concentric slot is inserted and a reverse L-formed stripe is expanded from the ground surface to enhance the isolation. The antenna parameters like S parameters and radiation pattern are calculated using Agilent N5230C VNA and microwave shield chamber. The values of R1, LS, WS, LP, and LP1 are parametrically varied to get wider bandwidth. The differences between tested and simulated curves are because of numerous losses like SMA soldering, fabrication, and measurement error.

### 6.2.2 Deviations in the ground plane of presented antenna:

The extension of the ground surface is presented in Figure 6.2. Figure 6.3 indicates the isolation of dissimilar ground surface; it is perceived that the best performance can be achieved utilizing ground C. Therefore, Ground C is used in the presented antenna.

**Table 6. 1:** Optimized size of the Ultra-Wide MIMO antenna with enhanced bandwidth

<b>Parameter</b>	$L_s$	$W_s$	$W_F$
<b>Units(mm)</b>	17	28	12
<b>Parameter</b>	$W_{GI}$	$W_G$	$L_f$
<b>Units(mm)</b>	4	14	1.6
<b>Parameter</b>	$L_{f1}$	$L_{GI}$	$L_G$
<b>Units(mm)</b>	4.5	0.7	10.8
<b>Parameter</b>	$R$	$LP1$	$LP$
<b>Units(mm)</b>	3	3.3	2.1

### 6.2.3 Surface Current circulation of the Ultra-Wide MIMO antenna

To further elaborate on the effectiveness of these proposed defected ground surface, the degree of mutual coupling in the presented structure can be perceived by presenting surface currents circulation. It is observed from Figure 6.4 the port 1 is agitated and port 2 is ended with 50 ohms. In Figure 6.4 (a) the entire current moving the presented antenna.

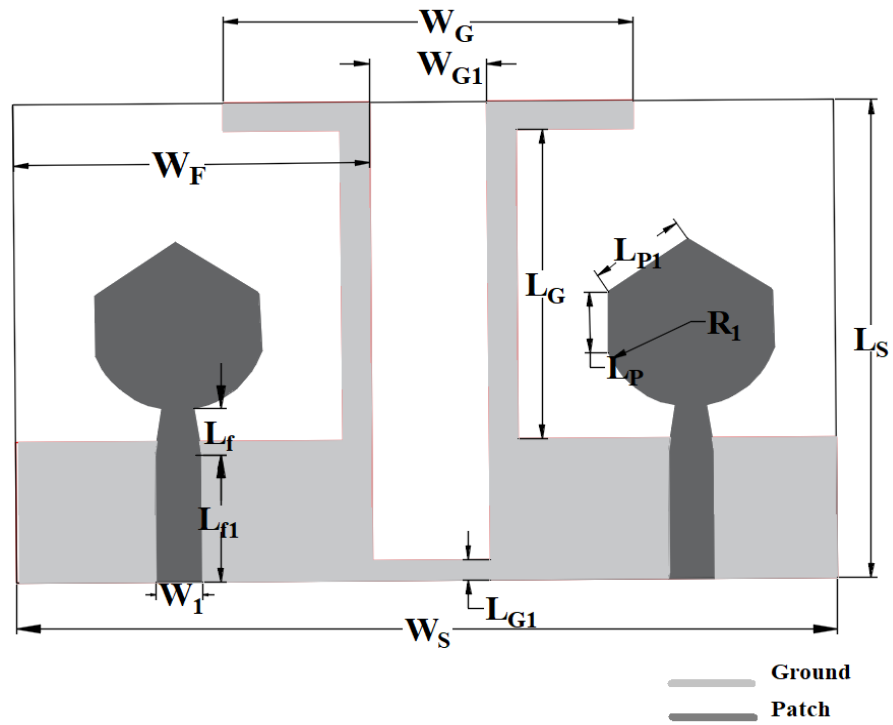


Figure 6. 1 Layout of the presented antenna

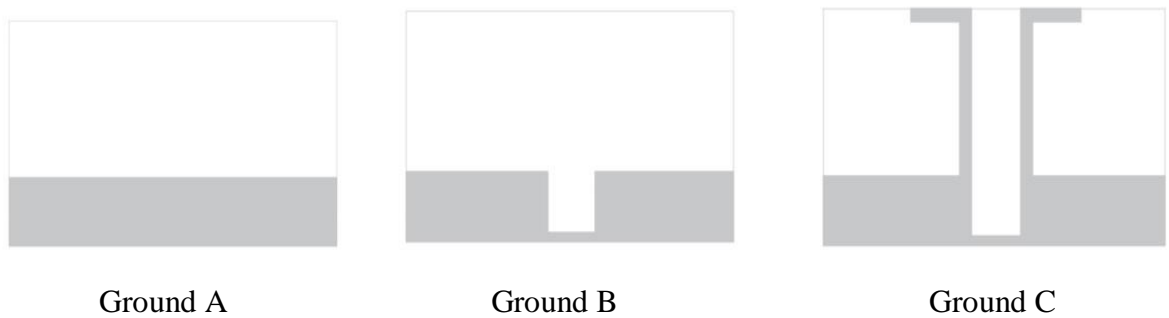


Figure 6. 2. Extension of the presented antenna

The  $|S_{12}|$  amid the radiating elements is enhanced by inserting the concentric slot on the ground plane as illustrated in Figure 6.4 (b). Though, combining the two inverse L shaped strip significantly increase the isolation as displayed in Figure 6.4(c).

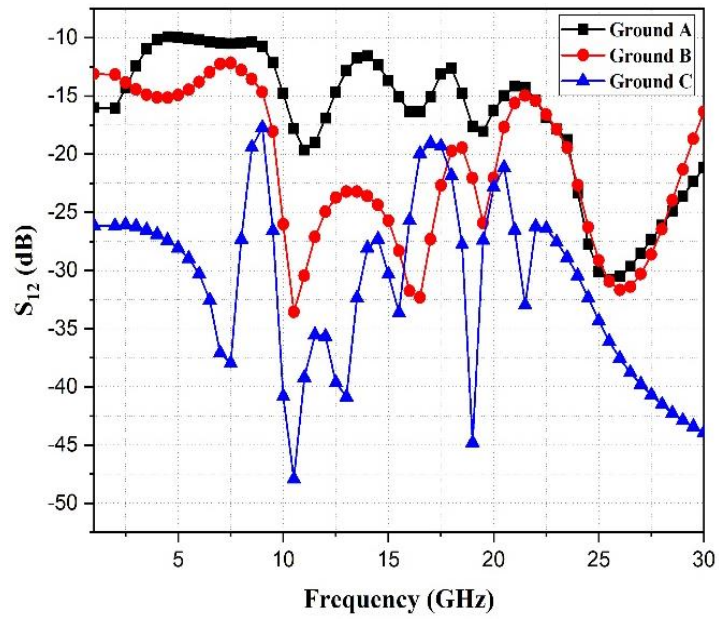
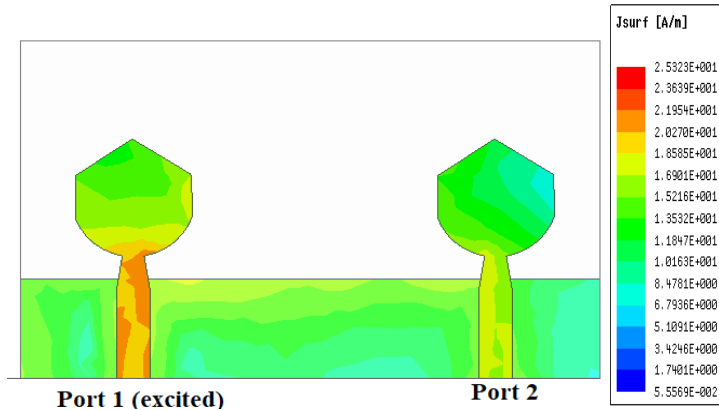
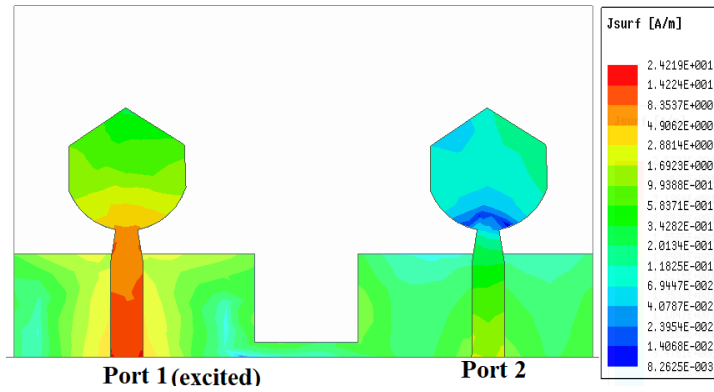


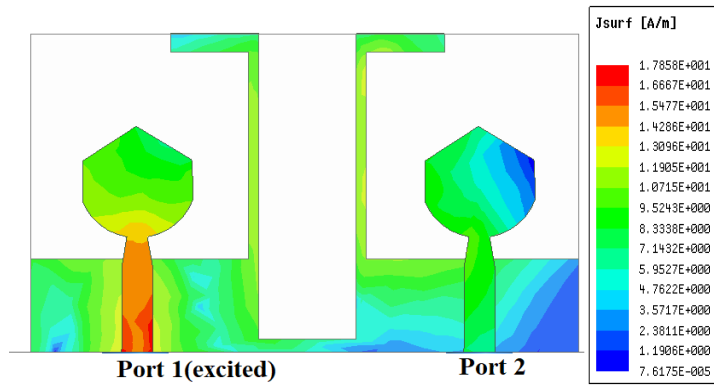
Figure 6.3: Deviation of the ground plane



(a)

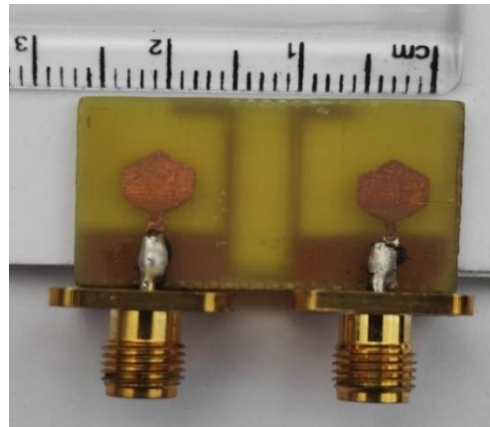


(b)

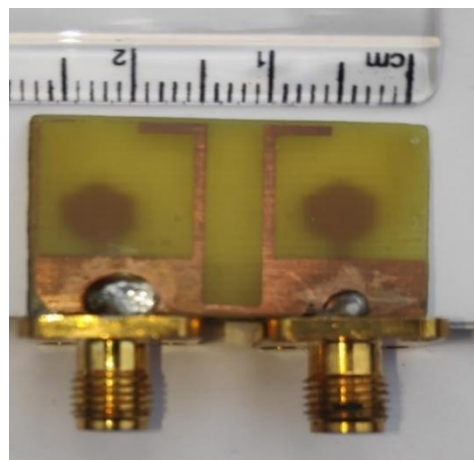


(c)

**Figure 6.4:** Circulation of the surface current on the presented structure



(a)



(b)

**Figure 6. 5:** (a) Topmost vision, (b) foot vision of the made-up presented structure.

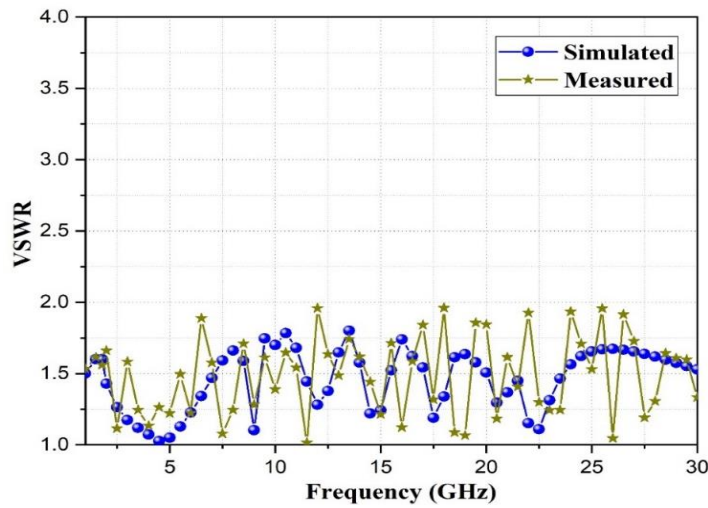


Figure 6. 6: Measures and simulated VSWR

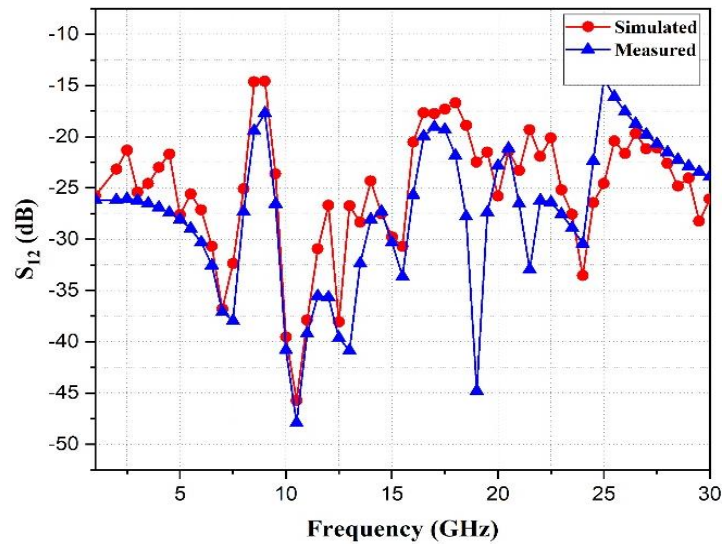
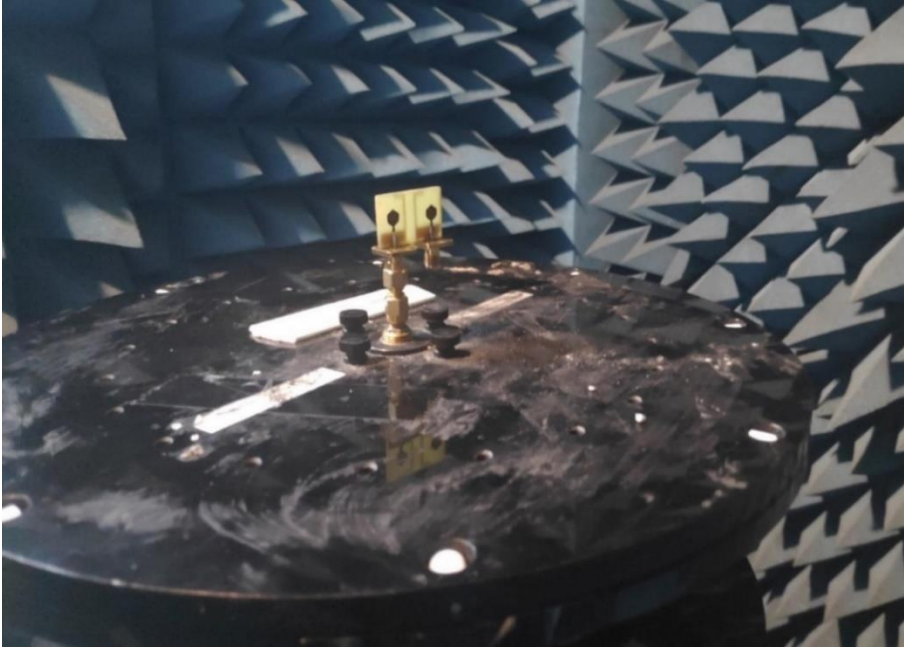


Figure 6. 7: Measures and simulated Mutual coupling

### 6.3. Experimental results and discussion

Integration of two elements together in a MIMO system to provide higher data throughput at the same operating band[332]–[333]. The designing of the multiple antennae is a difficult task, as the radiating patches are kept at very nearly. Because of this, the coupling between the port coupling and field coupling rises. The efficiency and channel capacity of the presented antenna are affected

by this coupling. Thus, there is a necessity for low mutual coupling between the ports and the low similarity level between the radiation patterns.

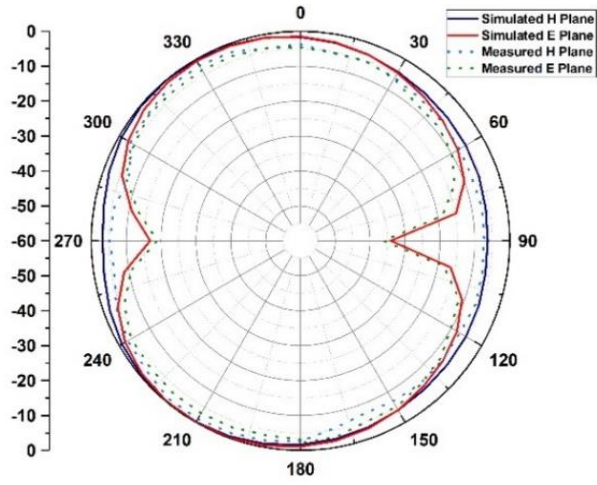


(a)

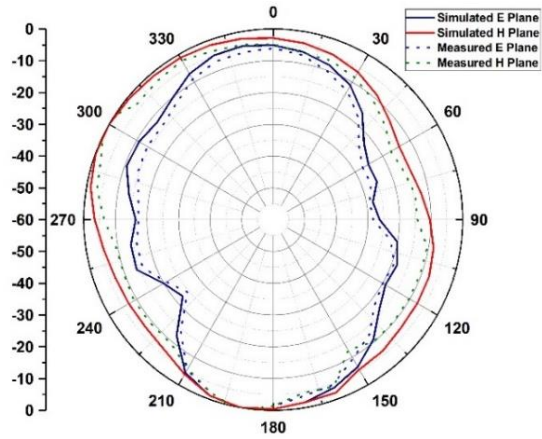


(b)

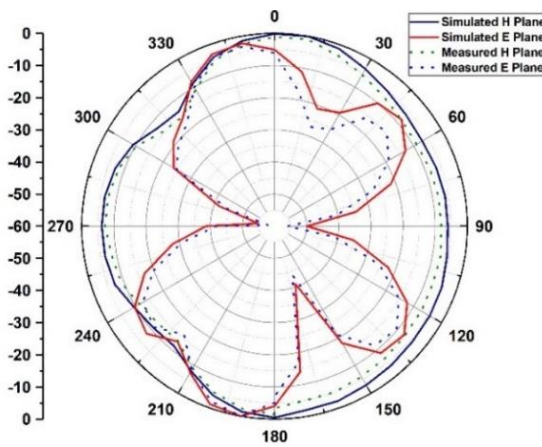
**Figure 6. 8:** Measurement set up for proposed dual notch fabricated prototype antenna in the anechoic chamber



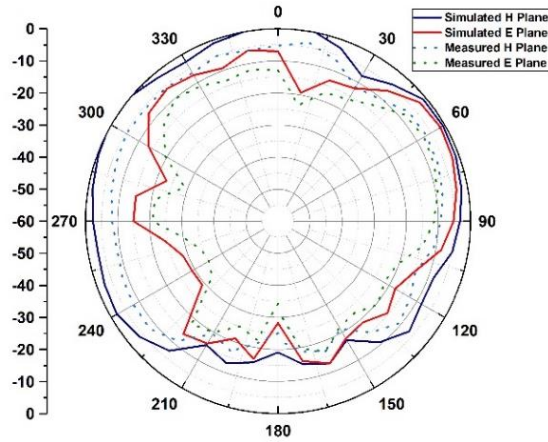
(a)



(b)



(c)



(d)

**Figure 6. 9.:** Difference between the measured and simulated radiation plot at for dissimilar frequencies  
(a) 5.5 GHz, (b) 14.5GHz (c) 24 GHz and (d) 27GHz

The diversity performance is evaluated using different parameters such as ECC[334], DG[335], TARC[336], EDG, RE, and CCL of the presented antenna. The extent of similarity amid the radiation curves of the presented MIMO elements can be estimated utilizing ECC[334]. The ECC is given below:

$$ECC = \frac{\left| \int_{\Omega} [XPR.E_{\theta_i}E_{\theta_j}^*P_{\theta} + E_{\phi_i}E_{\phi_j}^*P_{\phi}]d\Omega \right|^2}{\int_{\Omega} [XPR.E_{\theta_i}E_{\theta_i}^*P_{\theta} + E_{\phi_i}E_{\phi_i}^*P_{\phi}]d\Omega \int_{\Omega} [XPR.E_{\theta_j}E_{\theta_j}^*P_{\theta} + E_{\phi_j}E_{\phi_j}^*P_{\phi}]d\Omega} \quad (6.1)$$

$$XPR = \frac{P_V}{P_H}$$

ECC [334] is also related to S parameters given below

$$ECC = \frac{\left| S_{11}^*S_{12} + S_{21}^*S_{22} \right|^2}{\left( 1 - |S_{11}|^2 - |S_{21}|^2 \right) \left( 1 - |S_{22}|^2 - |S_{12}|^2 \right)} \quad (6.2)$$

where,  $S_{11}$  and  $S_{22}$  is the reflection coefficient.  $S_{12}$  and  $S_{21}$  are coupling among the different ports. It is essential to have ECC less than 0.5 for satisfactory results of a presented system. DG is the substation of power level in dB of the collective signals of the MIMO system and a single antenna system. DG [337] of the presented system is intended as:

$$DG = 10\sqrt{1 - ECC^2} \quad (6.3)$$

Figure 6.10 describes the difference between the measured and simulated ECC and DG of the presented structure. One more significant MIMO features are EDG. The DG does not assess the radiation losses while EDG contains the radiation losses. The EDG formulation is stated in equation (6.4). It is also the multiplication of DG and RE results EDG. The value of Effective diversity gain will be smaller than the DG. The achieved DG value is 9.98 dB however EDG is around 9.2 dB.

$$EDG = \eta_{Total} * DG \quad (6.4)$$

$$\eta_{Total} = \eta(1 - |S_{11}|^2 - |S_{21}|^2) \quad (6.5)$$

TARC formula is shown in equation (6.6) [338].

$$TARC = \frac{\sqrt{\sum_{i=1}^N |b_i|^2}}{\sqrt{\sum_{i=1}^N |a_i|^2}} \quad (6.6)$$

where,  $a_i$  and  $b_i$  is the onward moving wave and retrograde moving wave. The TARC of as given below.

$$TARC = \sqrt{\frac{(S_{11} + S_{12})^2 + (S_{21} + S_{22})^2}{2}} \quad (6.7)$$

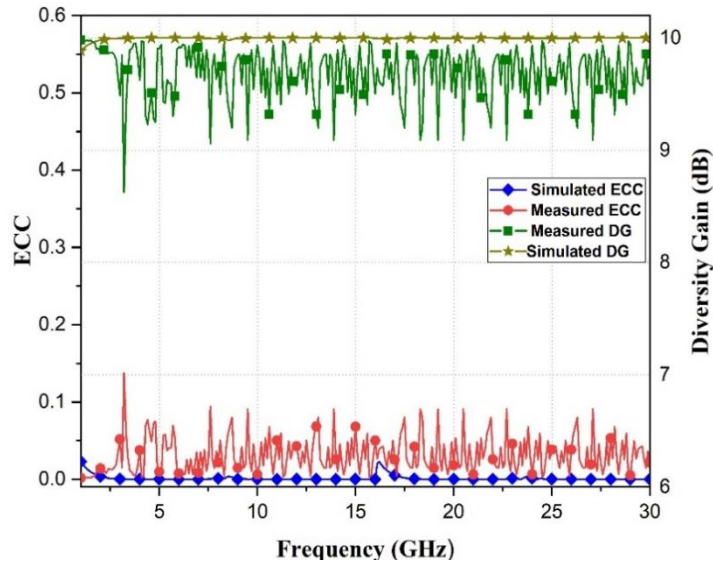


**Figure 6. 10:** Measured and simulated deviation of ECC and DG

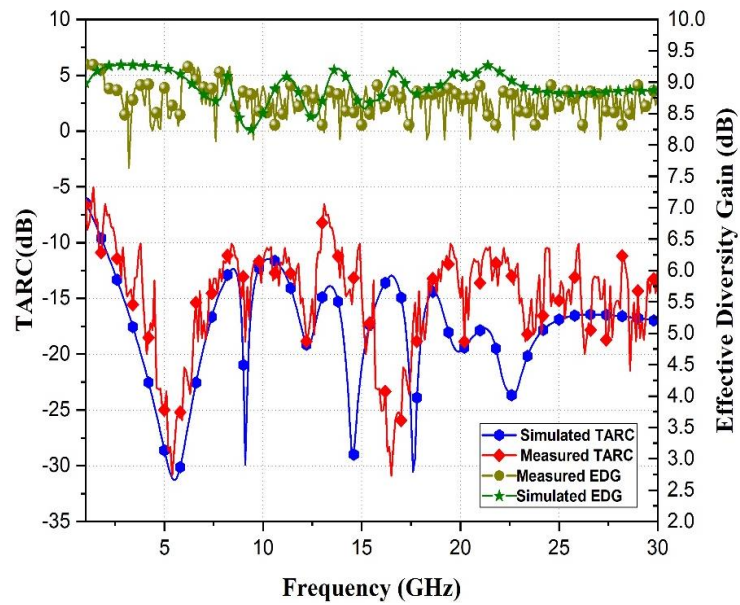


**Figure 6. 11:** Deviation of TARC vs frequency

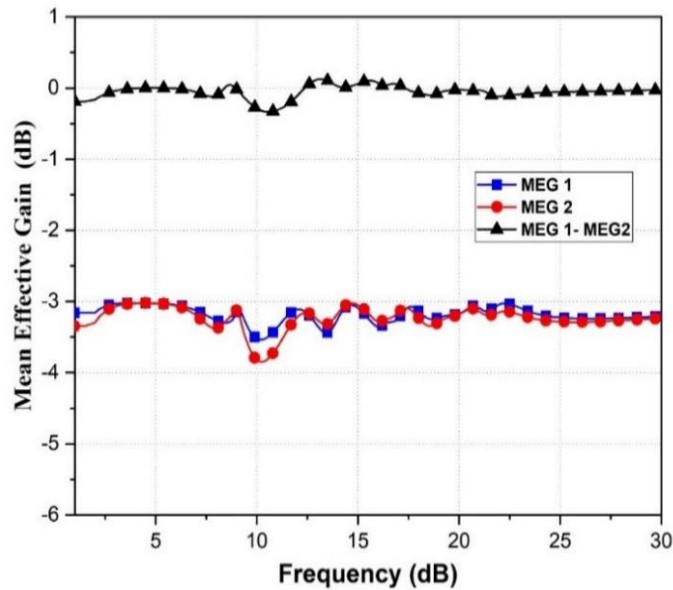


**Figure 6. 12:** MEGs of the presented system.

It is mandatory to have a TARC value of less than zero dB for the satisfactory performance of a presented system [339]. The curve of TARC is below  $-10$  dB and EDG is round  $9.2$  dB is shown in Figure 6.11. Low mutual coupling with the small dimension and radiation efficiency is around  $80\%$  for the whole UWB spectrum

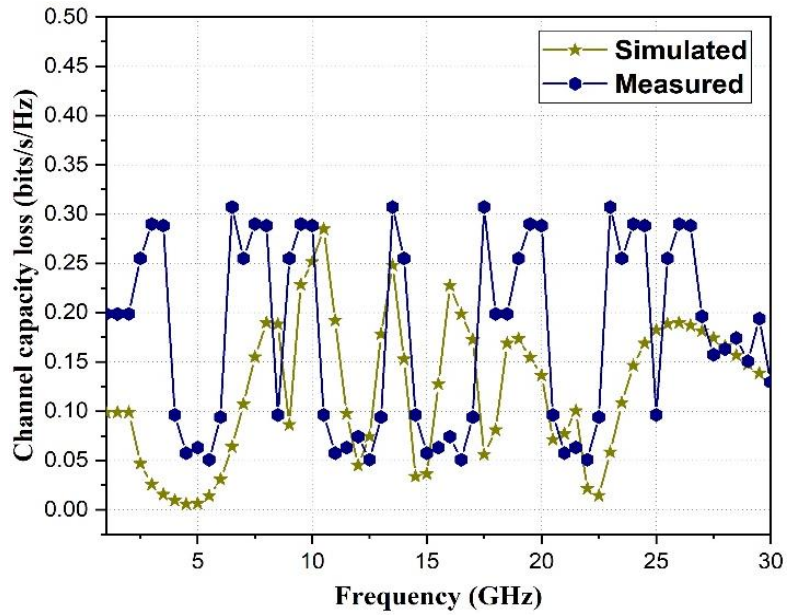


Figure 6. 13: Deviation of CCL vs frequency

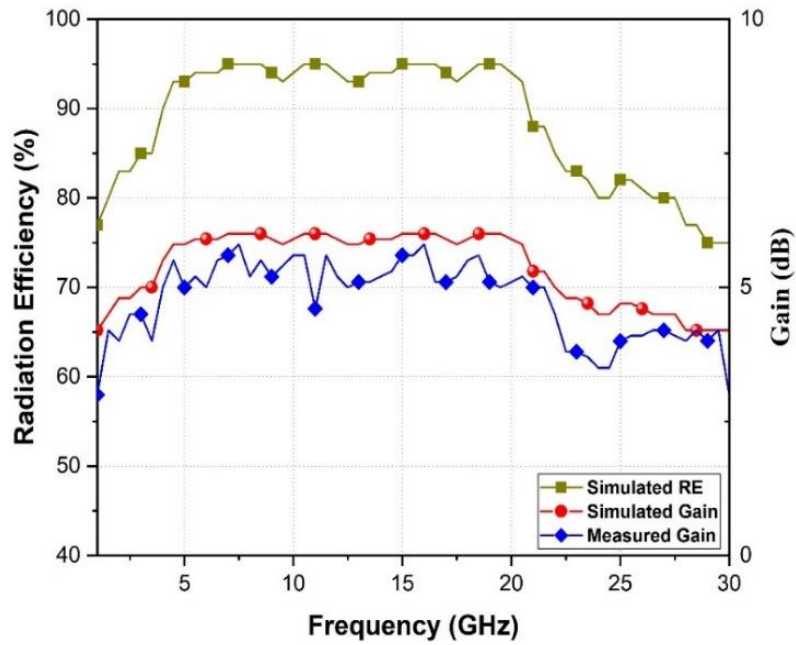


Figure 6. 14: Graph of radiation efficiency and Gain

In a multipath atmosphere, MEG is the variance of received power by the patch element to that of ref. structure. The MEG [338] is determined using equation (6.8) and (6.9). So, MEG<sub>i</sub> and MEG<sub>j</sub> is intended as given

$$MEG_i = 0.5 \left[ 1 - \sum_{j=1}^N |S_{ij}|^2 \right] < -3dB \quad (6.8)$$

$$\text{Also, } |MEG_i - MEG_j| < 3dB \quad (6.9)$$

$$MEG_i = 0.5 \left[ 1 - |S_{11}|^2 - |S_{12}|^2 \right] \quad (6.10)$$

$$MEG_j = 0.5 \left[ 1 - |S_{21}|^2 - |S_{22}|^2 \right] \quad (6.11)$$

Where, i, j denotes patch elements 1 and 2 respectively. Figure 6.12 demonstrates the MEG for the presented structure, we can see that the fraction of MEG is in between the desired limit[336] for the whole range of the UWB system. To estimate the enactment of the presented system one of the significant factors is CCL [324]. It can be intended using the equations (12).

$$C_{loss} = -\log_2 \det(\beta^R) \text{ Where, } \beta^R = \begin{bmatrix} \beta_{ii} & \beta_{ij} \\ \beta_{ji} & \beta_{jj} \end{bmatrix} \quad (6.12)$$

$$\beta_{ii} = 1 - \left( \sum_{j=1}^N |S_{ij}|^2 \right) \quad (6.13)$$

$$\beta_{ij} = -(S_{ii}^* S_{ij} + S_{ji}^* S_{ij}) \quad (6.14)$$

Figure 6.13 depicts that the intended CCL is below 0.4 bits/s/Hz for the entire functioning range. Figure 6.14 signifies the measured gain and RE. Many UWB MIMO antennae have been discussed in the literature. Table 6.2 indicates that the presented structure has a compact dimension than the antennas mentioned.

## 6.4 Summery

In this chapter, an improved bandwidth UWB MIMO antenna has been presented. Many antennae existing in the open works have stated good structure with wide bandwidth. However, these multiple microstrip structures agonize from big dimensions, great profile, small bandwidth (almost only dual bands) as well as complicated decoupling structures that can affect the fabrication cost.

**Table 6. 2:** Evaluation of the presented structure with present work

<b>S. No.</b>	<b>Reference</b>	<b>Bandwidth (GHz)</b>	<b>Gain (dBi)</b>	<b>Radiation Efficiency</b>	<b>Dimensions (mm×mm)</b>
1.	<b>Proposed Antenna</b>	<b>1-30</b>	<b>6</b>	<b>Around 85%</b>	<b>17×27</b>
2.	[337]	2.9-20	1.6 to 6	Around 60%	18×36
3.	[338]	3-20	0 to 7	Around 75%	18×34
4.	[339]	2-12	5	80%	32×32
5.	[340]	1-20	6	85%	32×28
6.	[341]	1-14	5	Around 85%	30 × 10
7.	[342]	2-12	5.5	-	22×26
8.	[343]	2-12	4	75%	42×24
9.	[344]	2-12	4	75%	23×29
10.	[345]	2-16	3.5 - 6	80%	50×30
11.	[ 346]	3.1-13.6	4.5	-	32×32
12.	[347]	3.1-17.3	1-5	85%	46×31
13.	[348]	3.1-17.5	6	-	65×65

Above mentioned concerns have been embarked in this chapter. The structure proposed in this chapter is small (total antenna dimensions of 17×27×1.6 mm<sup>3</sup>) and thin (fabricated on FR4 substrate), which makes them attractive for compact wireless devices. Designed UWB MIMO antenna is fabricated having a compact size and high efficiency. The presented structure has working BW from 1-30 GHz for numerous applications like GPS, WLAN, and radio astronomy. Mutual coupling is less than 15 dB improvement over the reference antenna

that has been obtained in each band. The presented structure indicates decent MIMO performance with ECC less than 0.2 and CCL is below 0.3. The ratio of MEG is in between the desired limits, DG is nearby 9.98, TARC is less than  $-10.5$  dB, and RE is nearby 80%. The tested curves indicate decent similarity to simulated ones.

**CHAPTER 7**  
**CONCLUSION AND**  
**FUTURE SCOPE**

## CHAPTER 7

### Conclusion and Future scope

#### 7.1 Overview of research

In this thesis extensive analysis of the UWB technology is done to avoid interference from the narrowband communication system. Antennas proposed in this thesis utilizes slots and TVC EBG structure to achieve a band-rejected UWB antenna design. The EBG structure attaining multiple notches independently and can be useful to most of the antennas. Compact EBG structures are achieved by inserting slots and multiple via in EBG structure. To overcome signal fading UWB MIMO antenna is designed. The defected ground surface is used to diminish the EM coupling among the patch elements in MIMO systems.

In Chapter 1 the introduction of UWB that is relevant to this thesis is carried out. This chapter starts with the introduction of UWB technology. Introduction to monopole antenna and MIMO antennas wave antenna is also given.

In Chapter 2 the introduction and literature review of band-notched UWB MIMO antenna using EBG Structure are discussed. This chapter starts with the historical background of monopole antennas with feeding techniques and their advantages, disadvantages are discussed. Then an introduction to MIMO antenna with challenges faced to design MIMO antenna is also discussed. Introduction to metamaterials with classifications like ENG, DNG, DPS, and MNG are discussed. Then an introduction to EBGs starts with their systematic evolutions through DGS, PBG, and FSS, etc. Different band gap methods used in this thesis like the dispersion diagram method, reflection phase method with basics are discussed. Introduction of polarization, different types of polarization, Antenna polarization loss factor, and advantages of polarization are also discussed. Then the application of the UWB MIMO antenna system with the literature review of EBGs to achieve band rejected features discussed. After this, some popular notched UWB antennas with single double and triple notches are introduced. It is understood from Table 2.4 that different feeding technique of the MPA provides dissimilar results for the same parameters. The important decision is to

pick the feed is since it interrupts the performance of the antenna. Different excitation methods provide unlike bandwidth, directivity, gain, and different efficiency, etc. From Table 4 it is observed coaxial feed achieved improved gain and directivity.

Chapter 3 deals with planar monopoles antenna that have been found a respectable illustration for UWB claims due to their benefits for example comfort of manufacture, acceptable radiation configuration, and enormous -10dB BW. To resolve this intrusion from the narrowband communication system it is essential to create a UWB structure with band rejection features. Numerous approaches have been suggested for band rejection features like inserting slots half-wavelength slots in patch/ground plane, placing parasitic element, and tuning stub. To attain compact antenna size in this chapter we use quarter wavelength slots on the patch element. Notch frequencies can be varied just by varying the length of the rectangular quarter wavelength slot. In the multipath environment, the signal fading issue of UWB using resolved by using the UWB MIMO antenna. A defected ground surface is used to diminish the mutual coupling amid the elements. Various diversity parameters are also discussed. A comparative study of the proposed antenna with lasted published work is also done.

In Chapter 4 two antenna designs are proposed that reject narrowband frequencies. A miniaturized UWB MIMO antenna with three rejection bands is generated using one EBG structure. Rather than using multiple EBG cells, a modified EBG cell with C slots is used to attained triple-band notches. Decoupling strips are used to enhance the isolation in radiating elements. MIMO characterizes of the proposed structure are also studied. To validate, the suggested antenna is fabricated and measured. The bandgap of the proposed TVC EBG unit cell is calculated using the transmission method. The proposed two elements antenna and four elements antenna attains an -10dB bandwidth from 2 to 11 GHz with three notched bands that are WiMAX, WLAN, and X band. The four-element UWB antenna attains decent MIMO performance with ECC less than 0.015, TARC less than -10 dB, and RE is nearly 80%. Therefore this chapter deals with TVC-EBG size reduction and the purpose of achieving multiple bands rejected using only EBG Structure.

Chapter 5 discusses the two circularly polarized UWB antennas. Firstly a ring-shaped planar antenna is suggested with wide ARBW. A slot is etched under the feed line and the strip is extended from the ground to obtain a wider AR. The proposed antenna has an impedance bandwidth of 3-11GHz, whereas the ARBW is 4-9 GHz. Further, the entire ARBW is coincided by impedance bandwidth, thus CP characteristics are satisfactory for the suggested antenna. In the interim, the suggested antenna has a simpler compact size with wider ARBW. The design process and measured outcomes are analyzed and discussed in this chapter. Further, a band-notched circularly polarized UWB MIMO antenna is fabricated. To produce the triple band-notched characteristics, the TVC EBG unit cell is located close to the feed of the planar monopole UWB structure. A rectangular slot and stub are removed in the ground of the presented structure to acquire wider axial ratio bandwidth. This circularly polarized UWB MIMO antenna yields measured impedance BW of (3.1-10.6 GHz) and ARBW of 5.52 GHz (81.42%, 4.02-9.54 GHz) with triple-band rejected centered at 3.5, 5.5 and 8.2 GHz. Additionally, the proposed antenna exhibits better MIMO properties like  $ECC > 0.05$ ,  $TARC > 10$  dB, and  $DG < 9.99$ .

In chapter 6, a miniaturized enhanced bandwidth UWB MIMO antenna is presented. The presented structure has a working -10dB bandwidth from 1-30 GHz for countless applications for example GSM/UMTS, GPS, ISM, WLAN/Wi-Fi, radio applications UWB communication, radio astronomy, and 5G. Virtuous isolation of more than 15 dB improvement over the reference antenna has been obtained in each band, for an antenna spacing less than a quarter wavelength of the lowest operating frequency. The antennas presented in this chapter are small (total antenna dimensions of  $17 \times 27 \times 1.6$  mm<sup>3</sup>) and thin (fabricated on FR4 substrate), which makes them attractive for compact wireless devices. The presented structure in this chapter displays excellent MIMO performance with ECC below than 0.2 and CCL less than 0.3. The ratio of MEG is in between the desired limits, DG is about 9.98, TARC below -10.5 dB, and RE is nearby 80%. Hence this chapter deals with UWB MIMO antenna reduction and the purpose to access various applications using a single antenna is achieved.

## 7.2 Conclusions

The research in this thesis covers basic properties, applications, advantages, disadvantages, and different feeding techniques of microstrip patch antennas. The various methods of analysis used in microstrip antennas are also explored. A literature review of EBGs and its applications with practical antenna designs are carried out. The bandstop property of EBG structures is verified mathematically. It is also shown mathematically that when a plain wave perpendicular or parallel polarized if impinges on the EBG structures the echoed wave is in phase. Different types of feeding techniques are designed to compare the different performance parameters like return loss, directivity, gain, and radiation efficiency. Multiple band-rejected antennae are fabricated having a small size of  $23 \times 40 \text{ mm}^2$  and high efficiency of 80%. Twisted  $\lambda/4$  wavelength slits are used to achieve band rejected feature with a decrease in antenna size. The designed band eliminated UWB MIMO antenna can be used in medical imaging etc. A band-rejected antenna is designed and fabricated having a compact size of  $21 \times 36 \text{ mm}^2$ . The band-notched antenna can be used in Radio Frequency Identification systems, radio altimeters, and radar applications. TVC EBG structures having three equivalent resonating circuit are proposed which are compact as compared to conventional mushroom EBG structures. The proposed TVC EBG structure is achieves band notch features foe WiMAX band (3.3 -3.7GHz), WLAN (5-6 GHz) and X Band (7.2-8.6 GHz). Then CP antenna with a band elimination feature is intended with a compact size of  $42.72 \times 55 \text{ mm}^2$ . To generate triple band-notched characteristics, the TVC-EBG cell is located close to the feed of the planar monopole antenna. A triple notches antenna that narrow band frequencies are reported. The equivalent circuit EBG structures are also shown. Wider axial ratio bandwidth 3-10.4 GHz excluding three bands are achieved using rectangular slots and stubs. The designed antenna is circularly polarized that avoids the polarization mismatch which makes it suitable for Radio Frequency Identification systems and Mobile communication systems. Lastly, an improved bandwidth UWB MIMO antenna is simulated with an impedance bandwidth of 1-30 GHz with a compact size of  $17 \times 27 \text{ mm}^2$ . To access various applications such as GSM/UMTS, GPS, ISM, WLAN/Wi-Fi, radio applications, UWB communication, radio astronomy, and 5G.

### **7.3 Future work**

The growing demand for wireless communication and information transfer has prompted the need to advance antenna design as an essential part of any wireless communication system. Metamaterials and various geometries for dimensions decrease the intended structure. Simulating a more miniaturized structure for the possible UWB MIMO applications.

- There are certain approaches to integrated EBG structure with UWB antenna which may support further improving antenna gain and bandwidth, reducing mutual coupling among antenna elements, and obtaining multiband characteristics in patch antenna.
- The band rejection characteristics can also be implemented on wearable antennas and conformal antennas.
- Finally, with the increasing number of antennas the data rate increases linearly, this leads to more number antenna in the MIMO system. But the problem of electromagnetic coupling degrades the performance of the MIMO system. Thus, unique solutions are prerequisites for the effective implementation of massive MIMO.

# **LIST OF PUBLICATIONS**

## PUBLICATIONS

### Book chapter:

1. **E. Thakur**, N. Jaglan, and S. D. Gupta, “Advances in Patch Antenna Design using EBG structures,” *Printed Antennas: Theory and Design*, July 2020.

### International Journals:

2. **E. Thakur**, N. Jaglan, S. D. Gupta, and B. K. Kanaujia, “A compact notched UWB MIMO antenna with enhanced performance,” *Progress in Electromagnetics Research C*, vol. 91, pp.39–53, March 2019. DOI: [10.2528/PIERC19083004](https://doi.org/10.2528/PIERC19083004)

*(Scopus Indexed)*

3. **E. Thakur**, N. Jaglan, and S. D. Gupta, “Design of Compact UWB MIMO Antenna with Enhanced Bandwidth,” *Progress in Electromagnetics Research C*, vol. 97, pp.83-94, November 2019. DOI: [10.2528/PIERC19083004](https://doi.org/10.2528/PIERC19083004)

*(Scopus Indexed)*

4. **E. Thakur**, N. Jaglan, and S. D. Gupta, “Design of triple band-notched UWB MIMO Antenna with TVC-EBG,” *Journal of Electromagnetic Waves and Applications*, pp. 1-15, June 2020. DOI: [10.1080/09205071.2020.1775136](https://doi.org/10.1080/09205071.2020.1775136)

*(SCI Indexed)(I.F:1.374)*

5. **E. Thakur**, N. Jaglan, and S. D. Gupta, “Ultra-wideband Compact Circularly Polarized Antenna,” *Wireless Personal Communications*, March 2020. (Under Review)

*(SCI Indexed)*

6. **E. Thakur**, N. Jaglan, and S. D. Gupta, “Miniaturized four-element UWB MIMO antenna with triple-band rejection using single EBG structure” *International Journal of Microwave and Wireless Technologies*, April 2020. (Under Review)

*(SCI Indexed)*

7. **E. Thakur**, N. Jaglan, and S. D. Gupta, “Circularly polarized Ultra wideband MIMO/Diversity antenna with triple band-notched characteristics,” *Wireless Network*, November 2020. (Communicated)

*(SCI Indexed)*

**International Conference:**

8. **E. Thakur**, D. Kumar, N. Jaglan, S.D. Gupta, and S. Srivastava, “Mathematical analysis of commonly used feeding techniques in rectangular Microstrip Patch Antenna,” *International Conference on Signal Processing and Communication*, Noida, India, pp.27-35, March 2018. DOI: [10.1007/978-981-13-2553-3\\_3](https://doi.org/10.1007/978-981-13-2553-3_3)

*(Scopus Indexed )*

# **REFERENCES**

## References

- [1] Deschamps G. A., “Microstrip Microwave Antennas”, Proc. 3rd USAF Symposium on Antennas, 1953.
- [2] Munson R. E., “Conformal Microstrip Antennas and Microstrip Phased Arrays”, *IEEE Trans. Antennas Propagation*, Vol. 22, pp. 74–78, 1974
- [3] Howell J. Q., “Microstrip Antennas”, *IEEE Trans. Antennas Propagation*, vol. 23, pp. 90–93, 1975.
- [4] Bahl I. J., Bhartia P., *Microstrip Antennas*, Dedham, MA: Artech House, 1980.
- [5] Pozar D. M., “Microstrip Antennas”, *Proceedings of IEEE*, vol. 80, No.1, 1992.
- [6] Carver K. R., Mink J. M., “Microstrip antenna technology”, *IEEE Antennas and Propagation*, vol.29, No.1, 1981.
- [7] Garg R., Bhartia P., Bahl I. J., Ittipiboon A., *Microstrip antenna design handbook*, Artech house, 2001.
- [8] James J. R., Hall P. S., Wood C., *Microstrip antenna theory and design*, Peter Petergrins, 1981.
- [9] Kumar G. and Ray K. P, *Broadband microstrip antennas*, Artech house, 2003.
- [10] Wong K. L, *Compact and broadband microstrip antennas*, John Wiley & sons, 2002.
- [11] Jensen M.A.,Wallace J.W., “A review of antennas and propagation for MIMO wireless communication”, *IEEE Trans. Antennas Propag.*,vol. 52, no. 11, pp. 2810–2824, Nov. 2004.
- [12] Song Y., Guo T. N., Qiu R. C.,Wicks M. C., “A real time UWB MIMO system with programmable transmit waveforms: Architecture, algorithms and demonstrations”, *IEEE Trans. Antennas Propag.*, vol.60, no. 8, pp. 3933–3940, Aug. 2012
- [13] S. Zhang, B. K. Lau, A. Sunesson, and S. He, “Closely-packed UWB MIMO/diversity antenna with different patterns and polarizations for USB dongle applications,” *IEEE Transactions on Antennas and Propagation*, vol. 60, pp. 4372–4380, Sep 2012
- [14] Fletcher P. N., Dean M., Nix A. R., “Mutual coupling in multi element array antennas and its influence on MIMO channel capacity”, *Electron. Lett.*, vol. 39, no. 4, pp. 342–344, Feb. 2003.

- [15] Li J. F., Chu Q. X., Li Z. H., Xia X. X., “Compact dual band-notched UWB MIMO antenna with high isolation”, *IEEE Trans. Antennas Propag.*, vol. 61, no. 9, pp. 4759–4766, Sep. 2013.
- [16] MacKinchan J. C., et al., “A Wide Bandwidth Microstrip Sub-Array for Array Antenna Application Using Aperture Coupling”, *IEEE AP-S Int. Symp. Digest*, pp. 878–881, 1989.
- [17] Menzel W., Grabherr W., “Microstrip Patch Antenna with Coplanar Feed Line”, *IEEE Microwave and Guided Wave Letters*, vol. 1, no. 11, pp. 340–342, 1991.
- [18] Smith R. L., Williams J. T., “Coplanar Waveguide Feed for Microstrip Patch Antenna”, *Electronics Letters*, vol. 28, no. 25, pp. 2272–2274, 1992.
- [19] Bhattacharya A. K., Garg R., “Generalized Transmission Line Model for Microstrip Patches”, *IEEE Proc. Microwaves Antennas Propagation*, vol. 132, no. 2, pp. 93–98, 1985.
- [20] Dubost G., Beauquet G., “Linear Transmission Line Model Analysis of a Circular Patch Antenna,” *Electronics Letters*, vol. 22, pp. 1174–1176, October 1986.
- [21] Babu S., Singh I., Kumar G., “Improved Linear Transmission Line Model for Rectangular, Circular and Triangular Microstrip Antennas”, *IEEE AP-S Int. Symp. Digest*, pp. 614–617, July 1997.
- [22] Lo Y. T., Solomon D., Richards W. F., “Theory and Experiment on Microstrip Antennas”, *IEEE Trans. Antennas Propagat.*, vol. 27, no. 2, pp. 137–145, March 1979.
- [23] Richards W. F., Lo Y. T., Harrison D. D., “An Improved Theory of Microstrip Antennas with Applications”, *IEEE Trans. Antennas Propagat.*, vol. 29, No. 1, pp. 38–46, January 1981.
- [24] J. Liang, C. C. Chiau, X. Chen, and C. G. Parini, “Study of a printed circular disc monopole antenna for UWB systems,” *IEEE Transactions on Antennas and Propagation*, vol. 53, pp. 3500–3504, November 2005
- [25] C. Y. D. Sim, W. T. Chung, and C. H. Lee, “Compact slot antenna for UWB applications,” *IEEE Antenna and Wireless Propagation Letters*, vol. 9, pp. 63–66, 2010
- [26] H. W. Liu and C. F. Yang, “Miniature hook-shaped monopole antenna for UWB applications,” *Electronics Letters*, vol. 46, pp. 265–266, February 2010.
- [27] R. Azim, M. T. Islam, and N. Misran, “Ground modified double-sided printed compact UWB antenna,” *Electronics Letters*, vol. 47, pp. 9–11, January 2011.

- [28] M. J. Ammann and Z. N. Chen, "A wide-band shorted planar monopole with bevel," *IEEE Transactions on Antennas and Propagation*, vol. 51, pp. 901–903, April 2003
- [29] N. P. Agrawall, G. Kumar, and K. P. Ray, "Wide-band planar monopole antennas," *IEEE Transactions on Antennas and Propagation*, vol. 46, pp. 294–295, February 1998.
- [30] Cho Y. J., Kim K. H., Choi D. H., Lee S. S., Park S. O., "A miniature UWB planar monopole antenna with 5-GHz band-rejection filter and the time-domain characteristics", *IEEE Trans. Antennas Propag.*, vol. 54, no. 5, pp. 1453–1460, May 2006.
- [31] Li W. T., Shi X. W., Hei Y. Q., "Novel planar UWB monopole antenna with triple band-notched characteristics", *IEEE Antennas Wireless Propag. Lett.*, vol. 8, pp. 1094–1098, 2009.
- [32] J. Jung, W. Choi, and J. Choi, "A small wideband microstrip-fed monopole antenna," *IEEE Microwave and Wireless Components Letters*, vol. 15, pp. 703–705, October 2005.
- [33] A. A. Deshmukh and K. P. Ray, "Compact broadband slotted rectangular microstrip antenna," *IEEE Antenna and Wireless Propagation Letters*, vol. 8, pp. 1410–1413, December 2009
- [34] M. Koohestani and M. Golpour, "U-shaped microstrip patch antenna with novel parasitic tuning stubs for ultra-wideband applications," *IET Microwaves, Antennas and Propagation*, vol. 4, no. 7, pp. 938–946, 2010.
- [35] J.G.Proakis, *Digital Communications*, 4th Edition. 2001.
- [36] Howell J. Q., "Microstrip Antennas", *IEEE Trans. Antennas Propagation*, Vol. 23, pp. 90– 93, 1975
- [37] Bahl I. J., Bhartia P., *Microstrip Antennas*, Dedham, MA: Artech House, 1980.
- [38] Kumar G. and Ray K. P, *Broadband microstrip antennas*, Artech house, 2003
- [39] Deschamps G. A., "Microstrip Microwave Antennas", *Proc. 3rd USAF Symposium on Antennas*, 1953
- [40] James J. R., Hall P. S., *Handbook of Microstrip Antennas*, vols. 1 and 2, Peter Peregrinus, London, UK, 1989
- [41] Collin R., *Field Theory of Guided Waves*, *IEEE Press*, 1991.
- [42] G. Chi, B. Li, and D. Qi, "Dual-band printed diversity antenna for 2.4/5.2-GHz WLAN application," *Microwave and Optical Technology Letters*, vol. 45, pp. 561–563, June 2005.

- [43] L. Kang, H. Li, X. Wang, and X. Shi, "Compact offset microstrip-fed MIMO antenna for band-notched UWB applications," *IEEE Antenna and Wireless Propagation Letters*, vol. 14, pp. 1754–1757, 2015.
- [44] James J. R., Hall P. S., *Handbook of Microstrip Antennas*, vols. 1 and 2, Peter Peregrinus, London, UK, 1989.
- [45] R. J. Mailloux, "Phased array antenna handbook, Artech, Boston, second edition," tech. rep., 2005.
- [46] Huang J., *Microstrip antennas for commercial applications*, *IEEE Press, Piscataway*, New Jersey, 1995
- [47] Lee H. F., and Chen W., *Advances in Microstrip and Printed Antennas*, New York: John Wiley & Sons, 1997.
- [48] Pozar D. M., Kaufman B., "Increasing the Bandwidth of a Microstrip Antenna by Proximity Coupling", *Electronics Letters*, Vol. 23, No. 8, pp. 368–369, 1987.
- [49] Pozar, D. M., "Microstrip Antenna Aperture-Coupled to a Microstrip Line", *Electronics Letters*, vol. 21, no. 2, pp. 49–50, 1985.
- [50] Rathi V., Kumar G., Ray K. P., "Improved Coupling for Aperture-Coupled Microstrip Antennas", *IEEE Trans. Antennas Propagation*, vol. 44, no. 8, pp. 1196–1198, 1996.
- [51] MacKinchan J. C., et al., "A Wide Bandwidth Microstrip Sub-Array for Array Antenna Application Using Aperture Coupling", *IEEE AP-S Int. Symp. Digest*, pp. 878–881, 1989.
- [52] Garg R., Bhartia P., Bhal I. J., Ittipiboon A., *Microstrip antenna design handbook*, Artech house, 2001.
- [53] Balanis C.A., *Antenna Theory: Analysis and Design*, 3rd ed, 811-876, Wiley India Edition 2012
- [54] Silvester P., "Finite Element Analysis of Planar Microwave Network", *IEEE Trans. Microwave Theory Tech.*, vol. 21, pp. 104–108, 1973.
- [55] Itoh T., Menzel W., "A Full-Wave Analysis Method for Open Microstrip Structure", *IEEE Trans. Antennas Propagation*, vol. 29, pp. 63–68, January 1981.
- [56] Elena Semouchkina, Wenwu Cao, Michael Lanagan, Raj Mittra and Wenhua Yu, "Combining FDTD simulations with measurements of Microstrip ring resonators for characterization of low and high K dielectrics at microwaves," *Microwave Opt. Technol Lett.*, vol.29, no. 1 , pp.21-24, 5 April 2001.

- [57] Kurt L. Shlager and John B. Schneider, "A selective survey of the Finite Difference Time-Domain literature," *IEEE Antennas Propagat. Mag.*, vol.37, no.4, pp.39-57, August 1995.
- [58] Elena Semouchkina, George Semouchkin, Raj Mittra and Wenwu Cao, "Finite-Difference Time-Domain simulation of resonant modes of rectangular dielectric resonators," *Microwave Opt. Technol. Lett.*, vol.136, no.3, pp.160-164, 5 February 2003.
- [59] Caloz C., Chang C.-C., Itoh T., "Full-wave verification of the fundamental properties of left-handed materials in waveguide configurations", *J. Appl. Phys.*, vol. 90, no. 11, pp. 5483– 5486, Dec. 2001.
- [60] Ying Shen, Zhiqiang Bi, Keli Wu and John Litva, "FD-TD analysis of open cylindrical dielectric resonators," *Microwave Opt. Technol Lett.*, vol.5, no.6, pp.261-265, 5 June 1992.
- [61] Karl S. Kunz and Raymond Luebbers, "The Finite Difference Time Domain Method for Electromagnetics" *CRC Press*, 1993
- [62] Werner Thiel and Linda P.B. Katehi, "Some Aspects of Stability and Numerical Dissipation of the Finite-Difference Time-Domain (FDTD) Technique including Passive and Active Lumped Elements," *IEEE Transactions on Microwave Theory and Techniques*, Vol 50, No.9, pp. 2159-2165, September 2002.
- [63] Takefumi Namiki and Koichi Ito, "Numerical Simulation using ADI-FDTD Method to estimate Shielding effectiveness of Thin Conductive Enclosures," *IEEE Transactions on Microwave Theory and Techniques*, Vol.49, No.6, pp. 1060-1066, June 2001.
- [64] Jaakko S. Juntunen and Theodoros D. Tsiboukis, "Reduction of Numerical Dispersion in FDTD Method through Artificial Anisotropy," *IEEE Transactions on Microwave Theory and Techniques*, Vol.48, No.4, pp. 582- 588, April 2000.
- [65] V.S.Reddy and Ramesh Garg, "Finite Difference Time Domain (FDTD) Analysis of Microwave Circuits-A Review with Examples," *FIETE Journal of Research*, Vol.45, No.1, pp.3-20, January 1999.
- [66] Young-Seek Chung, Tapan K. Sarkar, Baek Ho Jung & Magdalena SalazarPalma, "An Unconditionally Stable Scheme for the Finite-Difference Time Domain Method", *IEEE Transactions on Microwave Theory and Techniques*, vol.51, No.3, pp.697-704, March 2003.
- [67] Ryu K. S., Kishk A. A., "UWB antenna with single or dual band notches for lower WLAN band and upper WLAN band", *IEEE Trans. Antennas Propag.*, vol. 57, no. 12, pp. 3942–3950, Dec. 2009

- [68] Abbosh A. M., Bialkowski M. E., “Design of UWB planar band-notched antenna using parasitic elements”, *IEEE Trans. Antennas Propag.*, vol. 57, no. 3, pp. 796–799, Mar. 2009.
- [69] Kim K. H., Park S. O., “Analysis of the small band-rejected antenna with the parasitic strip for UWB”, *IEEE Trans. Antennas Propag.*, vol. 54, no. 6, pp. 1688–1692, Jun. 2006.
- [70] Ahmed O., Sebak A. R., “A printed monopole antenna with two steps and a circular slot for UWB applications”, *IEEE Antennas Wireless Propag. Lett.*, vol. 7, pp. 411–413, 2008
- [71] Jensen M.A.,Wallace J.W., “A review of antennas and propagation for MIMO wireless communication”, *IEEE Trans. Antennas Propag.*,vol. 52, no. 11, pp. 2810–2824, Nov. 2004.
- [72] Song Y., Guo T. N., Qiu R. C.,Wicks M. C., “A real time UWB MIMO system with programmable transmit waveforms: Architecture, algorithms and demonstrations”, *IEEE Trans. Antennas Propag.*, vol.60, no. 8, pp. 3933–3940, Aug. 2012
- [73] Song Y., Guo N., Qiu R.C., “Implementation of UWB MIMO time-reversal radio testbed”, *IEEE Antennas Wireless Propag. Lett.*,vol. 10, pp. 796–799, 2012
- [74] Ben I. M., Talbi L., Nedil M., Hettak K., “MIMO-UWB channel characterization within an underground mine gallery”, *IEEE Trans. Antennas Propag.*, vol. 60, no. 10, pp. 4866–4874, Oct. 2012
- [75] Lu S., Hui T., Bialkowski M., “Optimizing MIMO channel capacities under the influence of antenna mutual coupling”, *IEEE Antennas Wireless Propag. Lett.*, vol. 7, pp. 287–290, Jul. 2008.
- [76] Gao Y., Chen X., Ying Z., Parini C., “Design and performance investigation of a dualelement PIFA array at 2.5 GHz for MIMO terminal,” *IEEE Trans. Antennas Propag.*, vol. 55, no. 12, pp. 3433–3441, Dec 2007.
- [77] Jensen M.A.,Wallace J.W., “A review of antennas and propagation for MIMO wireless communication”, *IEEE Trans. Antennas Propag.*,vol. 52, no. 11, pp. 2810–2824, Nov. 2004.
- [78] Song Y., Guo T. N., Qiu R. C.,Wicks M. C., “A real time UWB MIMO system with programmable transmit waveforms: Architecture, algorithms and demonstrations”, *IEEE Trans. Antennas Propag.*, vol.60, no. 8, pp. 3933–3940, Aug. 2012.
- [79] V. P. Tran and A. Sibille, “Spatial multiplexing in UWB MIMO communications,” *Electronics letters*, pp. 931–932, August 2006.

- [80] L. Zheng and D. N. C. Tse, "Diversity and multiplexing: A fundamental tradeoff in multiple-antenna channels," *IEEE Transactions on Antennas and Propagation*, vol. 49, pp. 1073–1096, May 2003
- [81] C. Y. Chiu, C. H. Cheng, R. D. Murch, and C. R. Rowell, "Reduction of mutual coupling between closely-packed antenna elements," *IEEE Transactions on Antennas and Propagation*, vol. 55, pp. 1732–1738, June 2007
- [82] I. Kim, C. W. Jung, Y. Kim, and Y. E. Kim, "Low-profile wideband MIMO antenna with suppressing mutual coupling between two antennas," *Microwave and Optical Technology Letters*, vol. 50, pp. 1336–1339, May 2008.
- [83] K. Chung and J. Yoon, "Integrated MIMO antenna with high isolation characteristic," *Electronics Letters*, vol. 43, pp. 199–201, February 2007.
- [84] Y. Gao, X. Chen, Z. Ying, and C. Parini, "Design and performance investigation of a dual-element PIFA array at 2.5 GHz for MIMO terminal," *IEEE Transactions on Antennas and Propagation*, vol. 55, pp. 3433–3441, December 2007.
- [85] I. Kim, C. W. Jung, Y. Kim, and Y. E. Kim, "Low-profile wideband MIMO antenna with suppressing mutual coupling between two antennas," *Microwave and Optical Technology Letters*, vol. 50, pp. 1336–1339, May 2008.
- [86] S. Dossche, S. Blanch, and J. Romeu, "Decorrelation of a closely spaced four element antenna array," in *Antennas and Propagation Society International Symposium, 2005 IEEE*, vol. 1. IEEE, 2005, pp. 803–806.
- [87] J. Coetzee and Y. Yu, "Closed-form design equations for decoupling networks of small arrays," *Electronics Letters*, vol. 44, no. 25, pp. 1441–1442, 2008.
- [88] S.C. Chen, Y.-S. Wang, and S.-J. Chung, "A decoupling technique for increasing the port isolation between two strongly coupled antennas," *IEEE Transactions on Antennas and Propagation*, vol. 56, no. 12, pp. 3650–3658, 2008.
- [89] S. Park and C. Jung, "Compact MIMO antenna with high isolation performance," *Electronics letters*, vol. 46, no. 6, p. 1, 2010.
- [90] P.-S. Kildal, K. Rosengren, J. Byun, and J. Lee, "Definition of effective diversity gain and how to measure it in a reverberation chamber," *Microwave and Optical Technology Letters*, vol. 34, no. 1, pp. 56–59, 2002.
- [91] K. Rosengren and P.-S. Kildal, "Radiation efficiency, correlation, diversity gain and capacity of a six-monopole antenna array for a MIMO system: theory, simulation and

- measurement in reverberation chamber,” in *IEE Proceedings Microwaves, Antennas and Propagation*, vol. 152, no. 1. IET, 2005, pp. 7–16.
- [92] M. Manteghi, and Y.R. Sami, “Broadband characterization of the total active reflection coefficient of multiport antennas”, Proceeding of antennas and propagation society international symposium, June 22-27, 2003, Columbus, OH, USA, 2003.
- [93] M. Pelosi, M.B. Knudsen, and G.F. Pedersen, “Multiple antenna systems with inherently decoupled radiators”, *IEEE Transactions on Antennas and Propagation*, vol. 60, pp. 503-515, 2012.
- [94] M.S. Sharawi, “A dual-band dual-element compact MIMO antenna system for mobile 4G terminals”, *Microwave and Optical Technology Letters*, vol. 55, pp. 325-329, 2013.
- [95] G. Srivastava and B. K. Kanuijia, “Compact dual band-notched UWB MIMO antenna with shared radiator”, *Microwave and Optical Technology Letters*, vol. 57, pp. 2886-2891, 2015
- [96] G. Srivastava, A. Mohan, and A. Chakraborty, “A compact multidirectional UWB MIMO slot antenna with high isolation”, *Microwave and Opt. Technology Letters*, vol. 59, pp. 243-248, 2017.
- [97] J. Banerjee, A. Karmakar, R. Ghatak and D.R. Poddar, "Compact CPW-fed UWB MIMO antenna with a novel modified Minkowski fractal defected ground structure (DGS) for high isolation and triple band-notch characteristic", *Journal of Electromagnetic Waves and Applications*, vol. 31, pp. 1550-1565, 2017
- [98] P. Qin, Y. Jay Guo, and C. Liang, “Effect of antenna polarization diversity on MIMO system capacity”, *IEEE Antennas and Wireless Propagation Letters*, vol. 9, pp. 1092-1095, 2010.
- [99] C. Mao, and Q. Chu, “Compact co-radiator UWB-MIMO antenna with dual polarization”, *IEEE Transactions on Antenna and Propagation*, vol. 62, pp. 4474-4479, 2014.
- [100] Z. Charaabi, and M. Testard, “Optimized WiMAX MIMO antenna for base station applications with polarization and spatial diversity”, *Bell Labs Technical Journal*, vol. 16, pp. 217–234, 2011
- [101] J. Lu, Z. Kuai, X. Zhu, and N. Zhang, “A high-isolation dual-polarization microstrip patch antenna with quasi-cross-shaped coupling slot”, *IEEE Tran. on Ant. and Prop.*, vol. 59, pp. 2713-2717, 2011.

- [102] I. Yeom, H. Kim, K. J. Jung, and C. Won Jung, "Analysis of spatial/polarization diversity using a broadband slot-coupled patch antenna for the WLAN 802.11a/b/g/n access", *Microwave and Optical Technology Letters*, vol. 57, pp.1042-1048, May 2015
- [103] A. Moradikordalivand, C. Leow, T. A Rahman, S. Ebrahimi, and T. H. Chua, "Wideband MIMO antenna system with dual polarization for Wi-Fi and LTE applications", *International Journal of Microwave and Wireless Technologies*, vol.8, pp. 643-650, 2016.
- [104] Y. Sharma, D. Sarkar, K. Saurav, and K. V. Srivastava, "Three element MIMO antenna system with pattern and polarization diversity for WLAN applications, *IEEE Antennas and Wireless Propagation Letters*, vol. 16, pp. 1163 – 1166, 2016.
- [105] L. Malviya, R. K. Panigrahi, and M. V. Kartikeyan, "A  $2 \times 2$  dual band MIMO antenna with polarization diversity for wireless applications", *Progress in Electromagnetics Research C*, vol. 61, pp. 91–103, 2016.
- [106] H. Li, G. Zhang, J. Xu, J. Ding, and C. Guo, "Aperture coupling fed high isolation polarization diversity dual element MIMO antenna system for WLAN application", *Microwave and Optical Technology Letters*, vol. 59, pp. 1178-1182, 2017.
- [107] L. Malviya, R.K. Panigrahi, and M.V. Kartikeyan, "A low profile planar MIMO antenna with polarization diversity for LTE 1800/1900 applications", *Microwave and Optical Technology Letter*, vol. 59, pp. 533-538, 2017.
- [108] W. Q. Cao, Q. Wang, B. Zhang, and W. Hong, "Capacitive probe-fed compact dual-band dual mode dual-polarization microstrip antenna with broadened bandwidth", *IET Microw. Antennas Propag*, vol. 11, pp. 1003-1008, 2017.
- [109] G. Das, A. Sharma, and R.K. Gangwar, "Dielectric resonator based circularly polarized MIMO antenna with polarization diversity", *Microw Opt. Tech. Lett*, vol. 60, pp. 685-993, 2018.
- [110] X. Wang, Z. Feng, and K. M. Luk, "Pattern and polarization diversity antenna with high isolation for portable wireless devices," *IEEE Antenna and Wireless Propagation Letters*, vol. 8, pp. 209–211, 2009.
- [111] M. Sonkki, E. A. Daviu, M. F. Bataller, and E. T. Salonen, "Planar wideband polarization diversity antenna for mobile terminals," *IEEE Antenna and Wireless Propagation Letters*, vol. 10, pp. 939–942, 2011.

- [112] S. Zhang, B. K. Lau, A. Sunesson, and S. He, "Closely-packed UWB MIMO/diversity antenna with different patterns and polarizations for USB dongle applications," *IEEE Transactions on Antennas and Propagation*, vol. 60, pp. 4372–4380, Sep 2012.
- [113] H. Dane, K. Michael & S. F. Wamba (2010), RFID-enabled Inventory Control Optimization: A Proof of Concept in a Small-to Medium Retailer Hawaii International Conferences on System Sciences (HICSS), Organizational Systems and Technology, Implementation and Usage of Radio Frequency Identification (RFID), Koloa, Kauai, Hawaii, 5-10 January 2010.
- [114] Peter Jones, Colin Clarke-Hill, David Hillier, Peter Shears and Daphne Comfort (2004). Radio Frequency Identification in Retailing and Privacy and Public Policy Issues. Management Research News, Vol: 27 No: 8/9. Pp 46-56.
- [115] Ravi, R, Supply chain management in retail using Radio frequency identification(RFID) 17Th, IEEE International Conference on Industrial Engineering and Engineering Management (IE&EM), 2010 vol., no., pp.1907-1911, 29-31 Oct. 2010
- [116] Pfleuger Jr, P. R., Jeng-Chung Victor Chen, and William H. Ross Consumers' ethical perceptions of RFID in retail, *International Journal of Radio Frequency Identification Technology and Applications*, Volume 3, Number 1-2, Pages. 124-140, Oct. 2011.
- [117] Hong, S., Chung, K., Lee, J., Jung, S., Lee, S. S. and Choi, J. (2008), "Design of a diversity antenna with stubs for UWB applications," *Microwave and Optical Technology Letters*, vo. 50, no. 5, pp. 1352-1356
- [118] Kang, L., Li, H., Wang, X. and Shi, X. (2015), "Compact Offset Microstrip Fed MIMO Antenna for Band Notched UWB Applications," *IEEE Antennas and Wireless Propagation Letters*, vol. 14, pp. 1754-1757.
- [119] Kumar, R. and Malathi, P. (2011), "On the Design of CPW-Feed Diamond Shape Fractal Antenna for UWB Applications," *International Journal of Electronics*, vol. 98, no. 9, pp. 1157–1168.
- [120] Mandal, T. and Das, S. (2015), "Design of a Microstrip Fed Printed Monopole Antenna for Bluetooth and UWB Applications with WLAN Notch Band Characteristics," *International Journal of RF and Microwave Computer-Aided Engineering*, vol. 25, no. 1, pp. 66-74.
- [121] Mishra, S. K., Gupta, R. K., Vaidya, A. and Mukherjee, J. (2011), "A Compact Dual Band Fork-Shaped Monopole Antenna for Bluetooth and UWB Applications," *IEEE Antennas and Wireless Propagation Letters*, vol. 10, pp. 627-630.

- [122] Ren, J., Hu, W., Yin, Y. and Fan, R. (2014), “Compact Printed MIMO Antenna for UWB Applications,” *IEEE Antennas and Wireless Propagation Letters*, vol. 13, pp. 1517-1520.
- [123] Satyanarayana, B. and Mulgi, S. (2015), “Design of Planar Band Notched Monopole Antenna for 2.4 GHz WLAN and UWB Applications,” *Microwave Optical Technology and Letters*, vol. 57, no. 11, pp. 2496-2501.
- [124] Zouhdi S., Sihvola A., Vinogradov A.P., “Metamaterials and Plasmonics: Fundamentals, Modelling, Applications”, Springer, Marrakech, Morocco, 2009
- [125] Engheta N., Ziolkowski R.W., “Metamaterials Physics and Engineering Explorations”, 1st edition, John Wiley & Sons, USA, 2006.
- [126] Wu B.I, Wang W., Pacheco J., Chen X., Grzegorzczuk T.M., Kong J. A., “A Study of using Metamaterials as Antenna Substrate to Enhance Gain”, *Progress In Electromagnetics Research*, vol. 51, pp. 295–328, 2005.
- [127] Ziolkowski R.W., “Design, Fabrication, and Testing of Double Negative Metamaterials”, *IEEE Transactions on Antennas and Propagation*, vol. 51, pp. 1516– 1529, 2003.
- [128] Xu H.X., Wang G.M., Cai T., “Miniaturization of 3-D Anisotropic Zero-Refractive Index Metamaterials with Application to Directive Emissions”, *IEEE Transactions on Antennas and Propagation*, vol. 62, pp. 3141-3149, 2014.
- [129] Kumar A., Mohan J., Gupta H.O., “Novel Metamaterials with their Applications to Microstrip Antenna”, *International Journal of Microwave and Optical Technology*, vol. 11, pp. 188-195, pp. 188-195, 2016.
- [130] Andryieuski A., Malureanu R., Lavrinenko A.V., “Wave Propagation Retrieval Method for Metamaterials: Unambiguous Restoration of Effective Parameters”, *Physical Review B*, vol. 80, pp. 193101, 2009.
- [131] Smith D.R., Schultz S., Markos P., Soukoulis C.M., “Determination of Effective Permittivity and Permeability of Metamaterials from Reflection and Transmission Coefficients”, *Physical Review B*, vol. 65, pp. 195104, 2002
- [132] Ziolkowski R.W., “Design, Fabrication, and Testing of Double Negative Metamaterials”, *IEEE Transactions on Antennas and Propagation*, vol. 51, pp. 1516– 1529, 2003.
- [133] Smith D.R., Pendry J.B., “Homogenization of Metamaterials by Field Averaging”, *Journal of the Optical Society of America B*, vol. 23, pp. 391–403, 2006.
- [134] Popa B.I., Cummer S.A., “Determining The Effective Electromagnetic Properties of Negative–Refractive–Index Metamaterials from Internal Fields”, *Physical Review B*, vol. 72, pp. 165102, 2005.

- [135] Xu H.X., Wang G.M., Cai T., “Miniaturization of 3-D Anisotropic Zero-Refractive Index Metamaterials with Application to Directive Emissions”, *IEEE Transactions on Antennas and Propagation*, vol. 62, pp. 3141-3149, 2014
- [136] Kumar A., Mohan J., Gupta H.O., “Novel Metamaterials with their Applications to Microstrip Antenna”, *International Journal of Microwave and Optical Technology*, vol. 11, pp. 188-195, pp. 188-195, 2016.
- [137] A. Yu, F. Yang, and A. Elsherbeni “ A Dual Band Circularly Polarized Ring Antenna Based on Composite Right and Left Handed Metamaterials” Progress In Electromagnetics Research, *PIER* 78, 73–81, 2008
- [138] Andryieuski, A.; Malureanu, Radu; Alabastri, A.; Lavrinenko, A.V., "Bulk metamaterials: Design, fabrication and characterization," ICTON Mediterranean Winter Conference ICTON-MW 2009. 3rd, vol., no., pp.1,5, 10-12 Dec. 2009.
- [139] Ghanshyam Singh, “Double Negative Left-Handed Metamaterials for Miniaturization of Rectangular Microstrip Antenna”, *Journal Electromagnetic Analysis & Applications*, pp. 347-351, Feb 2010.
- [140] Andrea Alù, Filiberto Bilotti, Nader Engheta, and Lucio Vegni, “Subwavelength, Compact, Resonant Patch Antennas Loaded With Metamaterials”, *IEEE Transactions on Antennas and Propagation*, vol.55, NO.1, January 2007.
- [141] Ziolkowski, R.W., "Design, fabrication, and testing of double negative metamaterials," *Antennas and Propagation, IEEE Transactions on Antennas and Propagation*, vol.51, no.7, pp.1516, 1529, July 2003.
- [142] A. Yu, F. Yang, and A. Elsherbeni, A Dual Band Circularly Polarized Ring Antenna based on Composite Right and Left handed Metamaterials. Progress In Electromagnetics Research, *PIER*, 73–81, 2008.
- [143] Jia Chen, Enrang Zheng, and Wanzhao Cui “Symmetric Unit Cell Models for Composite Right/Left-handed Transmission Lines (CRLH-TL)” Metamaterials Progress In Electromagnetics Research Symposium, Beijing, China, pp: 619-624, March 23-27, 2009.
- [144] De Paulis, F, Cracraft, M, Olivieri, C, Connor, S, Orlandi, A & Archambeault, B 2015, EBG-based common-mode stripline Filters: Experimental investigation on interlayer crosstalk”, *IEEE Trans. Electromagn. Compat.*, vol. 57, no.6 pp. 1416-1424.

- [145] De Paulis, F, Cracraft, M, Olivieri, C, Connor, S, Orlandi, A & Archambeault, B 2015, „EBG-based common-mode stripline Filters: Experimental investigation on interlayer crosstalk“, *IEEE Trans. Electromagn. Compat.*, vol. 57, no.6 pp. 1416-1424.
- [146] Gujral, MJ, Li, LW, Yuan, T & Qiu, CW 2012, „Bandwidth improvement of microstrip antenna array using dummy EBG pattern on feedline“, *Prog. Electromagn. Res.*, vol. 127, pp. 79-92
- [147] Iglesias, ER, Sanchez, LI, Roy, SLV & Munoz, EG 2007, „Size reduction of mushroom-type EBG surfaces by using edge-located vias“, *IEEE. Microwave Wirel. Compon. Lett.*, vol. 17, pp. 670-672
- [148] Kim, KH & Schutt-Ain“e, JE 2007, „Design of EBG power distribution networks with VHF-band cutoff frequency and small unit cell size for mixed-signal systems“, *IEEE Microw. Wireless Compon. Lett.*, vol. 17, no. 7, pp. 489-491.
- [149] Kim, M 2015, „A compact EBG structure with wideband power/ground noise suppression using meander-perforated plane“, *IEEE Trans. Electromagn. Compat. Lett.*, vol. 57, no. 3, pp. 595-598.
- [150] Mohajer-Iravani, B & Ramahi, OM 2010, „Wideband circuit model for planar EBG structures“, *IEEE Transactions on Advanced Packaging*, vol. 33, no. 1, pp. 169-179.
- [151] Myunghoi Kim 2015, „Wideband and compact EBG structure with balanced slots“, *IEEE Transactions on Components Packaging and Manufacturing Technology*, vol. 5, no. 6.
- [152] Wu, TL, Chuang, HH & Wang, TK 2010, „Overview of power integrity solutions on package and PCB decoupling and EBG isolation“, *IEEE. Trans. Electromagn. Compat.*, vol. 52, pp. 346-356.
- [153] Q. Gao, Y. Yin, D. B. Yan, and N. C. Yuan, “A novel radar-absorbing material based on EBG structure,” *Microwave and Optical Technology Letters*, Vol. 47, No. 3, pp. 228–230, 2005
- [154] A. Yu, F. Yang, and A. Elsherbeni “ A Dual Band Circularly Polarized Ring Antenna Based on Composite Right and Left Handed Metamaterials” *Progress In Electromagnetics Research*, PIER 78, 73–81, 2008
- [155] Kim, SH, Nguyen, TT & Jang, JH 2011, „Rejection characteristics of 1-D EBG ground plane and its application to a planar dipole antenna“, *Progress In Electromagnetics Research*, vol. 120, pp. 51- 66.

- [156] Lee, S, Kim, H & Kim, J 2005, „High dielectric constant thin film EBG power-ground network for broad-band suppression of SSN and radiated emissions“, *IEEE. Microwave Wirel. Compon. Lett.*, vol. 15, pp. 505-507.
- [157] Ling-Feng Shi, Kai-Jing Li, Hua-Qing Hu & Sen Chen 2016, „Novel LEBG embedded structure for the suppression of SSN“, *IEEE Transactions on Electromagnetic Compatibility*, vol. 58, no. 1.
- [158] Mohajer-Iravani, B & Ramahi, OM 2010, „Wideband circuit model for planar EBG structures“, *IEEE Transactions on Advanced Packaging*, vol. 33, no. 1, pp. 169-179.
- [159] Wu, TL, Chuang, HH & Wang, TK 2010, „Overview of power integrity solutions on package and PCB decoupling and EBG isolation“, *IEEE. Trans. Electromagn. Compat.*, vol. 52, pp. 346-356.
- [160] Zhu, HR & Mao, JF 2013, „Localized planar EBG structure of CSRR for ultra wideband SSN mitigation and signal integrity improvement in mixed signal systems“, *IEEE Trans. Compon., Packag., Manuf. Technol.* vol. 3, no. 12, pp. 2092- 2100.
- [161] Yang F., Rahmat-Samii Y., “Reflection phase characterizations of the EBG ground plane for low profile wire antenna applications”, *IEEE Trans. Antennas Propagat.*, vol. 51, no. 10, pp. 2691–703, Oct. 2003.
- [162] Dellavilla A., Galdi V., Capolino F., Pierro V., Enoch S., and Tayeb G., “A Comparative Study of Representative Categories of EBG Dielectric Quasi-Crystals”, *IEEE Antennas Wireless Propagat. Lett.*, vol. 5, pp. 331–334, 2006.
- [163] Rajo-Iglesias E., Caiazzo M., Inclan-Sanchez L., Kildal P.-S., “Comparison of bandgaps of mushroom-type EBG surface and corrugated and strip-type soft surfaces”, *IET Proc. Microwave Antennas Propagation*, vol. 1, no. 1, pp. 184–189, 2007.
- [164] She W. H., Gong X., Chappell W. J., “Fundamental constraints on two-dimensional EBG substrates”, *IEEE APS Int. Symp. Dig.*, vol. 2, pp. 1419–22, June 2004.
- [165] Yu A., Zhang X., “A novel method to improve the performance of microstrip antenna arrays using a dumbbell EBG structure”, *Antennas Wireless Propagat. Lett.*, vol. 2, no. 1, pp. 170–172, 2003.
- [166] Boisbouvier N., Louzir A., Le Bolzer F., Tarot A.-C., Mahdjoubi K., “A double layer EBG structure for slot-line printed devices”, *IEEE APS Int. Symp. Dig.*, vol. 4, pp. 3553–6, June 2004.

- [167] Maci S., Caiazzo M., Cucini A., Asaletti M., “A pole-zero matching method for EBG surfaces composed of a dipole FSS printed on a grounded dielectric slab”, *IEEE Trans. Antennas Propag.*, vol. 53, no. 1, part 1, pp. 70–81, 2005.
- [168] Farahani, H. Veysi, S. Kamyab, et. al. 2010. Mutual Coupling Reduction in Patch Antenna Arrays Using a UC-EBG Superstrate. *IEEE Antennas and Wireless Propagation Letters*. 9 :57–59.
- [169] Alibakhshikenari, M. Khalily, M. B. Virdee, et. al . 2019. Mutual Coupling Suppression Between Two Closely Placed Microstrip Patches Using EM-Bandgap Metamaterial Fractal Loading. *IEEE Access*.7:23606–23614.
- [170] Kumar, N. and Kommuri, U. K. 2019. MIMO Antenna H-Plane Isolation Enhancement using UC-EBG Structure and Metal Line Strip for WLAN Applications. *Radioengineering*. 27:399–406.
- [171] Mavridou, M. Feresidis, A. P. and Gardner, P. 2016. Tunable Double-Layer EBG Structures and Application to Antenna Isolation. *IEEE Transactions on Antennas and Propagation*. 64:70–79.
- [172] Kushwaha, N. and Kumar, R .2013. An UWB fractal antenna with defected ground structure and swastika shape electromagnetic band gap. *Progress In Electromagnetics Research B*. 52:383–403.
- [173] Jaglan, N. Kanaujia, B. K. Gupta, S. D. et. al 2016. Triple band notched uwb antenna design using electromagnetic band gap structures. *Progress In Electromagnetics Research C*.66: 139–147.
- [174] Pandey, G. K. Singh, H. S. Bharti, P. K. and Meshram, M. K. 2013. Design of wlan band notched uwb monopole antenna with stepped geometry using modified EBG structure,” *Progress In Electromagnetics Research B*.50:201–217.
- [175] Mouhouche, Azrar, F. A. Dehmas, M. et. al 2018. Design a Compact UWB Monopole Antenna with Triple Band-Notched Characteristics Using EBG Structures. *Frequenz*,11. 479–487.
- [176] Peng, L. and Ruan, C.-L. 2011. UWB Band-Notched Monopole Antenna Design Using Electromagnetic-Bandgap Structures. *IEEE Transactions on Microwave Theory and Techniques*.59:1074–1081.
- [177] Mandal, T. and Das, S.2014. Design of dual notch band UWB printed monopole antenna using electromagnetic-bandgap structure. *Microwave and Optical Technology Letters*. 56:2195–2199.

- [178] Das, R. and Yoo, H. 2018. Application of a Compact Electromagnetic Bandgap Array in a Phone Case for Suppression of Mobile Phone Radiation Exposure. *IEEE Transactions on Microwave Theory and Techniques*.66:2363–2372.
- [179] Jaglan, N. Gupta, S. D., Thakur, et. al. 2018. Triple band notched mushroom and uniplanar EBG structures based UWB MIMO/Diversity antenna with enhanced wide band isolation. *AEU - International Journal of Electronics and Communications*.90: 36–44.
- [180] Jaglan, N. Kanaujia, B. K. Gupta, et. al .2017. Dual Band Notched EBG Structure based UWB MIMO/Diversity Antenna with Reduced Wide Band Electromagnetic Coupling. *Frequenz*.71:11–12.
- [181] Liu, H. and Xu, Z. 2013. Design of UWB Monopole Antenna with Dual Notched Bands Using One Modified Electromagnetic-Bandgap Structure. *The Scientific World Journal*. 1–9.
- [182] Wang, J. H. Yin, Y.-Z. Liu, X. L. 2013. Triple band-notched Ultra WideBand (UWB) antenna using a novel modified capacitively loaded loop (CLL) Resonator. *Progress In Electromagnetics Research Letters*.42:55–64.
- [183] Li, T. Zhai, H.-Q. Li, G.-H. et. al .2012. Design of compact UWB band-notched antenna by means of electromagnetic-bandgap structures. *Electronics Letters*.48: 601-608,
- [184] Ghosh, A. Mandal, T. and Das, S. 2019. Design and analysis of triple notch ultrawideband antenna using single slotted electromagnetic bandgap inspired structure. *Journal of Electromagnetic Waves and Applications*.1–15.
- [185] H. A. Majid, M. K. A. Rahim, and T. Masri, “Microstrip antenna’s gain enhancement using lefthanded metamaterial structure”, *Progress in Electromagnetics Research M*, Vol. 8, pp. 235–247, 2009.
- [186] I. Puscasu, and W. L. Schaich , “Narrow-band, tunable infrared emission from arrays of microstrip patches,” *Applied Physics Letters*, Vol.92, pp. 233102, 2008
- [187] Kumar A., Mohan J., Gupta H.O., “Novel Metamaterials with their Applications to Microstrip Antenna”, *International Journal of Microwave and Optical Technology*, vol. 11, pp. 188-195, pp. 188-195, 2016.
- [188] Ghosh C.K., “A Compact 4-Channel Microstrip MIMO Antenna with Reduced Mutual Coupling”, *AEU- International Journal of Electronics and Communication*, vol. 70, pp. 873-879, 2016.
- [189] Waterhouse R.B., “Microstrip Patch Antennas - A Designer’s Guide”, Boston, MA: Kluwer Academic Publishers, 2003.

- [190] Bao X.L., Ammann M.J., “Comparison of Several Novel Annular-Ring Microstrip Patch Antennas for Circular Polarization”, *Journal of Electromagnetic Waves and Application*, vol. 20, pp. 1427-1438, Aug. 2006.
- [191] Kumar A., Mohan J., Gupta H.O., “Novel Metamaterials with their Applications to Microstrip Antenna”, *International Journal of Microwave and Optical Technology*, vol. 11, pp. 188-195, pp. 188-195, 2016.
- [192] Wang, S., “A new compact printed triple band-notched UWB antenna,” *Progress In Electromagnetics Research Letters*, vol. 58, 67–72, 2016.
- [193] Tang, M.-C., H. Wang, T. Deng, and R. W. Ziolkowski, “Compact planar ultra wideband antennas with continuously tunable, independent band-notched filters,” *IEEE Transactions on Antennas and Propagation*, Vol. 64, No. 8, 3292–3301, Aug. 2016.
- [194] Pan, S., G. Luo, B. Ke, and K. Li, “A planar UWB antenna with triple-notched bands using triple-mode stepped impedance resonator,” *Progress In Electromagnetics Research Letters*, vol. 55,45–52, 2015.
- [195] Elhabchi, M., M. N. Srifi, and R. Touahni, “A tri-band-notched UWB planar monopoleantenna using DGS and semi arc-shaped slot for WIMAX/WLAN/X-band rejection,”*Progress In Electromagnetics Research Letters*, vol. 70, 7–14, 2017.
- [196] Jaglan, N., S. D. Gupta, B. K. Kanaujia, and S. Srivastava, “Design and development of efficient EBG structures based band notched UWB circular monopole antenna,” *Wireless Personal Communication*, 1–27, Springer, May 2017.
- [197] Ojaroudi, N. and M. Ojaroudi, “Small square monopole antenna having variable frequency bandnotch operation for UWB wireless communications,” *Microwave and Optical Technology Letters*, Vol. 54, 1994–1998, 2012.
- [198] Bakariya, P. S., S. Dwari, and M. Sarkar, “Triple band notch UWB printed monopole antenna with enhanced bandwidth,” *AEU — International Journal of Electronics and Communications*, vol. 69, 26–30, 2015.
- [199] Gorai, A., A. Karmakar, M. Pal, and R. Ghatak, “Multiple fractal-shaped slots-based UWB antenna with triple-band notch functionality,” *Journal of Electromagnetic Waves and Applications*, vol. 27, 2407–2415, 2013.
- [200] Gorai, A., A. Karmakar, M. Pal, and R. Ghatak, “Multiple fractal-shaped slots-based UWB antenna with triple-band notch functionality,” *Journal of Electromagnetic Waves and Applications*, vol. 27, 2407–2415, 2013.

- [201] Ali, W. A. E. and R. M. A. Moniem, “Frequency reconfigurable triple band-notched ultra-wideband antenna with compact size,” *Progress In Electromagnetics Research C*, vol. 73, 37–46, 2017.
- [202] Luo, C.-M., J.-S. Hong, and L.-L. Zhong, “Isolation enhancement of a very compact UWB-MIMO slot antenna with two defected ground structures,” *IEEE Antennas and Wireless Propagation Letters*, vol. 14, 1766–1769, 2015
- [203] Jaglan, N., S. D. Gupta, E. Thakur, D. Kumar, B. K. Kanaujia, and S. Srivastava, “Triple band notched mushroom and uniplanar EBG structures based UWB MIMO/Diversity antenna with enhanced wide band isolation,” *AEU — International Journal of Electronics and Communications*, vol. 90, 36–44, 2018.
- [204] Wang, J. H., Y.-Z. Yin, and X. L. Liu, “Triple band-notched ultra wideband (UWB) antenna using a novel modified capacitively loaded loop (CLL) resonator,” *Progress In Electromagnetics Research Letters*, vol. 42, 55–64, 2013.
- [205] Vendik, I. B., A. Rusakov, K. Kanjanasit, J. Hong, and D. Filonov, “Ultra-wideband (UWB) planar antenna with single-, dual-, and triple-band notched characteristic based on electric ring resonator,” *IEEE Antennas and Wireless Propagation Letters*, vol. 16, 1597–1600, 2017.
- [206] Tang, M.-C., H. Wang, T. Deng, and R. W. Ziolkowski, “Compact planar ultra-wide band antennas with continuously tunable, independent band-notched filters,” *IEEE Transactions on Antennas and Propagation*, vol. 64, No. 8, 3292–3301, 2016.
- [207] Zhu, J., B. Feng, B. Peng, L. Deng, and S. Li, “A dual notched band MIMO slot antenna system with Y-shaped defected ground structure for UWB applications,” *Microwave and Optical Technology Letters*, vol. 58, No. 3, 626–630, Mar. 2016.
- [208] Zhu, F.-G., J.-D. Xu and Q. Xu, “Reduction of mutual coupling between closely-packed antenna elements using defected ground structure,” *Electronics Letters*, vol. 45, 2009.
- [209] Ghosh, C. K., B. Mandal, and S. K. Parui, “Mutual coupling reduction of a dual-frequency microstrip antenna array by using U-shaped DGS and inverted U-shaped microstrip resonator,” *Progress In Electromagnetics Research C*, vol. 48, 61–68, 2014.
- [210] Park, J., J. Choi, J. Park, and Y. Kim, “Study of a T-shaped slot with a capacitor for high isolation between MIMO antennas,” *IEEE Antennas and Wireless Propagation Letters*, vol. 11, 1541–1544, 2012.
- [211] Ghosh, J., S. Ghosal, D. Mitra, and S. R. Bhadra Chaudhuri, “Mutual coupling reduction between closely placed microstrip patch antenna using meander line resonator,” *Progress In Electromagnetics Research Letters*, vol. 59, 115–122, 2016.

- [212] Vendik, I. B., A. Rusakov, K. Kanjanasit, J. Hong, and D. Filonov, "Ultra-wideband (UWB) planar antenna with single-, dual-, and triple-band notched characteristic based on electric ringresonator," *IEEE Antennas and Wireless Propagation Letters*, vol. 16, 1597–1600, 2017.
- [213] Zhang, S. and G. F. Pedersen, "Mutual coupling reduction for UWB MIMO antennas with a wideband neutralization line," *IEEE Antennas and Wireless Propagation Letters*, vol. 15, 166–169, 2016.
- [214] Mao, C. and Q. Chu, "Compact coradiator UWB-MIMO antenna with dual polarization," *IEEE Transactions on Antennas and Propagation*, vol. 62, No. 9, 4474–4480, 2014.
- [215] Chiu, C.-Y., J.-B. Yan, and R. D. Murch, "Compact three-port orthogonally polarized MIMO antennas," *IEEE Antennas and Wireless Propagation Letters*, vol. 6, 619–622, 2007.
- [216] Zhang, S., Z. Ying, J. Xiong, and S. He, "Ultra wide band MIMO/diversity antennas with a treelikestructure to enhance wideband isolation," *IEEE Antennas and Wireless Propagation Letters*, vol. 8, 1279–1282, 2009.
- [217] Vendik, I. B., A. Rusakov, K. Kanjanasit, J. Hong, and D. Filonov, "Ultra-wideband (UWB)planar antenna with single-, dual-, and triple-band notched characteristic based on electric ring resonator," *IEEE Antennas and Wireless Propagation Letters*, vol. 16, 1597–1600, 2017.
- [218] Bakariya, P. S., S. Dwari, and M. Sarkar, "Triple band notch UWB printed monopole antenna withenhanced bandwidth," *AEU — International Journal of Electronics and Communications*, vol. 69, 26–30, 2015.
- [219] Ryu, K. S. and A. A. Kishk, "UWB antenna with single or dual band-notches for lower WLAN bandand upper WLAN band," *IEEE Transactions on Antennas and Propagation*, vol. 57, 3942–3950, 2009.
- [220] Chandel, R., A. K. Gautam, and K. Rambabu, "Tapered fed compact UWB MIMO diversity antenna with dual band-notched characteristics," *IEEE Transactions on Antennas and Propagation*, vol. 66, No. 4, 1677–1684, 2018.
- [221] Jaglan, N., S. D. Gupta, E. Thakur, D. Kumar, B. K. Kanaujia, and S. Srivastava, "Triple band notched mushroom and uniplanar EBG structures based UWB MIMO/diversity antenna with enhanced wide band isolation," *AEU-International Journal of Electronics and Communications*, vol. 90, 36–44, 2018.
- [222] Jaglan, N., S. D. Gupta, B. K. Kanaujia, S. Srivastava, and E. Thakur, "Triple band notched DGC EBG structure based UWB MIMO/diversity antenna," *Progress In Electromagnetics Research C*, vol. 80, 21–37, 2018.
- [223] Chacko, B. P., G. Augustin, and T. A. Denidni, "Uniplanar polarisation diversity antenna for ultra wide band systems," *IET Microwaves, Antennas & Propagation*, vol. 7, 851–857, 2013.

- [224] Gao, P., S. He, X. Wei, Z. Xu, N. Wang, and Y. Zheng, “Compact printed UWB diversity slot antenna with 5.5-GHz band-notched characteristics,” *IEEE Antennas and Wireless Propagation Letters*, vol. 13, 376–379, 2014.
- [225] Kang, L., H. Li, X. Wang, and X. Shi, “Compact offset microstrip-fed MIMO antenna for band notched UWB applications,” *IEEE Antennas and Wireless Propagation Letters*, vol. 14, 1754–1757, 2015.
- [226] Zhu, J., B. Feng, B. Peng, L. Deng, and S. Li, “A dual notched band MIMO slot antenna system with y-shaped defected ground structure for UWB applications,” *Microwave and Optical Technology Letters*, vol. 58, 626–630, 2016.
- [227] Zhu, J., B. Feng, B. Peng, S. Li, and L. Deng, “Compact CPW UWB diversity slot antenna with dual band-notched characteristics,” *Microwave and Optical Technology Letters*, vol. 58, 989–994, 2016.
- [228] Yoon, H. K., Y. J. Yoon, H. Kim, and C.-H. Lee, “Flexible ultra-wideband polarisation diversity antenna with band-notch function,” *IET Microwaves, Antennas & Propagation*, Vol. 5, 1459–1463, 2011.
- [229] Banerjee, J., A. Karmakar, R. Ghatak, and D. R. Poddar, “Compact CPW-fed UWB MIMO antenna with a novel modified Minkowski fractal defected ground structure (DGS) for high isolation and triple band-notch characteristic,” *Journal of Electromagnetic Waves and Applications*, vol. 31, 1550–1565, 2017.
- [230] Jetti, C. R. and V. R. Nandanavanam, “Trident-shape strip loaded dual band-notched UWB MIMO antenna for portable device applications,” *AEU — International Journal of Electronics and Communications*, vol. 83, 11–21, 2018.
- [231] Wang JH, Yin YZ, Liu XL. Triple band-notched ultra wideband (UWB) antenna using a novel modified capacitively loaded loop (CLL) resonator. *Prog Electromagnet Res Lett*. vol. 42, 55–64, 2013.
- [232] Vendik IB, Rusakov A, Kanjanasit K, et al. “Ultra-wideband (UWB) planar -antenna with single-dual-, and triple-band notched characteristic based on electric ring resonator”, *IEEE Antennas Wirel Propag Lett.*, vol.16, 1597–1600, 2017.
- [233] Kushwaha N, Kumar R. “An UWB fractal antenna with defected ground structure and swastika shape electromagnetic bandgap”, *Prog Electromagnet Res B*, vol.52, 383–403, 2013.
- [234] Jiang W, Che W “A novel UWB antenna with dual notched bands for WiMAX and WLAN applications”, *IEEE Antennas Wirel Propag Lett*. vol.11, 293–296, 2012.

- [235] Alrabadi ON, Perruisseau-Carrier J, Kalis. “A MIMO transmission using a single RF source: theory and antenna design”, *IEEE Trans Antennas Propag.*, vol.60,654–664,2012
- [236] Thakur E., Jaglan, N. Gupta, S. D. & Kanaujia, B. K. “A compact notched UWB MIMO antenna with enhanced performance” .*Prog. Electromagn. Res. C*, vol.91, 39–53,2019. doi: 10.2528/PIERC18120202
- [237] Guichi, F. Challal M., and Denidni, T. A. “A novel dual band-notch ultra-wideband monopole antenna using parasitic stubs and slot”, *Microw. Opt. Technol. Lett.*, vol. 60, no.7, 1737–1744,2018. doi: 10.1002/mop.31231
- [238] Zitouni A. & Hacene, N B. “Triple Notched Band Characteristics UWB Antenna Using C-Shaped Slots and Slot-Type Capacitively-Loaded Loop (CLL)”,*J. Electromagn. Anal. Appl.*, vol.5,no.8, 342–345,2013. doi: 10.4236/jemaa.2013.58054.
- [239] Malviya, L. R. Panigrahi, K. & Kartikeyan, M. V. “low profile planar MIMO antenna with polarization diversity for LTE 1800/1900 applications,” *Microw. Opt. Technol. Lett.*, vol. 59, no. 3, pp. 533–538,2017, doi: 10.1002/mop.30329.
- [240] Thakur, E. Jaglan, N.& Gupta, S. D., “Design of compact UWB MIMO antenna with enhanced bandwidth”, *Prog. Electromagn. Res. C*,vol.97,83–94.2019.doi: 10.2528/PIERC19083004
- [241] Blanch, S. Romeu, J. & Corbella, I. “Exact representation of antenna system diversity performance from input parameter description”, *Electron. Lett.*, vol.39,no.9,701 705,2003. doi: 10.1049/el:20030495
- [242] Tang, Z. Zhan, J. X. Wu, Z. Xi, L. Chen, & S. Hu, “Design of a compact UWB-MIMO antenna with high isolation and dual band-notched characteristics,” *J. Electromagn. Waves Appl.*, vol.34, no.4, 500–513, 2020. doi: 10.1080/09205071.2020.1724200.
- [243] A. Dastranj, “Low-profile ultra-wideband polarisation diversity antenna with high isolation”, *IET Microw. Antennas Propag.*, vol.11,no.10,1363–1368,2017. doi: 10.1049/iet-map.2016.0937
- [244] Chae, S. H. Oh, S. & Park,S.-O., “ Analysis of Mutual Coupling, Correlations, and TARC in WiBro MIMO Array Antenna”, *IEEE Antennas Wirel. Propag. Lett.*. vol. 6,122–125. 2007. 10.1109/LAWP.2007.893109
- [245] Kumar, S. Kumar, R. Kumar Vishwakarma, R. & Srivastava, K. “An improved compact MIMO antenna for wireless applications with band-notched characteristics”, *AEU - Int. J. Electron. Commun.*, vol. 90,20–29,2018. doi: 10.1016/j.aeue.2018.04.008

- [246] Gujral, M. J. Li, L.-W. Yuan, T. & Qiu, C.-W, “Bandwidth improvement of microstrip antenna array using dummy EBG pattern on feedline”, *Prog. Electromagn. Res.*, vol.127, 79–92,2012. doi: 10.2528/PIER12022807
- [247] Liu H. & Xu, Z.(2013). Design of UWB Monopole Antenna with Dual Notched Bands Using One Modified Electromagnetic-Bandgap Structure. *Sci. World J.*, 1–9. doi: 10.1155/2013/917965.
- [248] Kiem NK, Phuong HN, Chien DN. Design of compact 4×4 UWB-MIMO antenna with WLAN band rejection. *Int J Antennas Propag.* 2014;2014:539094. DOI:10.1155/2014/539094
- [249] Peng L, Ruan CL. “UWB band-notched monopole antenna design using electromagnetic bandgap structures” *IEEE Trans Microw Theory Tech.*; vol.59:1074–1081,2011.
- [250] Xu F, Wang ZX, Chen X, et al. “Dual band-notched UWB antenna based on spiral electromagnetic band gap structure”, *Prog. Electromagnet Res B.*, vol.39:393–409,2012.
- [251] Jaglan N, Gupta SD, Kanaujia BK, et al. “Triple band notched DG-CEBG structure-Based UWB MIMO/diversity antenna”, *Prog Electromagnet Res C.*;80:21–37,2018.
- [252] Ghosh A, Mandal T, Das S. “Design and analysis of triple notch ultra-wideband antenna using single slotted electromagnetic bandgap inspired structure”, *J Electromagnet Waves Appl.* vol. 33,1–15,2019.
- [253] Rahman M, Jahromi MN, Mirjavadi SS, et al., “Compact UWB band-notched antenna with integrated bluetooth for personal wireless communication and UWB applications” *Electronics.*;vol. 8, no.2,154-158,2019.
- [254] Jaglan N, Gupta SD, Thakur E, et al. “Triple band-notched mushroom and uniplanar EBG structures based UWB MIMO/diversity antenna with enhanced wideband isolation”. *AEU - Int J Electron Commun*, vol. 90,36–44, 2018.
- [255] Jaglan N, Kanaujia BK, Gupta SD, et al., “ Dual band notched EBG structure-based UWB MIMO/diversity antenna with reduced wide band electromagnetic coupling”, *Frequenz.*;vol. 71,11–12,2017.
- [256] Jaglan N, Gupta SD, Kanaujia BK, et al., “ Triple band notched DG-CEBG structure-Based UWB MIMO/diversity antenna”, *Prog Electromagnet Res C*, vol. 80,21–37, 2018.
- [257] Mousazadeh A, Dadashzadeh G, “A novel compact UWB monopole antenna with triple bandnotched characteristics with EBG structure and two folded V-slot for MIMO/diversity applications”, *Prog Electromagnet Res C*, vol.50,1720–1731, 2016.

- [258] Jaglan N, Gupta SD, Kanaujia BK, et al. “Triple band notched DG-CEBG structure-Based UWB-MIMO/diversity antenna”, *Prog Electromagnet Res C*, vol. 80,21–37,2018.
- [259] Tang Z, Wu X, Zhan J, et al. “Compact UWB-MIMO antenna with high isolation and triple bandnotched characteristics” *IEEE Access*, vol.7, 19856–19865, 2019.
- [260] Biswal SP, Das S. “A low-profile dual port UWB-MIMO/diversity antenna with band rejection ability. *Int J RF Microw Comput Aided Eng*. 2018;28(1):e21159.
- [261] Chandel R, Gautam AK, Rambabu K. “Tapered fed compact UWB MIMO-diversity antenna with dual band-notched characteristics”, *IEEE Trans Antennas Propag.*; vol.66, 1677–1684, 2018.
- [262] Zhao Y, Zhang FS, Cao LX, et al. A compact dual band-notched MIMO diversity antenna for UWB wireless applications. *Prog Electromagnet Res C*, vol. 89,161–169, 2019.
- [263] Yadav D, Abegaonkar MP, Koul SK, et al., “ Two element band-notched UWB MIMO antenna withhigh and uniform isolation” *Prog Electromagnet Res M*, vol. 63,119–129,2018.
- [264] Ibrahim AA, Machac J, Shubair RM. “Compact UWB MIMO antenna with pattern diversity and band rejection characteristics”, *Microw Opt Technol Lett.*, vol. 59no.6, 1460–1464, 2017.
- [265] Xie,L. Zhao, G. Jiao, Y.-C. &.Zhang, S. “Ultra-wideband antenna using meandered slots for dual band-notched characteristic”, *Prog. Electromagn. Res. Lett.*, vol.16, 171–180, 2010. doi: 10.2528/PIERL10061703.
- [266] Chae, S. H. Oh, S. & Park,S.-O. “Analysis of Mutual Coupling, Correlations, and TARC in WiBro MIMO Array Antenna”, *IEEE Antennas Wirel. Propag. Lett.* vol. 6,122–125, 2007. 10.1109/LAWP.2007.893109.
- [267] Chandel, R. Gautam, A. K. & Rambabu, K , “Tapered Fed Compact UWB MIMO-Diversity Antenna With Dual Band-Notched Characteristics”, *IEEE Trans. Antennas Propag.*, vol.66,no.4,1677–1684,2018.doi: 10.1109/TAP.2018.2803134
- [268] A. Dastranj, “Low-profile ultra-wideband polarisation diversity antenna with high isolation”, *IET Microw. Antennas Propag.*,vol. 11,no.10,1363–1368, 2017. doi: 10.1049/iet-map.2016.0937
- [269] Kumar. S. Urooj, and F. Alrowais, “Design of Quad-Port MIMO/Diversity Antenna with Triple-Band Elimination Characteristics for Super-Wideband Applications,” *Sensors*, vol.20, no.3, 619-624, 2020. doi: 10.3390/s20030624.

- [270] Kumar, P. S. Urooj, and F. Alrowais, “Design and Implementation of Quad-Port MIMO Antenna with Dual-Band Elimination Characteristics for Ultra-Wideband Applications”, *Appl. Sci.*, vol. 10,no.5, 1701-1715,2020. doi: 10.3390/app10051715.
- [271] Raheja, D. K. Kumar, S. & Kanaujia. B K. Compact quasi-elliptical-self-complementary four-port super-wideband MIMO antenna with dual band elimination characteristics. *AEU-Int. J. Electron. Commun.*,vol.114, 2020. doi: 10.1016/j.aeue.2019.153001.
- [272] Srivastava, K. Kumar, A. Kanaujia, B. K. S.& Kumar, S., “A CPW-fed UWB MIMO antenna with integrated GSM band and dual band notches”, *Int. J. RF Microw. Comput.-Aided Eng.*, 29(1), 21433, 2019. doi: 10.1002/mmce.21433.
- [273] Kiem, N. K. H. Phuong, N. B.& Chien, D. N. “Design of Compact  $4 \times 4$  UWB-MIMO Antenna with WLAN Band Rejection”. *Int. J. Antennas Propag.*, 1–11. 2014. doi: 10.1155/2014/539094.
- [274] Wu, W. Yuan. & Wu, A., “Quad-Element UWB-MIMO Antenna with Band-Notch and Reduced Mutual Coupling Based on EBG Structures”, *Int. J. Antennas Propag.*, 1–10. 2018, doi: 10.1155/2018/8490740.
- [275] Liu Y.-Y.& Z.-H. Tu “Compact Differential Band-Notched Stepped-Slot UWB-MIMO Antenna With Common-Mode Suppression,” *IEEE Antennas Wirel. Propag. Lett.*, vol.16, 593–596,2017.doi: 10.1109/LAWP.2016.2592179.
- [276] Braaten,B. Iftikhar, D. A. Capobianco, A. Ijaz, D. Asif, B. S. & Khan, M. S , “Compact  $4 \times 4$  UWB-MIMO antenna with WLAN band rejected operation”, *Electron. Lett.*, vol. 51,no.14, 1048–1050,2015. doi: 10.1049/el.2015.1252
- [277] Irene, G. & Rajesh, A., “Penta-band reject inside cut koch fractal hexagonal monopole UWB MIMO antenna for portable devices”, *Progress In Electromagnetics Research C*, vol. 82,225–235, 2018.
- [278] Nguyen, D. T., Lee, D. H. & Park, H. C., “Very Compact Printed Triple Band-Notched UWB Antenna With Quarter-Wavelength Slots” *IEEE Antennas and Wireless Propagation Letters.* , vol.11, 411–414, 2012.
- [279] Babashah, H., Hassani, H. R. & Nezhad, S.M.A., “A compact UWB printed monopole MIMO antenna with mutual coupling reduction” *Progress In Electromagnetics Research C*. vol. 91, 55–67,2019.
- [280] Chamani, Z., & Jahanbakht, S., “Improved performance of double- T monopole antenna for 2.4/5.6 GHz dual-band WLAN operation using artificial magnetic conductors” *Progress In Electromagnetics Research M*,vol.61, 205–213,2017.

- [281] Tripathi, S., Yadav, S. & Mohan, A. “Hexagonal fractal ultra-wideband antenna using Koch geometry with bandwidth enhancement”, *IET Microwaves, Antennas & Propagation*, vol.8, 1445–1450, 2014.
- [282] Ooi, T.S. & Rahim, S. K. “A 2.45 GHz and 5.8 GHz compact dual band circularly polarized patch antenna”, *Journal of Electromagnets Waves and Application*. vol.24, 1473–1482, 2010.
- [283] Zhang, Y. P. “60-GHz antenna-in-package technology”, *IET Microwaves, Antennas & Propagation*, vol.5, 1743–1750,2011.
- [284] Weng, W.C, Sze, J.Y. Chen, C.F. “A dual-broadband circularly polarized slot antenna for WLAN applications”, *IEEE Trans Antennas Propag*, vol.62, 2837-2841, 2014.
- [285] Karamzadeh, S., Rafii, V. Kartal, M. & Saygin, H. “Compact UWB CP square slot antenna with two corners connected by a strip line” *Electron Lett.* 52,10-12,2016.
- [286] Tang, H., Wang, Wu, K. Yu, R. C. Zhang, J. & Wang, X., “A novel broadband circularly polarized monopole antenna based on C-shaped radiator”, *IEEE Antennas Wireless Propag Lett.* vol.16,964-967,2017.
- [287] Li, G.H., Li, H.Q. Li, T. L. & Liang, C.H, “CPW-fed S-shaped slot antenna for broadband circular polarization”, *IEEE Antennas Wireless Propag Lett.* , vol.12, 619-622, 2013.
- [288] Gyasi, K.O, Wen, G. J. Inserra, D. “A compact broadband cross-shaped circularly polarized planar monopole antenna with a ground plane extension”, *IEEE Antennas Wireless Propag Lett.*, vol. 17, 335-338, 2018.
- [289] Manas, M., Bhattacharjee, S. and Mitra, M., “Circularly polarized planar monopole antenna for ultra wide band applications”, *International Journal of RF and Microwave Computer-Aided Engineering*, vol.29, 1-9, 2019.
- [290] Hu, B.Y. & Nasimuddin, S.X. “Broadband circularly polarized moon-shaped monopole antenna” *Micro Opt Techno Lett.* vol. 57, 1135-1139,2015.
- [291] Tang, H. K., Wang, R. Wu, C. Zhang, Yu, J. & Wang, X., “ A novel broadband circularly polarized monopole antenna based on C-shaped radiator”, *IEEE Antennas Wireless Propag. Lett.*, vol.16, 964–967,2017.
- [292] Panahi, A., Bao, Ruvio, X.L. G, & Ammann, M. J. “A printed triangular monopole with wideband circular polarization”, *IEEE Trans Antenna Propag.* vol.63, 415–418, 2015.
- [293] Han, R. C. & Zhong, S. S. “Broadband circularly-polarized chifre-shaped monopole antenna with asymmetric feed”, *Electron. Lett.*,vol. 52, 256–258,2016 .

- [294] Martin, F. Falcone, F. Bonache, Marques, J. R. & Sorolla, M. “Miniaturized coplanar waveguide stop band filters based on multiple tuned split ring resonators”, *IEEE Microwave and Wireless Components Letters*, vol. 13, 511–513, 2003.
- [295] Zhang, H., Jiao, Y.C. Lu, L. “Broadband circularly polarized square-ring-loaded slot antenna with flat gains”, *IEEE Antennas Wireless Propag Lett.* vol.16, 29-32, 2017.
- [296] Hoang, T. V., Le, T. , Li, T. Q., & Park, H. C., “Quad-band circularly polarized antenna for 2.4/5.3/5.8-GHz WLAN and 3.5-GHz WiMAX applications”, *IEEE Antennas Wireless Propag. Lett.* vol. 15, 1032–1035, 2016.
- [297] Hu, B.Y., Nasimuddin, S.X., “Broadband circularly polarized moon-shaped monopole antenna”, *Microw Opt Technol Lett*, vol. 57, 1135-1139, 2015.
- [298] Yatendra, K., Gangwar, R. K., & Kanaujia, B. K, “Compact broadband circularly polarized hook-shaped microstrip antenna with DGS plane”, *Int J RF Microw Comput Aided Eng.* 28, e21275, 2018.
- [299] Chiu, C.Y., Yan, J.-B. & Murch, R. D Compact Three-Port Orthogonally Polarized MIMO Antennas. *IEEE Antennas and Wireless Propagation Letters*, 6, 619–622, 2007.
- [300] Xu, R., Li, J. Liu, Y. J. A design of broadband circularly polarized C-shaped slot antenna with sword-shaped radiator and its array for L/S-ban applications, *IEEE Access*, vol.6, 5891-5896, 2018.
- [301] Chandu, DS, and Karthikeyan, SS. “Broadband circularly polarized printed monopole antenna with protruded L-shaped and inverted L-shaped strips”, *Microw. Opt. Technol. Lett.*, vol.60, no.1, 242–248, 2018.
- [302] Chaudhary P, and Kumar A, “Compact ultra-wideband circularly polarized CPW-fed monopole antenna”, *AEU-International Journal of Electronics and Communications*, vol.107, 137–145, 2019.
- [303] Tran H H, and Park H.C. “Ultra wide band circularly polarized antenna with dual band-notched characteristics”, *Int J RF Microw Comput Aided Eng*, vol.29, no. 11, 2019.
- [304] Tang, H. K., Wang, R. Wu, C. Zhang, Yu, J. & Wang, X. “A novel broadband circularly polarized monopole antenna based on C-shaped radiator”, *IEEE Antennas Wireless Propag. Lett.* vol.16, 964–967, 2017
- [305] Panahi, A., Bao, Ruvio, X.L. G, & Ammann, M. J. “A printed triangular monopole with wideband circular polarization”, *IEEE Trans Antenna Propag*, vol. 63, 415–418. 1–9, 2019.

- [306] Han, R. C. & Zhong, S. S. “Broadband circularly-polarized chifre-shaped monopole antenna with asymmetric feed”, *Electron. Lett.* vol. 52, 256–258, 2019.
- [307] Martin F, Falcone F, Bonache J R & Sorolla M. “Miniaturized coplanar waveguide stop band filters based on multiple tuned split ring resonators”, *IEEE Microwave and Wireless Components Letters*, vol.13, 511–513,2003.
- [308] Zhang H, Jiao YC, Lu L. Broadband circularly polarized square-ring-loaded slot antenna with flat gains. *IEEE Antennas Wireless Propag Lett.*, vol.16, 29-32, 2017.
- [309] Hu BY, Nasimuddin, SX, “Broadband circularly polarized moon-shaped monopole antenna”, *Microw Opt Technol Lett*, vol.57, 1135-1139, 2015.
- [310] Zhang H, Jiao YC, Lu L. “Broadband circularly polarized square-ring-loaded slot antenna with flat gains” *IEEE Antennas Wireless Propag. Lett.*, vol.16, 29-32, 2017.
- [311] Panahi A, Bao Ruvio XLG, & Ammann M J. “A printed triangular monopole with wideband circular polarization” *IEEE Trans Antenna Propag*, vol. 63, 415–41852, 2015.
- [312] Ali, T., S. B K, and R. C. Biradar, “A miniaturized decagonal Sierpinski UWB fractal antenna,”*Progress In Electromagnetics Research C*, vol. 84, 161–174, 2018.
- [313] Nguyen, D. T., D. H. Lee, and H. C. Park, “Very compact printed triple band-notched UWB antenna with quarter-wavelength slots,” *IEEE Antennas and Wireless Propagation Letters*, vol. 11, 411–414, 2012.
- [314] Chattopadhyay, K., S. Das, S. Das, and S. R. Bhadra Chaudhuri, “Ultra-wideband performance of printed hexagonal wide-slot antenna with dual band-notched characteristics,” *Progress In Electromagnetics Research C*, vol. 44, 83–93, 2013.
- [315] Alkhatib, R. and M. Drissi, “Improvement of bandwidth and efficiency for directive superstrate EBG antenna,” *Electronics Letters*, vol. 43, 696–702, 2007.
- [316] Chamani, Z. and S. Jahanbakht, “Improved performance of double-T monopole antenna for 2.4/5.6GHz dual-band WLAN operation using artificial magnetic conductors,” *Progress In Electromagnetics Research M*, vol. 61, 205–213, 2017.
- [317] Tripathi, S., S. Yadav, and A. Mohan, “Hexagonal fractal ultra-wideband antenna using Koch geometry with bandwidth enhancement,” *IET Microwaves, Antennas & Propagation*, vol. 8, 1445– 1450, 2014.
- [318] Irene, G. and A. Rajesh, “A penta-band reject inside cut koch fractal hexagonal monopole UWB MIMO antenna for portable devices,” *Progress In Electromagnetics Research C*, vol. 82, 225–235, 2018.

- [319] Elwi, T. A., A. I. Imran, and Y. Alnaiemy, "A miniaturized lotus shaped microstrip antenna loaded with EBG structures for high gain-bandwidth product applications," *Progress In Electromagnetics Research C*, vol. 60, 157–167, 2015.
- [320] Kumar, A., A. Q. Ansari, B. K. Kanaujia, J. Kishor, and N. Tewari, "Design of triple-band MIMO antenna with one band-notched characteristic," *Progress In Electromagnetics Research C*, vol. 86, 41–53, 2018.
- [321] Thakur, E., N. Jaglan, S. D. Gupta, and B. K. Kanaujia, "A compact notched UWB MIMO antenna with enhanced performance," *Progress In Electromagnetics Research C*, vol. 91, 39–53, 2019.
- [322] Zhang, Y. P., "60-GHz antenna-in-package technology," *IET Microwaves, Antennas & Propagation*, vol. 5, 1743–1750, 2011.
- [323] Guo, Z., H. Tian, X. Wang, Q. Luo, and Y. Ji, "Bandwidth enhancement of monopole UWB antenna with new slots and ebg structures," *IEEE Antennas and Wireless Propagation Letters*, vol. 12, 1550–1553, 2013.
- [324] Chen, D., W. Yang, and W. Che, "High-gain patch antenna based on cylindrically projected EBG planes," *IEEE Antennas and Wireless Propagation Letters*, vol. 17, 2374–2378, 2018.
- [325] Huang, C., C. Ji, X. Wu, J. Song, and X. Luo, "Combining FSS and EBG surfaces for high-efficiency transmission and low-scattering properties," *IEEE Transactions on Antennas and Propagation*, vol. 66, 1628–1632, 2018.
- [326] Ghimire, J., K. Choi, and D. Y. Choi, "Bandwidth enhancement and mutual coupling reduction using a notch and a parasitic structure in a UWB-MIMO antenna," *International Journal of Antennas and Propagation*, vol. 15, 1–9, 2019.
- [327] Alrabadi, O. N., J. Perruisseau-Carrier, and A. Kalis, "MIMO transmission using a single RF source: Theory and antenna design," *IEEE Transactions on Antennas and Propagation*, Vol. 60, 654–664, 2012.
- [328] Zhu, J., B. Feng, B. Peng, L. Deng, and S. Li, "A dual notched band MIMO slot antenna system with Y-shaped defected ground structure for UWB applications," *Microvave and Optical Technology Letters*, Vol. 58, 626–630, 2016.
- [329] Kharche, S. U., G. S. Reddy, B. Mukherjee, R. K. Gupta, and J. Mukherjee, "MIMO antenna for Bluetooth, Wi-Fi, Wi-MAX and UWB applications," *Progress In Electromagnetics Research C*, Vol. 52, 53–62, 2014.
- [330] Martin, F., F. Falcone, J. Bonache, R. Marques, and M. Sorolla, "Miniaturized coplanar waveguide stop band filters based on multiple tuned split ring resonators," *IEEE Microwave and Wireless Components Letters*, Vol. 13, 511–513, 2003.

- [331] Zhang, S. and G. F. Pedersen, "Mutual coupling reduction for UWB MIMO antennas with a wide band neutralization line," *IEEE Antennas and Wireless Propagation Letters*, Vol. 15, 166–169, 2016.
- [332] Huang, H., Y. Liu, S. Zhang, and S. Gong, "Uniplanar differentially driven ultra wideband polarization diversity antenna with band-notched characteristics," *IEEE Antennas and Wireless Propagation Letters*, Vol. 14, 563–566, 2015.
- [333] Babashah, H., H. R. Hassani, and S. Mohammad-Ali-Nezhad, "A compact UWB printed monopole MIMO antenna with mutual coupling reduction," *Progress In Electromagnetics Research C*, Vol. 91, 55–67, 2019.
- [334] Braaten, B. D., A. Iftikhar, A. D. Capobianco, B. Ijaz, S. Asif, and M. S. Khan, "Compact  $4 \times 4$  UWB-MIMO antenna with WLAN band rejected operation," *Electronics Letters*, Vol. 51, 1048–1050, 2015.
- [335] Chiu, C.-Y., J.-B. Yan, and R. D. Murch, "Compact three-port orthogonally polarized MIMO antennas," *IEEE Antennas and Wireless Propagation Letters*, Vol. 6, 619–622, 2007.
- [336] Park, J., J. Choi, J. Park, and Y. Kim, "Study of a T-shaped slot with a capacitor for high isolation between MIMO antennas," *IEEE Antennas and Wireless Propagation Letters*, Vol. 11, 1541–1544, 2012.
- [337] Chandel, R., A. K. Gautam, and K. Rambabu, "Tapered fed compact UWB MIMO diversity antenna with dual band-notched characteristics," *IEEE Transactions on Antennas and Propagation*, Vol. 66, 1677–1684, 2018.
- [338] Chandel, R. and A. K. Gautam, "Compact MIMO/diversity slot antenna for UWB applications with band-notched characteristic," *Electronics Letters*, Vol. 52, No. 5, 336–338, 2016.
- [339] Karaboikis, M. P., V. C. Papamichael, G. F. Tsachtsiris, C. F. Soras, and V. T. Makios, "Integrating compact printed antennas onto small diversity/MIMO terminals," *IEEE Transactions on Antennas and Propagation*, Vol. 56, 2067–2078, 2008.
- [340] Elwi, T. A., A. I. Imran, and Y. Alnaiemy, "A miniaturized lotus shaped microstrip antenna loaded with ebg structures for high gain-bandwidth product applications," *Progress In Electromagnetics Research C*, Vol. 60, 157–167, 2015.
- [341] Ferrero, F., R. Addaci, R. Staraj, T. Fortaki, D. Seetharamdoo, and N. Hamdiken, "Simple bandwidth-enhancement technique for miniaturised low-profile UWB antenna design," *Electronics Letters*, Vol. 50, 1564–1566, 2014.
- [342] Ranga, Y., A. K. Verma, K. P. Esselle, and S. G. Hay, "An ultra-wideband quasi-planar antenna with enhanced gain," *Progress In Electromagnetics Research C*, Vol. 49, 59–65, 2014.

- [343] Alsath, M. G. N. and M. Kanagasabai, "Compact UWB monopole antenna for automotive communications," *IEEE Transactions on Antennas and Propagation*, Vol. 63, 4204–4208, 2015.
- [344] Khan, M. S., A.-D. Capobianco, S. M. Asif, D. E. Anagnostou, R. M. Shubair, and B. D. Braaten, "A compact CSRR-enabled UWB diversity antenna," *IEEE Antennas and Wireless Propagation Letters*, Vol. 16, 808–812, 2017.
- [345] Kumar, A., A. Q. Ansari, B. K. Kanaujia, J. Kishor, and N. Tewari, "Design of triple-band MIMO antenna with one band-notched characteristic," *Progress In Electromagnetics Research C*, Vol. 86, 41-53, 2018.
- [346] Irene, G. and A. Rajesh, "A penta-band reject inside cut koch fractal hexagonal monopole UWBMIMO antenna for portable devices," *Progress In Electromagnetics Research C*, Vol. 82, 225–235, 2018.
- [347] Kayabasi, A., A. Toktas, E. Yigit, and K. Sabanci, "Triangular quad-port multi-polarized UWBMIMO antenna with enhanced isolation using neutralization ring," *AEU — International Journal of Electronics and Communications*, Vol. 85, 47–53, 2018.
- [348] Ghimire, J., K.-W. Choi, and D.-Y. Choi, "Bandwidth enhancement and mutual coupling reduction using a notch and a parasitic structure in a UWB-MIMO antenna," *International Journal of Antennas and Propagation*, Vol. 2019, 1–9, 2019.

# **APPENDIX**

## Appendix

### Antenna Fabrication

The accuracy of the antenna dimension is very critical in microwave frequencies. Therefore EP 2006 PCB PROTOTYPE MACHINE is used to fabricate the antenna geometry. EP2006 series PCB Prototype Machine will bring you the most simple, quick precise way to make your own PCB prototype. The fabrication prototype machine is shown in Figure A.1.



**Figure A.1** Fabrication prototype machine

### Anechoic Chamber

The measurement setup in an anechoic chamber is shown in Figure A.2 The anechoic chamber provides a quiet zone and used to measure the antenna characteristics accurately. All the antenna characterizations are done in an anechoic chamber to avoid reflections from nearby objects. The absorbers fixed on the walls are highly loss at microwave frequencies. They have tapered shapes to achieve good impedance matching for the

microwave power impinges upon it. The chamber is made free from the surrounding EM interferences by covering all the walls and the roof with aluminum sheet.



**Figure A.2** Anechoic chamber

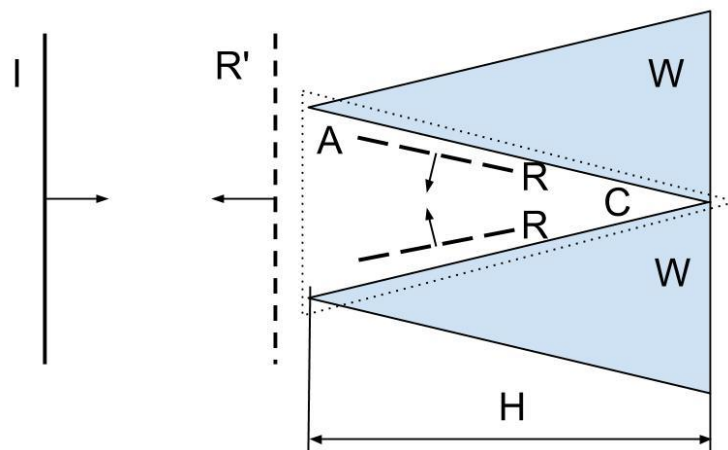


**Figure A.3.** Wedge absorbers in anechoic chamber

### **Radiation Pattern Measurement**

The mechanism by which anechoic chambers minimize the reflection of sound waves impinging onto their walls is as follows: In the included Figure, an incident sound wave  $I$  is about to impinge onto a wall of an anechoic chamber. This wall is composed of a series of wedges  $W$  with height  $H$ . After the impingement, the incident wave  $I$  is reflected as a series of waves  $R$  which in turn "bounce up-and-down" in the gap of air  $A$  (bounded by dotted lines) between the wedges  $W$ . Such bouncing may produce (at least

temporarily) a standing wave pattern in A. During this process, the acoustic energy of the waves R gets dissipated via the air's molecular viscosity, in particular near the corner C. In addition, with the use of foam materials to fabricate the wedges, another dissipation mechanism happens during the wave/wall interactions [4] . As a result, the component of the reflected waves R along the direction of I that escapes the gaps A and goes back to the source of sound, denoted R', is notably reduced.

## Vector Network Analyser

The Rohde and Schwarz ZVL vector network analyzer is used for measurements of S-parameters as shown in Figure A.4. It can be used from 9 KHz to 13.6 GHz which is sufficient for all fabricated antennas used in this thesis.



**Figure A.4.** Vector Network Analyzer

For accurate measurements it is mandatory to calibrate the VNA upto SMA connectors before each antenna testing. The reflection coefficient ( $S_{11}$ ) can be measured using only one port of VNA. The measurement transmission coefficients requires both ports of VNA. One port is acting as a source while the other is terminated with a match load. Agilent VNA PNA-L series is also used which is also based on similar principle.